



HAL
open science

Characterisation de l'ubiquitine Ligase PDZRN3 en tant que nouvel acteur des voies Wnt dans la morphogenese et l'integrite vasculaire

Raj Nayan Sewduth

► **To cite this version:**

Raj Nayan Sewduth. Characterisation de l'ubiquitine Ligase PDZRN3 en tant que nouvel acteur des voies Wnt dans la morphogenese et l'integrite vasculaire. Cellular Biology. Université de Bordeaux, 2014. English. NNT : 2014BORD0226 . tel-01399499

HAL Id: tel-01399499

<https://theses.hal.science/tel-01399499>

Submitted on 19 Nov 2016

HAL is a multi-disciplinary open access archive for the deposit and dissemination of scientific research documents, whether they are published or not. The documents may come from teaching and research institutions in France or abroad, or from public or private research centers.

L'archive ouverte pluridisciplinaire **HAL**, est destinée au dépôt et à la diffusion de documents scientifiques de niveau recherche, publiés ou non, émanant des établissements d'enseignement et de recherche français ou étrangers, des laboratoires publics ou privés.

THÈSE PRÉSENTÉE
POUR OBTENIR LE GRADE DE

**DOCTEUR DE
L'UNIVERSITÉ DE BORDEAUX**

ÉCOLE DOCTORALE SCIENCES DE LA VIE ET DE LA SANTE
SPÉCIALITÉ BIOLOGIE CELLULAIRE ET PHYSIOPATHOLOGIE

Par Raj Nayan SEWDUTH

**CARACTERISATION DE L'UBIQUITINE LIGASE PDZRN3 EN TANT QUE NOUVEL
ACTEUR DES VOIES WNT DANS LA MORPHOGENESE ET L'INTEGRITE VASCULAIRE**

**CHARACTERIZATION OF THE UBIQUITIN LIGASE PDZRN3 AS A NOVEL ACTOR
OF WNT PATHWAYS IN VASCULAR MORPHOGENESIS AND INTEGRITY**

Sous la direction de : Dr Cécile DUPLAA (Directeur de Recherche)
Soutenue le 18 Novembre 2014

Membres du jury :

Pr Elisabeth Tournier Laserve	Professeur Des Universités/ Praticien Hospitalier Hopital Lariboisière/Fernand Vidal – Inserm	Rapporteur
Dr Stéphane Germain	Directeur De Recherche– Collège De France/ Inserm	Rapporteur
Dr Nathalie Macrez	Chargée De Recherche– Institut Des Maladies Neurodégénératives/ Cnrs	Examineur
Dr Nathalie Sans	Chargée De Recherche– Neurocentre Magendie/ Inserm	Invité

Characterisation De L'ubiquitine Ligase PDZRN3 En Tant Que Nouvel Acteur Des Voies Wnt Dans La Morphogenese Et L'integrite Vasculaire

Résumé : Parmi les récepteurs Frizzled, Frizzled 4 est le seul à avoir un phénotype vasculaire fort. Par criblage, nous avons identifié l'ubiquitine ligase PDZRN3 en tant que nouveau partenaire de la protéine adaptatrice Dvl3 qui agit en aval de Fzd4. En utilisant des modèles murins inductibles, nous montrons que la délétion de PDZRN3 induit une létalité embryonnaire suite à des défauts de vascularisation du sac amniotique ; et que PDZRN3 est requis pour une vascularisation normale de la rétine. De par son activité d'ubiquitine ligase, PDZRN3 induit la prise en charge du complexe Fzd4/ Dvl3 par les vésicules d'endocytose ce qui permet la transduction du signal après fixation du ligand Wnt5a sur le récepteur Fzd4. PDZRN3 régule également le maintien des jonctions des cellules endothéliales et l'intégrité de la barrière hémato-encéphalique. La délétion de PDZRN3 stabilise les microvaisseaux après ischémie cérébrale. PDZRN3 induit la disruption des jonctions serrées et la rupture de la barrière hématoencéphalique en ubiquitinant la protéine d'échafaudage MUPP1.

Mots-clés: **PDZRN3, Wnt/ Frizzled, endocytose, ubiquitinylation, angiogenèse, perméabilité, développement, barrière hémato-encéphalique.**

Characterization Of The Ubiquitin Ligase PDZRN3 As A Novel Actor Of Wnt Pathways In Vascular Morphogenesis And Integrity

Abstract : Fzd4 is the only Frizzled receptor that is essential for angiogenesis. By using a yeast two hybrid screening, we have identified the ubiquitin ligase PDZRN3 as a potential partner of the adaptor protein Dvl3 that acts downstream of Fzd4. By using inducible mouse models, we have shown that loss of PDZRN3 leads to early embryo lethality due to vascular defects in the yolk sac when deleted *in utero*, and is then required during post natal retinal vascularization. PDZRN3 would target the Fzd4/ Dvl3 complex to endosome, leading to signal transduction upon binding of Wnt5a to Fzd4. PDZRN3 also regulates integrity of the blood brain barrier by acting on tight junctions stability. Loss of PDZRN3 stabilizes microvessels after cerebral ischemia. PDZRN3 would induce tight junction disruption and blood brain barrier leakage by ubiquitinylation of the scaffolding protein MUPP1.

Key words: **PDZRN3, Wnt/ Frizzled, endocytosis, ubiquitinylation, angiogenesis, permeability, development, blood brain barrier.**

REMERCIEMENTS

A tous les membres du jury, je vous remercie d'avoir accepté de juger ce travail

Je remercie tout le laboratoire pour leur soutien ; Catherine, Béatrice, Myriam, Annabel et Jérôme pour leur aide technique ; Christelle pour son aide au niveau administratif ; Aude, Claire, Nathalie, Marie-Lise et Laura pour leur bonne humeur ; Dr Marie-Ange Renault, Pr Pascale Dufourcq et Pr Thierry Couffinhal pour leur conseils et Dr Cécile Duplâa pour son encadrement au cours de ce travail.

Un merci aux étudiants en Master qui ont contribué au projet, Béatrice Desmoures, Nicolas Fritsch, Vincent Jecko et Robin Tellier.

Je tiens finalement à remercier mes parents et mes amis pour leur support moral. Je remercie tout spécialement Delphine pour son soutien tout le long de ce parcours.

TABLE OF CONTENTS

REMERCIEMENTS	1
TABLE OF CONTENTS	2
LIST OF FIGURES	5
ABBREVIATIONS.....	10
AVANT-PROPOS.....	12
INTRODUCTION	14
CHAPTER I. WNT SIGNALING AND ANGIOGENESIS	15
1) <i>The Wnt pathways</i>	15
a) The Wnt pathways	16
b) Wnt (wingless-type MMTV integration site family) Factors	19
c) Fzd receptors	24
d) Coreceptors of Fzd proteins	28
e) Downstream effectors of Wnt signaling	32
2) <i>Wnt signaling as a regulator of vascular development</i>	37
a) Wnt signaling is implicated in angiogenesis during development and in pathology	37
b) Molecular mechanisms of regulation of angiogenesis/cell migration by Wnt signaling	46
CHAPTER II. REGULATION OF WNT SIGNALING BY ENDOCYTOSIS AND UBIQUITINYLTATION.....	51
1) <i>Endocytosis as a regulator of Wnt signaling</i>	51
a) Role of the early endosome in signal transduction	51
b) Role of the early endosome in Wnt signaling	52
c) Caveolin and Clathrin mediated endocytosis would regulate balance between Wnt pathways	53
d) Role of the endocytosis in Wnt signaling during development	55
2) <i>Ubiquitylation as a regulator of Wnt signaling</i>	56
a) Role of ubiquitylation in protein stability or function	56
b) Ubiquitylation of Fzd proteins	57
c) Ubiquitylation of Dvl proteins	58
d) Ubiquitylation of β -catenin	60
3) <i>PDZRN3 E3 ubiquitin ligase</i>	61
a) Identification of PDZRN3.....	61
b) Structure and Function of PDZRN3 E3 ubiquitin ligase	62
c) PDZRN3 is a member of the LNX family of protein	64
CHAPTER III. WNT SIGNALING AND VASCULAR INTEGRITY	65
1) <i>Wnt signaling regulates endothelial permeability in the Blood brain barrier</i>	65
a) Wnt signaling as a regulator of brain vessels permeability	65
b) Wnt signaling as a regulator of brain vessels function in pathologies	69
2) <i>Molecular mechanisms of regulation of vascular permeability by Wnt signaling</i>	71
a) Structure of the tight junctions	71
b) Interplay between β -catenin and ZO1	73
c) Interplay between c-Jun and ZO2	75
3) <i>MUPP1 acts as a bridge between TJ and Wnt signaling</i>	77

- a) MUPP1 is important for tight junctions stability 77
- b) MUPP1 acts as a scaffold in the Crumbs complex 78
- c) MUPP1 as a bridge between Tight Junctions and Crumbs complex 80

METHODS..... 81

A) DETAILED PROTOCOLS	82
1) <i>Yeast Two Hybrid experiment</i>	82
2) <i>Expression constructs</i>	82
3) <i>Analysis of mRNA expression by quantitative RT-PCR</i>	83
4) <i>Cell culture</i>	84
a) Wnt conditioned media production.....	84
b) Cell transfection / transduction	84
c) Chemical treatments.....	85
d) Proliferation (MTT) assay.....	85
e) Luciferase reporter assay	85
5) <i>Protein analysis</i>	85
a) Western Blot	85
b) Immunoprecipitation assay	86
c) Cell fractionation.....	86
d) Ubiquitylation assay.....	87
6) <i>Immunocytochemistry</i>	87
a) Immunocytochemistry	87
b) Internalization assay.....	87
7) <i>Immunohistochemistry</i>	88
a) Paraffin sections.....	88
b) Cryosections.....	88
c) Vibratome sections.....	88
d) In toto embryo staining	88
e) Dab staining	88
f) Immunofluorescence	89
8) <i>Image analysis</i>	89
9) <i>In vitro assays on endothelial cells</i>	89
a) 2D tubulogenesis assay	89
b) Wound assay	90
c) 3D tubulogenesis (cytodex) assay.....	90
d) Chemotaxis assay.....	91
e) Permeability assay (Transwell assay).....	91
f) Junctions disruption by calcium chelation	91
10) <i>Experimental animals</i>	91
a) Cre – Lox system	91
b) Tetracyclin activated system.....	93
c) Injections.....	93
11) <i>Surgery</i>	94
a) Retinal vascularization analysis	94
b) Middle cerebral artery occlusion.....	95
c) Aortic ring assay	97

d)	Evaluation of vascular leakage in embryo and pups	97
e)	Micro computer tomography	97
f)	Isolation of primary endothelial cells from mouse kidney	98
g)	Vessel extraction	98
12)	<i>Statistical analysis</i>	99
B)	REAGENTS	100
1)	<i>List of used antibodies</i>	<i>100</i>
2)	<i>Chemical reagents</i>	<i>101</i>
3)	<i>Equipments</i>	<i>102</i>
RESULTS	103	
ARTICLE 1. FRIZZLED 4 REGULATES ARTERIAL NETWORK ORGANIZATION THROUGH NONCANONICAL WNT/PLANAR CELL POLARITY SIGNALING		
		104
a)	<i>State of art</i>	<i>105</i>
b)	<i>Hypothesis</i>	<i>105</i>
c)	<i>Summary</i>	<i>106</i>
ARTICLE 2. THE UBIQUITIN LIGASE PDZRN3 IS REQUIRED FOR VASCULAR MORPHOGENESIS THROUGH WNT/PLANAR CELL POLARITY SIGNALING		
		123
a)	<i>State of art</i>	<i>124</i>
b)	<i>Hypothesis</i>	<i>125</i>
c)	<i>Strategy</i>	<i>125</i>
d)	<i>Preliminary Results</i>	<i>126</i>
e)	<i>Summary</i>	<i>128</i>
ARTICLE 3. THE UBIQUITIN LIGASE PDZRN3 REGULATES BLOOD BRAIN BARRIER INTEGRITY BY CONTROLLING TIGHT JUNCTIONS STABILITY VIA A WNT DEPENDANT MECHANISM		
		145
a)	<i>State of art</i>	<i>146</i>
b)	<i>Hypothesis</i>	<i>146</i>
c)	<i>Preliminary Results</i>	<i>146</i>
d)	<i>Methods</i>	<i>147</i>
e)	<i>Summary</i>	<i>150</i>
CONCLUSION AND PROSPECTS	171	
1)	PROPOSED MODEL	173
2)	PROSPECTS	177
a)	<i>Expression of PDZRN3 in pathologies</i>	<i>177</i>
b)	<i>Interaction of PDZRN3 with MUPP1</i>	<i>179</i>
c)	<i>Phosphorylation status of PDZRN3</i>	<i>179</i>
d)	<i>Chemical inhibition of PDZRN3</i>	<i>180</i>
e)	<i>PDZRN3 in other tissues</i>	<i>180</i>
BIBLIOGRAPHY	181	

LIST OF FIGURES

Figure 1: The Wnt canonical and non canonical pathways (adapted from Saadeddin et al 2009)	15
Figure 2: Transcriptional targets of the Wnt/ canonical pathway (Wnt homepage, Stanford)	16
Figure 3: PCP induces asymmetrical organization of Fzd/ Dvl and Vangl2/ Pk (Schulte 2010)	17
Figure 4: Distribution of Wnt Genes in Metazoans. X indicate that no member of the Wnt subfamily found in the genome of the organism; the color is different for each Wnt; two blocks indicate presence of paralogue in the specie (adapted from Prud'homme et al. 2002)	19
Figure 5: Phylogenetic tree of the Wnt family (adapted from Prud'homme et al. 2002).....	20
Figure 6: List of Wnt genes (Wnt homepage, Stanford).....	22
Figure 7: Schematic presentation of Wnt/ Fzd signaling kinetics (Schulte and Shenoy 2011).....	23
Figure 8: Phylogenetic tree of the human Frizzled receptors FZD (Schulte and Shenoy 2011)	24
Figure 9: Schematic representation of Frizzled protein (binding sites for Dvl/ PDZ and G proteins indicated) (Schulte and Shenoy 2011).....	24
Figure 10: Conservation of the PDZ binding domain (TXV-COOH) in the Fzd family; functional and non functional PDZ binding domain is noted as (+) or (-) respectively (Schulte and Shenoy 2011).....	25
Figure 11: List of Frizzled receptors (Wnt homepage, Stanford).....	26
Figure 12: Diagram of Fzd-4 showing mutations associated to the disease (Robitaille et al. 2002, Robitaille et al. 2011).....	27
Figure 13: Competition between Wnt ligands would regulate activation of Wnt pathways by modulating phosphorylation of LRP5/6 and Ror2 (adapted from Grumolato et al 2010)	28
Figure 14: Structure of LRP5 (He et al 2005)	29
Figure 15: Structure of the Ror2 protein (adapted from Scopus)	30
Figure 16: Structure of the Ryk protein.....	31
Figure 17: Structure of Dvl (SCOPUS).....	32
Figure 18: List of Dvl proteins (adapted from Wnt homepage, Stanford).....	33
Figure 19: Positive (left) and negative (right) regulators of Dvl activity (Gao et al 2010)	33
Figure 20: The β -catenin destruction complex (Kimelman and Xu 2006).....	34
Figure 21: Canonical Wnt signaling is up-regulated after Wnt5a KO (Topol et al 2003).....	37

Figure 22: a- Expression of various components of Wnt signaling in placenta and yolk sac; b- Placenta and Yolk Sac of Fzd5 ^{-/-} embryos are not vascularized correctly; Vascular pattern is normal in Fzd5 ^{-/-} embryo but vasculature remains superficial in placenta of Fzd5 ^{-/-} embryos (Tomo et al 2001).	37
Figure 23: a- The yolk sac of the junB KO embryo at E9.5 is translucent and shows no vessels; b- Morphological phenotypes of JunB deficient embryos (Schorpp-Kistner 1999).....	38
Figure 24: a- Wnts and Fzd4 are mediators of Brain angiogenesis (right) and differentiation of the Blood brain barrier (left) (Paolinelli et al 2011); b- Lrp5/6 and β -catenin are also essential for vessel formation in the hindbrain as KD of both proteins lead to vascular leakage (in white) (Zhou et al. 2014).....	39
Figure 25: Schematic of retina during its vascularization (adapted from Franco et al 2009).....	40
Figure 26: a- Neutralizing FZD4 alters development of the intermediate and deep plexus; b- leading to leakage as shown by fluorescein extravasation and PLVAP expression (Ye et al 2010)	41
Figure 27: a - Fzd4 deletion leads to expression of PLVAP; the cells expressing PLVAP are progressively lost, indicating that endothelial cells deleted for Fzd4 are eliminated; b- Proliferation is increased in Fzd4 ^{-/-} cells as indicated by Edu staining.	42
Figure 28: Retinal myeloid cells (in red) interact with descending vertical sprouts (in green).....	43
Figure 29: Retinal myeloid cells flow sorted from the deep plexus are subjected to PCR for Wnt pathway components (Stefater, Lewkowich et al. 2011)	43
Figure 30: a-c micro-CT images of control and stem cells injected hindlimb after ischemia; d - quantification of vessel density and connectivity; e- expression of Wnt factors as detected in ischemic muscle after injection of normal/ hypoxic stem cell (adapted from Leroux et al.).....	44
Figure 31: Events that occur after cerebral ischemia (Sandoval 2009)	45
Figure 32: Wnt5a induces migration by relocalizing c-Jun to the leading edge (Nomachi 2008)	46
Figure 33: Cell migration and adhesion regulated by the Wnt5a pathway (Kikuchi et al. 2012).....	46
Figure 34: Regulation of migration via the actin skeleton by Dvl and Daam (Chen et al 2003).....	47
Figure 35: Regulation of migration via microtubules by Dvl and Daam (Chen et al 2003).....	48
Figure 36: Sprouting endothelial cells are hierarchically organized into tips cells and stalk cells during retinal angiogenesis. Tip cell formation is induced by VEGF signaling, while stalk cell are determined by Notch signaling (Herbert et al. 2011).....	49
Figure 37: Different effects of Wnt/ β -catenin and Notch signaling during sprouting angiogenesis (Gerhardt et al. 2009).....	50
Figure 38: Endosome regulates signaling by different manner (Dobrowolski et al 2011).....	51
Figure 39: Endocytosis of Wnt receptors can lead to signal transduction / recycling or signal termination depending on context (Gagliardi et al 2008)	52
Figure 40: Endosome and Wnt signal transduction (adapted from Drobowski et al 2011).....	54

Figure 41: The dorsal determinants of the <i>Xenopus</i> egg may be Wnt endosomal components (adapted from Drobowski et al 2011)	55
Figure 42: a - different types of ubiquitin chains, b- 3D structure of Lysine 63 linked diubiquitin, c- 3D structure of Lysine 48 linked diubiquitin (Ikeda, Dikic 2008)	56
Figure 43: a- position of the different lysines residues on intracellular domains of Fzd4; ubiquitinylation of Fzd4 (smear) is mediated by Wnt3a and UBPY (Mukai et al 2010).....	57
Figure 44: UBPY deubiquitin ligase controls availability of FZD4 for Wnts (Mukai et al 2010)	57
Figure 45: Different regulators of Dvl ubiquitinylation (adapted from Tauriello 2010)	58
Figure 46: a- Cyld mediated K63 dependant ubiquitinylation of Dvl (detected as a smear); b- model of regulation of Dvl activity by CYLD (Tauriello et al. 2010).....	58
Figure 47: Inversin regulation of Dvl (adapted from Simons 2006)	59
Figure 48: Ubiquitin mediated regulation of core Wnt proteins such as β -catenin (adapted from Tauriello et al. 2010).....	60
Figure 49: Orthologues of PDZRN3 (Gene Ontology)	61
Figure 50: Structure of the protein (Scopus, EMBL)	62
Figure 51: Process of ubiquitinylation (Dikic et al. 2012)	62
Figure 52: ClustalX alignment of the last amino acids of murine PDZRN3 (mm LNX3), PDZRN3 4 (mm LNX4) as well as orthologues from invertebrate species(Flynn et al. 2011).....	63
Figure 53: Molecular evolution of the LNX family (Flynn et al 2011).....	64
Figure 54: Brain capillaries under normal and pathological conditions (Paolinelli et al 2011)	65
Figure 55: VE-cadherin traps FoxO1 and β -catenin at the membrane. In the nucleus, both would block claudin-5 transcription. In acute permeability condition, VE-cadherin adhesion is destabilized and FoxO1 and β -catenin are phosphorylated and translocate to the nucleus where they block claudin-5 transcription (Gavard et al 2008).....	66
Figure 56: a- Transcription of claudin 3 is activated by β -catenin (Liebner et al 2008); b- Conditional loss of β -catenin leads to vascular leakage during development (Catellino et al 2003).....	67
Figure 57: a/b- Injection of Evans Blue of Fz4 deficient in EC mice shows leakage in the cerebellum and retina; c- Leakage arises from the fact that vessels are fenestrated as indicated by Biotin / Mouse igG extravazation(adapted from Wang et al 2013/ Zhou et al 2014)	68
Figure 58: Response to stroke (adapted from Kahle et al. 2014)	69
Figure 59: Structure of the tight junctions (adapted from González-Mariscal et al 2000).....	71
Figure 60: Structure of MAGUK Proteins (adapted from González-Mariscal et al 2000).....	72
Figure 61: Proposed model for the formation of TJ (Rajasekaran et al 1996)	73

Figure 62: Differential expression and localization of β -catenin and ZO-1 in migratory versus stationary MCF10A human breast cells (adapted from Polette et al 2007).....	73
Figure 63: Interaction of ZO1/ β -catenin during EMT transition (Polette et al 2007)	74
Figure 64: In subconfluent cultures, ZO-2 and Jun are found at the nuclei and cell borders, while in the confluent condition, they are only detected at the cell membrane (Betanzos et al 2007).....	75
Figure 65: In subconfluent cultures, ZO-2 and Jun are found at the nuclear fraction, while in confluent cultures, they are only detected in the membrane fraction as indicated by cell fractionation (Betanzos et al 2007).....	75
Figure 66: ZO-2 immunoprecipitation realized from membrane (a) and nuclear extracts (b) from sparse and confluent cell cultures (Betanzos et al. 2004).....	76
Figure 67: a -Interaction of claudins with scaffolding proteins ZOs and MUPP1; b- Western blot showing expression of MUPP1 in brain tissues (adapted from Soini et al 2011 and Sitek et al 2003)	77
Figure 68: a- Interactions of MUPP1/ Patj (first 10 PDZ domains are identical in MUPP1 and Patj); b- Relocalization RhoA to Leading edge by the Crumbs complex (Ernkvist et al. 2009).....	78
Figure 69: a- Syx /RhoA /Amot /MUPP1 and Rab13 colocalize in response to VEGF.A , as detected 2mins after treatment in vesicles and 30mins after treatment at the leading edge of migrating cells; b - Recycling vesicles are essential for polarized migration as depletion of Rab13 dirupts polarity of migrating cells (Wu et al. 2011).....	79
Figure 70: a -Depletion of MUPP1 and Syx disrupts junctional integrity as shown by ZO1 stainin and Transmission electron micrographs of sections of ventricle myocardium; b- Model of regulation of Junctional stability via MUPP1 (Ngok et al. 2012)	80
Figure 71: Dvl3 sequence used for cloning in each corresponding plasmids in red.....	82
Figure 72: PDZRN3 sequence used for cloning in each corresponding plasmids in red.....	83
Figure 73: Formation of tube-like structures after cytodex plating (control condition).....	90
Figure 74: Floxed PDZRN3 mice construct	91
Figure 75: Mating of PDGF-icre Pdzn3fl/fl males with Pdzn3 fl/fl females	92
Figure 76: Validation of the PDGF icre recombinase system using the mT/mG reporter mice.....	93
Figure 77: Quantification of Vascular area/ Regression and Proliferation.....	94
Figure 78: Region of retina imaged for quantification ; Representative view of the superficial plexus; a plane of the intermediate plexus and the deep plexus.....	95
Figure 79: View of the module of Tracking (Image J) and data analysis (Chemotaxis and migration tool Ibidi) ..	95
Figure 80: Scheme of the cerebral artery occlusion procedure (Rousselet et al 2012).....	95
Figure 81: Evans Blue diffusion after MCAO: a- whole brain; b- 100 μ m vibratome slice observed under white light; c- observed at 545nm	96
Figure 82: Scheme indicating position of the x-ray lamp, sample and camera in the microCT	97

Figure 83: Vessel extracts from adult - PDGF cre+ mT/mG mice injected with tamoxifen (vessels fluoresce in green; Hoechst staining of nuclei in blue)	98
Figure 84: Phenotype of Fzd4 ^{-/-} mice	105
Figure 85: Effect of deletion of Fzd4 on vessel density	106
Figure 86: Interaction of Fzd4 and Dvl favor Wnt non canonical pathway to favor angiogenesis	107
Figure 87: Alignment of the Dvl1/ 2 and 3 sequences	124
Figure 88: Yeast two Hybrid Strategy and Structure of the PDZRN3 protein	125
Figure 89 A few of the proteins found to be interacting with Dvl3 Dix using the screening	126
Figure 90 PDZRN3 (V5) colocalizes with clathrin, Rab5 and Rab11; with ubiquitin	127
Figure 91 Depletion of Pdzrn3 using two siRNAs reduces migration of endothelial cells	127
Figure 92 Loss of PDZRN3 modifies the ability of endothelial cells to form tubes	128
Figure 93: Role of PDZRN3 for transduction of Wnt signaling and vascular morphogenesis	129
Figure 94: EDTA treatment induces disruption of cell to cell junctions in control Huvecs; a delay is observed in Pdzrn3 depleted cells	146
Figure 95: Huvec cells are orientated in a flow of 10, 20 or 30dyn/cm ² ; Pdzrn3 depleted cells are unable to align to the flow and reorganize their junctions accordingly	147
Figure 96: a - validation of the PDGF Cre activation using a mt/mg reporter; b- vessel extracts were purified from pdgf cre mt/mg mice and subjected to confocal microscopy	148
Figure 97: Validation of the enrichment of the brain vessel fraction by q RT PCR	148
Figure 98: Expression of PDZRN3 in vessel / wash fraction	149
Figure 99: Proposed Model	150
Figure 100: Expression of the Pdzrn3 in Carcinoma (Oncomine)	177
Figure 101: Correlation of expression of PDZRN3 with other genes in Carcinoma – inset represent the scaling colour (Oncomine)	178
Figure 102: Phosphorylation of PSD-95 on Y397 makes access to the 3rd PDZ domain of PSD 95 possible (Zhang et al. 2011)	179
Figure 103: Interaction of compound 3289-8625 (blue) and Dpr peptide(brown) with the PDZ domain of Dvl (Grandy et al. 2009)	180

ABBREVIATIONS

ABC: Active β catenin
APC : Adenomatous Polyposis Coli
AJ: adherens junctions
BBB: blood brain barrier
BrdU : BromoDésoxyUridine
BSA : Bovine Serum Albumin
CD31 : Cluster of Differentiation 31
CM: conditioned medium
CNS: Central nervous system
CRD : Cystein rich Domain
Ctl: control
DAAM: Dishevelled-associated activator of morphogenesis
DAB : Diaminobenzidine
DAG : Diacylglycérol
DEP: Dishevelled, EGL-10, Pleckstrin
Dgo: Diego
DIX: Dishevelled/Axin
Dkk : Dickkopf
(D)MEM: (Dulbecco's) Modified Eagle's Medium
DMSO: Dimethyl sulfoxide
DNA : Deoxyribonucleic acid
dNTPs : Dinucleotidtriphosphate
dpc : days post-coitum
Dsh /Dvl : Dishevelled
DTT : 1,4-dithio-threitol
EC : Endothelial Cells
EDTA :ethylenediaminetetraacetic acid
E: Embryonic day
ERK : Extracellular signal-Regulated Kinase
FEVR: Familial exudative vitreoretinopathy
FGF : Fibroblast Growth Factor
FITC : Fluorescein IsoThioCyanate
Fmi: Flamingo

Fzd: Frizzled
GSK3 β : Glycogen Synthase Kinase 3 beta
I(sch): Ischemic
IB: immunoblot
i(EC)KO: inducible (endothelial cell specific) knock-out
IP: intermediate plexus OR immunoprecipitate
LiCl:Lithium Chloride
KO: Knock-Out
P: post natal day OR probability
PAGE : polyacrylamid gel electrophoresis
PBS : phosphate buffer saline
PCR : Polymerase chain reaction
PDZ: PSD95, Dlg1, ZO-1
PFA : Paraformaldehyde
PMA: Phorbol Myristate Acetate
MCAO: middle cerebral artery occlusion
NI: non ischemic
NVU: neurovascular unit
RNA : Ribonucleic acid
RT-PCR : Reverse-transcriptase PCR
SDS :sodium dodecyl sulfat
TCF : T-cell Factor
TGF- β : transforming growth Factor β
TJ: tight junctions
TNF α : Tumor Necrosis Factor alpha
TTA: tetracyclin transactivator
Ub: Ubiquitin
UBC: Ubiquitin C
Vang: Van Gogh
VE-cadhérine : Vascular Endothelial-cadhérine
VEGF : Vascular Endothelial Growth Factor
W/O: without
WT: wild - type
ZO: Zona occludens

AVANT-PROPOS

Les maladies cardiovasculaires sont la première cause de mortalité en France ; environ 170 000 décès sont recensés chaque année. Parmi les plus fréquentes, les cardiopathies ischémiques sont responsables de 27% des décès, les accidents vasculaires cérébraux de 25 % et les insuffisances cardiaques de 23 %. Les mécanismes d'adaptation à l'ischémie requièrent une adaptation vasculaire au niveau du tissu ischémique, avec le développement de nouveaux vaisseaux sanguins afin de corriger le défaut de perfusion tissulaire. Mieux comprendre les mécanismes favorisant la formation et le maintien de néo-vaisseaux fonctionnels dans un tissu ischémique est un pré-requis pour améliorer le traitement des ces pathologies. Ma recherche s'inscrit dans l'étude des mécanismes de formation et de maintien des vaisseaux en condition physiologique et pathologique au cours de l'embryogenèse et chez l'adulte. Les protéines Wnt et leurs récepteurs Frizzled régulent la formation des vaisseaux sanguins via une signalisation intracellulaire complexe. Comme les acteurs en aval des Frizzled restent méconnus, le laboratoire a mis en place une stratégie de criblage qui a permis d'identifier de nouveaux acteurs des voies Wnt/ Frizzled. Mes travaux ont porté sur l'étude d'un d'entre eux, l'ubiquitine ligase PDZRN3 et de son rôle dans la formation des vaisseaux sanguins.

L'introduction de ce manuscrit comporte trois chapitres. J'ai tout d'abord décrit le rôle de la voie Wnt/Frizzled dans la régulation de l'angiogenèse, en décrivant les différentes voies et en présentant les acteurs du système. J'ai détaillé les données concernant le rôle du ligand Wnt5a, du récepteur Frizzled, de la protéine adaptatrice Dishevelled 3 et de l'effecteur c-Jun, des protéines retrouvées en filigrane au cours du travail, avant de détailler les différents modèles de régulation proposés dans la littérature. La 2^{ème} partie de l'introduction décrit comment l'endocytose permet de réguler les voies Wnt, avec différents modèles proposés qui pourraient notamment expliquer comment la balance entre les différentes voies Wnt se fait. J'ai ensuite abordé comment l'ubiquitination permet de réguler l'endocytose pour favoriser la transduction du signal dans les voies de signalisation Wnt. Dans une 3^{ème} partie, j'ai abordé la régulation de la perméabilité vasculaire par les voies Wnt, avant de mettre en avant

les liens existant entre les voies Wnt et les jonctions serrées qui sont essentielles au maintien de l'intégrité vasculaire au niveau cérébral.

Dans le cadre de l'étude du système Wnt/Frizzled dans la formation des vaisseaux sanguins, j'ai participé à un premier travail décrivant l'implication de Frizzled 4 dans le développement vasculaire au cours du développement et dans un modèle d'ischémie du membre inférieur. Ce travail a mis en avant le rôle de Frizzled4 en tant qu'activateur des voies Wnt, requis pour la migration des cellules endothéliales.

A la suite de ce travail, une approche de criblage par double hybride a été menée permettant d'identifier un nouveau partenaire de la voie, l'ubiquitine ligase PDZRN3. Un premier travail a porté sur le rôle de la protéine dans l'angiogenèse. Des souris délétées pour la protéine de façon ubiquitaire ou spécifiquement dans les cellules endothéliales ont été générées. J'ai étudié le rôle de PDZRN3 dans le développement vasculaire au cours de l'embryogenèse et du développement de la rétine. J'ai ensuite utilisé des approches biochimiques et de culture cellulaire pour comprendre comment PDZRN3 jouait sur les voies Wnt pour favoriser le développement vasculaire.

Dans un dernier travail, le rôle physiologique de la voie Wnt via PDZRN3 dans le maintien des jonctions serrées des cellules endothéliales du cerveau et le contrôle de la barrière hémato-encéphalique a été analysé. J'ai notamment étudié l'impact de la surexpression de PDZRN3 dans les cellules endothéliales au cours de l'embryogenèse et qualifié les mutants délétés pour PDZRN3 dans les cellules endothéliales dans un modèle d'ischémie cérébral. Nous montrons par des approches de biochimie que PDZRN3 fait le lien entre voies Wnt et stabilité des jonctions en ubiquitinant la protéine associée aux jonctions MUPP1 et en favorisant la rupture des jonctions serrées.

Cet ensemble de travaux montre l'importance de la voie Wnt non canonique et de PDZRN3 dans le développement vasculaire et le maintien des fonctions vasculaires chez l'adulte.

INTRODUCTION

Chapter I. Wnt signaling and Angiogenesis

1) The Wnt pathways

Wnt signaling plays a key role in many biological processes as it regulates cell proliferation, migration and polarity establishment. Wnts are essential during development as they guide body axis specification (Barolo 2006). Ectopic placement of Wnts in *Xenopus* eggs during early gastrulation leads to formation of a secondary body axis and head, while inhibition of Wnt signaling results in a lack of dorsal structures in the frog embryo. Wnts are produced from specific sites during development, such as the edge of the developing fly wing or the dorsal region of the neural tube in vertebrates. Failure of closure of the neural tube is characteristic of knock-out mice of proteins of the Wnt pathway (Wang et al. 2006). Dysregulation of Wnt signaling is associated with cancer development (Saadi-Kheddouci et al. 2001) as alteration of proteins implicated in the pathway such as Axin or Ror2 are linked to carcinogenesis (Saadeddin et al. 2009, Ford et al. 2013).

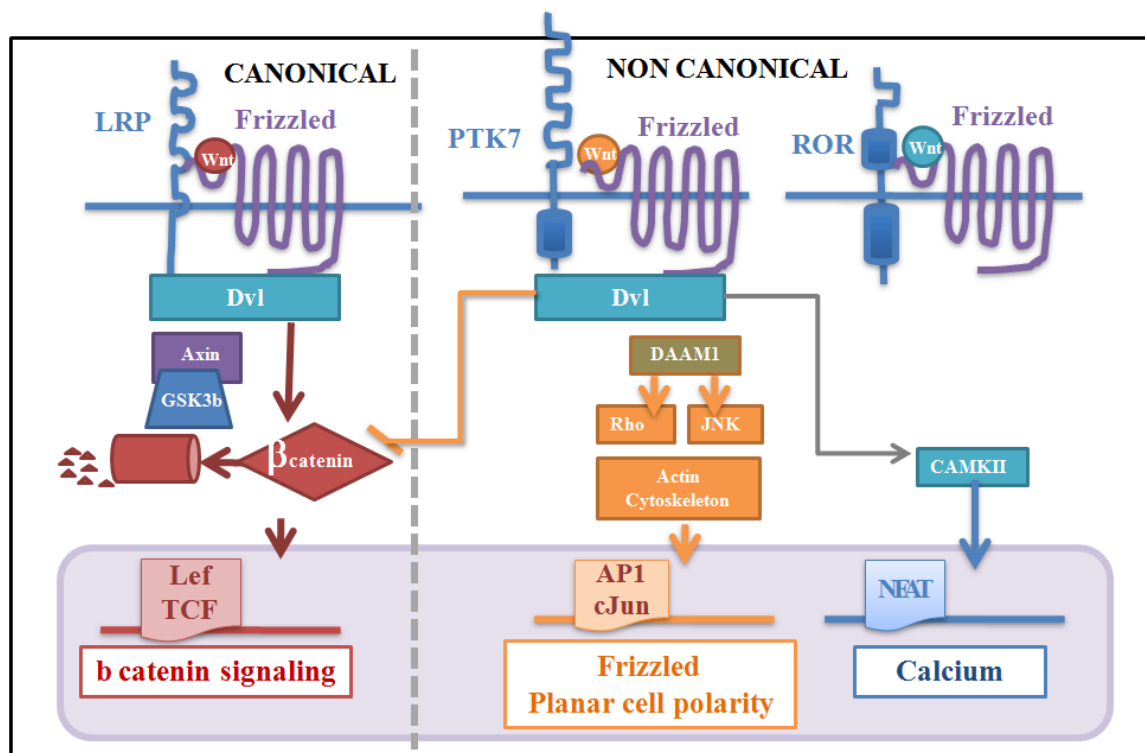


Figure 1: The Wnt canonical and non canonical pathways (adapted from Saadeddin et al 2009)

a) The Wnt pathways

i) *Canonical pathway*

The canonical Wnt signaling pathway requires β -catenin (Fig 1). Level of β -catenin is regulated by the GSK-3 containing β -catenin destruction complex. Upon binding of Wnt ligands to the Frizzled receptor (Fzd) and to its coreceptor - low density lipoprotein receptor-related protein 5/6 (LRP5/6), Fzd recruits the intracellular protein dishevelled (Dvl). Dvl then recruits the β -catenin destruction complex to the membrane, leading to inhibition of destruction of cytoplasmic β -catenin. β -catenin then accumulates in the cytoplasm and translocates to the nucleus where it functions as a coactivator for the lymphoid-enhancing factor/T-cell factor (LEF/TCF) family of transcription factors.

Gene	Organism/system	Direct/Indirect	up/down
c-myc	human colon cancer	Yes	Up
n-myc	mesenchyme limbs		Up
Cyclin D	human colon cancer	Yes	Up
Tcf-1	human colon cancer	Yes	Up
LEF1	human colon cancer	Yes	Up
PPAR	human colon cancer	Yes	Up
matrix metalloproteinase MMP-7	human colon cancer	Yes	Up
Axin-2	human colon cancer	Yes	Up
EphB/ephrin-B	human colon cancer		up/down
claudin-1	human colon cancer	Yes	Up
VEGF	human colon cancer	Yes	Up
endothelin-1	human colon cancer		Up
Frizzled 7	EC cells	Yes	Up
Wnt3a	EC cells		
E-cadherin	ES/EB		Down

Figure 2: Transcriptional targets of the Wnt/ canonical pathway (Wnt homepage, Stanford)

The canonical pathway is implicated in proliferation as transcriptional activation of Cyclin D1 is a hallmark of the activation of the pathway upon β -catenin stabilization. C-myc / axin2 / VEGF/ endothelin and claudin 5 are also transcriptional targets of the pathway (Zeng et al. 2008).

ii) Non canonical / Planar cell polarity (PCP) pathway

The non-canonical pathways do not require β -Catenin or LRP5/6. Their activation usually leads to inhibition of the canonical pathway (Grumolato et al. 2010). One of the non canonical pathways is the planar cell polarity signaling. PCP is distinct from apical/ basal polarity and can be defined as the alignment of cells within a cell sheet (Fig 2). PCP signaling creates an orientation of the cell by producing asymmetrical organization of Wnt signaling components: Fzd/Dvl are present at the distal side of the cell and Vangl2/ Prickle at the proximal side (Veeman et al 2003)(Montcouquiol et al. 2006). Both complex exclude each other: Prickle antagonizes Fzd/ Dvl by inducing removal of Fzd/ Dvl from the cell membrane by endocytosis while Dvl recruits E3 ubiquitin ligase Smurf to Prickle, leading to its loss (Narimatsu et al 2007).

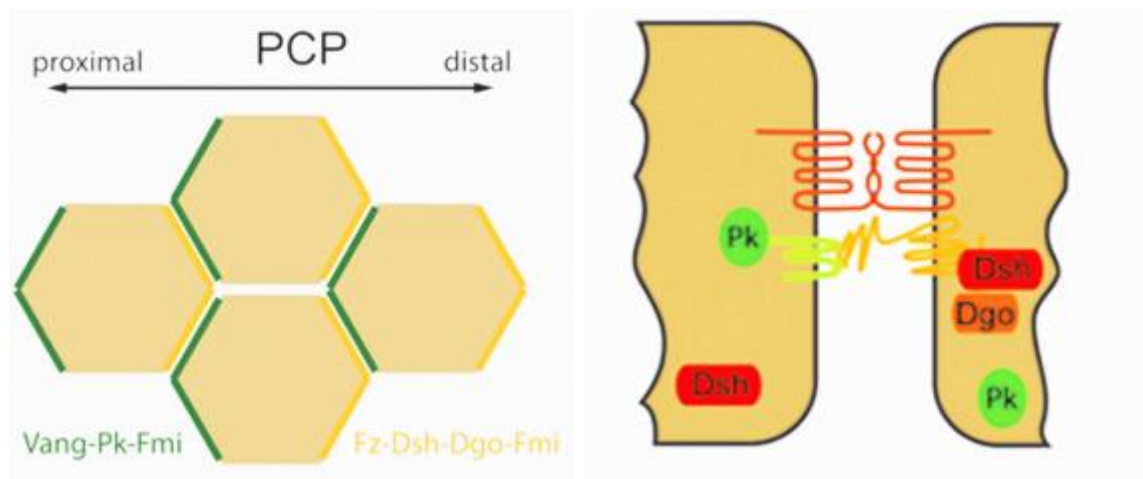


Figure 3: PCP induces asymmetrical organization of Fzd/ Dvl and Vangl2/ Pk (Schulte 2010)

The current consensus is that for activation of the PCP pathways, Wnt ligand would bind to their receptor (Fzd with Ror2 or Ryk) and recruit Dishevelled, which then forms a complex with Dishevelled-associated activator of morphogenesis 1, Daam1. Activation of Dvl leads to phosphorylation/ relocalization to the nucleus of c-JUN, where it acts as a transcription factor with c-FOS and to

activation of the small G-protein Rac, leading to activation of JNK (Gan et al. 2008). In parallel, Daam1 has been identified as a regulator of cell migration as it activates the small G-protein Rho, leading to activation of ROCK (Rho-associated kinase), which is one of the major regulators of the remodeling of the actin cytoskeleton (Ju et al. 2010, Tsuji et al. 2010). Most of the proteins involved in planar cell polarity in drosophila wing formation are conserved and used in vertebrates during regulation of cell movements during events such as gastrulation. Both processes imply control of actin filaments by the small G-proteins Rho and/ or Rac (van Amerongen and Nusse 2009). Other mechanisms are activated by PCP such as inflammation; phosphorylation of mitogen activated protein kinase p-38 would be induced by the non canonical pathway but not the canonical pathway, leading to inflammation (Verkaar et al. 2011). Interestingly, the PDZ protein GIPC is also a regulator of the localization of Vangl2 and of PCP in general (Wang et al. 1999, Giese et al. 2012).

iii) Other non canonical pathways

In the Wnt/Calcium pathway, Wnt5a and Frizzled regulate intracellular calcium levels. Wnt ligand binding to Frizzled receptor causes coupled G-protein to activate mechanisms that lead to an increase of intracellular calcium concentration. This increase activates Cdc42 (cell division control protein 42) through PKC (phosphokinase C), and calcineurin through CamKII (calcium/calmodulin-dependent kinase II). Calcineurin then induces activation of the transcription factor NFAT, which regulates ventral patterning. CamKII can also activate TAK1 and NLK kinase, which inhibit the canonical pathway (Kelly et al. 2011).

Finally, in the Wnt/GSK3 pathway, Wnt inhibition of GSK-3 activates mTOR without involvement of β -Catenin. It's why the mTOR inhibitor, Rapamycin inhibits Wnt-induced cell growth and cancer formation independently of β -Catenin. The Wnt/ m-Tor pathway regulates cell cycle and is important in carcinogenesis (van Amerongen and Nusse 2009).

b) Wnt (wingless-type MMTV integration site family) Factors

i) Overview of the Wnt family of proteins

Mouse mammary tumor virus (MMTV) is a retrovirus that utilizes an insertional mutagenesis strategy to infect mammalian cells, leading to malignant transformation only in mammary epithelium, having a potent role in breast cancer formation. MMTV activates aberrant expression of number of developmental genes, via proviral insertion, leading to oncogenetic transformation. These normally silent genes activated by the MMTV have been named as ints. The association of MMTV with the Wingless family of proteins (drosophila) began with int-1 that shares 54% identity with Drosophila Wng, with a conservation of 20 cysteine residues. Thus, an amalgam was created out of the wingless-int-1 similarity (Wnt) that served for naming of the family. The Wnt family includes 19 members in mammals. Ligands such as Wnt1, Wnt3a, and Wnt8 interact with Fzd and LRP5/6 to activate the canonical pathway, while Wnt4, Wnt5a, Wnt7a and Wnt11 activate non canonical pathways.



Figure 4: Distribution of Wnt Genes in Metazoans. X indicate that no member of the Wnt subfamily found in the genome of the organism; the color is different for each Wnt; two blocks indicate presence of paralogue in the specie (adapted from Prud'homme et al. 2002)

Wnt5 and 10 are the only Wnt factors expressed in all species, indicating that their function are vital and conserved during evolution (Fig 4). Wnt3, 5 and 7 are not part of a subfamily suggesting that their function is not redundant with other Wnt factors (Fig 5).

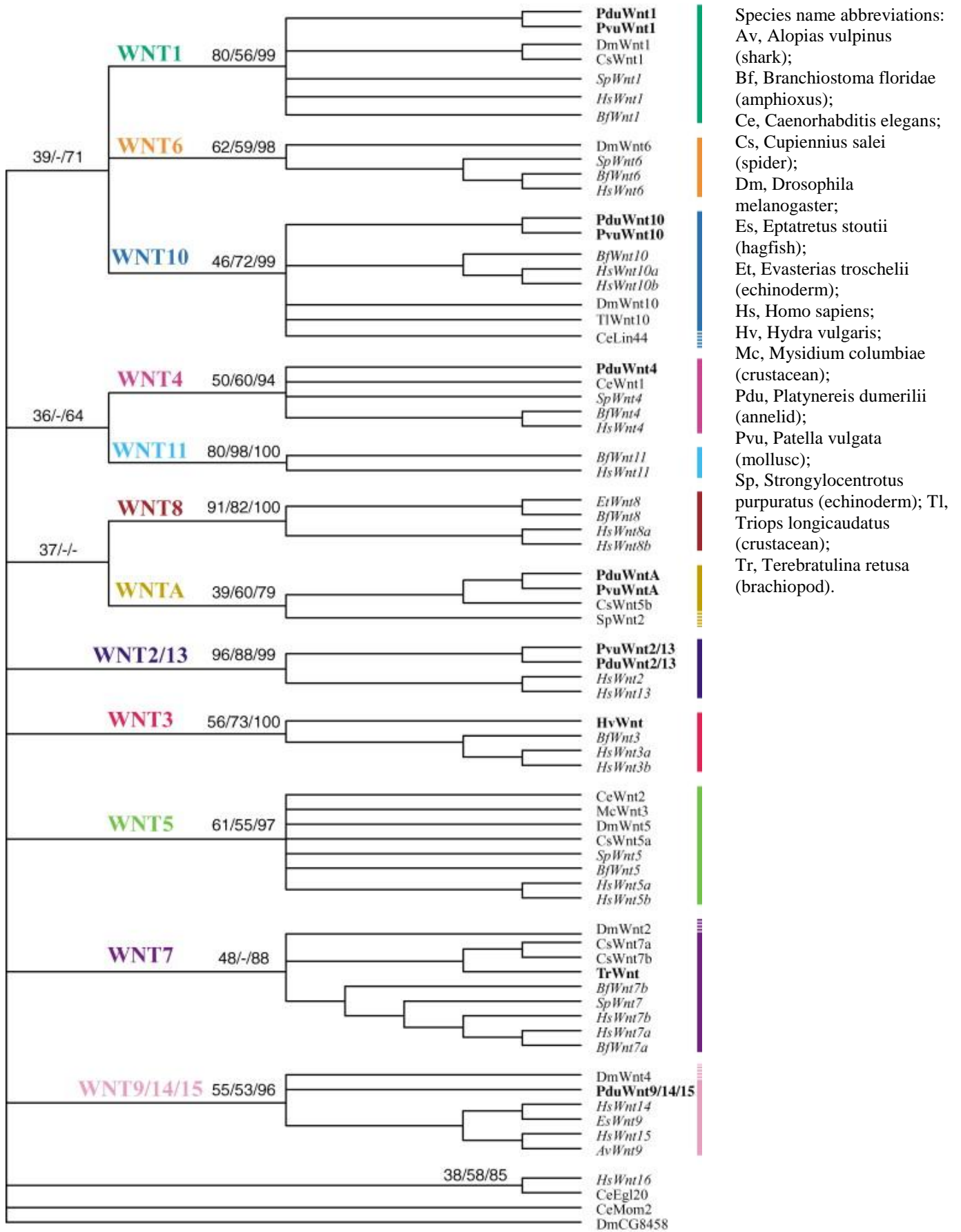


Figure 5: Phylogenetic tree of the Wnt family (adapted from Prud'homme et al. 2002)

ii) Phenotypes of Knockout Mice for Wnt factors

Loss of Wnt factors leads to severe phenotypes where various territories are affected. For example, loss of Wnt3 leads to gastrulation and neurogenesis defects. Loss of Wnt5 is associated to defects of morphogenesis and of formation of the reproductive apparatus. Loss of Wnt7 induces defects of the Central nervous system vascularization (Fig 6).

Gene	Phenotype of Knockouts Mouse or other functions	Associated diseases in Human
Wnt1	<ul style="list-style-type: none"> • Loss of midbrain and cerebellum • With Wnt3a deletion: reduction of number of neural precursors in the neural tube • With Wnt4 deletion: reduction of number of thymocytes 	
Wnt2	<ul style="list-style-type: none"> • Placental defects • With Wnt2b : defective lung development 	
Wnt2b/13	<ul style="list-style-type: none"> • Retinal cell differentiation defects • With Wnt2: defective lung development 	
Wnt3	<ul style="list-style-type: none"> • Early gastrulation defect • Hair growth defects • Apical ectodermal ridge defects • Medial-lateral retinotectal topography • Hippocampal neurogenesis defects 	<ul style="list-style-type: none"> • Tetra-Amelia
Wnt3a	<ul style="list-style-type: none"> • Somites, tailbud defects • With Wnt1: reduction in number of neural precursors in the neural tube together • Loss of hippocampus • Segmentation oscillation clock defects • Left right asymmetry • Hematopoetic stem cell self-renewal defects 	
Wnt4	<ul style="list-style-type: none"> • Kidney defects • Defects in female development due to absence Mullerian Duct, leading to ectopic testosterone synthesis • Side-branching in mammary gland • With Wnt1: decrease in the number of thymocytes • Repression of the migration of steroidogenic adrenal precursors into the gonad 	<ul style="list-style-type: none"> • Mullerian-duct regression and virilization • SERKAL syndrome
Wnt5a	<ul style="list-style-type: none"> • Truncated limbs and anteroposterior axis • Distal lung morphogenesis defects 	<ul style="list-style-type: none"> • Associated with Susceptibility to type

	<ul style="list-style-type: none"> • Longitudinal skeletal outgrowth • Female reproductive tract defects • Shortened and widened cochlea • Mammary gland defects • Prostate gland defects • Intestinal elongation defects • Required for endothelial differentiation of ES cells 	2 diabetes
Wnt5b		
Wnt6		
Wnt7a	<ul style="list-style-type: none"> • Limb polarity defects • Infertility due to lack of Mullerian duct regression • Delayed maturation of synapses in Cerebellum • Promotes neuronal differentiation • With Wnt7b: required for central nervous system vasculaturization and maturation 	<ul style="list-style-type: none"> • Fuhrmann syndrome
Wnt7b	<ul style="list-style-type: none"> • Placental development defects • Respiratory failure due to defects in mesenchymal proliferation, required for lung development • With Wnt7a: required for central nervous system vasculaturization and maturation • Determines cortico-medullary axis in the kidney 	
Wnt8a		
Wnt8b	<ul style="list-style-type: none"> • Changes in gene expression profile in neurons 	
Wnt9a	<ul style="list-style-type: none"> • Joint integrity defects 	
Wnt9b	<ul style="list-style-type: none"> • Regulates of mesenchymal/ epithelial transitions • Regulates renal vesicle induction • Planar cell polarity defects of the kidney 	
Wnt10a		<ul style="list-style-type: none"> • Odonto-onycho-dermal dysplasia
Wnt10b	<ul style="list-style-type: none"> • Decreased trabecular bone (Bennett 2005) and bone mass loss • Required for taste papilla development • Loss activates adipogenesis • Overexpression inhibits adipogenesis 	<ul style="list-style-type: none"> • Mutations in Obesity patients • Split-Hand/Foot Malformation
Wnt11	<ul style="list-style-type: none"> • Ureteric branching defects • Cardiogenesis defects 	
Wnt16		

Figure 6: List of Wnt genes (Wnt homepage, Stanford)

iii) Wnt3a (wingless-type MMTV integration site family, member 3A)

Wnt3a can bind Fzd1, Fzd2, Fzd4 and LRP6 directly. WIF1 and SFRP1 bind to Wnt3a and inhibit its activity (Dufourcq et al. 2008). Wnt3a is able to induce the canonical pathway by promoting caveolin-dependent internalization of LRP6/ Fzd after binding of LRP6 (Yamamoto et al. 2008).

iv) Wnt5a (wingless-type MMTV integration site family, member 5A)

Wnt5a can interact with Fzd1, Fzd2, Fzd4, Fzd7 or Ror2. Wnt5a can activate or inhibit canonical Wnt signaling, depending on receptor context. It can activate β – catenin signaling by inducing caveolin-mediated endocytosis of Fzd receptors or inhibit the canonical Wnt pathway by promoting clathrin-mediated endocytosis of Fzd / Ror2(Grumolato et al. 2010). Wnt5a is required during embryogenesis for extension of the primary anterior-posterior axis and for gastrulation.

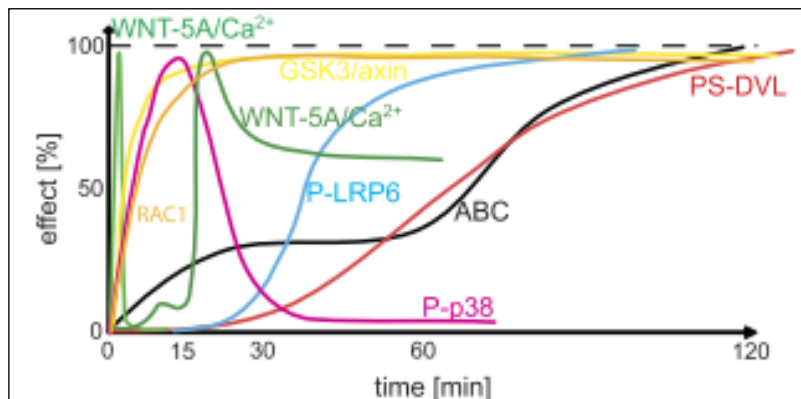


Figure 7: Schematic presentation of Wnt/ Fzd signaling kinetics (Schulte and Shenoy 2011)

Activation of β -catenin (active β -catenin - ABC, Fig 7, in black) or LRP6 (in blue) and interaction between GSK3 and Axin are induced by Wnt3a. Phosphorylation of Dvl or Rac1 (in red/ orange) is induced by Wnt3a or Wnt5a. Phosphorylation of mitogen activated protein kinase p-38 is induced by Wnt5a only, indicating that both proteins induce signal transduction via similar protein, leading to activation of different targets (Schulte et al. 2010, Schulte and Shenoy 2011).

c) Fzd receptors

i) Overview of the Frizzled protein family

‘Frizzled’ refers to the phenotype of the frizzled mutant in *Drosophila* that has irregular patterned and curled hairs on the thorax, wings, and feet (Bridges and Brehme, 1944). Frizzled receptors family is a family of G protein- that act as receptors in the Wnt signaling pathway. These proteins are formed of seven-transmembrane domains, an extracellular N terminus, and an intracellular C terminus domain. Their basic architecture is reminiscent of conventional G protein-coupled receptor. Phylogenetic analysis reveals that Fzd form 4 subfamilies indicating potential redundancy of function between Fzd1,2 and 7; Fzd 3 and 6; Fzd4,9 and 10 and between Fzd5 and 8 respectively (Fig 8).

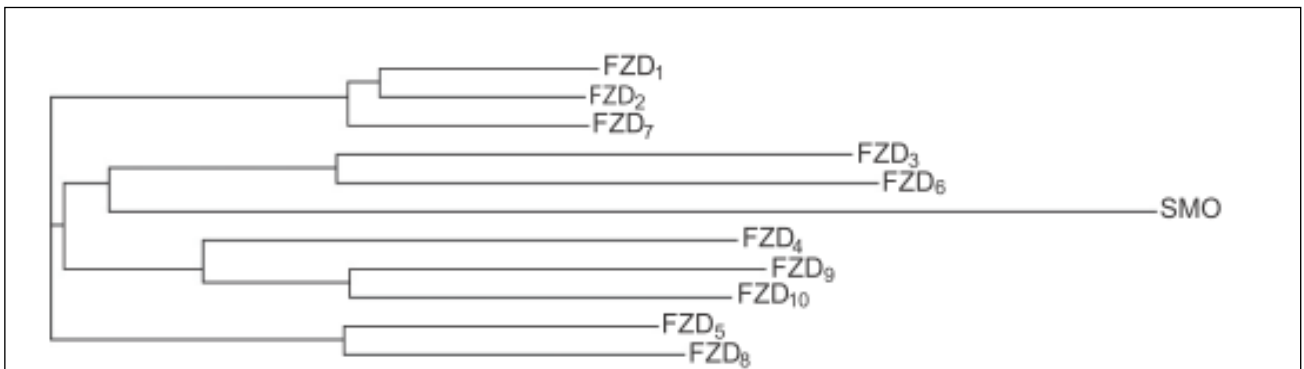


Figure 8: Phylogenetic tree of the human Frizzled receptors FZD (Schulte and Shenoy 2011)

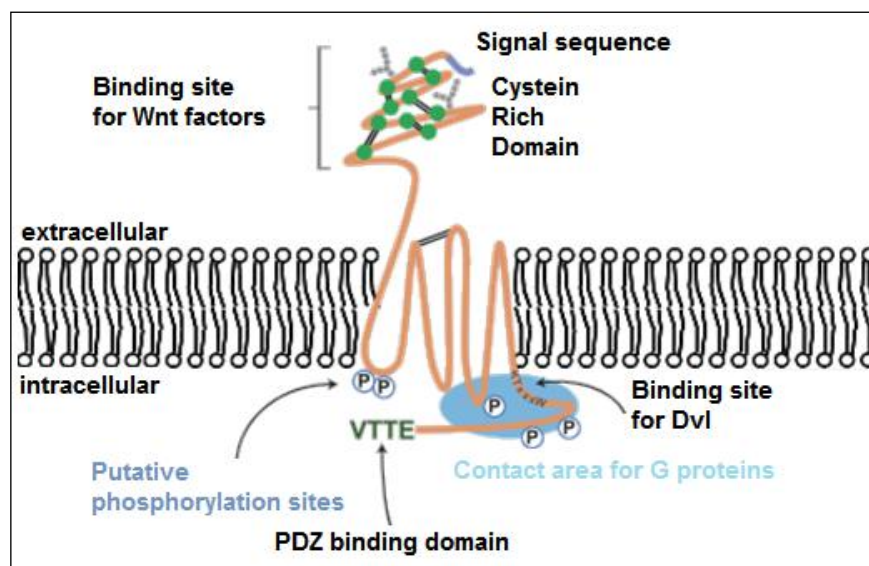


Figure 9: Schematic representation of Frizzled protein (binding sites for Dvl/ PDZ and G proteins indicated) (Schulte and Shenoy 2011)

The extracellular region (Fig 9) of all Frizzled receptors consists of an N-terminal signal sequence (amino acid 1 to 36 in human FZD4) that is important for the insertion of the protein in the membrane. This is followed by a cysteine-rich domain (CRD; aa 40–161 in hFZD 4), which constitutes the binding site for Wnt ligands and Norrin (Schulte 2010). It is also hypothesized that Fzd receptors could form dimers via the CRD domain. The Fzd dimers would be sufficient to activate Wnt/ β -catenin signaling. Homology analysis indicates that Fzds share only 20 to 40% of amino acid identity, but the ten cysteines that form the five disulfide bonds in the CRD domain are highly conserved between the Fzd isoforms, indicating a strong pressure of selection on these positions. The CRD domain is followed by seven transmembrane regions that form three intracellular loops, three extracellular loops, and a C-terminus of variable length. These intracellular domains are essential because they mediate various protein-protein interactions and post-translational processing through phosphorylation, ubiquitinylation, nitrosylation, or hydroxylation. The K-T-x-x-x-W domain that is very close to the membrane is highly conserved in the family. This sequence serves as the domain for interaction with the DEP domain of Disheveled. Additionally, Fzd proteins have an additional C-terminal typical PDZ binding domain for interaction with proteins such as PSD95 and with the PDZ domain of Dvl, this binding domain is conserved between most members of the family(Fig 10) (Schulte 2010)

Receptor	Chromosomal Location	Protein Length	Molecular Mass	Number of		C Terminus
				Transcripts	Exons	
		aa	kDa			
FZD ₁	7q21	647	71,158	1	1	ETTV (+)
FZD ₂	17q21.1	565	63,554	1	1	ETTV (+)
FZD ₃	8p21	666	76,263	1	8	GTSA (+)
FZD ₄	11q14.2	537	59,881	1	2	ETVV (+)
FZD ₅	2q33-q34	585	64,507	1	2	LSHV (+)
FZD ₆	8q22.3-q23.1	706	79,292	1	7	HSDT (-)
FZD ₇	2q33	574	63,620	1	1	ETAV (+)
FZD ₈	10p11.22	694	73,300	1	1	LSQV (+)
FZD ₉	7q11.23	591	64,466	1	1	PTHL (-)
FZD ₁₀	12q24.33	581	65,336	1	1	PTCV (+)
SMO	7q32.3	787	86,397	4	25	DSDF (+)

Figure 10: Conservation of the PDZ binding domain (TXV-COOH) in the Fzd family; functional and non functional PDZ binding domain is noted as (+) or (-) respectively (Schulte and Shenoy 2011)

ii) Phenotypes of Knockout Mice for Fzd receptors

Loss of Fzd receptors leads to severe phenotypes where various territories are affected. Current works indicate that Fzd4 would be the only Fzd receptor shown to be essential for angiogenesis in adult, while Fzd5 would be essential for placental angiogenesis.

Gene	Functions	Phenotype of Knockouts Mouse	Associated diseases
FZD1		<ul style="list-style-type: none"> • Viable 	
FZD2		<ul style="list-style-type: none"> • Viable 	
FZD3	<ul style="list-style-type: none"> • Activates PKC • Activates β-catenin 	<ul style="list-style-type: none"> • Defect in guidance of axons • With Fzd6: Midbrain morphogenesis defect 	
FZD4	<ul style="list-style-type: none"> • Activates PKC • Becomes internalized after adding Wnt5a • Activates Wnt reporter with norrin • Activates Wnt reporter with LRP5 	<ul style="list-style-type: none"> • Cerebellar, Auditory, and Esophageal Defects • Impaired Corpora Lutea Formation • Defects in vascular growth, endothelial defects • With Fzd8: Kidney phenotype 	<ul style="list-style-type: none"> • Retinal angiogenesis in familial exudative vitreoretinopathy
FZD5		<ul style="list-style-type: none"> • Essential for yolk sac and placental angiogenesis • Paneth cell phenotype • Neural potential in the developing <i>Xenopus</i> retina • Mammalian ocular development 	
FZD6	<ul style="list-style-type: none"> • Activates PKC 	<ul style="list-style-type: none"> • Hair patterning, tissue polarity • With Fzd3: Midbrain morphogenesis defect 	
FZD7		<ul style="list-style-type: none"> • Viable 	
FZD8	<ul style="list-style-type: none"> • Activates Wnt with Respondin 	<ul style="list-style-type: none"> • With Fzd4: Kidney phenotype 	
FZD9		<ul style="list-style-type: none"> • B cell development • Hippocampal defects 	
FZD10			

Figure 11: List of Frizzled receptors (Wnt homepage, Stanford)

iii) *Frizzled 4*

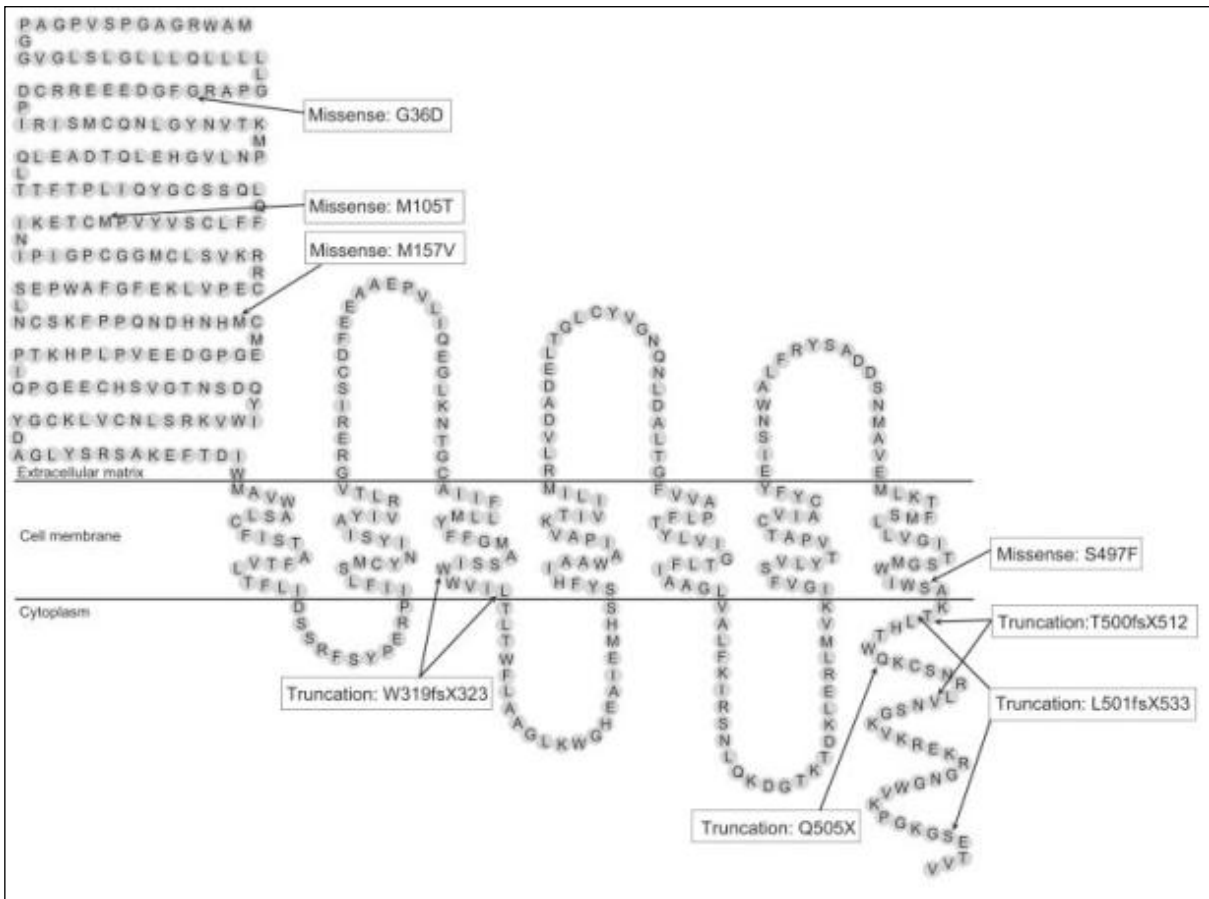


Figure 12: Diagram of Fzd-4 showing mutations associated to vitreoretinopathy (Robitaille et al. 2002, Robitaille et al. 2011)

Fzd4 is the only representative of frizzled family members that binds an additional ligand Norrin structurally different from Wnt ligands. Fzd4 and Norrin are major regulators of the vascular development of vertebrate retina. Mutations in the *frizzled-4* gene have been notably associated with autosomal dominant familial exudative vitreoretinopathy (Robitaille et al. 2002). The main process in the disease is the destabilization of retinal vessels, causing retinal ischemia. Abnormal vessels then develop at the edges of the ischemic retina causing subretinal exudation and formation of scar tissue that produces tractional forces on the retina, leading to retinal detachment. The disease appeared to be linked with missense mutations of Fzd4 coding gene in the region coding for the CRD domain or truncation mutations in the internal domains (Nikopoulos et al. 2010), indicating that these domains are essential for the function of the protein (Fig 12). In 2004, Xu et al. indicated that vascular defects in *fzd4* and *Norrin* (Ndp) mutant mice were very similar. By showing that interaction between Fzd4 and Norrin was

specific and that FEVR-Associated Fz4 mutants bind Norrin but were unable to transduce signal, they were able to place Norrin as one of the activator of Fzd4 during retinal vascularization(Xu et al. 2004). Furthermore, Ye et al found that endothelial specific deletion of fzd4 lead to retardation of vascular development of the retina, reduction in retinal capillaries and alteration of vessels of the vitreal surface that penetrate the retina that formed end in ball-like structures (Ye et al. 2010). Inhibition of Fzd4 using a blocking antibody would also lead to abnormal vascularization of the retina (Paes et al. 2011), confirming the role of the protein in the process of retinal vaculature. Fzd4 is also important in other organs. Loss of Fzd4 is also associated to cerebellar, auditory, and esophageal dysfunction (Wang et al. 2001). In a similar manner, it was demonstrated recently that Fz4 is required for blood barrier maintenance and plasticity in the central nervous system, as loss of Fzd4 leads to leakage in the cerebellum (Wang et al. 2012). These evidence shows that Fzd4 is vital for angiogenesis. That's why our laboratory has focused part of its research on this protein.

d) Coreceptors of Fzd proteins

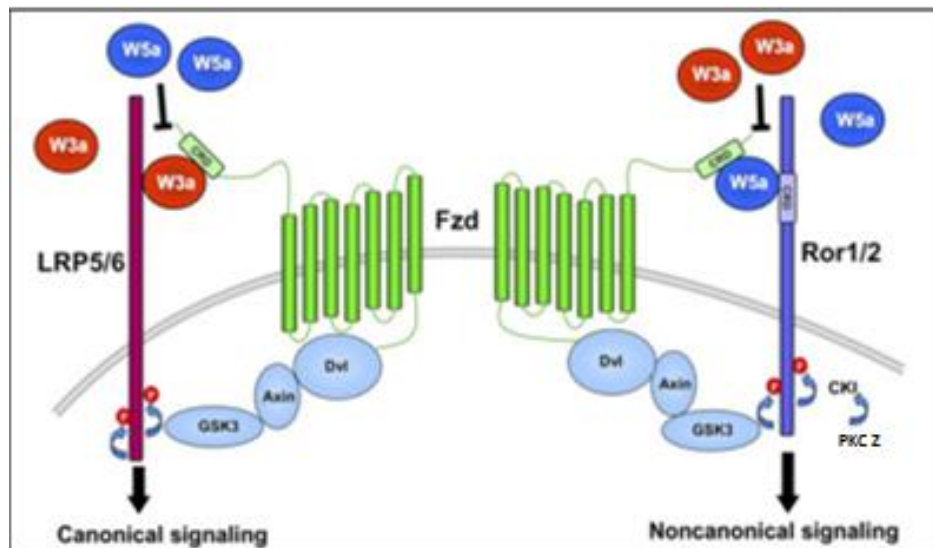


Figure 13: Competition between Wnt ligands would regulate activation of Wnt pathways by modulating phosphorylation of LRP5/6 and Ror2 (adapted from Grumolato et al 2010)

Wnt factors can activate the canonical and non canonical Wnt pathways through common mechanisms. Canonical Wnt3a and non canonical Wnt5a ligands bind Fzd receptor and recruit the same components. However, canonical Wnt ligands would induce phosphorylation of the Fzd receptor LRP5/6, while non canonical ligands would induce phosphorylation of the Fzd coreceptor Ror2 (Ser864) (Liu et al. 2008). Interestingly, it was shown more recently that canonical and noncanonical Wnts ligands inhibit each other by competing for Fzd binding at the cell surface leading to this differential phosphorylation of Ror2 and LRP5/6 (Grumolato et al. 2010) (Fig 13).

i) *LRP5/6*

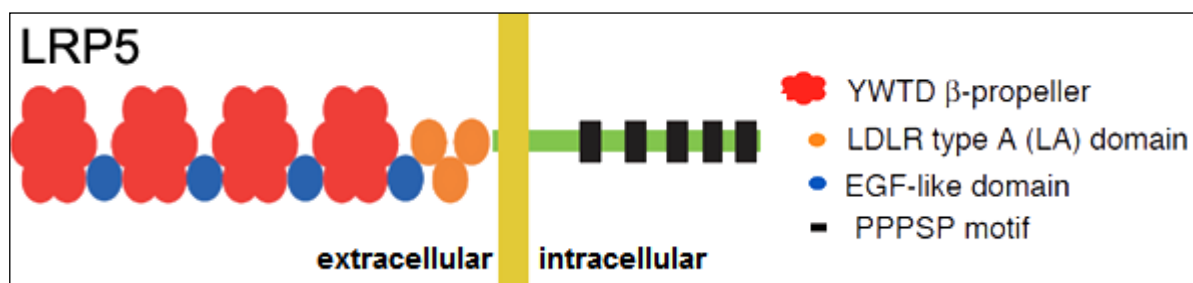


Figure 14: Structure of LRP5 (He et al 2005)

LRP5 and 6 are highly homologous proteins. LRP5 contains a large extracellular domain containing four beta-propeller motifs and four epidermal growth factor-like repeats that form the binding sites for extracellular ligands. These domains are followed by three LDLR type A domains. The intracellular domain of LRP5 contains 5 PPPSP motifs. These motifs are phosphorylated upon binding of Wnt ligands and lead to binding of Ror2 to Axin, leading to activation of the canonical pathway (Grumolato et al. 2010). Zeng et al proposed a similar model in which Wnt-induced Fz-Lrp5/6 complex formation would lead to recruitment of the axin-Gsk3 complex, Gsk3 would then induce Lrp5/6 phosphorylation to initiate B-catenin signaling (Zeng et al. 2008). Interestingly, the phosphorylated forms of LRP5/6 have been shown to be internalized in clathrin-dependant vesicles with Dvl/ Fzd upon activation of the Wnt pathway, suggesting that LRP5/6 has a role for signal transduction that initiate in the early endosome (Bilic et al. 2007, Yamamoto et al. 2008). LRP5/6 is essential for angiogenesis as loss of the protein can also cause familial exudative vitreoretinopathy in humans, independently of loss of Fzd4 or Norrin

(Toomes et al. 2004). As LRP5 knockout mice display incomplete vasculature in the deeper plexus of the retina while FZD4 and Norrin knockout mice develop severe defects in both the superficial and deep plexus of the retina, Xia et al hypothesised that LRP5 would mediate Wnt signaling in Muller cells present in the deep plexus to regulate vascularization of this layer of the retina (Xia 2010). This demonstration correlates with recent findings showing that Wnt signaling is the main signaling pathway implicated in the formation of the deep retinal plexus.

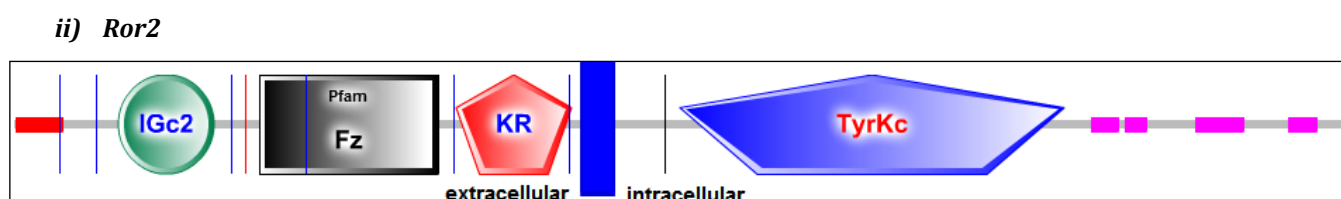


Figure 15: Structure of the Ror2 protein (adapted from Scopus)

ROR2 is a member of the receptor tyrosine kinase-like orphan receptor (ROR) family. The protein is composed of an extracellular part composed of an Immunoglobulin C-2 Type domain, a Fzd domain and a Kringle domain. The Fzd domain would be essential for binding of Wnt ligands, while function of the immunoglobulin and Kringle domain are unknown. Interestingly, the tyrosine kinase domain of Ror2 is functional. The tyrosine kinase activity would be essential for signal transduction in the non canonical pathway, as activation of c-Jun/ Dishevelled would be dependant on this activity, but no targets have been found yet (Mikels et al. 2009, Ford et al. 2013). Ror2 is phosphorylated on serine/threonine residues in its c-Terminal cystein rich domain upon stimulation of cultured cells with Wnt5a, but not with Wnt3a. Phosphorylation of Ror2 would be GSK3 dependant as blockade of GSK3 would block Ror2 induced migration of endothelial cells (Yamamoto et al. 2007). Phosphorylation of Ror2 on this domain would depend on various kinases such as Casein Kinase 1- ϵ (CKI ϵ) or Phosphokinase C ζ (PKC- ζ). Casein Kinase 1 would be directly responsible for phosphorylation of Ror2 while PKC- ζ would activate kinases upstream of Casein Kinase 1 (Kani et al. 2004). Interestingly, use of the PKC- ζ pseudosubstrate that blocks the kinase activity of PKC- ζ blocks the phosphorylation of Ror2 and the

activation of non canonical Wnt pathway (Nomachi et al. 2008). Using the PKC- ζ pseudosubstrate and *ror2* targeting siRNA, it was shown that Ror2 activity was essential for formation of the lamellipodia and reorientation of microtubule-organizing center in Wnt5a-induced cell migration. The proposed model is that Ror2 would associate with the actin-binding protein filamin A to regulate reorganization of the actin cytoskeleton to induce migration of endothelial cell; and would be required for c-Jun / JNK activation that is essential for activation of the small GTPases Rho and Rac (Nomachi et al. 2008).

iii) *Ryk*

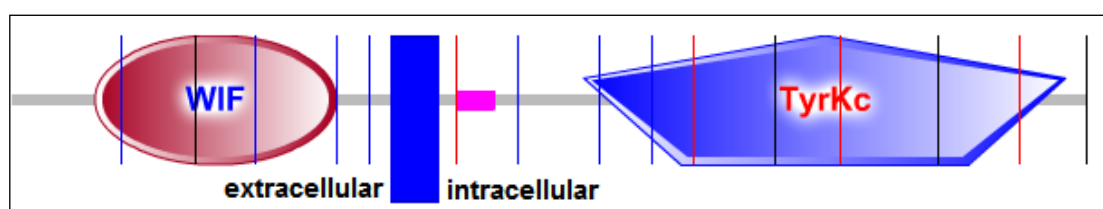


Figure 16: Structure of the Ryk protein (adapted from Scopus)

Ryk is an atypical member of the family of growth factor receptor protein tyrosine kinases, whose activity is not regulated by phosphorylation. The protein has a leucine-rich extracellular domain with a WIF-type Wnt binding region, a single transmembrane domain, and an intracellular tyrosine kinase domain. This protein is involved in stimulating Wnt signaling in processes such as the regulation of axon pathfinding. Ryk functions as a coreceptor with Fzd and binds Dvl to activate the canonical Wnt pathway (Lu et al. 2004). More recently, it was shown that the E3 ubiquitin ligase Mindbomb1 would reduce cell surface levels of Ryk leading to activation of the Wnt canonical pathway, indicating that Ryk would activate the non canonical pathway (Berndt et al. 2011).

e) Downstream effectors of Wnt signaling

i) *Dishevelled adaptor proteins*

Dvl is the cytoplasmic link between Frizzled and downstream components of the Wnt signaling pathway. Dvl has no known enzymatic activity and functions as a scaffold protein bridging the receptors and downstream signaling components.

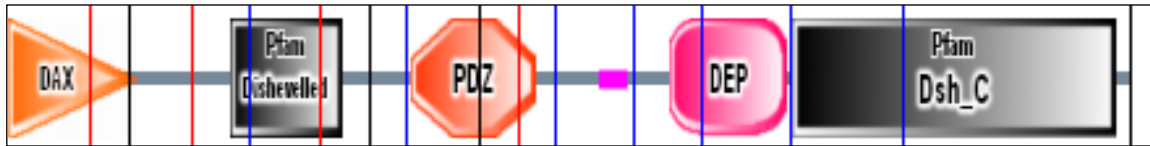


Figure 17: Structure of Dvl (adapted from Scopus)

The DIX domain is essential for β -catenin activation, the DEP domain is implicated in the activation of the non canonical pathway, while the PDZ domain is required for both. Dvl can bind Axin2 via its DIX domain – blocking Axin-induced degradation of β -catenin (Fiedler et al. 2011). The PDZ domain is required for the interaction with the C-terminal regions of Vangl1 and 2. Dvl interacts with Fzd4 (Chen et al. 2003) via both the PDZ and DEP domains (Fig 17). In presence of Wnt5a, cytoplasmic Dvl is recruited to the membrane via endocytic vesicles where it is phosphorylated (Bryja et al. 2007). Human and murine orthologues share more than 95% sequence identity and are each 40-50% identical to *Drosophila* Dvl where a single member of the family is found. Sequence similarity is concentrated around the DIX domain, the PDZ domain and the DEP domain, indicating that the three domains are essential. Three members of the Dishevelled family exist in mammals (Dvl-1 to 3). Dvl2 is strongly expressed in majority of mammalian cells, while levels of Dvl1 and 3 are much lower. Dvl1 and 3 play the major role for the activation of both Wnt pathways. The three Dvl isoforms are essential during development as knock-out of Dvl2 or 3 leads to cardiovascular defects while the knock-out mouse for Dvl1 and 2 presents an open neural tube, a characteristic of knock-out mice of genes implicated in the Wnt/PCP pathway (Wang et al. 2006).

Gene	Functions	Phenotype of knockouts mouse	Associated diseases in human
Dvl1	<ul style="list-style-type: none"> Activates Wnt canonical and calcic pathway Overexpression leads to cardiac hypertrophy and is rescued by inhibition of CamKII 	<ul style="list-style-type: none"> Social interaction and sensorimotor gating abnormalities With Dvl2: Open neural tube With Dvl2: Convergent extension phenotype 	Activity of LRRK2 that is mutated in Parkinson is regulated by Dvl1/2/3
Dvl2		<ul style="list-style-type: none"> Cardiovascular outflow tract defect. With dvl1:open neural tube With dvl1: convergent extension phenotype 	
Dvl3	<ul style="list-style-type: none"> Activates canonical and PCP pathway 	<ul style="list-style-type: none"> Cardiac outflow tract defects 	

Figure 18: List of Dvl proteins (adapted from Wnt homepage, Stanford)

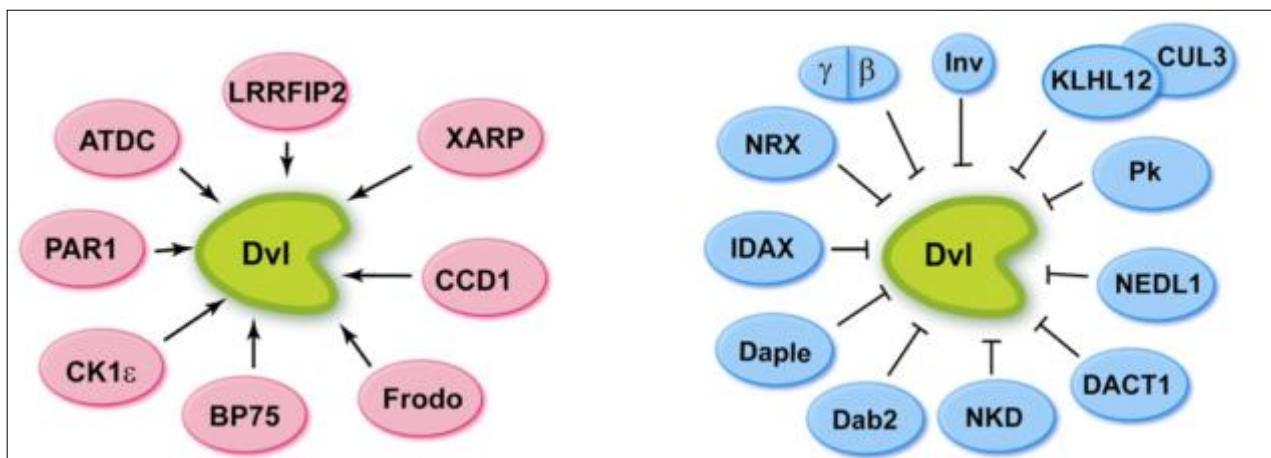


Figure 19: Positive (left) and negative (right) regulators of Dvl activity (Gao et al 2010)

Dvl is phosphorylated upon activation of the Wnt pathways by Casein kinase 1- ϵ , or PAR-1 depending on context (Tian-Qiang Sun and Williams 2001, Bryja et al. 2007). Several proteins have been reported to regulate stability of Dvl by facilitating its poly-ubiquitination and/or degradation. The HECT-type ubiquitin ligase NEDL1 induces degradation of Dvl1. KHL12 recruits the ubiquitin complex Cullin-3 to Dvl, causing its degradation. Prickle 1 also negatively regulates the Wnt/PCP pathway by enhancing Dvl3 degradation (Gao and Chen 2010).

ii) β -catenin

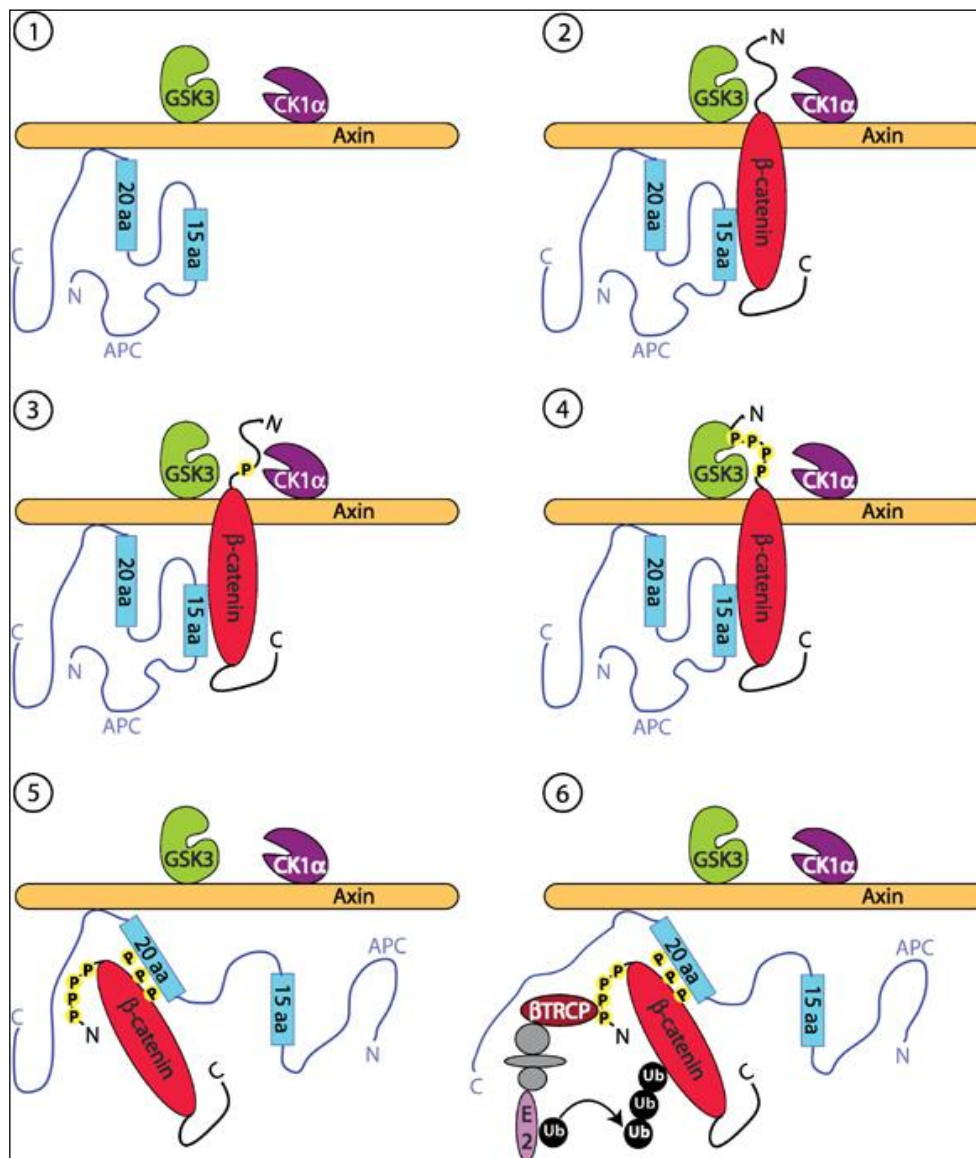


Figure 20: The β -catenin destruction complex (Kimelman and Xu 2006)

β -catenin, protein composed of armadillo repeats was first identified as a scaffold protein and is one of the key components of the canonical Wnt signaling pathway. In the absence of the Wnt signal, β – catenin levels are down-regulated by a complex, composed of Axin/ CKI- α (casein kinase 1- α) / APC(Adenomatous Polyposis Coli) and GSK-3 β (glycogen synthase kinase 3) (Fig20 – 1). Axin and APC act as scaffold protein bringing GSK3 and its substrate (β -catenin) into close physical proximity (Fig 20 – 2and3). This positions the N-terminus of β -catenin near CK1 and GSK3. CK1 phosphorylates β -catenin at Ser45 and GSK3 phosphorylates β -catenin at Thr41, Ser37 and Ser33 (Fig20 – 3and4). The

E3 ubiquitin ligase β -TRCP1 then binds the phosphorylated N-terminus of β -catenin, causing its degradation (Fig 20- 6). Transcription of β -catenin target genes is then repressed as the transcription factors LEF/TCF form a complex with groucho, inducing histone deacetylation of the target genes of β -catenin (Saadeddin et al. 2009). In the presence of Wnt ligand, Fzd recruits Dvl which in turn brings to the membrane the axin–GSK3 complex that promotes phosphorylation of LRP5/6 by GSK3 and CK1 (Zeng et al. 2008). Phosphorylated LRP5/6 leads to inhibition of GSK3/Axin/APC complex; β -catenin is not ubiquitinated and is dephosphorylated by cadherin 2 on Ser37 or Thr41. This active form of β -catenin translocates to the nucleus where it complexes with transcription factors LEF/ TCF to favor transcription of genes such as Cyclin D (Sadot E et al. 2002). The membrane bound β -catenin has a different function. It is part of a complex of proteins that constitute adherens junctions by interacting with Ve-cadherin. Therefore, it is also implicated in processes of adhesion and permeability. Mutations in the gene coding for β -catenin are a cause of colorectal cancer, pilomatrixoma, medulloblastoma, and ovarian cancer. β catenin is typically a protein that can localize to Nuclear and Adhesion Complex (NACos)(Balda 2003) that stabilizes junctions when located at the adherens junction and act as pro-proliferative transcription factor when located to the nucleus.

iii) C-JUN

c-Jun is a transcription factor of the MAPK family composed of a basic region leucine zipper domain, that recognizes and binds to the enhancer heptamer motif 5'-TGA[CG]TCA-3'. It is part of the SMAD3/ SMAD4/ JUN/ FOS complex which forms at the AP1 promoter site. The SMAD3/SMAD4 heterodimer acts synergistically with the JUN/FOS heterodimer to activate transcription in response to Wnt signaling. C-Jun is phosphorylated by CAMK4, PRKCD, DYRK2 or HIPK2 and notably at Ser-63 by PLK3 upon Wnt5a activation, leading to increase of its DNA-binding activity. The phosphorylation of c-Jun at this site will be used as an indicator of the activation of the Wnt non canonical pathway in this work. C-Jun is also phosphorylated at Thr-239, Ser-243 and Ser-249 by GSK3 β ; reducing its ability to bind DNA (Wong et al. 2004, Gan et al. 2008, Saadeddin et al. 2009). Various works have shown a role of c-Jun in development and specifically in vascular development. *Jun*-null mice die between

midgestation and late gestation and exhibit impaired hepatogenesis, altered fetal liver erythropoiesis, and generalized edema (Hilberg et al. 1993), indicating an essential function of Jun in hepatogenesis and vascular permeability. Jun is also essential for placental and yolk sac vascularization (Schorpp-Kistner 1999, Schreiber 2000). Behrens et al. 1999 demonstrated that phosphorylation of Jun on ser63 is required for apoptosis. Jun can induce oncogenic transformation and was also found to be highly expressed in breast cancers (Johnson et al. 1999). Jun is also one of the first proteins to be upregulated after stroke, when the blood brain barrier is disrupted (McColl et al. 2008).

iv) RhoA

The small guanosine triphosphatase (GTP) Ras homolog family member A (Rho A) is a major regulator of actin remodeling during cell morphogenesis and motility. Rho activates its effector ROCK1, which phosphorylates and activates LIM kinase, which in turn, phosphorylates cofilin, inhibiting its actin-depolymerizing activity (Maekawa et al 1999). RhoA was shown to be implicated in migration as exoenzyme C3, a Rho inhibitor, inhibits corneal epithelial migration (Nakamura et al 2001). Pertz et al (2006) used a fluorescent biosensor to visualize the spatiotemporal dynamics of RhoA activity during cell migration. In randomly migrating cells, RhoA activity is concentrated at the leading edge while PDGF-induced membrane protrusions have low RhoA activity, potentially because PDGF strongly activates Rac, which had been shown to antagonize RhoA activity, showing that different stimuli induce distinct patterns of signaling during migration. Many elements link RhoA to Wnt signaling. Binding of DAAM1 to Dvl and the small GTPase Rho has been shown to coordinate Wnt signaling cues (Habas et al 2001), while the RhoGEF p114 was shown to transduce Wnt signaling, leading to RhoA activation (Tsuji et al. 2010). These elements place RhoA directly downstream of Wnt/PCP signaling.

2) *Wnt* signaling as a regulator of vascular development

a) *Wnt* signaling is implicated in angiogenesis during development and in pathology

i) *During embryonic development*

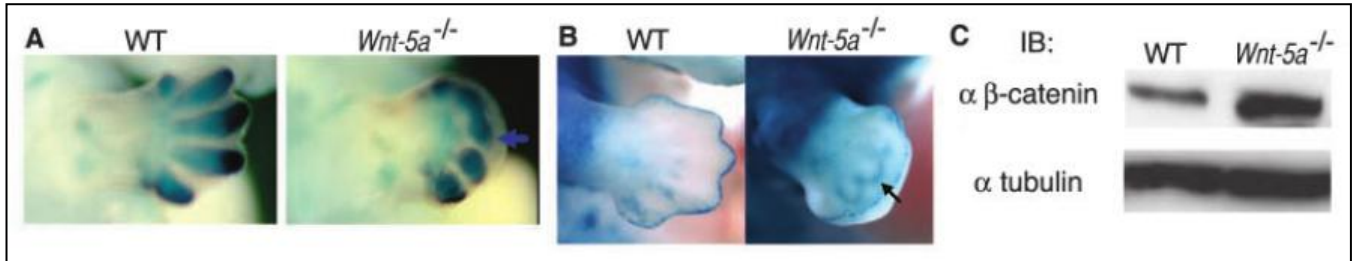


Figure 21: Canonical *Wnt* signaling is up-regulated after *Wnt5a* KO (Topol et al 2003)

Wnt-5a is strongly expressed in the limb bud during development and its expression gradually fades (Yamaguchi et al., 1999). In the *Wnt-5a* KO embryos, the fingers are missing, due to massive activation of the canonical pathway, detected as an increase of β-catenin protein level, indicating that *Wnt-5a* would regulate the balance between the *Wnt* pathways (Fig 21) (Topol et al. 2003).

❖ *Yolk sac and placenta vascularization*

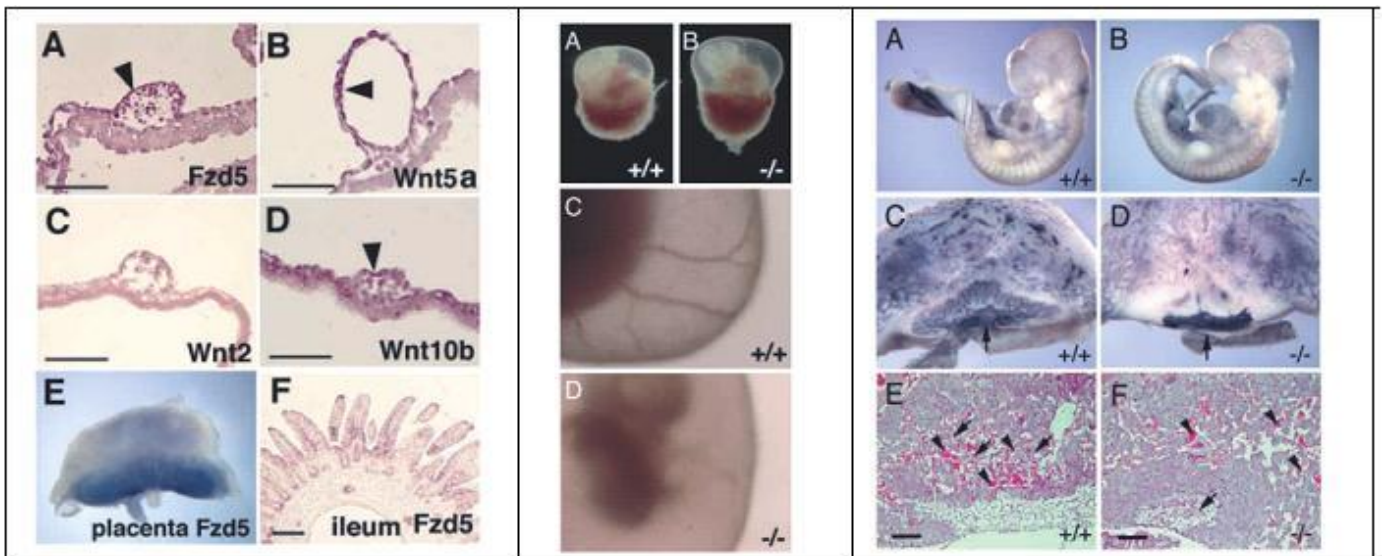
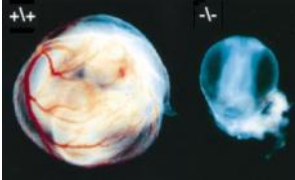


Figure 22: a- Expression of various components of *Wnt* signaling in placenta and yolk sac; b- Vascular pattern is normal in *Fzd5*^{-/-} embryo but vasculature remains superficial in placenta/ yolk sac of *Fzd5*^{-/-} embryos (Tomo et al 2001).

Wnt signaling is also important for sac yolk angiogenesis. Yolk sac angiogenesis occurs between E8.5 and E10.5. *Fzd5* is strongly expressed in vessels of the yolk sac at E9.5 (Fig 22a) and *Fzd5*^{-/-} embryo die in utero around E10.5, due to defects in yolk sac angiogenesis, as indicated by a poorly developed vascular bed when compared to Wt mice (Fig 22b). Vasculogenesis in the placenta is also defective as embryonic vessels do not invade the placental labyrinth in *Fzd5*^{-/-} mouse (Fig 22c). Because *Wnt5a* and *Wnt10b* co-localize with *Fzd5* in the developing yolk sac, these two Wnts are likely physiological ligands for *Fzd5*-dependent signaling for endothelial growth in the yolk sac (Fig 22a) (Tomo-o Ishikawa and Shin-ichi Nishikawa 2001).



Defects	E7.5 (7)	E8.5 (12)	E9.5 (13)
Retarded in growth and development ^b	57% (4)	83% (10)	85% (11)
Giant cells accumulated at the antimesometrial pole	43% (3)	25% (3)	–
Abnormal peri-vitelline meshwork	43% (3)	58% (7)	69% (9)
Abnormal yolk sac	–	61% (8)	–
Non-vascularized labyrinth	–	–	100% (3)

Figure 23: a- The yolk sac of the *junB* KO embryo at E9.5 is translucent and shows no vessels; b- Morphological phenotypes of *JunB* deficient embryos (Schorpp-Kistner 1999).

Interestingly, the non canonical pathway is essential for yolk sac angiogenesis as deletion of *jun* or other members of the AP1 pathway such as *c-Fos* lead to vascular defects of the yolk sac and placenta leading to growth retardation of the embryo as from E7.5dpc (Schorpp-Kistner 1999, Schreiber 2000). This body of evidence shows that the PCP pathway is required for angiogenesis in the placenta and yolk sac, implying that the pathway is essential for embryonic development.

❖ *Brain vascularization*

Vascularization of the central nervous system starts at embryonic day 9 via angiogenesis from a previously developed primitive vascular plexus (Paolinelli et al. 2011). The newly formed vessels acquire specific characteristics in the brain as they establish unique barrier characteristics called blood–brain barrier. The blood brain barrier (BBB) has a protective role as it prevents the flow of molecules from the blood to the tissue via expression of tight junction proteins that seal the space between endothelial cells.

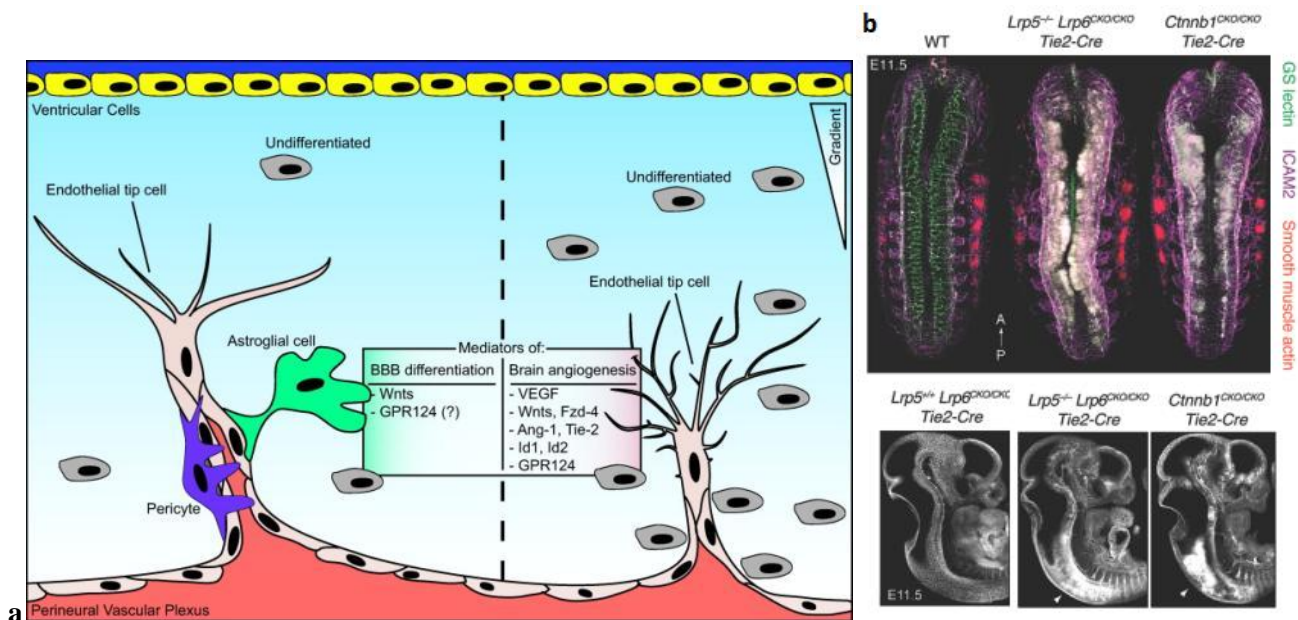


Figure 24: a- Wnts and Fzd4 are mediators of Brain angiogenesis (right) and differentiation of the Blood brain barrier (left) (Paolinelli et al 2011); **b-** Lrp5/6 and b-catenin are also essential for vessel formation in the hindbrain as KD of both proteins lead to vascular leakage (in white) (Zhou et al. 2014)

During development of the brain vasculature, vascular sprouts migrate towards a gradient of growth factors such as VEGF or Wnt proteins. The ligands Wnt7a and Wnt7b are expressed by neural progenitor cells in the spinal cord and forebrain. Inactivation of both ligands causes defects in brain angiogenesis due to reduced migration of ECs and loss of the BBB function, indicating that communication between neurons and ECs occur via Wnt7 (Liebner et al. 2008). The receptor Fzd4 is also present in endothelial progenitors (Kuhnert et al., Science, 2013) (Fig 24, right). Interestingly, loss of *Fzd4* results in loss of blood brain barrier function, as *Fzd4* deficient ECs are not able to maintain integrity of their tight junctions (Wang et al. 2012). Endothelial specific inactivation of β -catenin also leads to vascular leakage in the embryonic brain (Liebner et al. 2008). The proposed model by the group of Liebner is that activation of the canonical pathway would activate transcription of claudin 3 and PDGF β . These proteins are required for formation of tight junctions and recruitment of pericytes respectively. Both processes are required for induce vessel stabilization during brain development (Fig24, left) (Reis and Liebner 2013).

ii) ***In adult: Retinal vascularization***

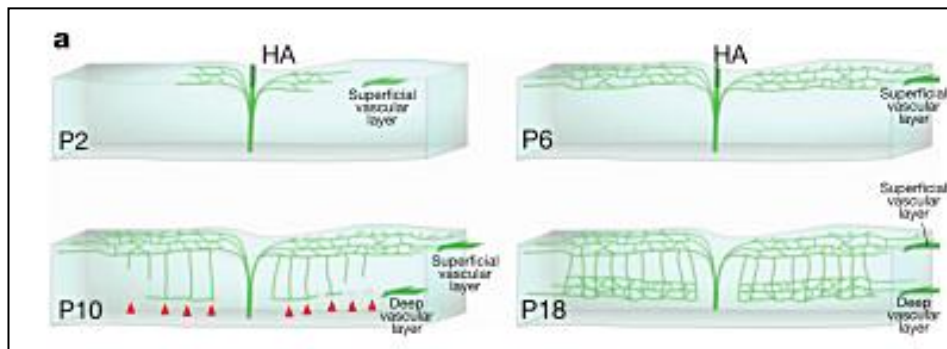


Figure 25: Schematic of retina during its vascularization; the superficial plexus is formed between P2 and P6; the intermediate and deep plexus between P10 and P18 (Franco et al 2009)

The retinal vasculature is formed between day 0 and day 21 after birth in mice. The superficial plexus is formed first between day 0 and day 6, the deep plexus and intermediate plexus linking the deep and superficial plexus are formed between day 6 and day 21 (Fig25). Endothelial tip cells are present at the leading edge of the superficial plexus and present filopodia that invade the retina by responding to VEGF or Wnt ligands. The gene expression profile of tip cells shows up-regulation of proteins such as caveolin1 and Fzd7, indicating implication of Wnt signaling in their activity (Fruttiger 2007, Franco et al. 2009).

❖ ***Role of Fzd4 in retinal vascularization***

Knock –out mice for the secreted protein *Norrin* or *Fzd4* present severe retardation of the retinal vascularization; both the superficial and deep plexus were massively impacted by the deletions (Robitaille et al. 2002). As this phenotype is extreme and makes it unclear what the function of Fzd4 is, Paes et al. proposed a model using a monoclonal antibody that neutralizes Fzd4 function, making it possible to study impact of Fzd4 deletion at various time-points during development or in pathogenesis.

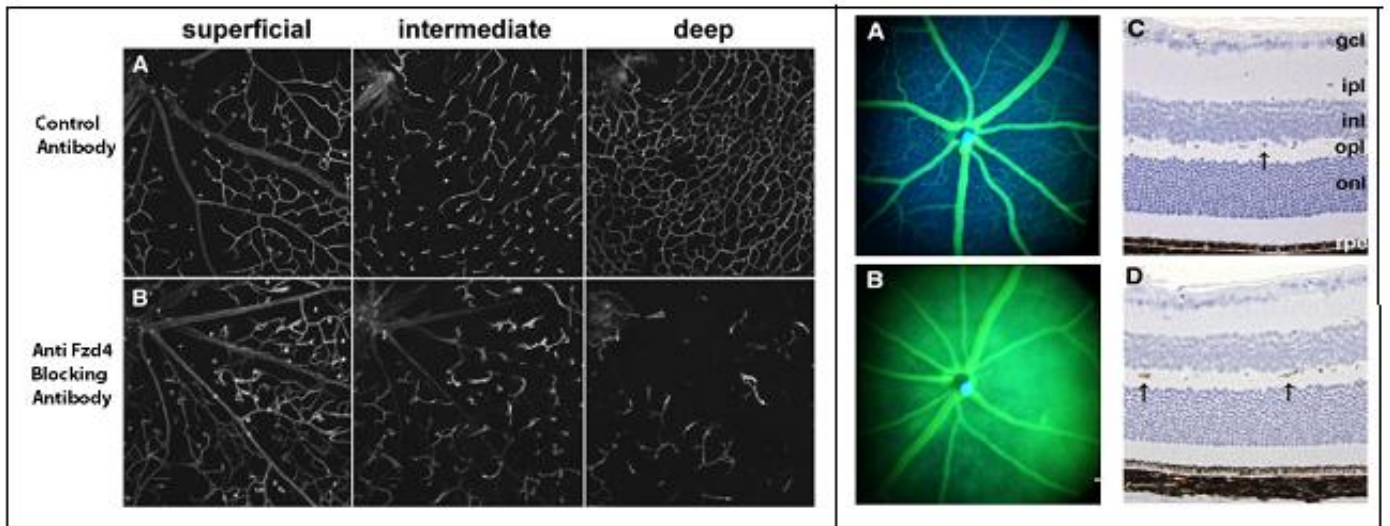


Figure 26: a- Neutralizing Fzd4 alters development of the intermediate and deep plexus; b- leading to leakage as shown by fluorescein extravasation and PLVAP expression (Ye et al 2010)

Inhibition of Fzd4 by injection of the blocking antibody during retinal vascularization alters retinal vascularization in the superficial and deep plexus (Fig 26a). After injection, the deep plexus is incomplete and the intermediate plexus that bridges the other plexus is disorganized, while the superficial plexus is less impacted. Administration of the antibody also induced extravasation of fluorescein through the blood-retina barrier, indicating that loss of Fzd4 makes the blood–retinal barrier more permeable (Fig 26b). The injection of the antibody also induced expression of PLVAP, a protein normally associated with fenestrated / immature endothelium (Fig 26b) (Paes et al. 2011). This indicates that Fzd4 is essential for acquisition and maintenance of the ‘blood retinal barrier’ integrity but also for formation of the intermediate and deep plexus. These findings echo the work done by Xia et al 2010 that showed that deletion of the coreceptor of Fzd4, *Lrp5* induced disorganization of the deep plexus of the retina. This indicates that the Fzd4/LRP5 complex is important for formation of this plexus.

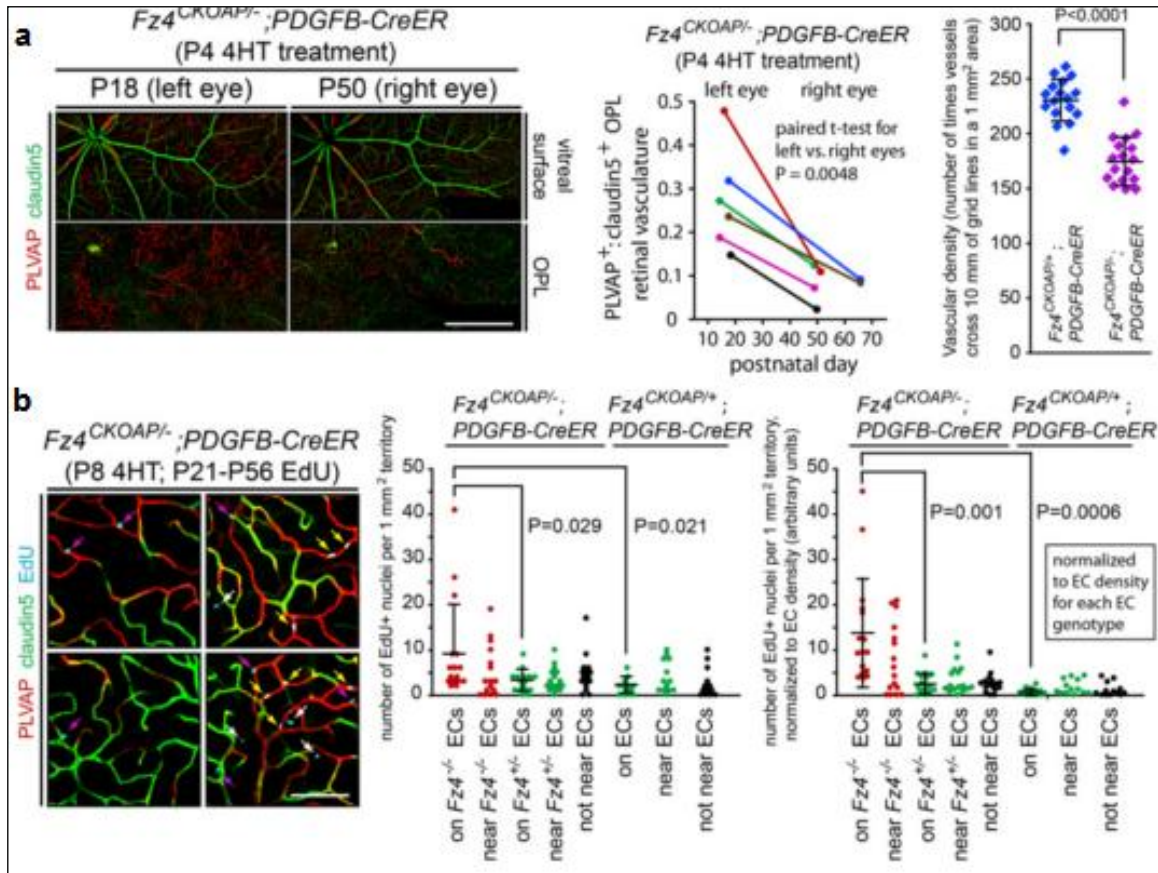


Figure 27: a - *Fzd4* deletion leads to expression of PLVAP; the cells expressing PLVAP are progressively lost, indicating that endothelial cells deleted for *Fzd4* are eliminated; b - Proliferation is increased in *Fzd4*^{-/-} cells as indicated by Edu staining.

More recently, Wang et al showed that in a mosaic mouse model, deletion of *Fzd4* in retinal endothelial cells lead to expression of PLVAP, a protein normally expressed in fenestrated endothelium (Fig 27a). The cells deficient for *FZD4* are progressively eliminated during development as PLVAP positive endothelial cells are lost in mosaic retinas. To determine whether the progressive loss of *Fz4* deficient ECs in the mosaic retina is associated with a reduction of a proliferation, the mosaic mice were injected with EdU. Interestingly, EdU positive nuclei were substantially enriched on *Fz4*^{-/-} ECs, indicating that proliferation is indeed increased in *Fzd4*^{-/-} cells (Fig 27b), suggesting that *Fzd4* deletion activates the pro-proliferative canonical Wnt pathway. The proposed model would be that *Fz4* deficient ECs lose their capacity to maintain the integrity of the blood retinal barrier and would be selectively eliminated, independently of their high level of proliferation (Wang et al. 2012).

❖ *Role of myeloid cells*

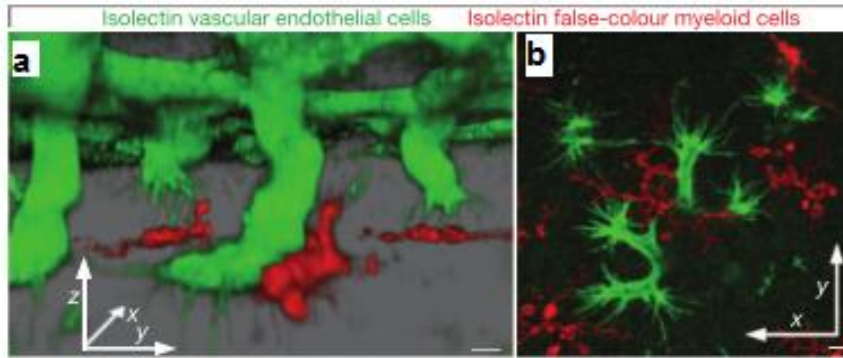


Figure 28: Retinal myeloid cells (in red) interact with descending vertical sprouts (in green)

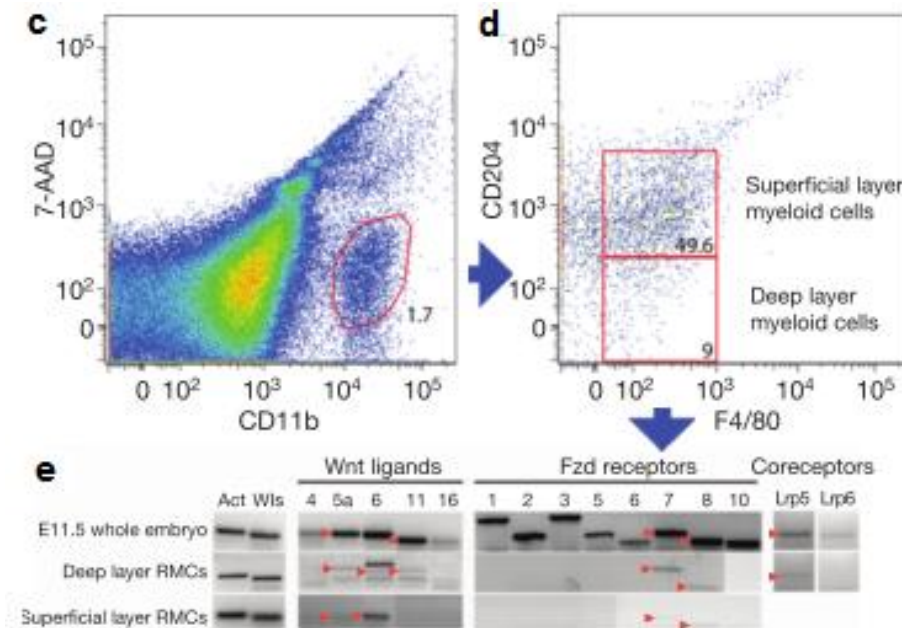


Figure 29: Retinal myeloid cells flow sorted from the deep plexus are subjected to PCR for Wnt pathway components (Stefater, Lewkowich et al. 2011)

An additional study demonstrated that Wnt factors control vessel formation in the deep retinal plexus. It was shown that the myeloid cells of the deep plexus produce Wnt ligands such as Wnt5a and Wnt6 (Fig 28, 29). These ligands would promote blood vessel branching as deletion of *Wnt5a* in retinal myeloid cells is sufficient to alter vessel structure of the deep plexus. This confirms that the non canonical Wnt pathway is essential for retinal angiogenesis at the level of the deep plexus (Stefater et al. 2011). Using these evidences, we can propose that retinal angiogenesis in the deep plexus would be regulated by the Wnt5a ligand secreted by myeloid cells that would activate endothelial cells via Fzd4/LRP5, as deletion of *Wnt5a* in myeloid cells and *Fzd4 / Lrp5* in endothelial cells both lead to disorganization of the retinal deeper plexus (Ye et al. 2010).

iii) In adult: Hindlimb Ischemia

Barandon et al. have shown that the competitor of Fzd, secreted frizzled-related protein-1 (sFRP-1) would regulate response to myocardial infarction. Overexpression of sFRP-1 reduces neutrophil infiltration in ischemic tissue, by switching the balance of pro- and antiinflammatory cytokine expression, leading to a reduction in scar formation (Barandon et al. 2011).

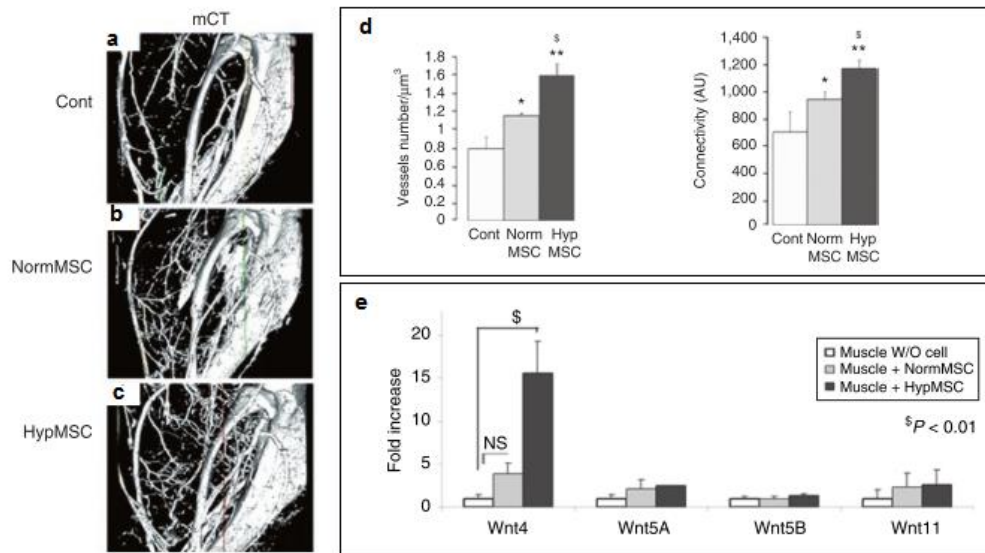


Figure 30: a-c micro-CT images of control and stem cells injected hindlimb after ischemia; d - quantification of vessel density and connectivity; e- expression of Wnt factors as detected in ischemic muscle after injection of normal/ hypoxic stem cell (adapted from Leroux et al.)

Many works show that the Wnt canonical pathway controls neovascularization after ischemia, using notably the hindlimb ischemia model (Oses et al. 2009). Ezan et al. showed that blockade of Wnt signaling by injection of virus expressing Secreted frizzled related proteins 1 (sFRP1) induced degradation of β -catenin and reduces neovascularization in ischemic muscle (Ezan et al. 2004). In a similar manner, the Wnt canonical pathway antagonist Dickkopf-1 blocked neovascularization (Smadja et al. 2010), while expression of β -catenin favored capillary formation after muscle ischemia by inducing recruitment of angiogenic progenitors and promoting proliferation of endothelial cell (Kim et al. 2006). Finally, Leroux et al showed that injection of hypoxia pretreated mesenchymal stem cells would promote neovascularization after ischemia (Fig 30 a to d). The stem cells after hypoxia strongly expressed Wnt4 (Fig 30e); suggesting a pivotal role of Wnt4 in promoting capillary formation (Leroux et al. 2010).

iv) *In adult: Cerebral Ischemia and Brain tumors*

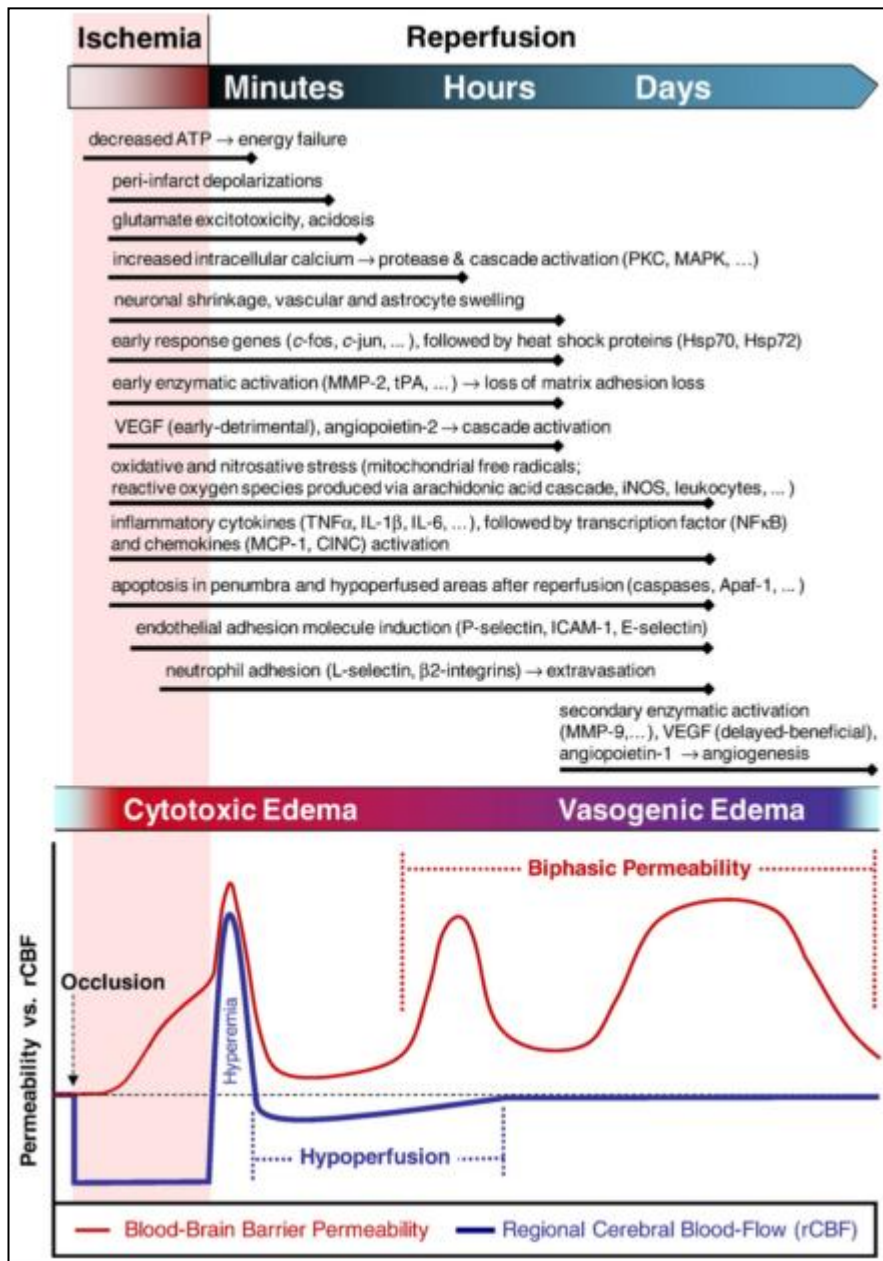


Figure 31: Events that occur after cerebral ischemia (Sandoval 2009)

Interestingly, the targets of Wnt signaling c-Jun and c-Fos are activated extremely early after cerebral ischemia. It would be interesting to assess how Wnt signaling is modulated by cerebral ischemia. The angiogenesis regulating pathways implicating PKC and VEGF are also activated a few hours after ischemia, indicating that vascular activation occurs (Sandoval and Witt 2008). In human brain tumors, genes related to Wnt signaling such as Dkk1 and Wnt5a are upregulated, indicating that Wnt signaling is activated in this context (Reis et al. 2012).

b) Molecular mechanisms of regulation of angiogenesis/cell migration by Wnt signaling

i) Wnt5a as a regulator of cell migration

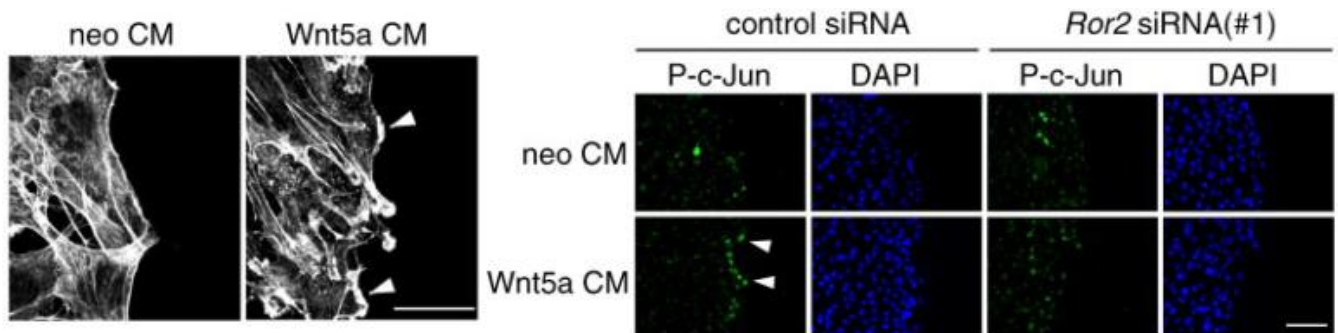


Figure 32: Wnt5a induces migration by relocating c-Jun to the leading edge (Nomachi 2008)

Wnt5a was shown to stimulate migration of endothelial cell by inducing formation of the lamellipodia (Fig 32a). Wnt5a induces accumulation of c-Jun at the lamellipodia of migrating cell. The Fzd coreceptor Ror2 would be essential for Wnt5a action on migration, as depletion of *Ror2* blocks relocation of c-Jun to the leading edge (Fig 32b) (Nomachi et al. 2008).

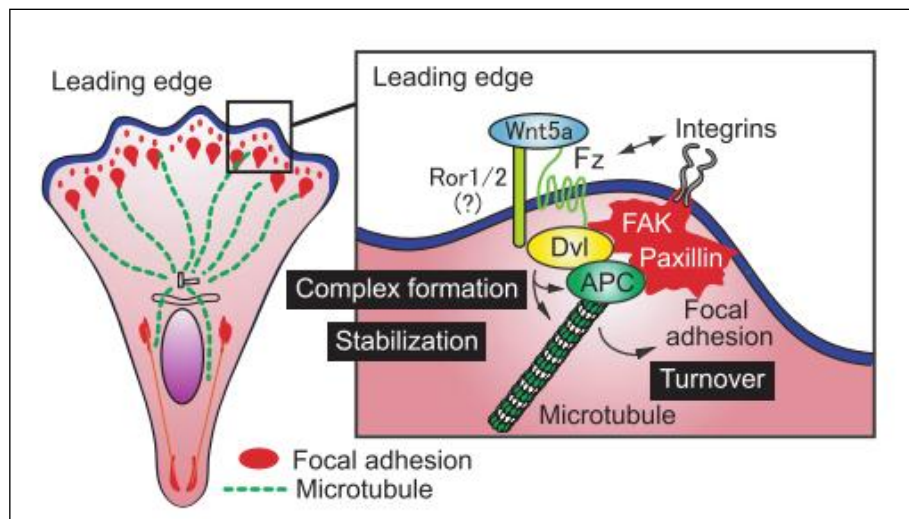


Figure 33: Cell migration and adhesion regulated by the Wnt5a pathway (Kikuchi et al. 2012)

Several mechanisms have been proposed for the involvement of Wnt5a in cell migration. For instance, binding of Wnt5a to Ror2 would induce cell migration by mediating the formation of filopodia via the actin-binding protein filamin A, leading to lamellipodia formation and reorientation of the microtubule organizing center(MTOC) (Nishita et al. 2006). This process requires JNK that

phosphorylates paxillin, the focal adhesion molecule, essential for cell migration (Huang et al. 2003). Another proposed mechanism is that Wnt5a would induce binding of Dvl to APC that interacts directly with microtubule-plus-end binding protein, FAK and paxillin. Both proteins are involved in the stabilization of microtubules at the cell periphery, which is important for the disassembly of the focal adhesion to stimulate cell migration (Matsumoto et al. 2010) (Fig 33). Additionally, Wong et al (2003) showed that Fzd2 and integrin $\beta 1$ co-localize at the leading edge of polarized migrating cells, and that they would compete for binding with Paxillin. Taken together, these observations suggest that Wnt5a signaling through Fzd / Dvl and APC complex regulates adhesion negatively to promote cell migration (Fig33).

ii) Dvl and Daam1 regulate migration by remodeling the actin cytoskeleton or the microtubule network

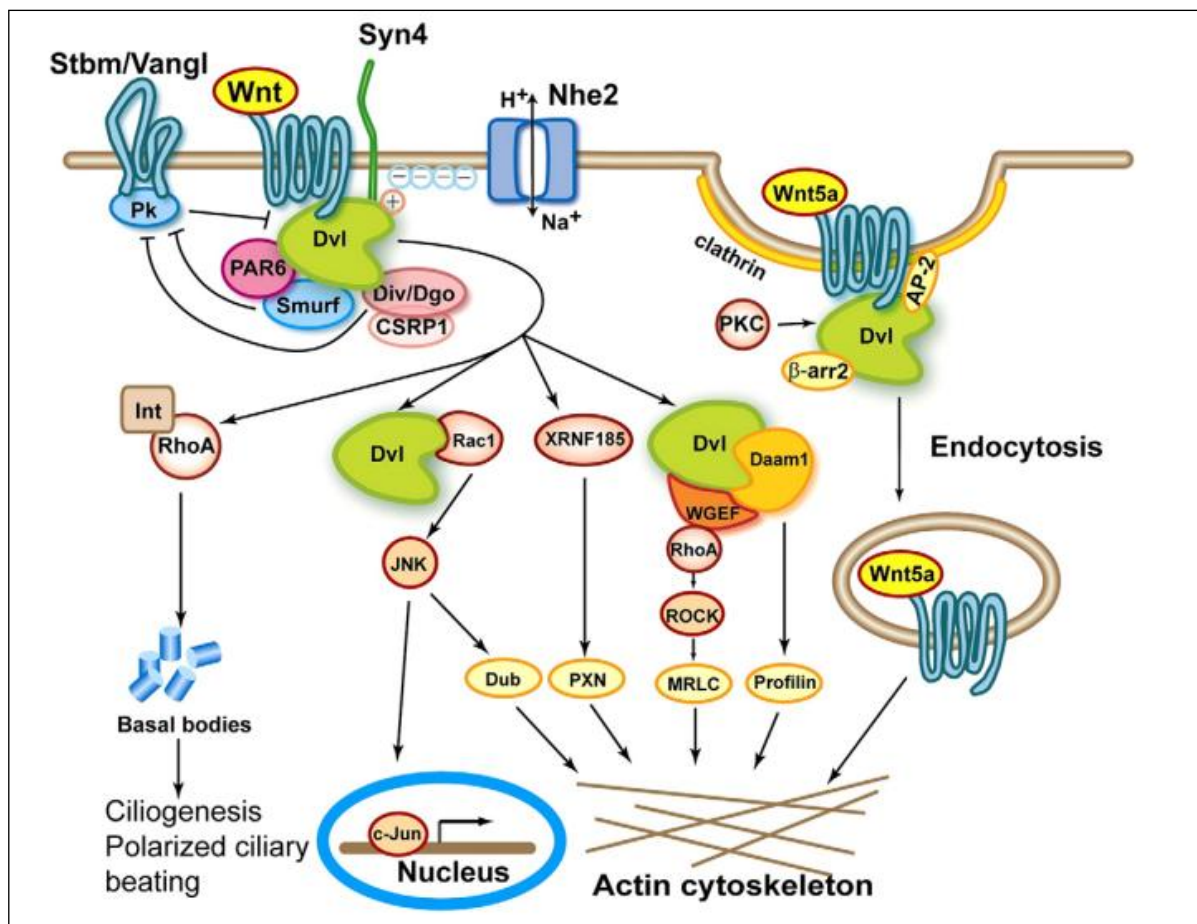


Figure 34: Regulation of migration via the actin skeleton by Dvl and Daam (Chen et al 2003)

Dvl proteins 1 and 3 can regulate cell migration by promoting remodeling of the actin cytoskeleton (Gao and Chen 2010). Dvl can associate with Daam1 that interacts with the Rho guanine nucleotide exchange factor WGEF (weak-similarity GEF), leading to the formation of the Rho-GTP complex, which activates the ROCK kinase and leads to remodeling of the cytoskeleton (Habas et al 2001). Additionally, Daam1 can interact directly with the actin-binding protein Profilin1 that can control directional movement of the cell by promoting reorganization of the actin cytoskeleton (Sato et al 2006). Other partners of Dvl can also control migration. In *Xenopus*, Dvl can interact with XRNF185 that induces paxillin destabilization, leading to cytoskeleton rearrangement and migration (Lioka et al 2007). Dvl can also activate another small GTPase of the Rho family, Rac that can directly regulate migration and cell polarity / movement (Habas et al 2003).

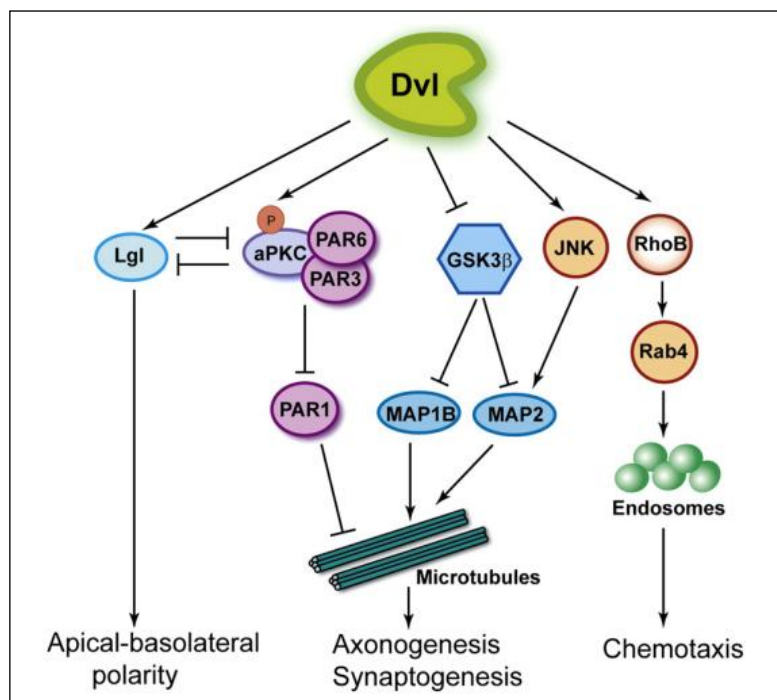


Figure 35: Regulation of migration via microtubules by Dvl and Daam (Chen et al 2003)

Dvl can also control migration through microtubules. For example, during axonogenesis, Dvl stabilize microtubules through activation of JNK and GSK3β inhibition. GSK3β blocks migration by phosphorylating the microtubule-associated protein MAP1B (Ciani et al 2006) (Fig35). Interestingly, overexpression of the Daam1 would also be able to induce microtubule stabilization for unknown

reasons (Ju et al. 2010). In ciliated cells, Dvl is essential for apical docking and planar polarization of basal bodies, a short cylindrical array of microtubules that serve as a core for the growth of cilium axoneme. Silencing of Dvl causes failure to localize basal bodies to the apical surface of ciliated cells, leading to defects in ciliogenesis (Park et al 2008). Other proteins interacting with Dvl such as Vangl2 also regulate position of the cilium (Giese et al. 2012, Ezan et al. 2013)

iii) Interplay between Wnt and Notch signaling during sprouting retinal angiogenesis

Sprouting angiogenesis in the retina would be dependent on two types of cells: the tip and stalk cells. Notch signaling would be central to the establishment of these identities (Fig 36).

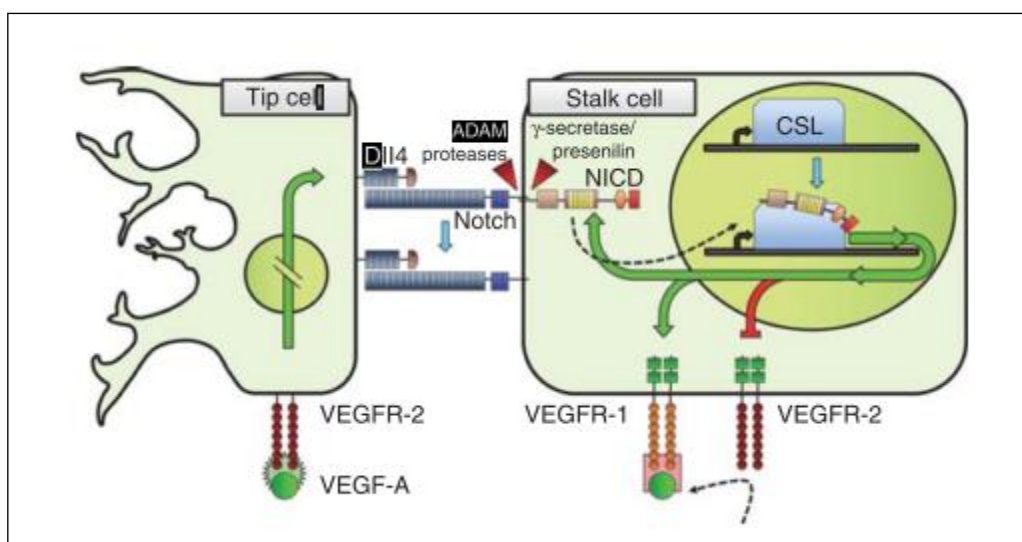


Figure 36: Sprouting endothelial cells are hierarchically organized into tips cells and stalk cells during retinal angiogenesis. Tip cell formation is induced by VEGF signaling, while stalk cell are determined by Notch signaling (Herbert et al. 2011)

The Notch gene was first identified when a mutant allele in *Drosophila melanogaster* caused a ‘notching’ of their wings. Notch signaling is initiated when a Notch family receptor binds one of its ligands. This induces cleavage of the Notch receptor; the separated Notch intracellular domain (NICD) translocates to the nucleus to regulate transcription of genes such as Hair/Enhancer of Split genes (Tung et al. 2012). The formation of a tip cell is induced when extracellular VEGF-A binds VEGF receptor 2 (VEGFR-2) causing up-regulation of the Notch ligand Delta-like 4 (Dll4). Membrane-bound Dll4 then

interacts with Notch1 receptors on the adjacent endothelial cells. This leads to the down-regulation of VEGFR-2 and up-regulation of VEGFR-1 in these cells, which is a high-affinity/ low-activity receptor of VEGF-A. This creates a situation in which one cell expresses high VEGFR-2 levels and its neighbor cell is less sensitive to VEGF-A signaling (Liu et al. 2003, Hellstrom et al. 2007). The cell expressing VEGFR-2 and Dll4 becomes a “tip” cell by producing filopodia that extend in the direction of the angiogenic factors. The neighbor of the tip cell becomes a “stalk” cells that proliferate and contribute to the elongation of the sprout (Fig36) (Herbert and Stainier 2011).

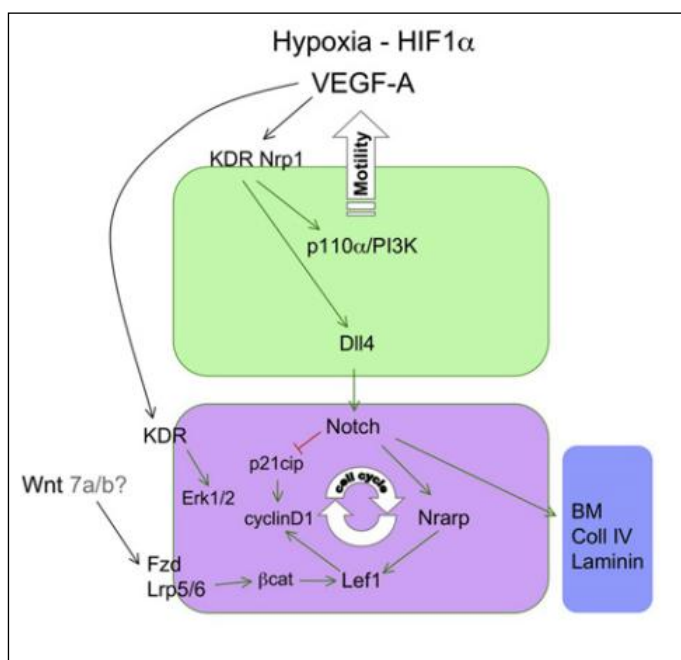


Figure 37: Different effects of Wnt/ β -catenin and Notch signaling during sprouting angiogenesis (Gerhardt et al. 2009)

Many evidence indicate interplay between Notch signaling and Wnt pathways in the tip/ stalk differentiation. Dll4–Notch interactions between tip and stalk cells can activate Wnt signaling in stalk cells to maintain EC connections, leading to expression of Notch-regulated ankyrin repeat-containing protein (NRARP). NRARP limits Notch activity and stimulates the Wnt canonical pathway to stabilize stalk cells, induce proliferation and prevent regression (Fig37) (Tung et al. 2012, Reis and Liebner 2013). Interestingly, overexpression of β -catenin positively regulates Dll4 expression in ECs, inducing Notch signaling and EC regression at the level of stalk cells (Reis et al. 2012).

Chapter II. Regulation of Wnt signaling by endocytosis and ubiquitinylation

1) Endocytosis as a regulator of Wnt signaling

Endocytosis has recently emerged as a regulator of various pathways including Wnt signaling. Endocytosis would regulate availability of Fzd receptors on the cell surface and would be essential for signal transduction after binding of Wnt ligands of the Fzd receptors.

a) Role of the early endosome in signal transduction

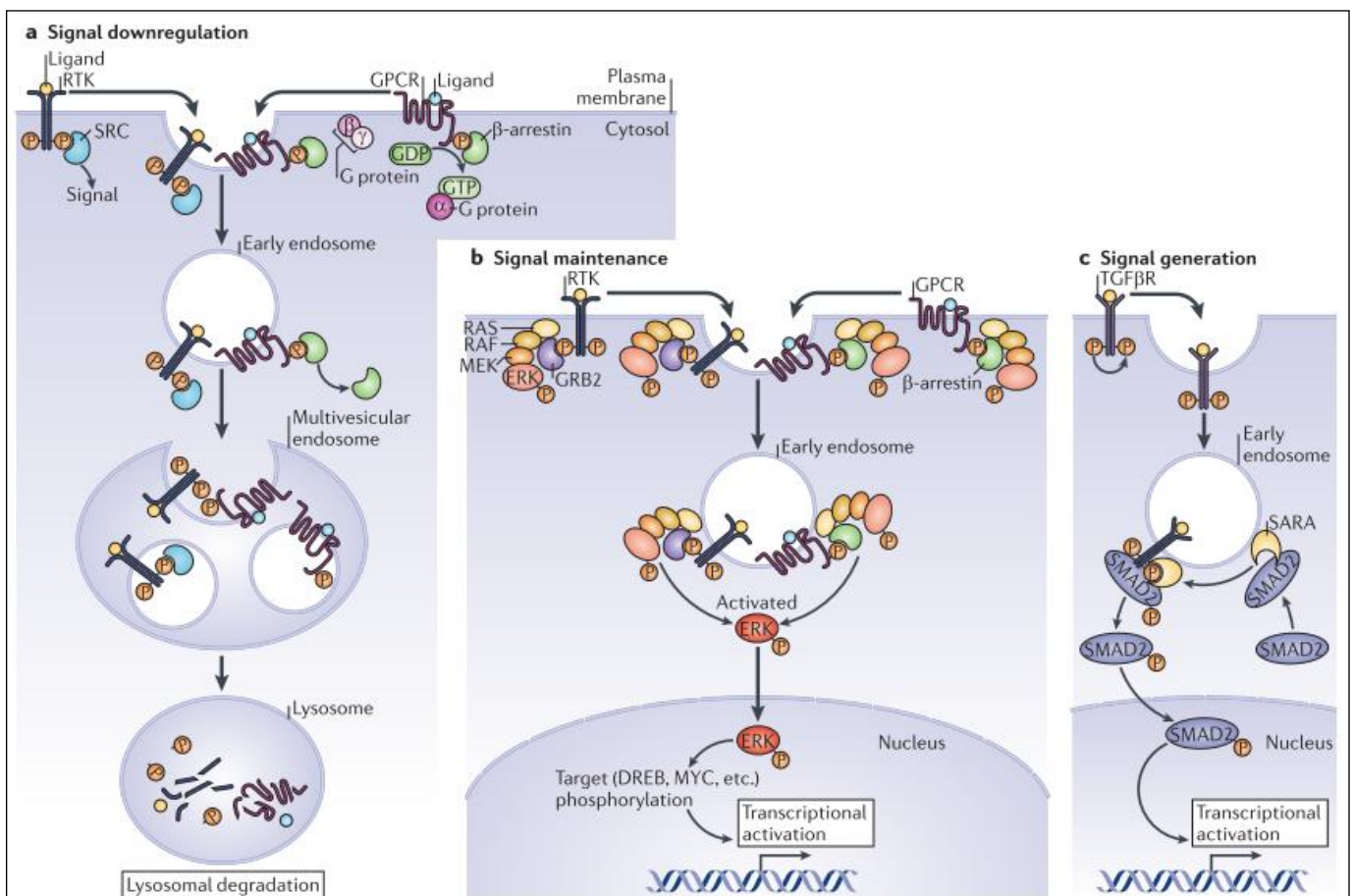


Figure 38: Endosome regulates signaling by different manner (Dobrowolski et al 2011)

Endocytosis can mediate cell signaling in different ways. Endocytosis can downregulate signaling by promoting degradation of receptors – as it is the case for some small G protein-coupled proteins that are internalized and fused with the lysosome for degradation (Fig 38a). Endocytosis can also maintain

signaling complex after their formation at the plasma membrane – as it is the case for activation of the mitogen activated protein kinase (MAPK) that leads to formation of the RAS-RAF-MAPK-ERK complex in endosome and activation of ERK (Fig 38b). Endocytosis can also generate signal – as in the case of transforming growth factor- β receptor that is internalized into endosomes leading to recruitment and phosphorylation of SMAD2 leading to signal transduction (Fig 38c) (Grant and Donaldson 2009, Sadowski et al. 2009, Dobrowolski and De Robertis 2011).

b) Role of the early endosome in Wnt signaling

In the case of Wnt signaling, endocytosis is required at different levels. Early endosomes would sequester GSK3- β in vesicles, leading to protection of its cytosolic substrates (β catenin or c-Jun) from phosphorylation, stabilizing newly translated β -catenin protein. Interestingly, GSK3- β would be recruited to the multivesicular endosome after binding to the Dvl/Axin-2 complex in the cytosol (Jibin Zhou 2005).

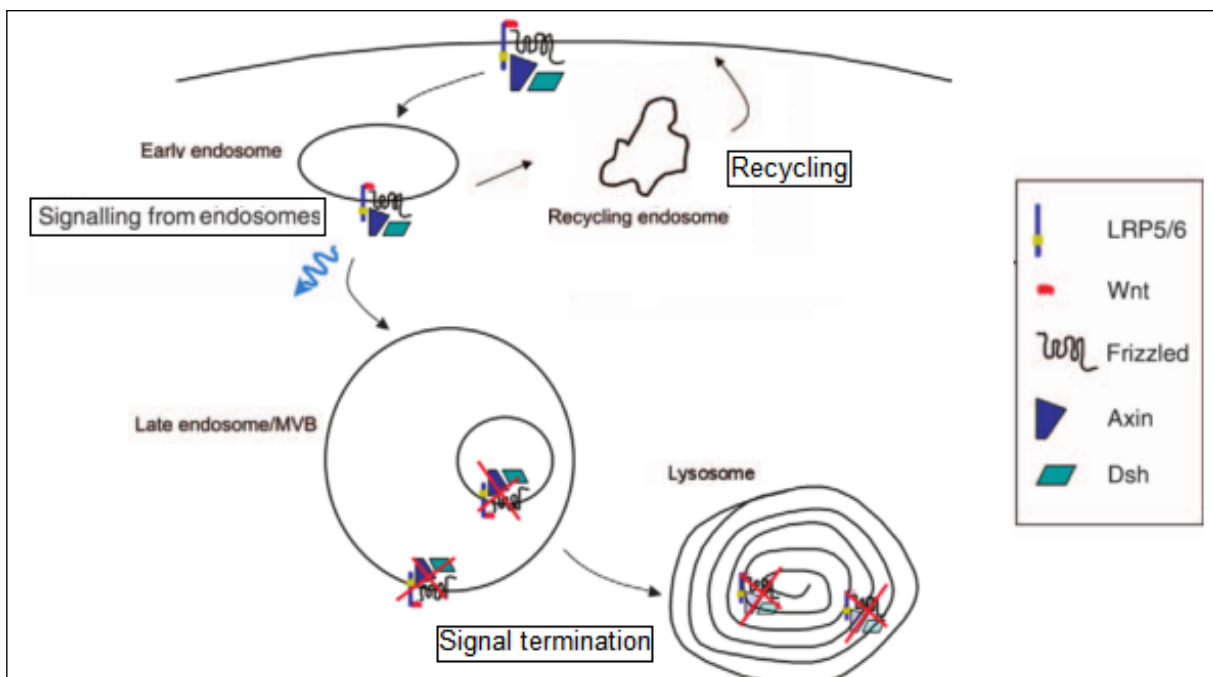


Figure 39: Endocytosis of Wnt receptors can lead to signal transduction / recycling or signal termination depending on context (Gagliardi et al 2008)

Endocytosis can also regulate the level of expression of Wnt receptors by targeting them to lysosome for degradation or recycling endosome for receptor recycling. Receptors are protected from

degradation when they are sequestered in early endosome. The receptors can then only be restored to endosomal membrane via the recycling endosome. It is possible for membrane lipid components of the early endosome to recycle back to the plasma membrane but not to be degraded by fusion with the lysosome (back-fusion) (Fig 39) (Gagliardi et al. 2008).

c) Caveolin and Clathrin mediated endocytosis would regulate balance between Wnt pathways

Recent evidences strongly indicated that Wnt ligands would induce different pathways via the same components by promoting endocytosis of the Fzd/ Dvl complex via caveolin or clathrin mediated endocytosis. Caveolin – dependant endocytosis of Fzd and Fzd correceptors would favor the Wnt canonical pathway, while clathrin –dependant endocytosis would favor the Wnt non canonical/ PCP pathway (Fig 40). First evidences were that Wnt3a induces the caveolin-dependent internalization of Fzd coreceptor, low-density-lipoprotein receptor-related protein 6 (LRP6) leading to recruitment of Axin to the cell surface membrane and to subsequent accumulation of B-catenin (Fig 40) (Yamamoto et al. 2008). In contrast, Dkk1 induces the internalization of LRP6 with clathrin and inhibits Wnt3a response, reducing distribution of LRP6 in caveolin rich-lipid rafts (Fig 40) (Yamamoto et al. 2008). In a similar manner, Dvl2 interacts with m2-adaptin, a subunit of the clathrin adaptor AP-2; leading to handling of Frizzled4 by the endocytic machinery and subsequent activation of the PCP (Yu et al. 2007). These results echoes findings of Chen et al. 2003 who showed that Wnt5a induces endocytosis of Fzd4 to clathrin dependant vesicles, leading to recruitment of Dvl2 (Chen et al. 2003). Recent evidence also show that upon binding of Wnt5a to Fzd7, Respondin 3 (Rspo3) binds to syndecan 4, leading to clathrin-mediated endocytosis of Fzd7 and activation of PCP in xenopus (Ohkawara et al. 2011). This body of evidence indicates that endocytosis of the Fzd complex via clathrin vesicles would favor non canonical pathway, while endocytosis in lipid rafts via caveolin would favor the canonical pathway.

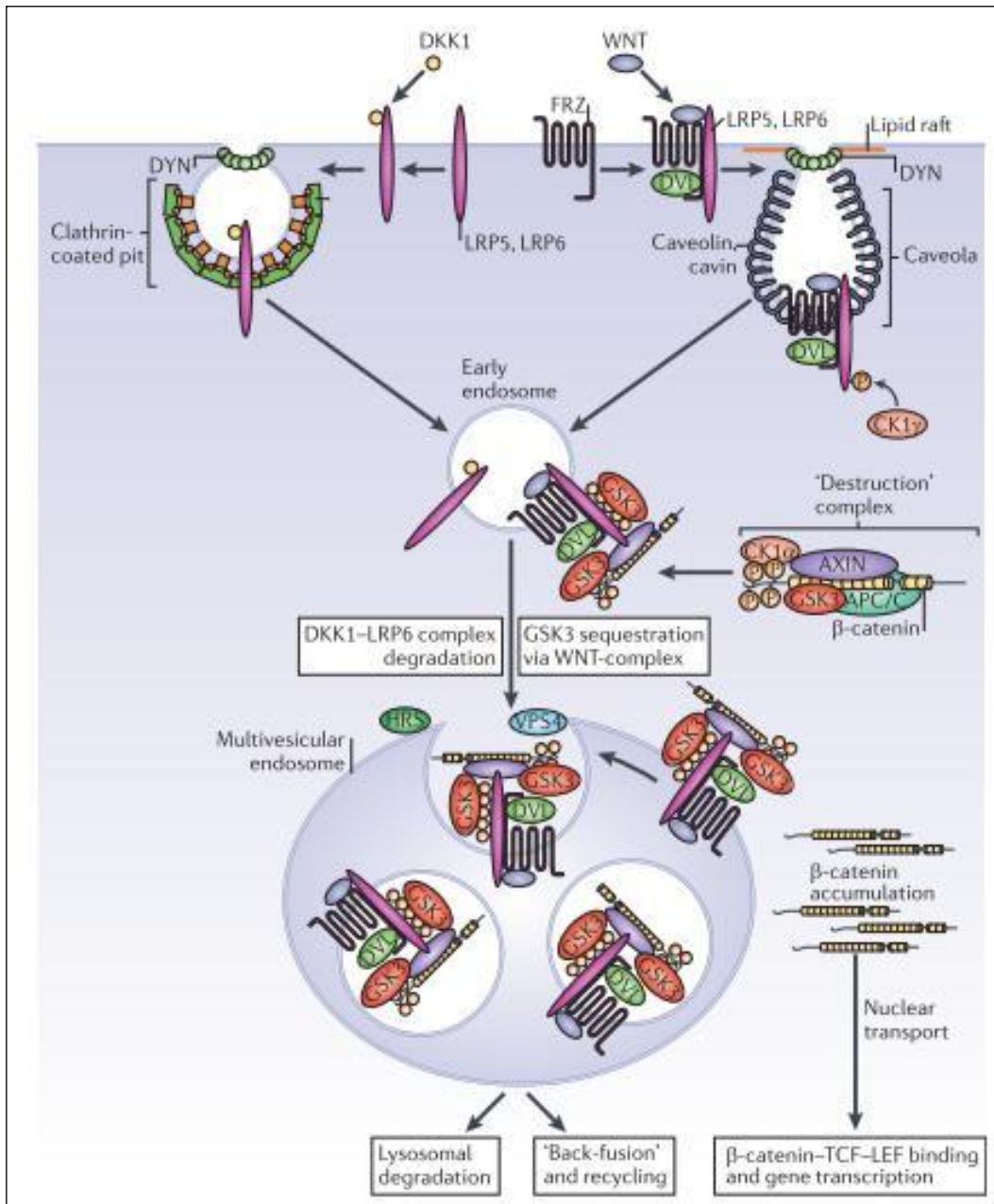


Figure 40: Endosome and Wnt signal transduction (adapted from Drobowolski et al 2011)

d) Role of the endocytosis in Wnt signaling during development

Drobolowki et al. suggested that the regulation of Wnt signaling through sequestration would be important in the formation of the dorsal axis during *Xenopus laevis* development.

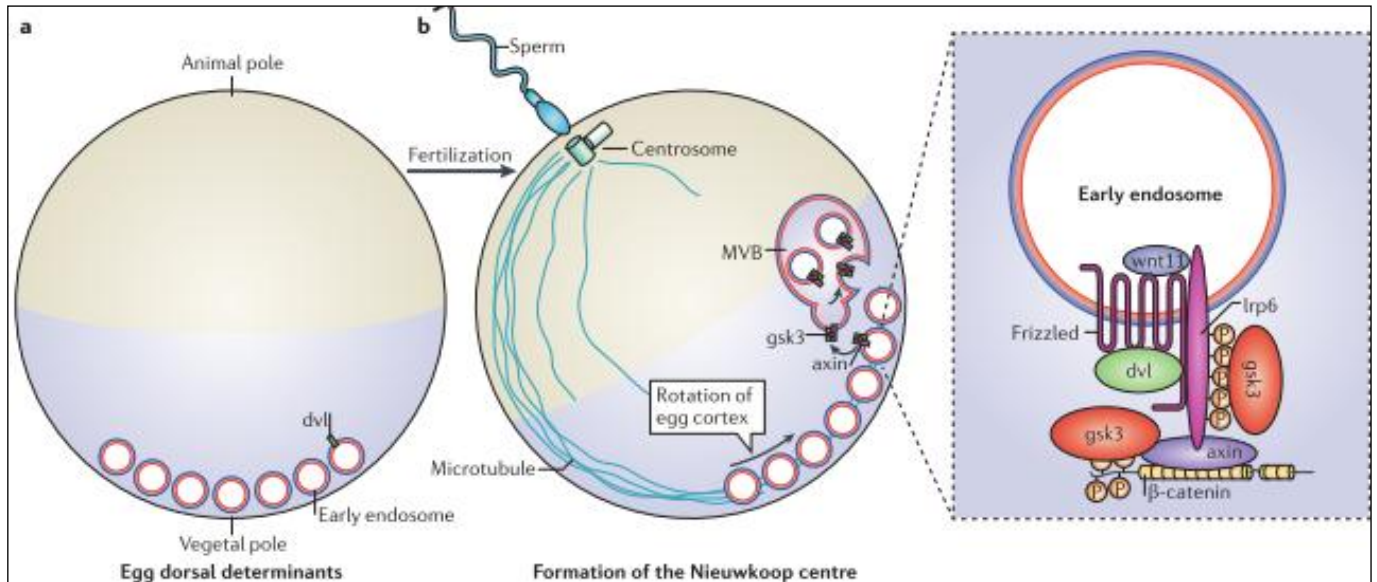


Figure 41: The dorsal determinants of the *Xenopus* egg may be Wnt endosomal components (adapted from Drobowski et al 2011)

The vegetal pole of the egg would contain ‘maternal determinants’ such as Wnt-containing early endosomes that would be incorporated into multivesicular bodies (MVB) on the dorsal side of the egg. These MVB would sequester GSK3, making Wnt induced embryonic differentiation possible, leading notably to formation of the Nieuwkoop signaling center. The vegetal pole is transported to the opposite of the site of entry of the sperm, forming the dorsal side (Fig 41). This hypothesis is clearly relevant as injection in the egg of interfering RNAs targeted against Wnt key proteins coding RNAs doesn’t block development of the embryo, even if Wnt signaling is essential for the process (as shown using KO strategy). This model would also explain why injection of Wnt inhibitors, such as dkk1 or sfrps cannot inhibit Wnt signaling in the early embryo: as the Wnt signaling complex would be protected inside early endosomes at this stage of embryonic development (Leyns et al. 1997, Kemp et al. 2007).

2) Ubiquitylation as a regulator of Wnt signaling

Ubiquitylation has emerged as a key process for regulation of endocytosis and Wnt pathway, by acting as a targeting system of proteins to vesicular systems, such as the endosome or lysosome.

a) Role of ubiquitylation in protein stability or function

Ubiquitylation can control trafficking/ degradation / localization or function of signaling components depending on the type of ubiquitin – chains attached to the cargo (Tauriello et al 2010). Following addition of an ubiquitin molecule to a substrate, further ubiquitin molecules can be added, leading to formation of a polyubiquitin chain. In addition, some substrates are modified by addition of ubiquitin molecules to multiple lysines residues in a process termed multiubiquitylation (Fig 42a).

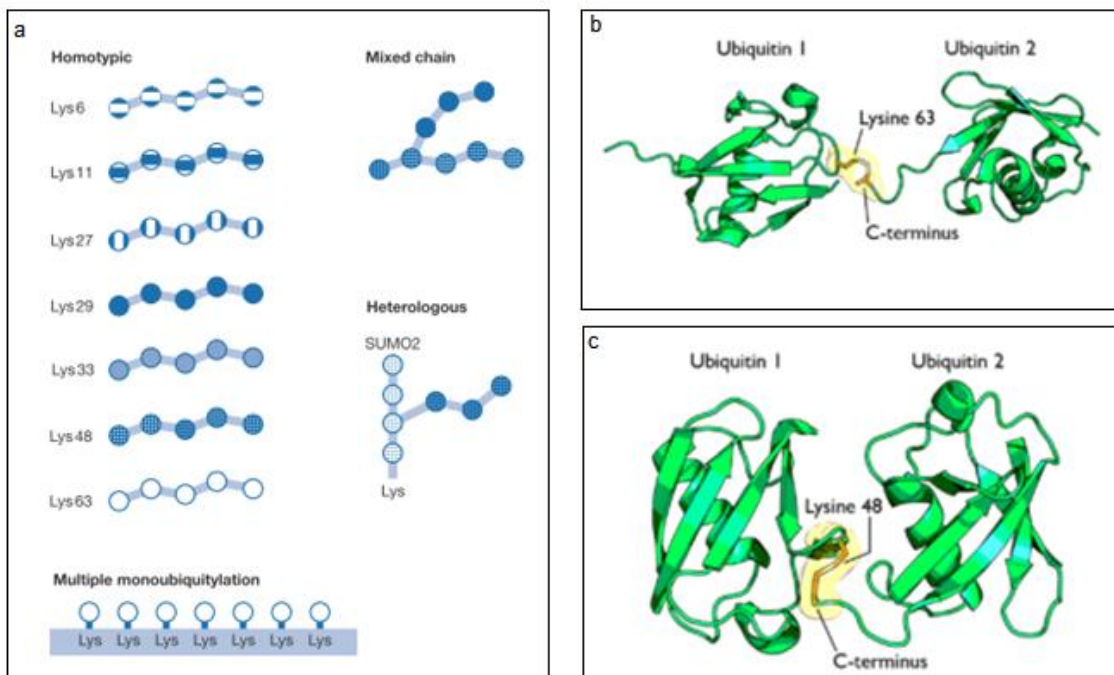


Figure 42: a - different types of ubiquitin chains, b- 3D structure of Lysine 63 linked diubiquitin, c- 3D structure of Lysine 48 linked diubiquitin (Ikeda, Dikic 2008)

Ubiquitin possesses a total of 7 lysine residues. The first type of ubiquitin chains identified were those linked via lysine 48 that targets proteins to the proteasome (Fig 42b). The formation of a chain of at least four ubiquitin molecules is required for degradation of the cargo. Lysine 63 linked chains direct the subcellular localization of proteins, as it is a signal for recruitment of the cargo to various endocytic vesicles (Fig42c).

b) Ubiquitylation of Fzd proteins

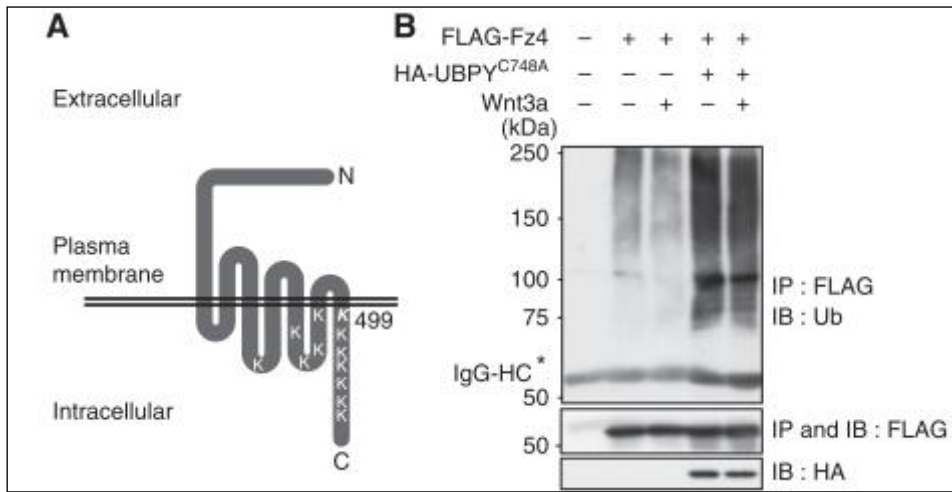


Figure 43: a- position of the different lysines residues on intracellular domains of Fzd4; ubiquitylation of Fzd4 (smear) is mediated by Wnt3a and UBPY (Mukai et al 2010)

Fzd4 presents many lysines residues on its intracellular domain that could be used for ubiquitylation (Fig43a) (Mukai et al. 2010). Balance of ubiquitylation / deubiquitylation of Frizzled4 by the deubiquitylating enzyme UBPY would determine availability of the protein at the cell surface level and subsequently, condition the cell response to Wnts.

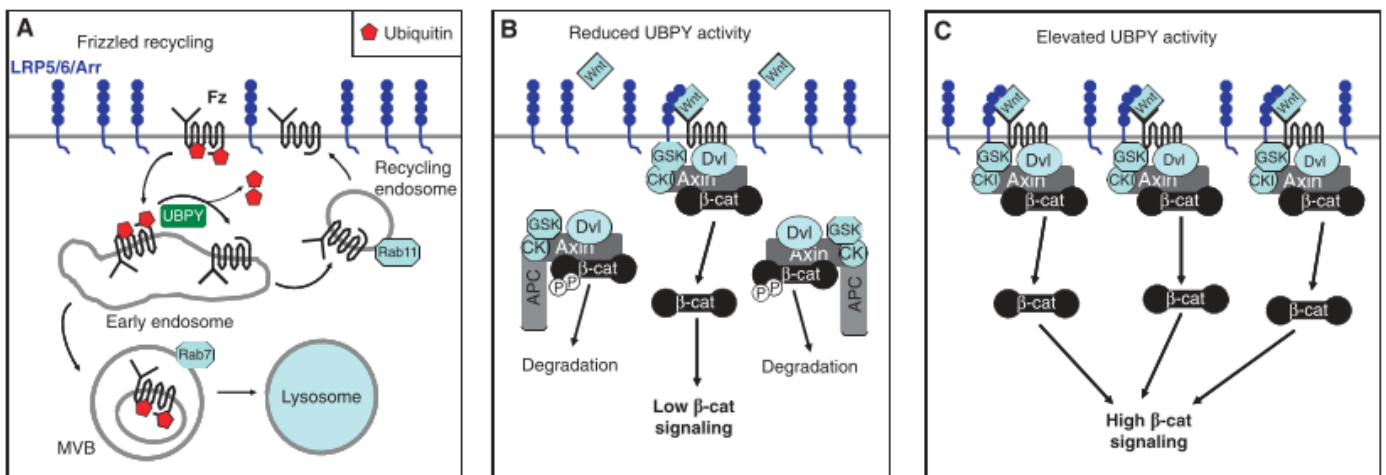


Figure 44: UBPY deubiquitin ligase controls availability of FZD4 for Wnts (Mukai et al 2010)

The model proposed by Mukai is that in absence of UBPY, Fzd4 is not deubiquitylated and degraded. In presence of UBPY, Fzd4 is deubiquitylated and recycled to the membrane where it is available for binding of Wnt ligands to activate Wnt pathways (Fig 44).

c) Ubiquitylation of Dvl proteins

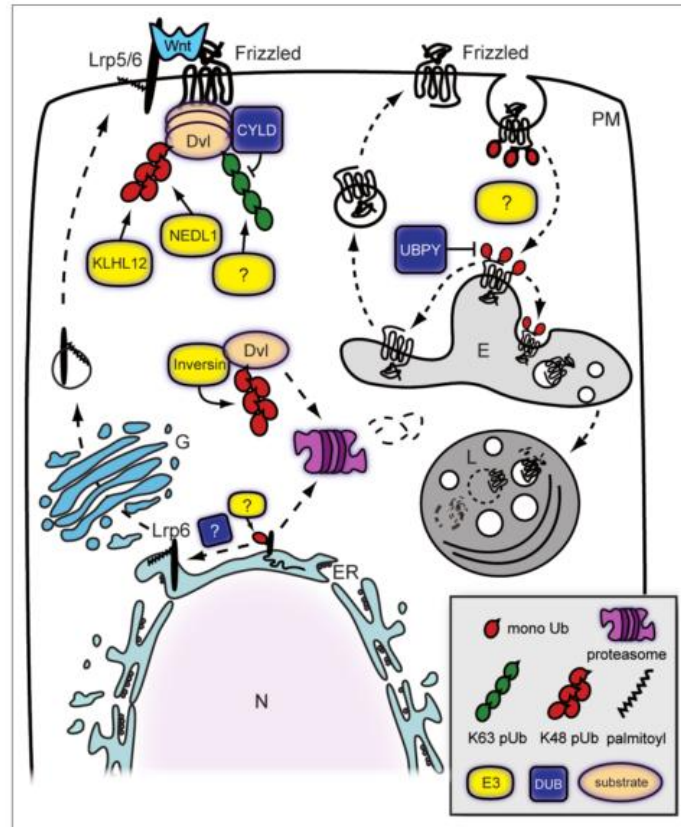


Figure 45: Different regulators of Dvl ubiquitylation (adapted from Tauriello 2010)

Many proteins have been shown to induce Dvl degradation via K48-linked ubiquitylation (in red, Fig 44). The E3 ubiquitin ligase Kelch-like 12 and Prickle via its destruction box facilitate Dvl degradation while Nucleoredoxin (NRX) blocks K48-linked ubiquitylation of Dvl3 (Chan et al. 2006, Funato et al. 2010).

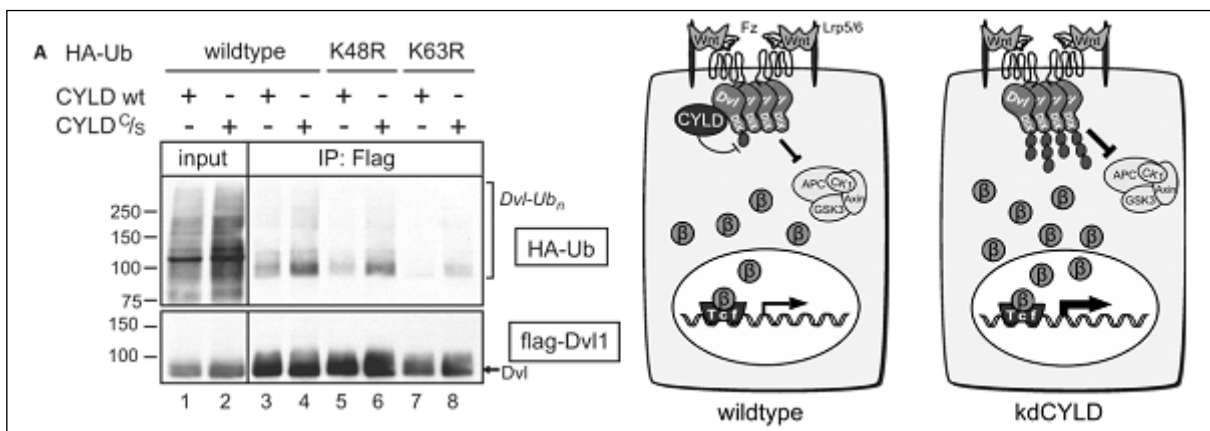


Figure 46: a- Cyld mediated K63 dependant ubiquitylation of Dvl (detected as a smear); b- model of regulation of Dvl activity by CYLD (Tauriello et al. 2010)

d) Ubiquitylation of β -catenin

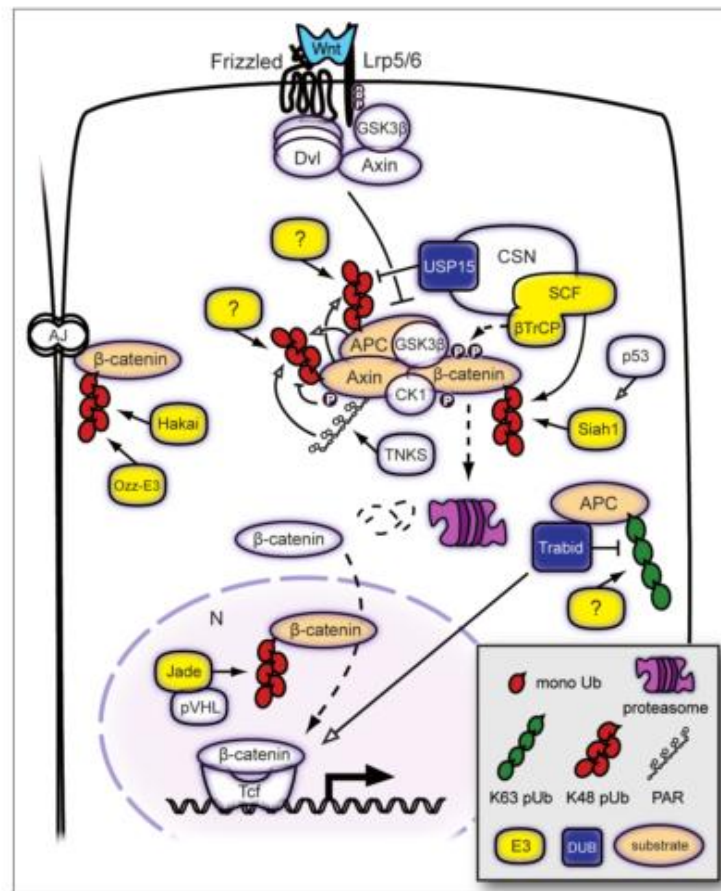


Figure 48: Ubiquitin mediated regulation of core Wnt proteins such as β -catenin (adapted from Tauriello et al. 2010)

Degradation of cytoplasmic β -catenin was first shown to be mediated by GSK3 β -mediated phosphorylation (Ser33, Ser37) and subsequent proteolytic degradation by the Skp1-Cullin-F-box (SCF) RING-type E3 ligase. SCF ubiquitinylates β -catenin on Lys-19 and Lys-49. Mutations of β -catenin on these sites correlate with many cancers. An alternative degradation pathway for cytoplasmic β -catenin is mediated by the kidney specific nucleic ubiquitin ligase Jade-1 in a von Hippel-Lindau (VHL) dependant manner (Fig 48). Independent of Wnt signaling, cytoplasmic β -catenin levels can be regulated by Siah-1 in response to DNA damage via P53. The pool of Adherens junctions associated β -catenin can be targeted to degradation by two E3 ubiquitin ligases, Hakai and Ozz-E3(Jibin Zhou 2005).

3) *PDZRN3 E3 ubiquitin ligase*

During my PhD, a large part of my work focused on the ubiquitin ligase PDZRN3 that we have sorted out using a yeast two hybrid screening using Dvl3 as bait.

a) Identification of PDZRN3

PDZRN3 was identified in 2006 as a regulator of the differentiation of myoblast in myotubes. In another study, the protein was shown to bind and ubiquitinylate MUSK. The overexpression of PDZRN3 would induce degradation of MUSK and was shown to alter the structure of neuromuscular junctions (Lu et al. 2007). In 2010, PDZRN3 was shown to negatively regulate BMP-2-induced osteoblast differentiation through inhibition of Wnt canonical signaling (Ji-Ae Ko 2006, Lu et al. 2007, Honda et al. 2010). PDZRN3 could also interact with Neuroligin1 and EphrinB2 (by similarity, in silico predictions).

Organism	Taxonomic classification	Gene	Description	Human Similarity
mouse (Mus musculus)	Mammalia	Pdzn3	PDZ domain containing RING finger 3	88.51(<i>n</i>) 94.54(<i>a</i>)
zebrafish (Danio rerio)	Actinopterygii	Dr.5264		78.8(<i>n</i>)

Figure 49: Orthologues of PDZRN3 (Gene Ontology)

PDZRN3 is coded by a gene on the chromosome 3 in humans. Many Single Nucleotide Polymorphisms (SNPs) exist in the coding gene but none of them correlate with specific diseases. The protein is highly conserved as there is 88,51% of nucleotidic homology between the coding gene in humans and in mice (Fig49). This low mutation rate indicate a strong pressure of selection on the gene and a key role of the protein. A paralogue for PDZRN3 exists in humans, PDZRN4 has no known function, and there doesn't seem to be redundancy between the function of the two proteins.

b) Structure and Function of PDZRN3 E3 ubiquitin ligase

The 1066 amino acid protein is composed of a RING domain, a deprecated zf-TRAF domain, two PDZ domains and a C-terminal PDZ binding domain.

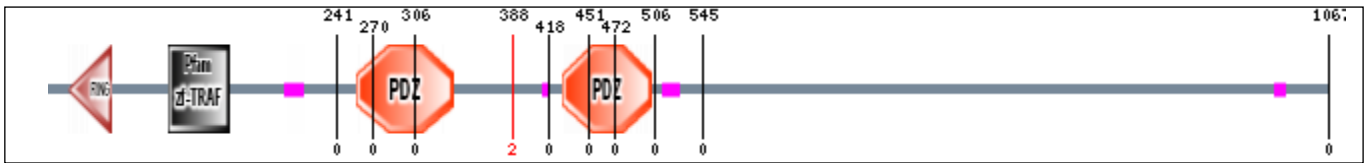


Figure 50: Structure of the protein (Scopus, EMBL)

i) The RING domain carries the ubiquitylation function

A RING (Really Interesting New Gene) finger domain is a protein structural domain of zinc finger type which contains from 40 to 60 amino acids. Many proteins containing a RING finger play a key role in the ubiquitination pathway. An E3 ubiquitin ligase such as PDZRN3 is a protein that after association with a E2 ubiquitin-conjugating enzyme causes the attachment of ubiquitin to a lysine on a target protein.

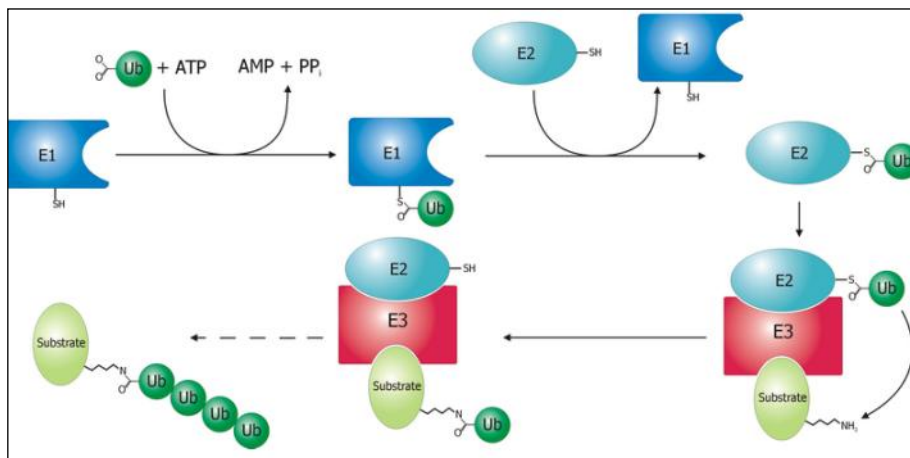


Figure 51: Process of ubiquitylation (Dikic et al. 2012)

ii) PDZ binding domain

PDZ is the acronym combining the first letters of three proteins where the domain was first found — post synaptic density protein (PSD95), Drosophila disc large tumor suppressor (Dlg1), and zonula occludens-1 protein (ZO-1). The PDZ domains of PDZRN3 are formed of 80-90 amino-acids. PDZ domains bind to specific short region of the C-terminus of other proteins.

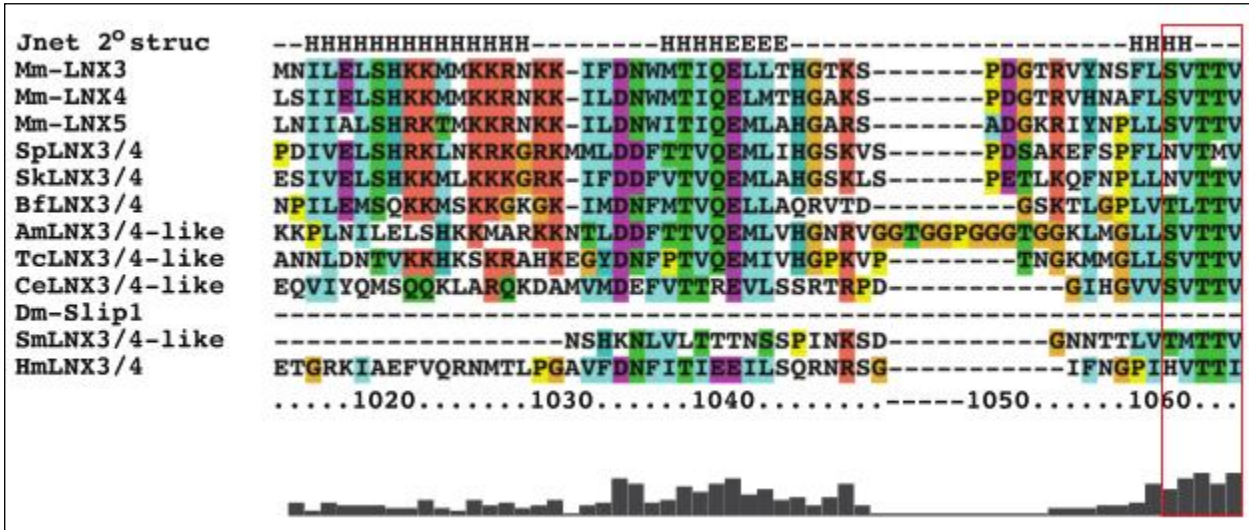


Figure 52: ClustalX alignment of the last amino acids of murine PDZRN3 (mm LNX3), PDZRN3 4 (mm LNX4) as well as orthologues from invertebrate species (Flynn et al. 2011).

PDZRN3 possesses a PDZ binding domain. These are usually composed of Thr –X –Val –COOH (Nie et al. 2004, Valiente et al. 2005). The last 150 amino acid region of PDZRN3, including the PDZ binding domain (Fig 52) are highly conserved across diverse species, suggesting that this domain is essential for the function of the protein (Flynn et al. 2011).

iii) Endocytic scaffolding

Proteins carrying PDZ and PDZ binding domains can form scaffolds. It has been suggested that because these proteins interact with junctions, they could be implicated in formation of ‘endocytic scaffold’. These structures would promote endocytosis of transmembrane proteins after binding of a ligand. Kandansku suggested in 2006 that a paralogue of PDZRN3, ligand of Numb X (LNX) would provide an endocytic scaffold for JAM4, after binding of the Notch antagonist NUMB, leading to reorganization of cell junctions. (Kansaku et al. 2006). PDZRN3 could have similar functions.

iv) Homology with GIPC / Synectin

PDZRN3 shares homology of sequence with SEMACAP 1 and 2 (GIPC 1 and 2 or Synectin). GIPC are small proteins with a single C-terminal PDZ domain, implicated in clathrin-mediated endocytosis (Djiane and Mlodzik 2010). GIPC1 also interacts with Endoglin that in turn phosphorylates Smad1

/Smad5 /Smad8, leading to inhibition of endothelial cell migration. The GIPC-null mice has reduced numbers and altered pattern of arteries, whereas the venous system is normal (Lee et al 2008).

c) PDZRN3 is a member of the LNX family of protein

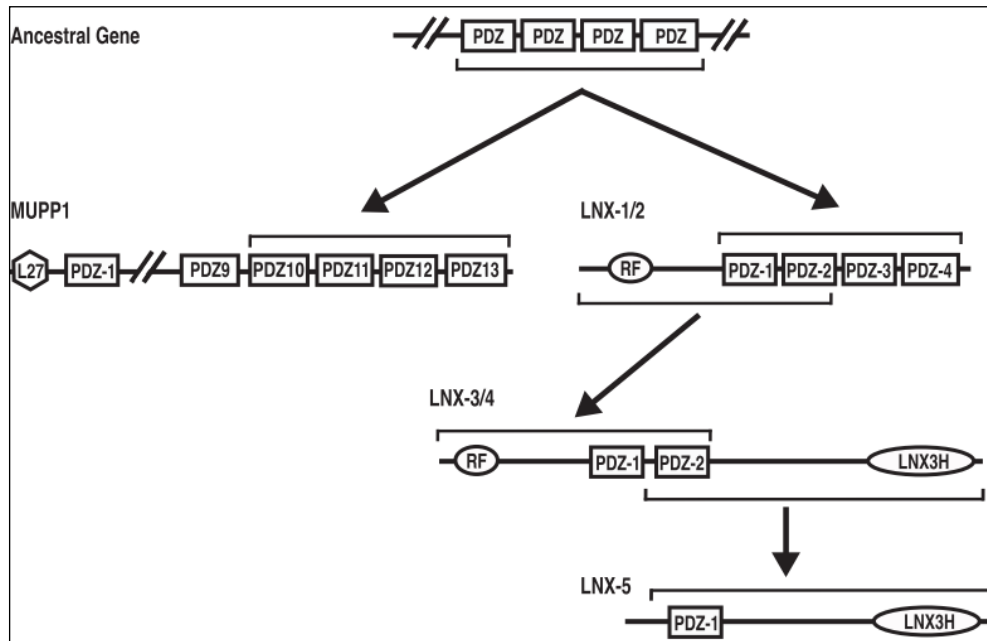


Figure 53: Molecular evolution of the LNX family (Flynn et al 2011)

PDZRN3 was first called LNX3 because of its homology of sequence with LNX1 and 2. Ligand of Numb Protein-X (or LNX) proteins contains an amino-terminal RING domain and PDZ domains. LNX proteins function as E3 ubiquitin ligases and their ubiquitin ligase activity would be targeted to specific substrates or subcellular locations by PDZ domain-mediated interactions. Interestingly, LNX1 regulates activity of NUMB, a protein that regulates balance between Notch and Wnt signaling by inhibiting Notch signaling to favor Wnt pathway (Cheng et al. 2008). Flynn et al (2011) did a phylogenetic study of the family and found that PDZRN3 arose from a duplication of the LNX1/LNX2 -coding gene. The PDZ domains of LNX1/2 and 3 are closely related to the four carboxy-terminal domains from multiple PDZ domain containing protein-1 (MUPP1) that acts as a scaffolding protein in the Crumbs complex (Fig 53) (Flynn et al. 2011).

Chapter III. Wnt signaling and vascular integrity

1) Wnt signaling regulates endothelial permeability in the Blood brain barrier

Wnt signaling is required for differentiation of brain vessels during development, during which it is essential for formation of TJ or recruitment of pericytes. It is also required for maintenance of the blood brain barrier (BBB) integrity in adulthood.

a) Wnt signaling as a regulator of brain vessels permeability

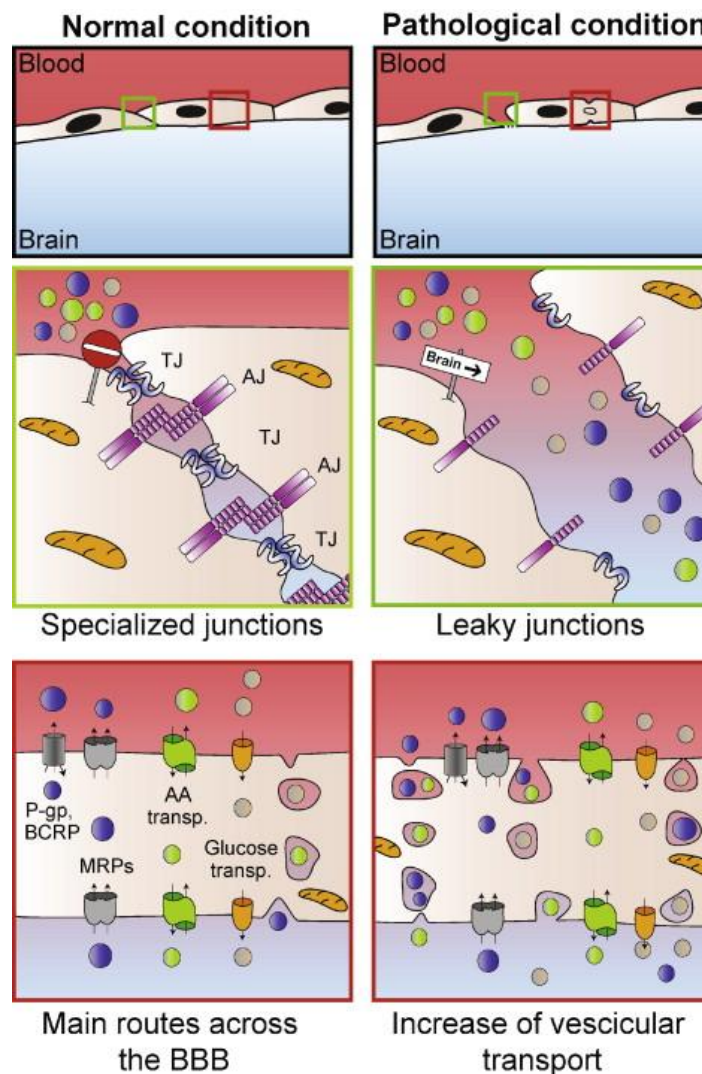


Figure 54: Brain capillaries under normal and pathological conditions (Paolinelli et al 2011)

Permeability of the BBB depends on the stability of adherens and tight junctions (TJ). In normal conditions, cerebral endothelial cells form complex junctions that block the passage of large

molecules. Nutrients such as amino acids or glucose are able cross the barrier through specific transporters, while large molecules (such as antibodies, lipoproteins, peptides) can be transferred by vesicular-based systems. In pathological condition (such as ischemia), TJ become leaky and vesicular transport strongly increased. This results in the entry of fluids in the brain leading to edema and other pathological reactions (Paolinelli et al 2011). Wnt signaling would be one of the signaling pathways essential for maintenance of blood brain barrier integrity.

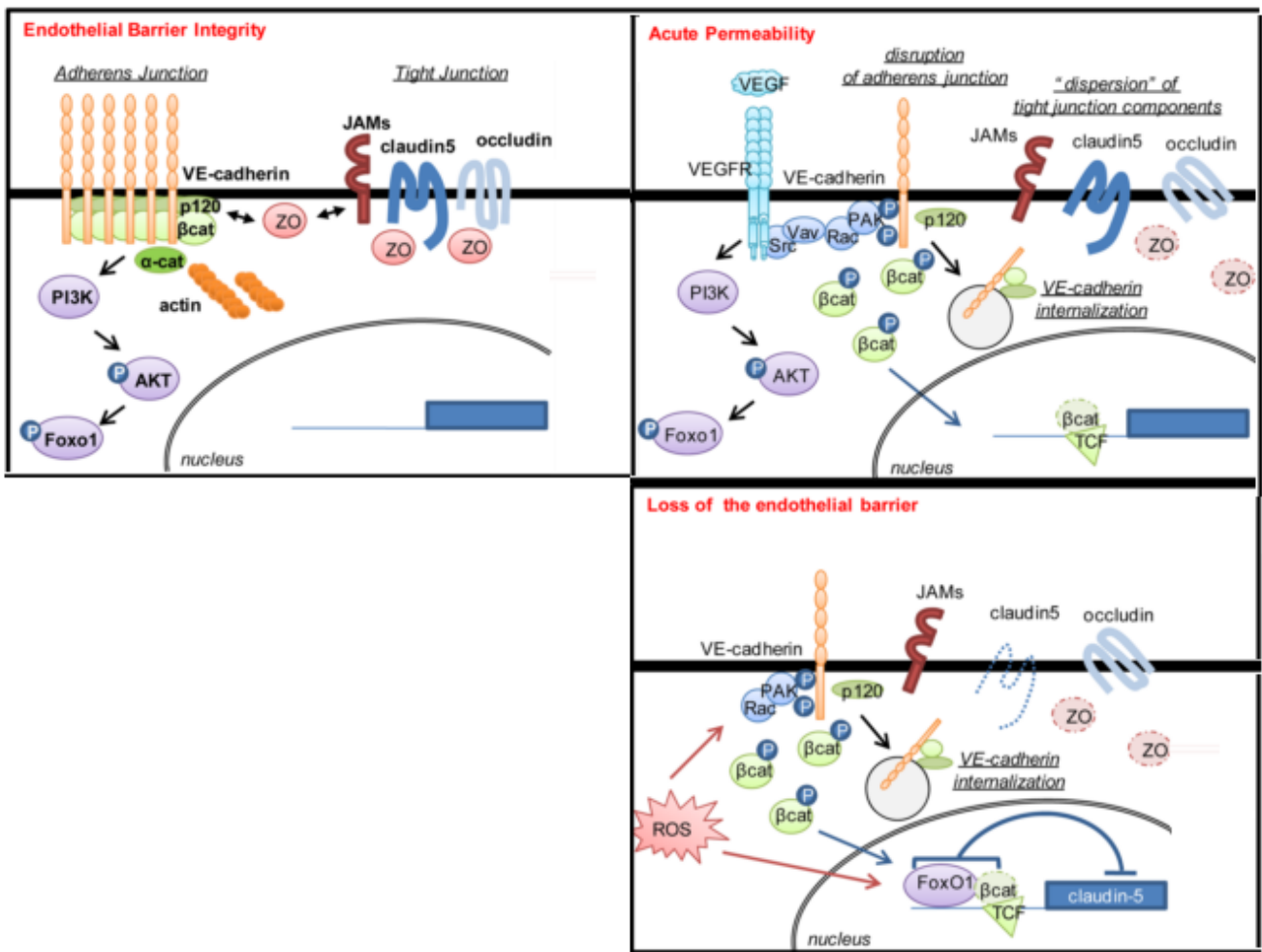


Figure 55: VE-cadherin traps FoxO1 and β-catenin at the membrane. In the nucleus, both would block claudin-5 transcription. In acute permeability condition, VE-cadherin adhesion is destabilized and FoxO1 and β-catenin are phosphorylated and translocate to the nucleus where they block claudin-5 transcription (Gavard et al 2008)

The integrity of the blood brain barrier would be regulated by VE-cadherin and claudin-5 but also by β -catenin. VE-cadherin when expressed at the adherens junctions (AJ) enables claudin-5 expression by preventing the accumulation at the nucleus of FoxO1 and β -catenin, which repress claudin-5 expression in the nucleus when VE-cadherin is absent or not functional (Fig 55). These findings place VE-cadherin and β -catenin upstream of claudin-5 in the establishment, maturation and maintenance of endothelial cell-cell junctions in development (Gavard and Gutkind 2008). Phosphorylation of Foxo1 is also used to assess the integrity of the BBB (Wang et al. 2013).

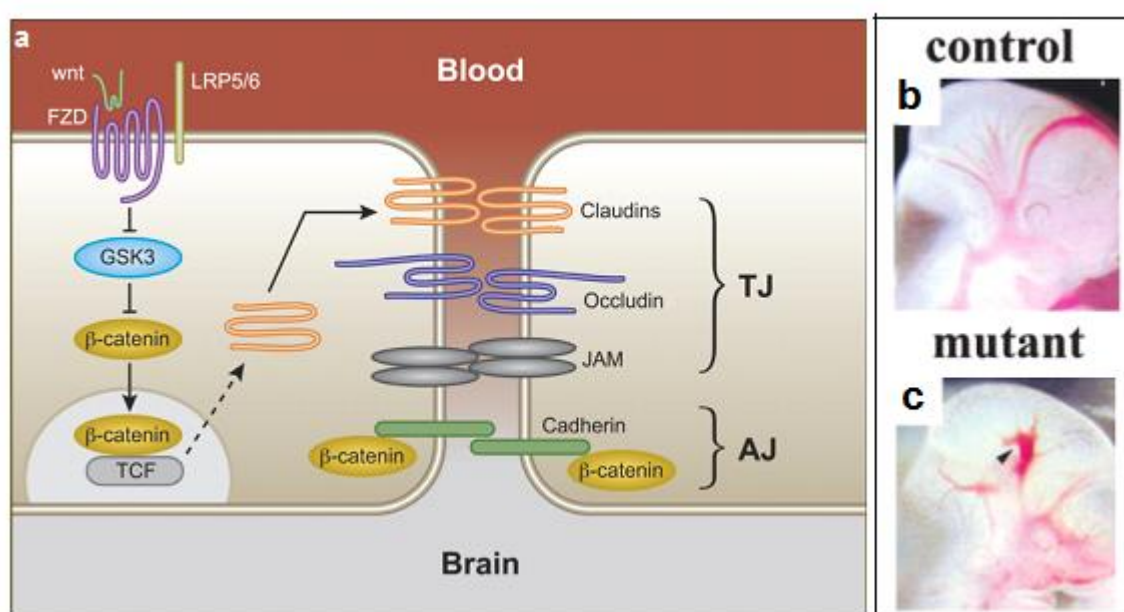


Figure 56: a- Transcription of claudin 3 is activated by B-catenin (Liebner et al 2008); b- Conditional loss of β -catenin leads to vascular leakage during development (Catellino et al 2003)

Interestingly, the team of Liebner had different findings. They showed that loss of β -catenin leads to vessel dilatation and vascular leakage in the brain during embryogenesis (Fig 56b, c) (Cattellino et al. 2003). They proposed that translocation of cytosolic β -catenin to the nucleus upon binding of Wnts to Fzd receptor would activate transcription of claudin 3 to stabilize tight junctions (Fig 56a). Both works indicate an important but different role of Wnt signaling for maintenance of the BBB, suggesting that relocalization to the nucleus of AJ-associated β -catenin or cytosolic β -catenin would have different functions (Polakis 2008).

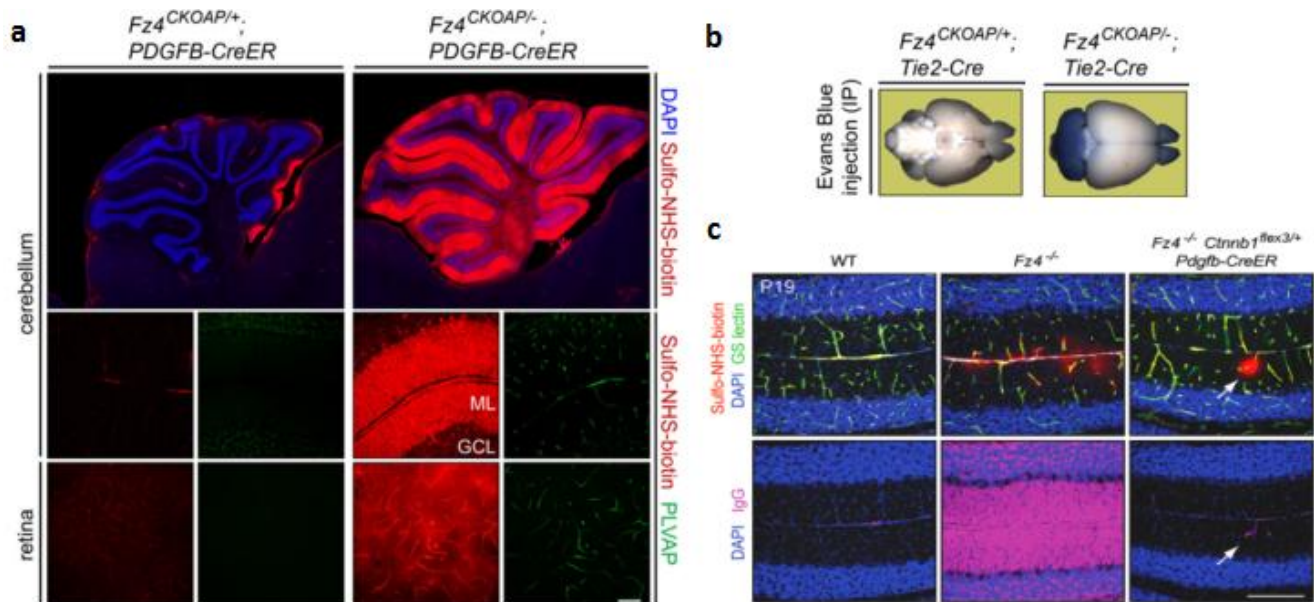


Figure 57: a/b- Injection of Evans Blue of Fz4 deficient in EC mice shows leakage in the cerebellum and retina; c- Leakage arises from the fact that vessels are fenestrated as indicated by Biotin / Mouse igG extravazation(adapted from Wang et al 2013/ Zhou et al 2014)

In a similar manner, Fzd4 is essential for maintenance of the BBB. Deletion of Fz4 in endothelial cells leads to loss of blood brain and retinal barrier integrity as assessed by injection of Evans Blue (Fig 57 a / b). BBB disruption in the Fzd4 EC KO mice was assessed by Biotin extravazation and Mouse igG staining (Fig 57b). Biotin and mouse igG is usually not extravagated. Presence of both out of the vessel indicating loss of the specific properties of the BBB was found in Fzd4 EC KO mice, but not in the Fzd4 EC KO/ β -catenin overexpressing mutant (Fig 57c). This suggests that expression of Fzd4 is essential for maintenance of the integrity and properties of the BBB in adult (Wang et al. 2012). β -catenin would act downstream of Fzd4 to enable expression of BBB specific markers such as Claudin 5(Zhou et al. 2014). These various works show that Wnt signaling is required for acquisition of the BBB characteristics during embryonic development, but also maintenance of the BBB integrity in adult. Both processes seem to implicate different members of the pathway such as the Fzd receptor of β -catenin.

b) Wnt signaling as a regulator of brain vessels function in pathologies

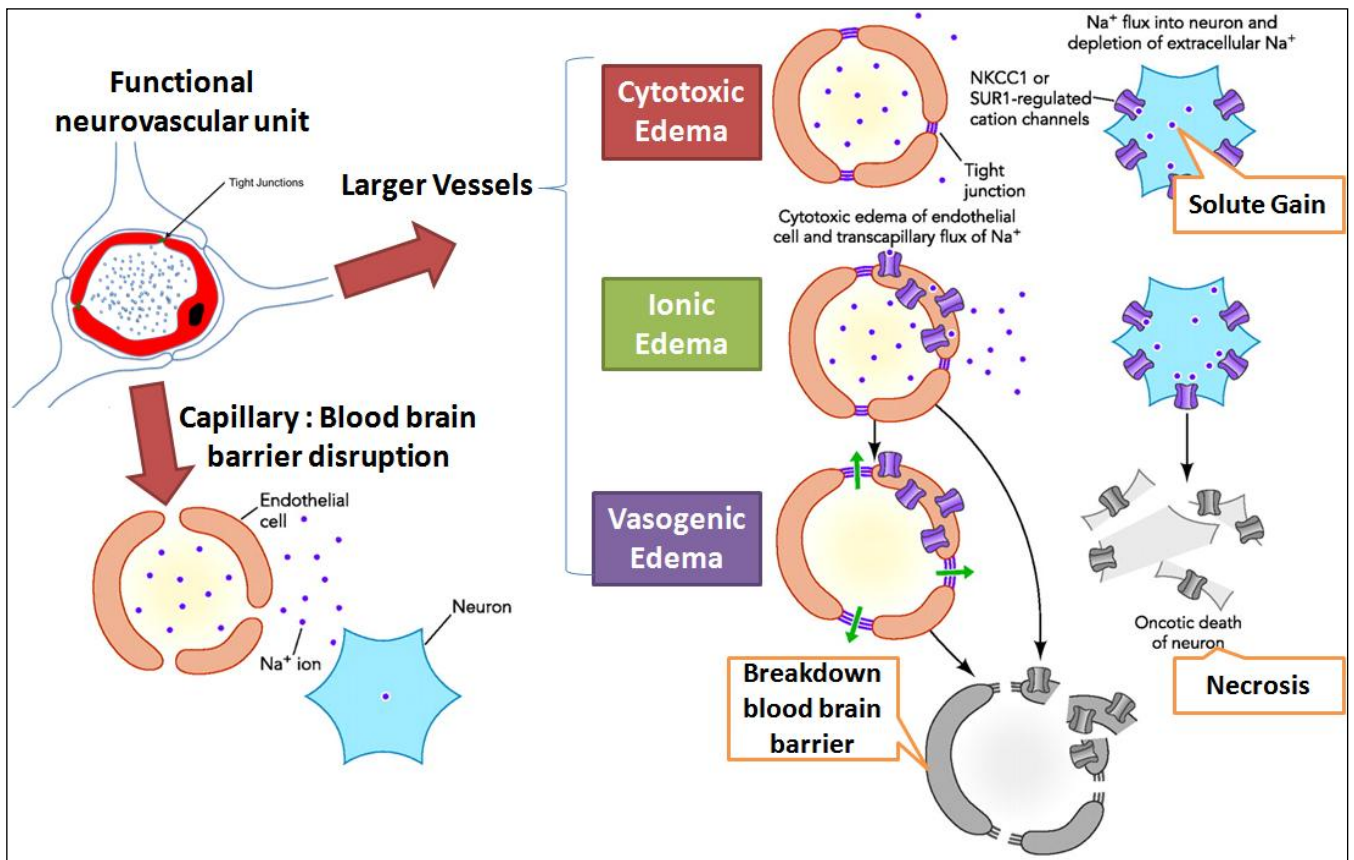


Figure 58: Response to stroke (adapted from Kahle et al. 2014)

Brain vessels are altered in various neurological pathologies. First of all, brain vessels structure is altered after stroke. Stroke leads to cytotoxic edema that affects endothelial cells and neurons leading to solute gain in the cytoplasm of both cells. Ionic edema that consists of transcapillary flux of Calcium Ions then occurs; leading to the vasogenic edema. Leakage occurs and both endothelial cells/ neurons become necrotic (Fig 58). Interestingly, the downstream effectors of the Wnt signaling c-Jun and c-Fos are accumulated early after stroke; indicating that Wnt signaling is activated at early steps of the process (cytotoxic edema)(Sandoval and Witt 2008). Non canonical/ Wnt5a dependant Wnt signaling is also regulated positively by Calcium influx (Liu et al. 2008, Kelly et al. 2011). As calcium flux occurs early in stroke, it could be related to the observed activation of the pathway.

Brain vessels are also altered in Alzheimer disease. Endothelial inflammation and increase of blood flow have been observed in patients suffering from the disease (Kalaria 2002, Marchesi 2011). Increases of permeability of capillaries and leakage have also been described (Biron et al. 2011). Interestingly, modulation of the canonical Wnt pathway has been observed in neurons of Alzheimer affected subjects. This pathway would be downregulated in such subjects and restoring the pathway using chemical agents would decrease the severity of the pathology (Kitazawa et al. 2011, Wang et al. 2011). More recently, it was shown that Wnt5a and Fzd-5 were up-regulated in brain of mice suffering from Alzheimer and that the constituent of amyloid plaques, beta-amyloid peptide stimulated Wnt5a and Fz5 expression in cortical cultures. The Wnt5a activated pathway would be able to regulate neuroinflammation and would aggravate the pathology (Bei Li. 2011).

Parkinson disease is also a pathology where brain vessel function is altered. Increase of blood flow in subjects affected by the disease has been described (Kortekaas et al. 2005, Rite et al. 2007, Hutton. 2010). Several proteins have been shown to have a role in the process such as Glucose transporters; ApoE or PKC (Nassia Methia 2001, Youdim et al. 2003). However, no direct links between Wnt signaling and Parkinson disease have been described for the moment. Interestingly, various ubiquitin ligases have been linked to the disease; Parkin that gave the name to the disease (Shimura et al. 2000) but also various other proteins linked to the proteasome (Fornai et al. 2005, Li et al. 2006, Meray and Lansbury 2007, Fishman-Jacob et al. 2009, Ullrich et al. 2010). These processes have been described in the neuronal cell but not in the endothelial cell.

Finally, Wnt signaling has been linked to formation of neuroblastoma. Wnt3a and Dvl would favor RhoA signaling and neural retraction in these cells (Tsuji et al. 2010). Proapoptotic stimuli would induce GSK3 activation in these cells (Bijur and Jope 2001), while the Wnt5a/Ror2 pathway would be upregulated in these cancer cells (Rebagay et al. 2012). Augmentation of blood flow and pressure has also been described in this disease (Wong et al. 2013)

SH3 domain of ZO-1 recruits a serine protein kinase leading to its phosphorylation. The GK module is homologous to the enzyme that catalyzes the conversion of GMP to GDP. However, ZOs are assumed to be enzymatically inactive. The C-terminal domain is different between the ZOs and would be responsible for their specific functions (Fig 60). These functions can be modified by a variety of agents. Glucocorticoid augments expression of ZO1, increasing transendothelial flow resistance, while Wnt factors such as Wnt3a would also increase monolayer permeability via ZO-1 (Polette et al. 2005).

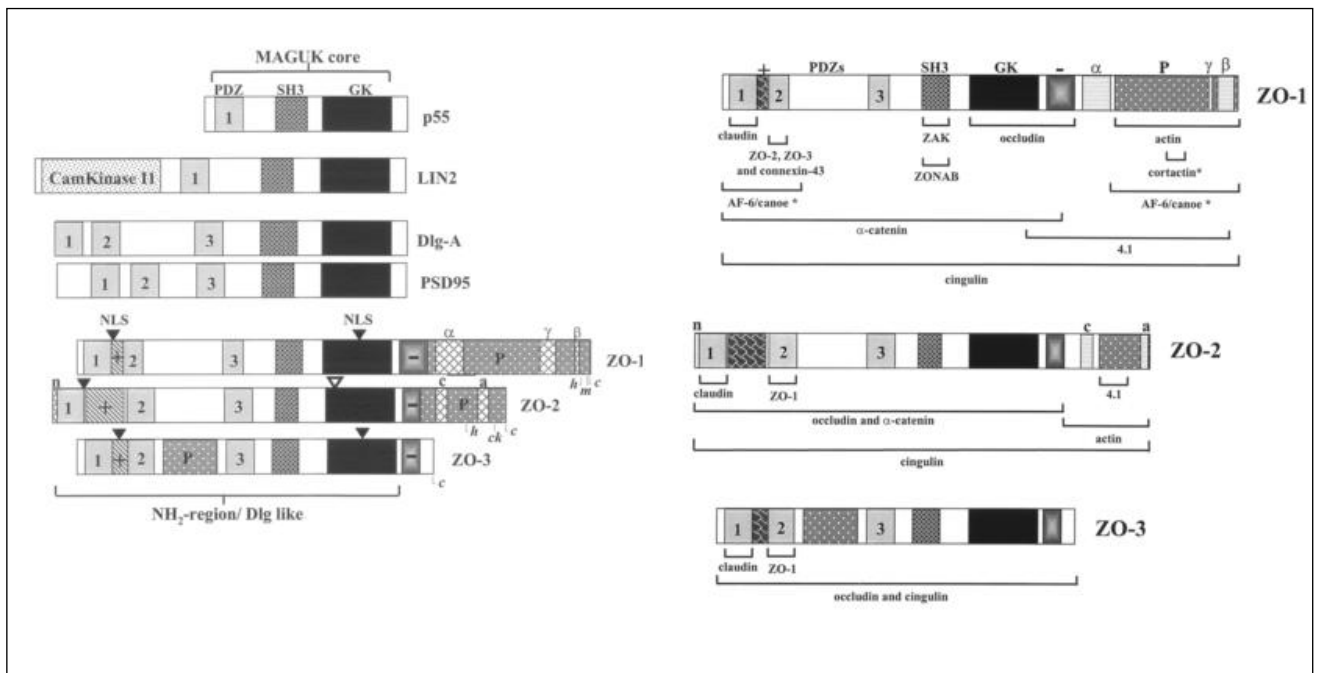


Figure 60: Structure of MAGUK Proteins (adapted from González-Mariscal et al 2000)

The three MAGUK proteins of the TJ are phosphorylated. Initially, it was observed that ZO-1 from a low-trans epithelial electrical resistance (TER) strain of MDCK cells contained almost twice as much phosphate as that from the high-TER strain. This suggests that tyrosine phosphorylation of ZO proteins would weaken junctional sealing (Gonzalez-Mariscal et al. 2000). In a similar manner, the phosphorylation level of ZO-2 is significantly higher in cells with disassembled TJ via Calcium chelation when compared with confluent monolayers. This is due to the action of both PKC and cAMP-dependent protein kinase. This suggests that the phosphorylated state of ZO-2 restrains its capacity to operate at the junctional complex (Avila-Flores et al. 2001).

b) Interplay between β -catenin and ZO1

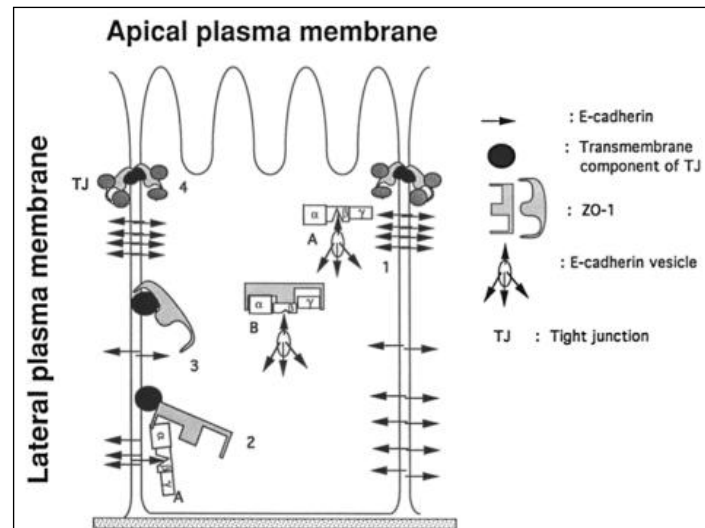


Figure 61: Proposed model for the formation of TJ (Rajasekaran et al 1996)

Interplay between ZO-1 and β -catenin was first described in 1996. ZO-1 coprecipitated with β -catenin, while E-cadherin was detected in β -catenin immunoprecipitates that exclude ZO-1, suggesting that the binding of ZO-1 to β -catenin would weaken the interaction of the proteins with E-cadherin. The proposed model was that β -catenin would form a shuttle with ZO-1 from the cytosol to the cell surface early in the development of tight junctions, β -catenin would then dissociate from ZO-1 to bind E-cadherin (Fig 61) (Rajasekaran et al. 1996).

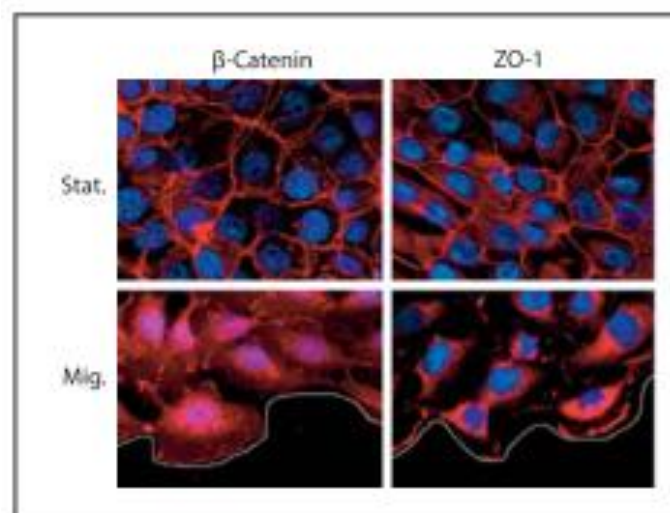


Figure 62: Differential expression and localization of B-catenin and ZO-1 in migratory versus stationary MCF10A human breast cells (adapted from Polette et al 2007)

More recently, it was shown that while ZO-1 is specifically enriched at the TJ of confluent epithelial and endothelial cells, it can localize at the nucleus of subconfluent cells or at the edge of wounded monolayers, suggesting that its nuclear localization is inversely related to the extent and maturity of cell contact (Fig 62) (Balda 2003). ZO-1 interacts with ZONAB that co-localizes with ZO1 at the TJ and the nucleus, where ZONAB acts as a transcription factor to activate targets that regulate permeability and cell cycle progression (Nie et al. 2009, Pozzi and Zent 2010). In a similar manner, β -catenin is junctional in confluent cells and translocates to the nucleus in migrating cells, where it acts as a transcription factor (Fig 62) (Polette et al. 2005).

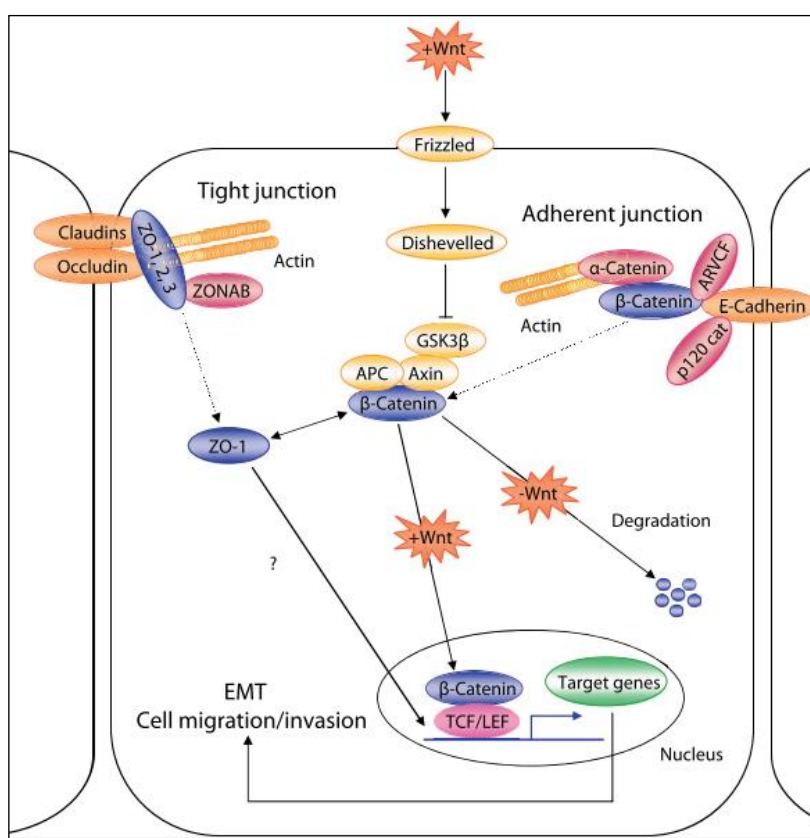


Figure 63: Interaction of ZO1/ β -catenin during EMT transition (Polette et al 2007)

Further evidence of the interplay between β -catenin and ZO-1 is that the cytoplasmic/nuclear relocalization of β -catenin and ZO-1 from the adherens and tight junctions is a common process of the epithelial-mesenchymal transition (EMT) associated with tumor invasion, leading to expression of vimentin and matrix metalloproteinase-14 (Fig 63) (Polette et al. 2007).

c) Interplay between c-Jun and ZO2

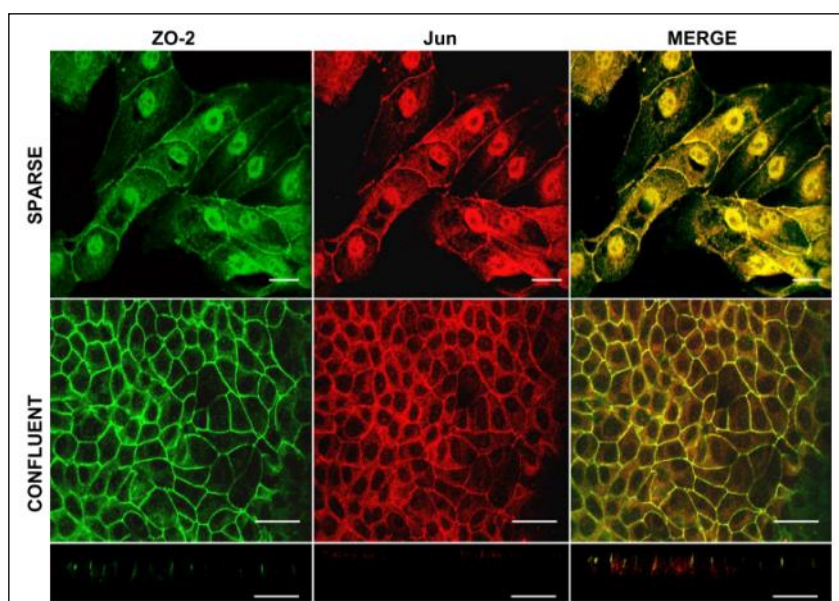


Figure 64: In subconfluent cultures, ZO-2 and Jun are found at the nuclei and cell borders, while in the confluent condition, they are only detected at the cell membrane (Betanzos et al 2007)

ZO-2 was first identified as a ZO-1 binding protein. ZO-2 also has a shuttling activity. As ZO1, ZO-2 localizes to the nucleus in sparse cells, where it co-localizes with the splicing factor SC-35 and relocalizes at the cell membrane in confluent cells (Fig 64)(Avila-Flores et al. 2001, Jaramillo et al. 2004).

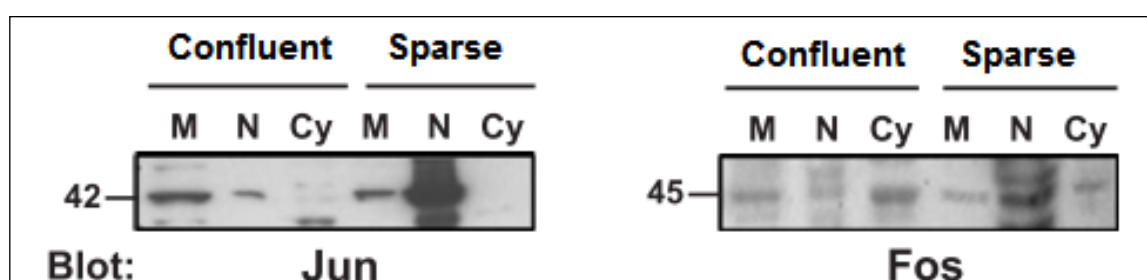


Figure 65: In subconfluent cultures, ZO-2 and Jun are found at the nuclear fraction, while in confluent cultures, they are only detected in the membrane fraction as indicated by cell fractionation (Betanzos et al 2007)

After cell fractionation, in a similar manner as ZO1, ZO2 is detected in the nuclear fraction(N) in sparse cell culture and only at the cytoplasmic membrane fraction(M) in confluent cell cultures (Fig 65) (Betanzos et al. 2004).

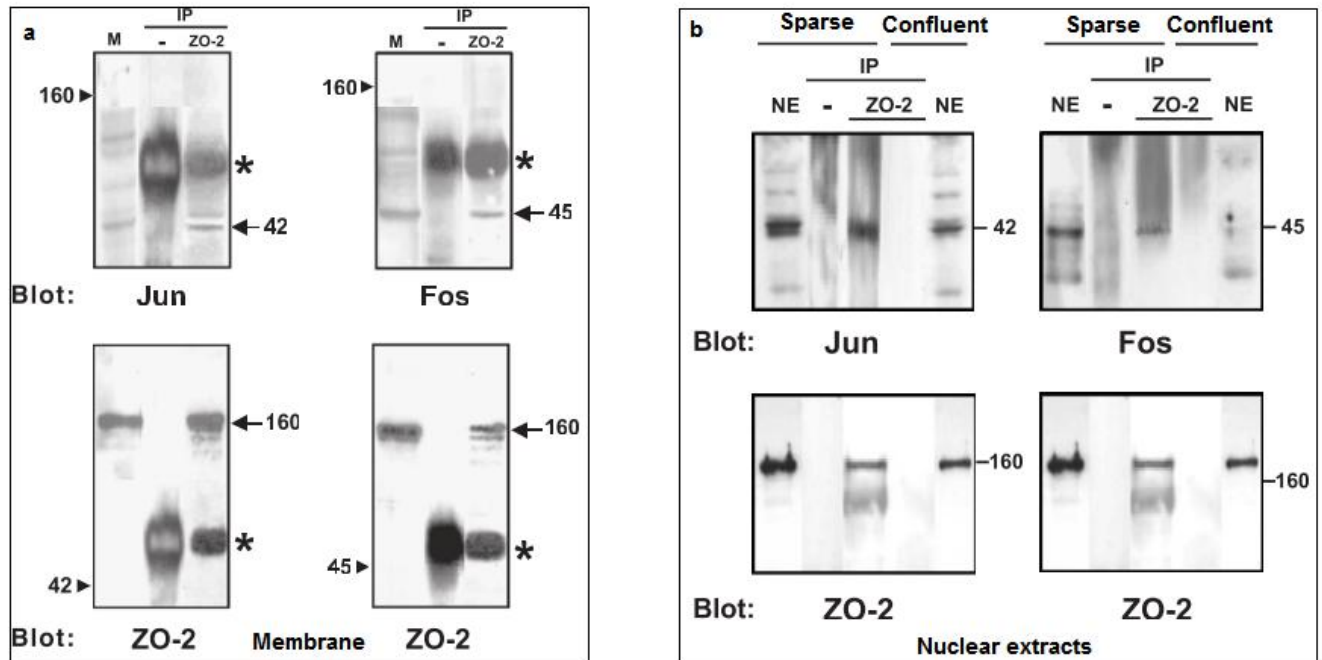


Figure 66: ZO-2 immunoprecipitation realized from membrane (a) and nuclear extracts (b) from sparse and confluent cell cultures (Betanzos et al. 2004)

Pull-down were realized on membrane (M) or nuclear (N) fraction from confluent and sparse cell cultures. Interaction between ZO-2 and transcription factors Jun and Fos was detected in the membrane fraction in confluent cells and in the nuclear fraction in sparse cells, indicating that both proteins would translocate together to activate their target in the nucleus (Fig 66). ZO-2 (but not ZO-1) down-regulates in a dose-dependent manner the expression of a AP-1 reporter system, that indicates activation of the non canonical Wnt pathway. Although both ZO proteins have the capacity to travel to the nucleus under conditions of diminished cell-cell contact, each one modulates different gene promoters. The current model is that ZO2 segregates c-Jun at the TJ, inhibiting non canonical pathway, while under activation, ZO2 detaches from the TJ – liberating c-Jun, thus promoting the non canonical Wnt pathway (Betanzos et al. 2004).

3) MUPP1 acts as a bridge between TJ and Wnt signaling

MUPP1 (multiple PDZ domain containing protein-1) is a member of the LNX family of protein that is present at the TJ. *In silico* predictions indicate that PDZRN3 could interact with MUPP1, indicating that the protein could be a link between PDZRN3 and TJ. MUPP1 is a member of the LNX protein family that shares a high degree of similarity with LNX1/2 and its paralogue PATJ. MUPP1 contains an amino terminal L27 domain and 13 PDZ domains, while PATJ has the same architecture but with ‘only’ 10 PDZ domains. MUPP1 can form homodimers or dimers with LNX1 and 2 via their PDZ domains (Flynn et al. 2011); suggesting that PDZRN3 would also be able to interact with MUPP1.

a) MUPP1 is important for tight junctions stability

MUPP1 was first identified as an interacting partner of the serotonin receptor type 2C. Hamazaki et al. showed that MUPP1 is located at tight junctions of epithelial and endothelial cells, where it binds claudins and acts as a scaffolding protein, anchoring these proteins to the F-actin cytoskeleton.

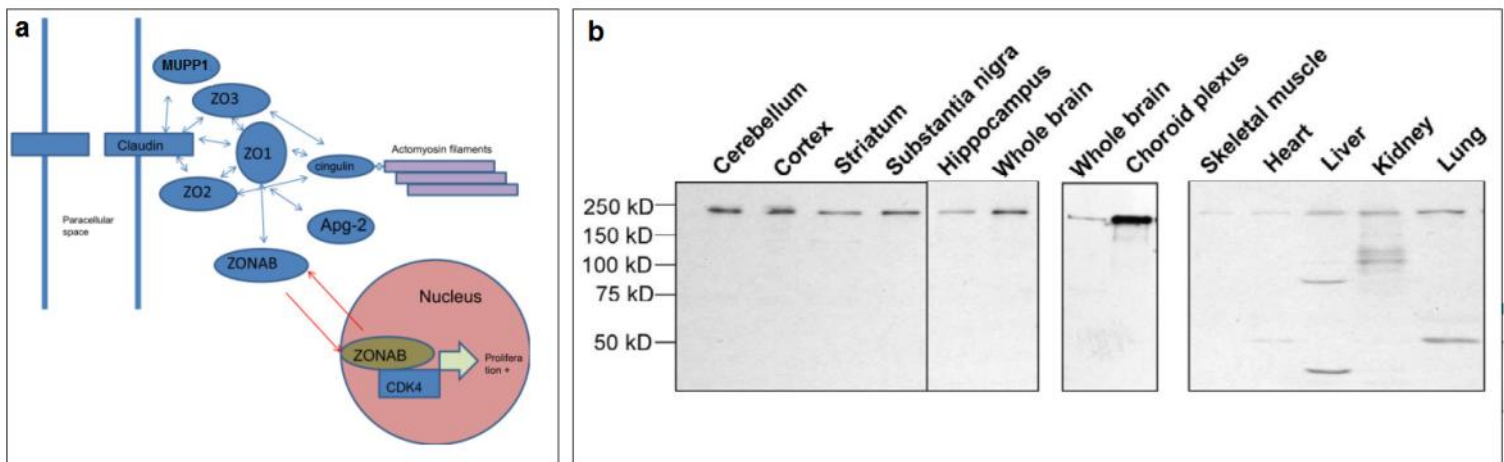


Figure 67: a- Interaction of claudins with scaffolding proteins ZOs and MUPP1; b- Western blot showing expression of MUPP1 in brain tissues (adapted from Soini et al 2011 and Sitek et al 2003)

Disruption or redistribution of MUPP1 compromises the epithelial/ endothelial barrier in a similar manner as ZO1. Oncoproteins have been shown to induce mislocalization of MUPP1 or its paralog PATJ, resulting in disruption of TJs and causing apicobasal polarity defects in epithelial cells leading to the EMT transition (Fig 67a) (Lanasa et al. 2007). Finally, in a similar manner to ZO-1, MUPP1 is

phosphorylated and detaches from TJs in response to hypertonic stress, making the TJs more porous (Then et al. 2011). Consistent with this role, MUPP1 was shown to be strongly expressed in brain, where TJs are important for the integrity of the blood brain barrier (Fig 67b) (Sitek, Poschmann et al. 2003).

b) MUPP1 acts as a scaffold in the Crumbs complex

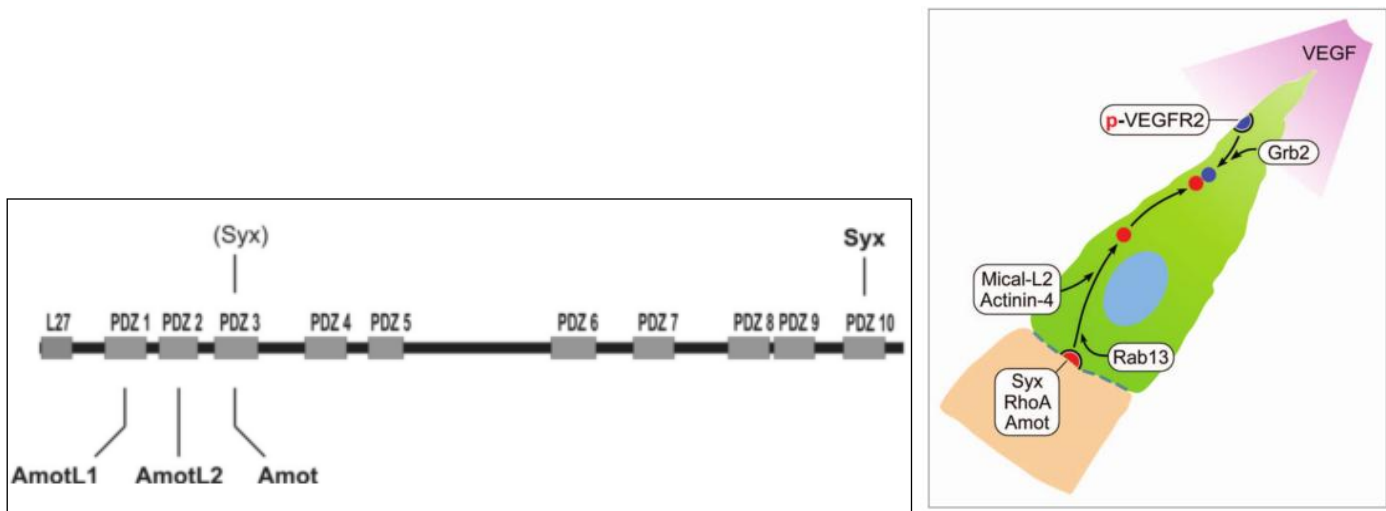


Figure 68: a- Interactions of MUPP1/ Patj (first 10 PDZ domains are identical in MUPP1 and Patj); b- Relocalization RhoA to Leading edge by the Crumbs complex (Ernkvist et al. 2009)

The ternary complex formed of MUPP1 (or its paralogue Patj), Angiomotin (Amot) and Syx is called the Crumbs complex. MUPP1 (or its paralogue Patj) acts as a scaffolding protein in the complex by interacting with Angiomotin (Amot) via its 3 first PDZ domain and Syx via its 10th PDZ domain (Fig 68a). The crumbs complex is a regulator of migration. Angiomotin (Amot) and Syx bind the RhoA GTPase exchange factor (Rho-GEF) at the tight junctions, and control the targeting of RhoA to the lamellipodia (Fig 68b). Knock-down of *Amot* or *Syx* blocks migration of intersegmental arteries in zebrafish, confirming that the directional migration of capillaries is maintained by the the Amot - Patj/Mupp1 - Syx complex (Ernkvist et al. 2009).

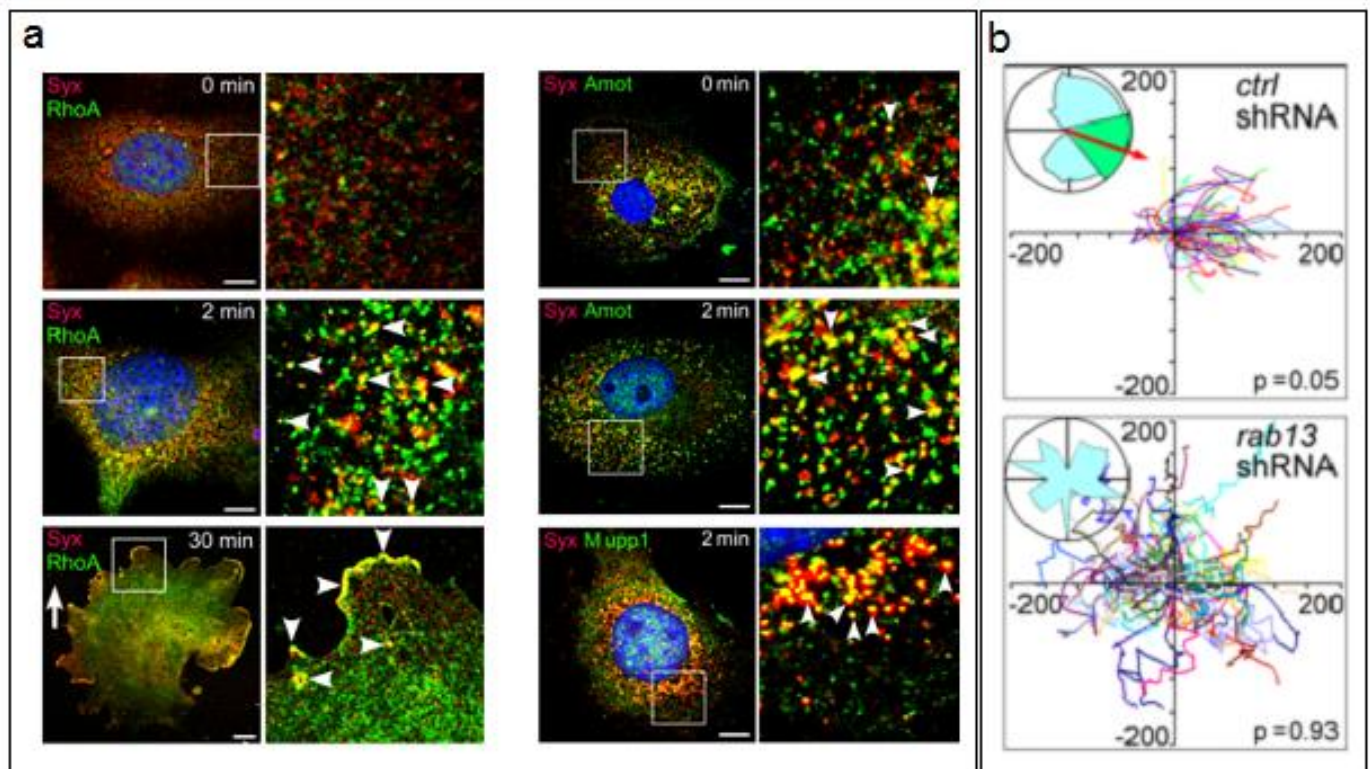


Figure 69: a- Syx /RhoA /Amot /MUPP1 and Rab13 colocalize in response to VEGF.A , as detected 2mins after treatment in vesicles and 30mins after treatment at the leading edge of migrating cells; b - Recycling vesicles are essential for polarized migration as depletion of *Rab13* disrupts polarity of migrating cells (Wu et al. 2011)

The Crumbs complex would regulate relocalization of RhoA to the lamellipodia via endocytic vesicles, as RhoA / Syx / MUPP1 colocalize with Rab13. The Syx/ /MUPP1 / Amot associated complex would induce recruitment of RhoA in Rab13-positive vesicles at the TJs (Fig 69a). The vesicles would then translocate to the leading edge of migrating cells by membrane trafficking. At the leading edge, Rab13 associates with Grb2, targeting Syx and RhoA to Tyr1175- phosphorylated VEGFR2 (Wu et al. 2011). Interestingly, knock-down of *Rab13* impairs directional migration (Fig 69b), confirming that the recycling endosome is essential for polarization of endothelial cell. Together with previous studies that demonstrated regulation of Rac signaling by Rab5-dependent trafficking, this confirms that membrane trafficking is an important regulator of Rho GTPases localization and activity.

c) MUPP1 as a bridge between Tight Junctions and Crumbs complex

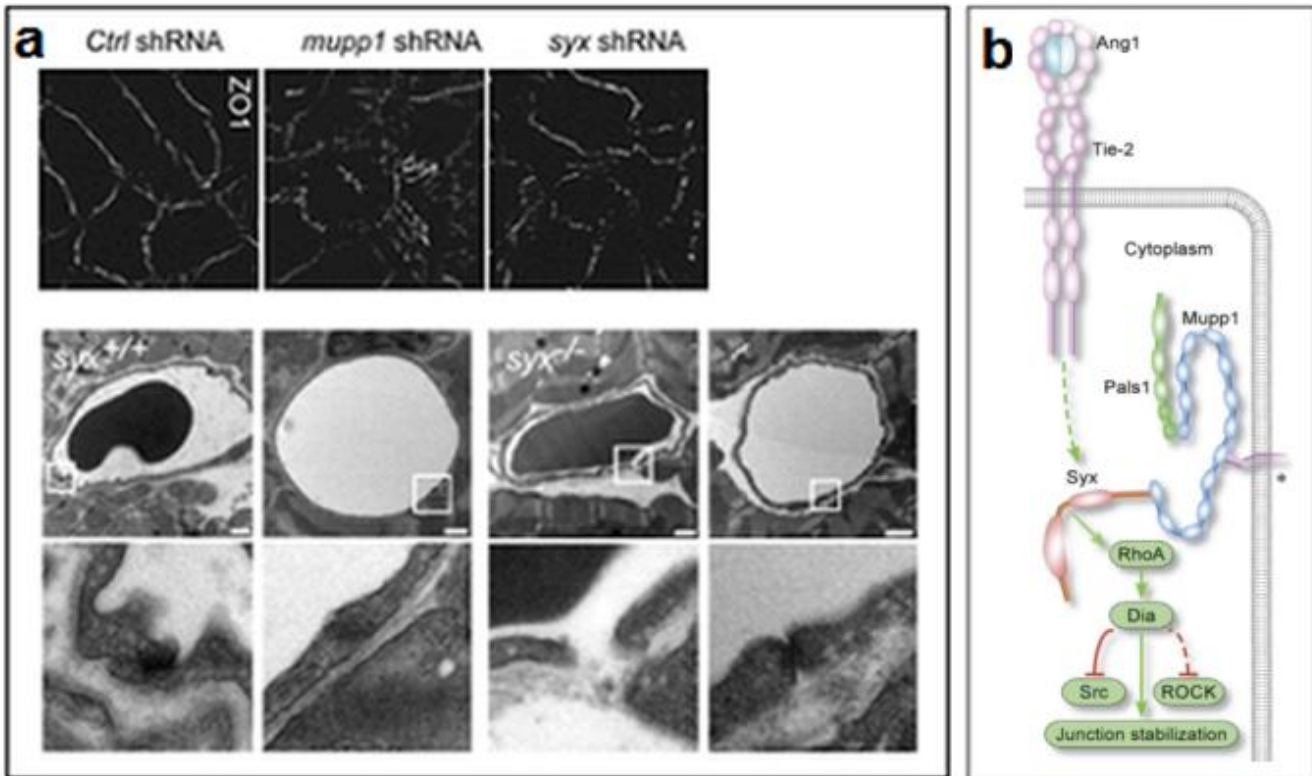


Figure 70: a -Depletion of *Mupp1* and *Syx* disrupts junctional integrity as shown by ZO1 stainin and Transmission electron micrographs of sections of ventricle myocardium; b- Model of regulation of Junctional stability via MUPP1 (Ngok et al. 2012)

Loss of *Mupp1* and *Syx* alters structure of junctions *in vitro*, while the KO mice of *Syx* shows malformation of capillaries associated to vascular leakage, indicating that both are required for maintenance of TJs and Endothelial barrier integrity (Fig 70a) (Ngok et al. 2012). The model proposed by Ngok et al is that *Syx* is recruited to endothelial junctions by *Mupp1*, where it forms a complex with members of the polarity complex. This interaction results in the localized activation of *RhoA* and *Dia* that suppresses activities of *Src* and *ROCK*, leading to junctional stabilization. In contrast, the absence of *Syx* or *MUPP1* would result in junction disassembly and increased permeability, through the unopposed activities of *Src* and *ROCK* (Fig 70b) (Ngok et al. 2012). These different works show that *MUPP1* is required for both TJ stability and endothelial migration.

METHODS

A) Detailed protocols

1) Yeast Two Hybrid experiment

mDvl3 lacking the DIX domain (amino acid 106 to 716) was subcloned into pGBTK7 in-frame with the DNA binding domain of galactosidase-4 (GAL4). Yeast two-hybrid screening and assays were performed as described in the Clontech protocol (MatchMaker system3, Clontech, K1612-1). AH109 cells expressing GAL4–Dvl3 Δ DIX were combined with Y187 cells expressing the mouse E11 embryo cDNA library (Clontech, 638868). The mating mixture was plated on SD/ -TRY, -LEU, -HIS, -ADE plates. From colonies obtained after transformation, more of 500 colonies tested were His positive/LacZ positive. The library plasmids from those colonies were rescued, amplified by PCR, and sequenced.

2) Expression constructs

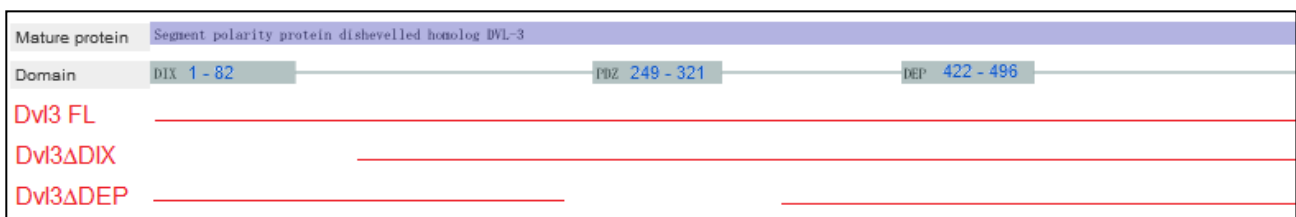


Figure 71: Dvl3 sequence used for cloning in each corresponding plasmids in red

The cloning of Dvl3-green was described previously (Descamps et al. 2012). To generate Dvl3-Myc, the full coding sequence of mDvl3 (amino acid 1 to 716) was cloned in pcDNA3.1-mDvl3-myc his. To generate Dvl3 Δ DIX -Myc, the coding sequence of mDvl3 excluding the DIX domain (amino acid 106 to 716) was cloned in pcDNA3.1-mDvl3-myc his. To generate Dvl3 Δ PDZ, the coding sequence of Dvl3 excluding the PDZ domain (amino acid 1 to 218 and 329 to 716) was cloned in pcDNA3.1-mDvl3-myc his. Fzd4-HA was provided by Dr. Tomas Kirchhausen (Yu et al. 2007). Fzd4- GFP was provided by Dr. M. Montcouquiol.

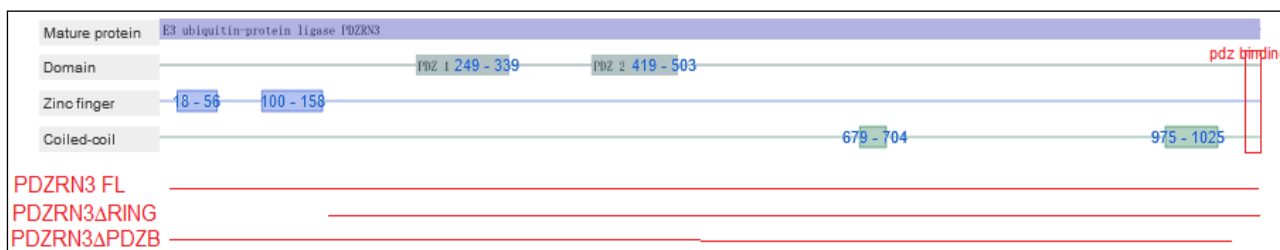


Figure 72: PDZRN3 sequence used for cloning in each corresponding plasmids in red

The full coding sequence of PDZRN3 (amino acid 1 to 1066) was cloned in pcDNA3.1-V5-His (Invitrogen) to generate PDZRN3-V5, using the plasmid coding for human PDZRN3 (NM_015009.1) provided by Dr. Makoto Inui (Ji-Ae Ko 2006). The PDZRN3 Δ PDZB-V5 plasmid was produced by cloning the sequence of PDZRN3 excluding the PDZ binding motif TTV (amino acid 1 to 1056) in pcDNA3.1-V5-His. The PDZRN3 Δ RING plasmid was provided by Dr. Makoto Inui.

3) Analysis of mRNA expression by quantitative RT-PCR

For RT-PCR analysis, 1 μ g of total RNA from mouse tissue or cell extracts was reverse-transcribed: PCR was performed using IQ SYBR Green supermix (Bio-Rad). An MJ Research Opticon and the following parameters were used for real-time PCR: 95°C for 5 minutes followed by 34 cycles of 95°C for 30 seconds, 60°C for 1 minute, 72°C for 30 seconds, 76°C for 1 minute and 80°C for 1 minute. Negative controls without RT were prepared in parallel for each RNA sample. All experiments were performed in triplicate and differences in cDNA input were compensated by normalization to expression of B-actin. Selected primers indicated below:

		Forward primer (5' to 3')	Reverse primer (5' to 3')
<i>m beta-actin</i>	NM_007393	ATTTCTTTTGACTTGCAGGC	GGAGGAGCTGGAAGCAGCC
<i>m PDZRN3</i>	NM_018884.2	CTGACTCTTGCTCCTGCATCGGGACTC	ATGGGCTCCTTGGCTGTCTTGAAAGC
<i>h beta-actin</i>	NM_001101	ATTTCTTTTGACTTGCAGGC	GGAGGAGCTGGAAGCAGCC
<i>h PDZRN3</i>	NM_015009.1	ATTATTGAGGTCAACGGCAG	AGGGCCATGATATGTTCAAAG-

4) Cell culture

HEK293T were cultured in DMEM supplemented with 10% FBS (Hyclone) and penicillin-streptomycin. HeLa cells were cultured in RPMI supplemented with 10% FBS and penicillin-streptomycin. Human umbilical vein endothelial cells (HUVEC) were cultured in EGM-2 media (Lonza, CC-3156) supplemented with EGM-2 Single Quots (Lonza, CC-4176), and plated on 1% gelatin-coated dish. MS1 (mouse pancreatic islet endothelial cell line) were cultured in RPMI supplemented with 10% FBS and penicillin-streptomycin, and plated on 0,2% gelatin-coated dish. All these cells were serum starved with DMEM plus 1% FBS/0.25%BSA.

a) Wnt conditioned media production

Wnt3a and Wnt5a producing mouse L cells (American Type Culture Collection ATCC) were cultured in DMEM medium, 10% fetal bovine serum (FBS) and penicillin-streptomycin supplemented with G418 (0,4 and 0,6mg/ml respectively). Conditioned medium (CM) was harvested as described in ATCC protocol. Wnt5a CM was produced in DMEM medium, 0.5% FBS and penicillin-streptomycin, while Wnt3a CM was produced in DMEM medium, 10% FBS and penicillin-streptomycin.

b) Cell transfection / transduction

Plasmids were transfected using Jetprime (Polyplus) following the manufacturer's protocol (final concentration of 1.5 µg/ml for HEK293, 0.5µg/ml for HeLa). Lentivirus were transduced using Protamin sulfate (4µg/ml) at a multiplicity of infection of 20 (MOI). SiRNA were transfected using Interferin (Polyplus) at a final concentration of 30nM. Selected siRNAs sequence are detailed below

		Reference / Produced by	Sequence
<i>h PDZRN3</i>	NM_015009.1	SR307944A (Origene)	CGGCACTAGAGTATACAATTCCTTC
<i>h PDZRN3</i>	NM_015009.1	SR307944B (Origene)	CGATCCAAATGACTACATTGGAGAC
<i>h PDZRN3</i>	NM_015009.1	SR307944C (Origene)	GCATGTACAGGAAAGTTGTGGATG

c) Chemical treatments

Ly.72632 (sigma) was used at 10 μ m (sigma). Phorbol myristate acetate(pma) (sigma) was used at 1 μ g/ml (YU ET AL. 2007). Dynasore (Santa Cruz) was used at 0,25M (MIKELS AND NUSSE 2006).

d) Proliferation (MTT) assay

Proliferation was assessed 0, 24, 48, 72 hours after cell seeding. MTT (3-(4, 5-dimethyl-2-thiazolyl)-2, 5-diphenyl-2H-tetrazolium bromide) (0,5mg/ml) was added to cell media for 4hours. The MTT is incorporated into living cells and reduced to formazan. Addition of DMSO induces solubilization of formazan into a purple soluble solution that can be quantified by fluorescence at 570nm. The measured optical density correlates with the number of living cells.

e) Luciferase reporter assay

In order to study the canonical pathway, HELA cells grown in 48-well culture plates were transiently transfected at 60-70% confluence with 0.2 μ g/ml of 8XTOPflash reporter (Nusse lab), 0.1 μ g/ml of b galactosidase reporter and 0,2 μ g/ml of various plasmids. The total quantity of DNA in the transfection mixes was adjusted to a total of 0,5 μ g/ml using an empty vector. 24 after transfection, cells were activated overnight with Wnt3a conditioned medium as indicated. Luciferase activities were measured using the Luciferase Reporter Assay system (Promega) according to the manufacture's specifications. The firefly luciferase activity was normalized to b galactosidase activity. In order to analyze the non canonical pathway, HELA cells were transiently transfected with 0.2 μ g of AP1 reporter, 0.1 μ g of b galactosidase reporter (to evaluate efficiency of transfection) and various plasmids as indicated for individual experiments.

5) *Protein analysis*

a) Western Blot

For Western Blot analysis, organ tissues or cells were lysed for 30 minutes in RIPA buffer (1% Nonidet P-40, 0.5% deoxycholate, 0.1% sodium dodecyl sulphate, 50mmol/L Tris, pH 8.0, 2 μ g/ml aprotinin, 10 μ g/ml leupeptin, 200 μ M AEBSF, 1mM benzamidine, 1 μ M orthovanadate, 1nM okadaic

acid). Cell lysates were cleared by centrifugation at 14 000 g for 10 min. The various fractions were dosed using BCA quantification kit (Thermo scientific). 25µg of each fraction were then resolved by 7,5% SDS-PAGE (1mm) and probed with indicated antibodies. Binding of antibodies to the blots was detected using Odyssey Infrared Imaging System (LI-COR Biosciences).

b) Immunoprecipitation assay

Immunoprecipitation assays were done on HEK293T after transfection or tissue homogenates. Lysates were incubated 1hour with primary antibody at +4°C with gentle agitation. After this 25 µl of protein G-Sepharose slurry were added and samples were incubated overnight at +4°C. Beads were washed three times and subsequently resuspended and boiled in 60µl of loading buffer for SDS-PAGE (H2R).

c) Cell fractionation

For Cell fractionation, cell lysates or tissues lysates are resuspended in BH Buffer (Pipes pH6.8, KCl 10mM, MgCl₂ 1,5mM, Sucrose 250mM, EGTA 1mM, EDTA 1mM) and potterized 20times on ice. After a centrifugation at 800g for 5mins, the supernatant is collected and spinned at 100.000g for 1hour. The pellet is then resuspended in BH buffer + Triton1% + SDS 1% and identified as the 'cell membrane fraction'. The supernatant is collected and corresponds to the 'cytoplasmic fraction'. The pellet obtained after the 800g centrifugation is washed in BH buffer and spinned at 2700g for 5mins 3 times. The cleaned pellet is then resuspended, placed as a cushion on top of a sucrose buffer (Sucrose 1M) and spinned at 2700g for 5mins. The pellet is then resuspended in a Tris buffer (Tris pH 7.4, NaCl 10mM, MgCl₂ 3mM, EGTA 1mM, NP40 0.05%) and spinned at 2700g for 20mins. The pellet is resuspended in a HEPES buffer (Hepes pH 7.9, NaCl 300mM, MgCl₂ 1,5mM, EDTA 2mM) that lyses the nuclear membrane. After a 20 min incubation, the lysate is spinned at 10000g for 20mins. The pellet is identified as the 'nuclear membrane fraction' and the cytoplasm as the 'soluble nuclear fraction'. The cytoplasmic fraction is normalized using tubulin, the nucleic fractions with Histone H1 and the membrane fraction using Ve-cadherin.

d) Ubiquitylation assay

For ubiquitylation assay, pRK5-HA-UB-Wt (17608, Addgene), pRK5-HA-UB K48 (17605, Addgene) that codes for lysine 48-only-ubiquitin and pRK5-HA-UB K63 (17606, Addgene) that codes for lysine-63-only ubiquitin were purchased at Addgene. HEK293T were transfected with Dvl3-myc (0,5µg/ml), one of the ubiquitin coding plasmids (0,5µg/ml) and PDZRN3-V5 OR empty plasmid (0,5µg/ml). Immunoprecipitation was then realized as described before using a myc antibody.

6) Immunocytochemistry

a) Immunocytochemistry

Immunofluorescence analyses were realized on HELA cells or Huvecs. The cells were fixed in Formalin 4% for 20mins and permeabilized using Triton 0,2% for 2mins before 30min of saturation in PBS+5% BSA. The cells were incubated with the primary antibody (diluted in PBS +1% BSA) for 1 hour at 37°C and with the secondary antibody for 30mins at room temperature.

b) Internalization assay

For Internalization assay, the cells were transfected with the protein we wanted to follow. After activation, the cells were fixed and incubated with a first primary/ secondary antibody directed against the target diluted in PBS + 1% BSA. After a step of permeabilization (Triton 0,1% for 5mins), the cells are incubated with a second couple of primary / secondary antibody directed against the target. For example, we could use a rabbit – polyclonal antibody revealed with a Alexa 568 anti rabbit before permeabilization, and a mouse – monoclonal antibody revealed with Alexa 488 anti mouse. The first antibody reveals the membrane located target (Alexa 568 – in red) and the second antibody reveals the membrane located and endocytosed target (Alexa 488 – in green).

7) Immunohistochemistry

a) Paraffin sections

Tissues are fixed in Methanol / Methanol80% + DMSO 20% or Paraformaldehyde 4%. The samples are then dehydrated with successive ethanol/ xylene baths and then included in a paraffin block. 7 μ M sections are then realized. Cells are colored in blue using Hemalun for 2mins. Red blood cells were stained in pink using Eosin (Sigma) for 30secs.

b) Cryosections

Tissues are fixed in paraformaldehyde 4% and transferred in Sucrose 30%. Once tissue has sunk in sucrose solution, it is embedded in OCT embedding solution. 10 μ M sections are then realized.

c) Vibratome sections

Tissues are fixed in paraformaldehyde 4% and included in agarose 4%. 100 μ M slices are realized using a vibratome (Leica).

d) In toto embryo staining

Embryos (10.5dpc maximum) are dissected and fixed in 4% paraformaldehyde overnight (or Methanol 80%+DMSO 20% for 2 hours). Once the embryo sunk to the bottom of the solutions, it is permeabilized in 0,5% Triton for 2hours. Embryos are then blocked in milk 5%+ Triton 0,5% for 2hours. Embryos are then incubated with antibody for 24-48h in milk 5%+Triton 0,5%. Embryos are then placed in 100% glycerol for 48h. Once the embryo sunk to the bottom of the solution, it is transferred in 75% glycerol+ 25% gelatin and finally transferred in 50% glycerol before being mounted. The embryos were imaged using a confocal microscope (Olympus FSV 100).

e) Dab staining

Endogenous peroxydases are saturated by incubated the samples in PBS + 3% H2O2 for 20mins. The cells were incubated with the primary antibody (diluted in PBS +1% Horse serum and 0,5% Triton)

overnight at 4°C, with the secondary antibody and then peroxylase for 2h at room temperature respectively. The DAB revelation Kit is then used for the revelation of the peroxylase.

f) Immunofluorescence

Immunofluorescence analyses were realized on various tissue samples. The samples were incubated with the primary antibody (diluted in PBS +1% HS+0,5% Triton) for 1 hour at 37°C or ON at 4°C and with the secondary antibody for 1 to 4 hours at room temperature. Alexa 488/ 568 / 647 goat-anti mouse/ rabbit and donkey anti-goat were used as secondary antibody. The DNA was counterstained by 4',6-diamidino-2-phenylindole (DAPI) or Hoechst.

8) Image analysis

Cells were imaged using a ZEISS microscope at 63X and analyzed using AXIOVISION. For colocalization studies, cells were analyzed with a Olympus laser scanning confocal microscope using multichannel scanning using a 63x/1.4 ApoPlan oil immersion objective. Three-dimensional projections were deconvoluted using Autoquant(Mediacybernetics) and digitally reconstituted from stacks of confocal optical slices by Imaris software (Bitplane).

9) In vitro assays on endothelial cells

a) 2D tubulogenesis assay

The Capillary-like tube formation assay was carried out by plating Growth factor-reduced Matrigel® (Becton Dickinson) plated on the bottom of μ -slide angiogenesis plate (Ibidi), and allowing it to gel at 37 °C for 1 hr. 150,000 cells/well, were seeded on Matrigel and incubated at 37 °C, in growth media with 20 ng/ml purified recombinant human VEGF165 (RandD Systems). After 6 h at 37 °C, formation of tube-like structures was examined under an inverted light microscope (Olympus) at 4.2 \times magnification. Two images were taken for each well. The number of lumen per field, the length/number of branches per branch point and cell covered area were quantified (Axiovision, Cell profiler).

b) Wound assay

The assay was carried out by plating endothelial cells on each well of culture-inserts (Ibidi) and allowing them to reach confluence. After a 4h serum starvation, culture-inserts were removed, and cells were stimulated with control or Wnt3a conditioned medium (diluted 1/20). The subsequent gaps were imaged at baseline and 8 hr later. The area of the gaps was quantified using Axiovision.

c) 3D tubulogenesis (cytodex) assay

For 3D tubulogenesis assay, HMVECs were transduced with a GFP expressing lentivirus and transfected with various siRNAs. Gelatin-coated microcarrier beads (Cytodex 3; Sigma) were incubated with the HMVECs. When the cells reached confluence on the beads, equal numbers of HMVECs-coated beads were embedded in fibrin gels in a μ -slide angiogenesis plate (Ibidi). For preparation of fibrin gels, bovine fibrinogen (2.5 mg/mL; Sigma) was dissolved in Dulbecco's modified eagle medium (DMEM)/10% FBS. Aprotinin (0.05 mg/mL; Sigma) was added. Clotting was induced by the addition of thrombin (1.2 U/mL) (Sigma). Following 60 min of incubation, human fibroblast were plated on the top of gel and EBM2 medium added. The model of Cytodex was validated in many studies (Larrivee et al. 2007, Bignon et al. 2011)

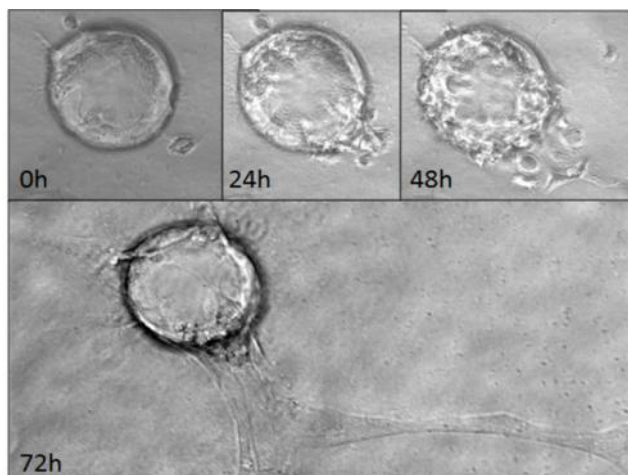


Figure 73: Formation of tube-like structures after cytodex plating (control condition)

The formation of tube-like structure was imaged by time-lapse videomicroscopy (brightfield) for 72 h under an inverted microscope (Fig 73) (Zeiss). Each sprout was then imaged using Imaris (Bitplane) for analysis.

d) Chemotaxis assay

6 μ l of a solution of Huvecs cells (3millions cells/ml) are seeded in an Ibidi chemotaxis slide (Ibidi). Two chambers are filled with media, and a chemotactic attractant added to one of the chamber, creating a chemotactic gradient in the well containing the endothelial cells. The track of each cell was imaged by time-lapse videomicroscopy (in fluorescence) for 12 h under an inverted microscope (Zeiss). The tracks were analyzed using the Chemotaxis and Migration tool from Ibidi.

e) Permeability assay (Transwell assay)

100.000 Huvecs cells are seeded on the upper chamber of a Transwell in a volume of 250 μ l. 1hour after seeding; the lower chamber is filled with 750 μ l of medium. 24h after seeding, Dextran-FITC (40kDA Sigma) is added to the the upper chamber (C°). 25 μ l of the medium of the lower chamber is collected 5/10/15/30/45/60/90 mins after addition of Dextran. Quantity of Dextran in these samples is assessed by measuring the optical density at Xnm.

f) Junctions disruption by calcium chelation

Treating cells with PBS supplemented with the calcium chelator EDTA (2,5nM) induces disruption of the junctions maintaining cell monolayer progressively. Junctions in Huvecs cells monolayers are disrupted totally after 30mins. This process was imaged by time-lapse videomicroscopy each 30sec under an inverted microscope (Zeiss). The movies were analyzed using Imaris (Bitplane).

10) Experimental animals

a) Cre – Lox system

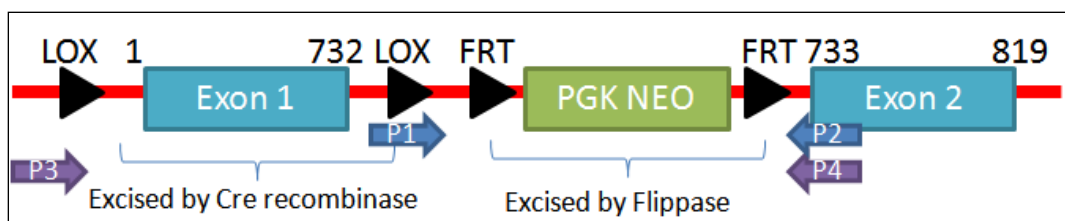


Figure 74: Floxed PDZRN3 mice construct

Floxed *Pdznr3* mice (stock 01750, Riken institute) were generated by Dr Y. Saga (National Institute of Genetics, Japan). The neomycin cassette was removed by flippase-mediated recombination by breeding with *Flp* mice. Floxed *Pdznr3* ($PDZRN3^{fl/+}$) mice were subsequently backcrossed on C57BL6/J background. Interbred, homozygous $Pdznr3^{fl/fl}$ mice exhibit apparently normal development, and are viable and fertile. Tails of pups were genotyped by PCR using the P1/P2 primer set for the wild-type allele and for the Flox allele and the P3/P4 primer set for the KO allele: P1: 5' cgaccacttgctccagtaaccggaag -3'; P2: 5'-gaggctgacataattcccgatcagc -3'; P3: 5' – TCTGGCCTGTCCCATCCAGACAGCTGGAG – 3'; P4: 5'- GGAGATGTTTTAATTCAAGGAGGCTATCAC – 3' (Fig 74). For ubiquitous deletion of the gene, *Ubiquitin C-icre* transgenics were bred in a background of $Pdznr3^{fl/fl}$ mice. *Ubiquitin C-icre Pdznr3^{fl/fl}* male were then mated with $Pdznr3^{fl/fl}$ females.

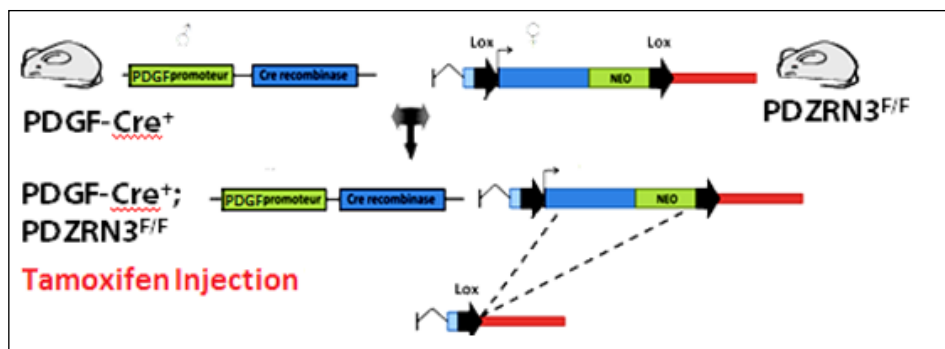


Figure 75: Mating of PDGF-icre *Pdzrn3*^{fl/fl} males with *Pdzrn3*^{fl/fl} females

For endothelial cell-specific deletion, *PDGF-icre* (Claxton et al. 2008) transgenics were bred in a background of $Pdznr3^{fl/fl}$ mice. *PDGF-icre Pdznr3^{fl/fl}* male were then mated with $Pdznr3^{fl/fl}$ females. Deletion of the *Pdznr3* gene was induced by activation of the cre recombinase by tamoxifen injection. *Pdznr3* gene deletion was induced in utero by an injection of 3mg of tamoxifen intraperitoneally at 7.5 or 10.5 day post coitum (Boulday et al. 2011). For retinal vascularization analysis, *Pdznr3* gene deletion was induced by intragastric injection of 50µg of tamoxifen at day 1 and day 3 after birth. For gene deletion in adults, 1mg of tamoxifen was injected subcutaneously for three successive days.

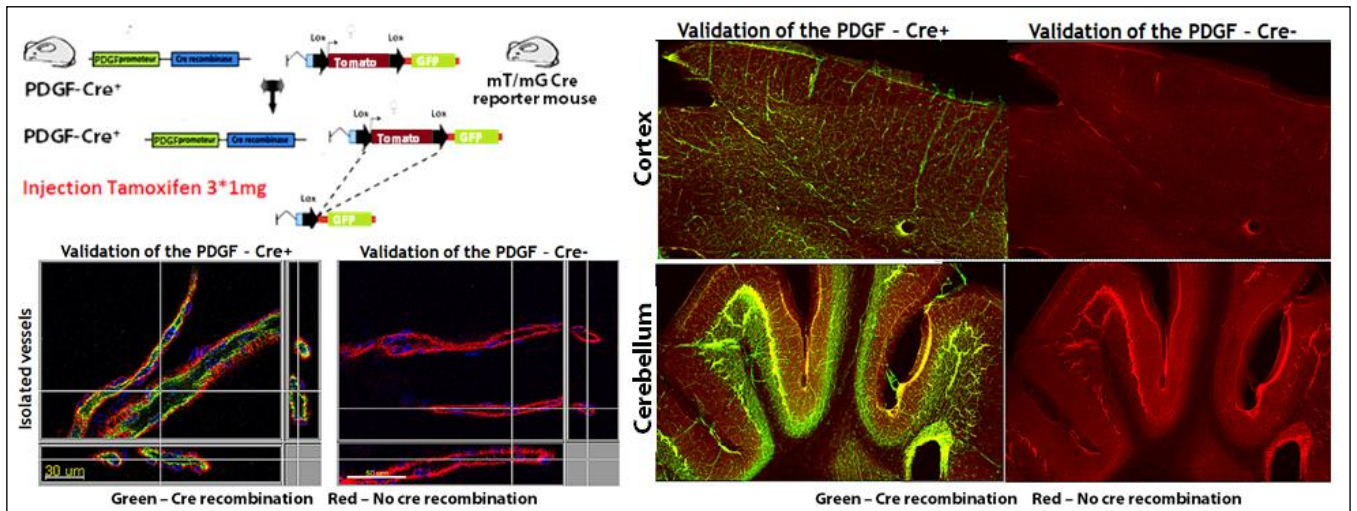


Figure 76: Validation of the PDGF icre recombinase system using the mT/mG reporter mice

Efficiency and specificity of activation of the cre – recombinase efficiency was assessed by mating *PDGF-icre* males with *mT/mG* reporter mice. The *mT/mG* mice expressing red fluorescence prior to, and green fluorescence following, Cre-mediated recombination. Recombination (as indicated by green fluorescence) is detected only in endothelial cells after 3 injections of 1mg of tamoxifen in adults.

b) Tetracyclin activated system

We have generated mice that had integrated the gene coding for *Pdzrn3* followed by the sequence coding for a V5 cassette under the control of a transactivator. These mice were subsequently backcrossed on C57BL6/J background. Interbred, homozygous *Pdzrn3 – V5* mice exhibit apparently normal development, and are viable and fertile. For endothelial cell-specific overexpression, *Tie2 – tta* (Tet-off) transgenics were bred in a background of *Pdzrn3-V5* mice. *Tie2 - tta* male were mated with *Pdzrn3- V5* females. Tails of pups were genotyped by PCR using the P1/P2 primer set for the PDZRN3-V5 coding gene: 5' CAGCTTGAGGATAAAGGCGCT-3'; P2: 5'- CTTCGAGCTGGACCGCTTC-3'.

c) Injections

Intraocular injection was performed using the injector from World precision instruments. 0.5μl of Dynasore (200μM in 6%DMSO; 94 % Ethanol) was injected in one eye of the animal at the speed of 50nl/sec; the other eye was injected with a solution of 6%DMSO; 94% Ethanol.

11) *Surgery*

a) Retinal vascularization analysis

For immunofluorescence of mouse retinas, eyes from mice sacrificed at P5 were fixed in 4% paraformaldehyde at 4 °C for 1 h and dissected, before being incubated at 4 °C overnight with FITC labeled - isolectin B4 (Sigma Aldrich) diluted in PBS buffer with 0.5% Triton X-100, and 5% horse serum. Ratio of Vascular area was quantified by delineating the area where vessels were present and related to the total area of the retina. The number of branch points per field was quantified after Isolectin staining of the retina. The number of regressing branches was quantified by counting the number of collagen positive/ isolectin negative branches. Proliferation was quantified by counting the number of Brdu positive nuclei in the vessels and related to the isolectin stained area per field (Fig 77).

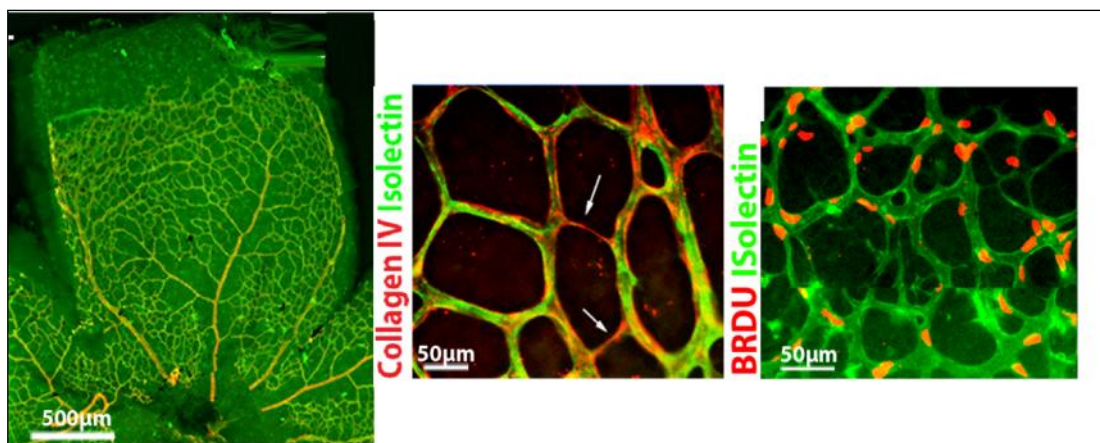


Figure 77: Quantification of Vascular area/ Regression and Proliferation

Retinas were analyzed at P12. At this stage, a deep plexus parallel to the superficial plexus and an intermediate plexus that is orthogonal to the deep and superficial plexus (Fig78). The number of branch points in the superficial and deep plexus was quantified; the orientation of the vessels of the intermediate plexus was quantified using the manual tracking module of Image J. The angles formed by each of the descending vessels were then compared and analyzed using the Chemotaxis and Migration tool from Ibidi (Fig 79).

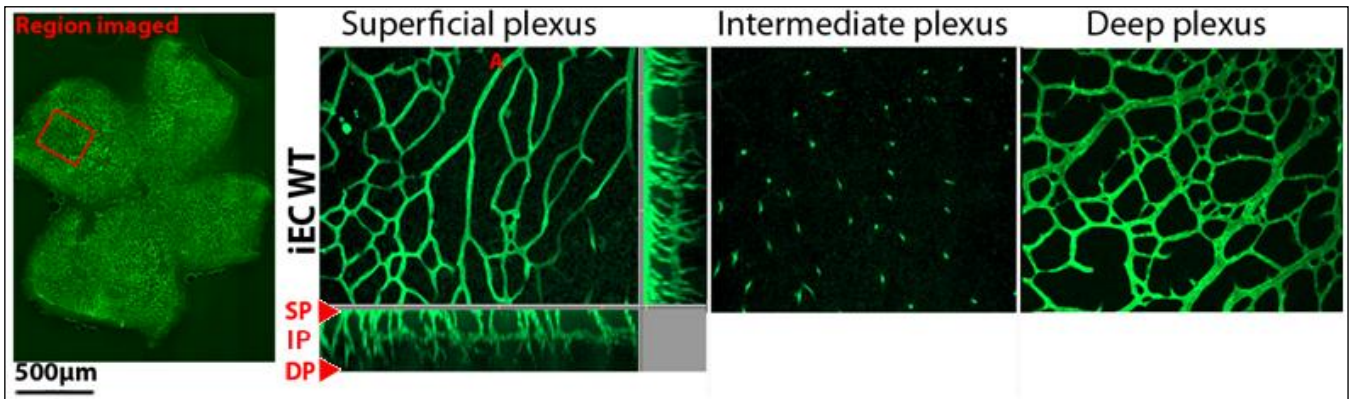


Figure 78: Region of retina imaged for quantification ; Representative view of the superficial plexus; a plane of the intermediate plexus and the deep plexus

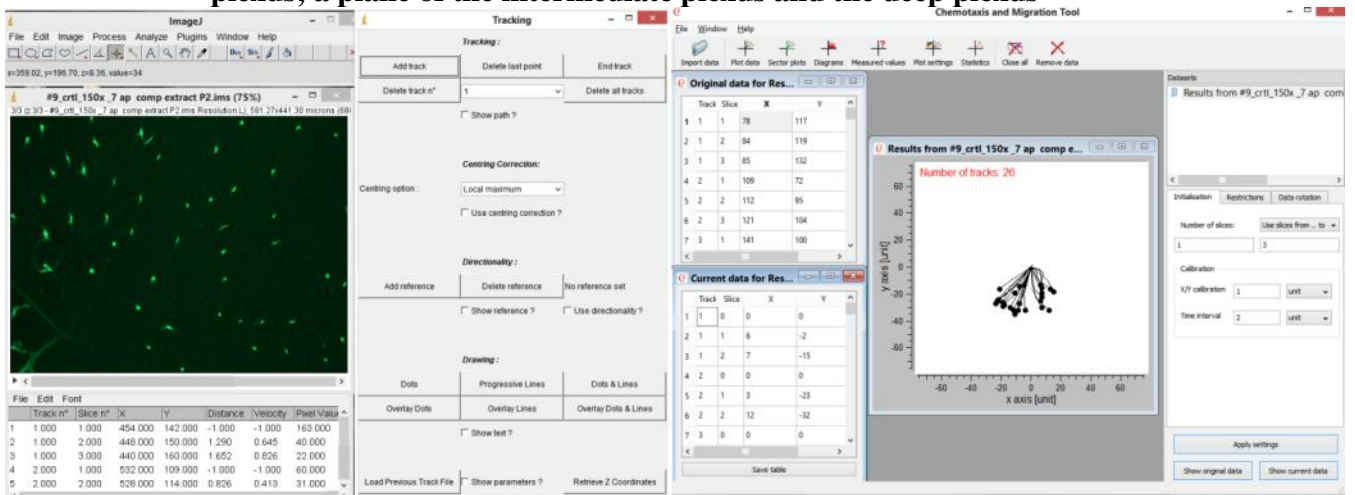


Figure 79: View of the module of Tracking (Image J) and data analysis (Chemotaxis and migration tool Ibidi)

b) Middle cerebral artery occlusion

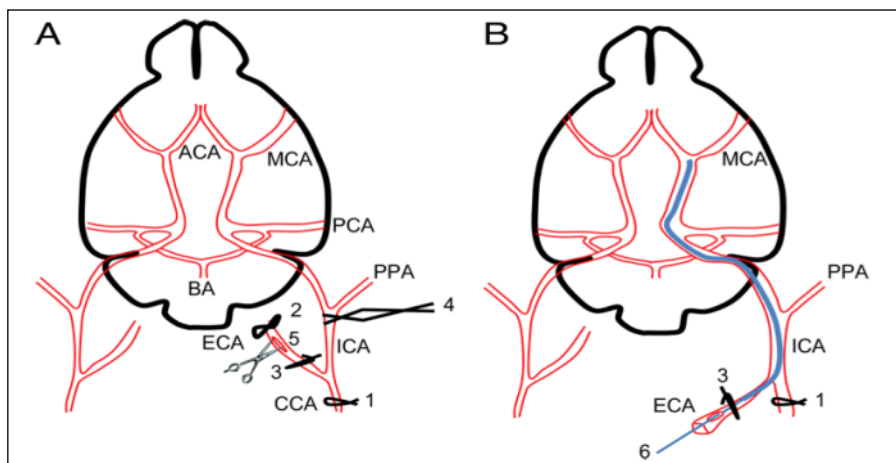


Figure 80: Scheme of the cerebral artery occlusion procedure (Rousselet et al 2012)

Cerebral infarcts were produced by 90mins occlusion of the middle cerebral artery (MCAO) followed by reperfusion. A silicone-coated 8-0 monofilament (Doccol) was introduced into the internal carotid artery and advanced of a distance of about 10mm to occlude the middle cerebral artery under anesthesia (isoflurane). After 90mins, the animals were anesthetized again and the filament withdrawn. Animals are monitored 1, 3 and 24 hours after MCAO using these criterias. On a scale of 1 to 6, 1 denotes animals showing a normal comportement; 2 denotes animals showing rotation of the ischemic side; 3 - constant rotation on the ischemic side; 4 - barelling; 5 - unconsciousness; 6 - death.

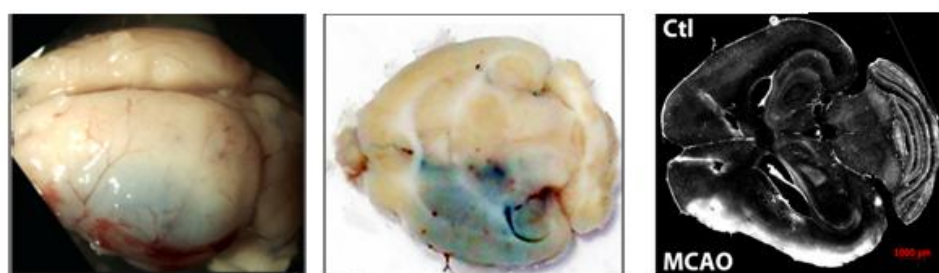


Figure 81: Evans Blue diffusion after MCAO: a- whole brain; b- 100µm vibratome slice observed under white light; c- observed at 545nm

For Evans blue extraction, both brain hemispheres were separated, weighed and stored at -80°C . The tissues were lysed in 1ml of PBS using a tissue-lyser and spinned at 15000g for 30mins. To 500µl of the supernatant, 500µl of trichloroacetic acid was added – and the mixture stored at 4°C overnight. After a centrifugation at 15000g for 30mins, the supernatant is collected and optical density measured at 610 and 690nm. The quantity of Evans blue per gram of tissue is then calculated using a standard curve.

For evaluation of Dextran extravasation, 500µl of a solution of FITC - Dextran 70kDa (Sigma) was injected in the ventricle. After 5mins of circulation, the mouse was decapitated and the brain prepared for OCT embedding and cryosection (Hoffmann et al. 2011, Bouleti et al. 2013).

MRI imaging was done in collaboration with the RMSB (www.rmsb.u-bordeaux2.fr). Diffusion, volume of edema and anisotropy were measured. A strategy of diffusion tensor imaging was also put in place. Interestingly, MRI strategies have shown that volume of the edema was reduced in some knock out mice(Bouleti et al. 2013), while only diffusion was modified in other cases(Badaut et al. 2011).

c) Aortic ring assay

Dorsal aortas from mice sacrificed at P5 were surgically removed, cut in several rings. A 10- μ L drop of Matrigel® (Becton Dickinson) was added to a well of a μ slide angiogenesis plate (Ibidi). Aortic explants were put on top of the gel, covered with a 10- μ L drop of gel, and incubated 15 min to solidify. 40 μ L of EGM-2 media (Promocell) was then added and the explants were cultured for 72h.

d) Evaluation of vascular leakage in embryo and pups

Pregnant mice were anesthetized and 15.5dpc embryos were extracted from the yolk sac with the umbilical chord still attached. 5 μ L of a 4mg/ml solution of Rhodamin –Dextran (Invitrogen) was injected in the kidney; after 5mins, the embryo was killed by decapitation and the head embedded in OCT for cryosection. In pups, 10 μ L of the same solution was injected in the ventricle (Choi 2011).

e) Micro computer tomography

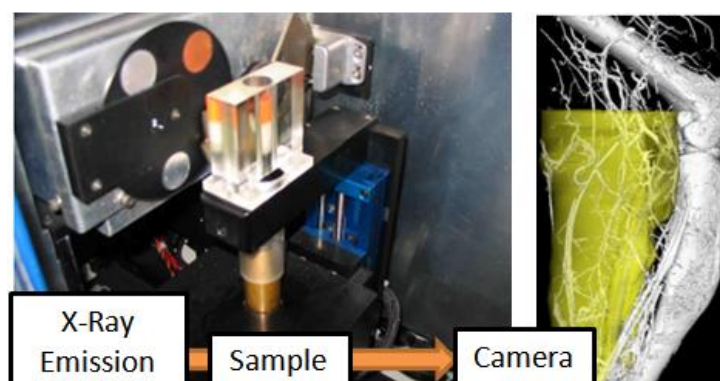


Figure 82: Scheme indicating position of the x-ray lamp, sample and camera in the microCT

The liver, heart and the hind limb vasculature were imaged with a high-resolution micro-CT imaging system (GE eXplore Locus SP), set to a 0.08-mm effective detector pixel size. The apparatus used for imaging the vessels was the eXplore Locus Micro-CT scanner from General Electric Healthcare® with spatial resolutions of 36 to 7 μ m, and used with the Scan Control® and Reconstruction Utility® programs. Data were acquired in an axial mode as described before (Tirziu and Simons 2005). The quantification parameters were obtained using the Microview ABA® program.

f) Isolation of primary endothelial cells from mouse kidney

Kidneys were removed in PBS-containing CaCl₂ and MgCl₂ (Gibco), minced and incubated for 45 min at 37 ° C in PBS supplemented with collagenase type I (Sigma). The suspensions were triturated with a cannula, filtered through a 70 microns (BD) and 30 microns filter (Miltenyi). Cells were cultured in MEM medium supplemented with D-valine for 5 days. After trypsinization, the cell suspension was incubated with anti-CD31 (Pharmingen) and anti-endoglin (Santacruz) antibodies for 30 min, placed in the presence of microbeads coupled with rat IgG (Miltenyi) for 15 min and passaged through a magnetic column (MACS MS columns, Miltenyi), the endothelial cell preparation was recolted.

g) Vessel extraction

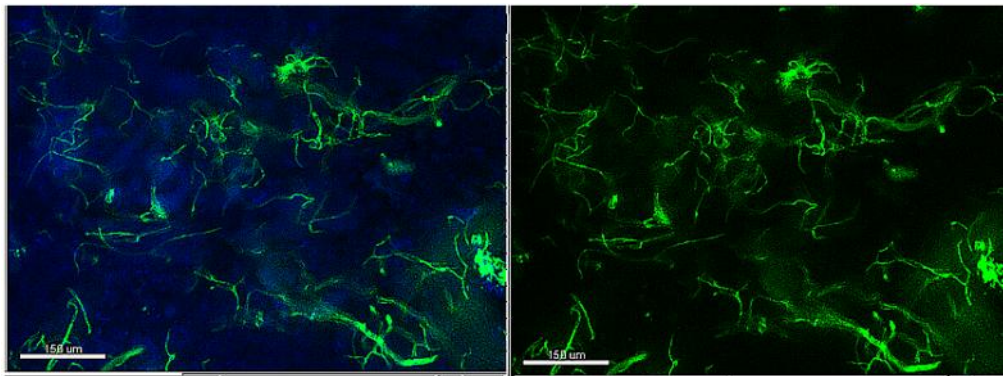


**Figure 83: Vessel extracts from adult - PDGF cre⁺ mT/mG mice injected with tamoxifen
(vessels fluoresce in green; Hoechst staining of nuclei in blue)**

Brain or retina were frozen at -20°C. The tissue is potterized 20times on ice in PBS. After a 10min / 1000g centrifugation, the pellet is resuspended in PBS and placed on top of a PBS / Dextran 17,5% gradient. After a 10min / 4400g centrifugation, the pellet is resuspended and filtered via a 40μm filter (BD). The fraction retained on the filter is then eluted with PBS by inversion of the filter. For optimal extraction of vessels, the vessel fraction can be loaded on a column containing glass beads. After washing with PBS, the purified vessel fraction is recolted by gentle agitation. This fraction is collected as is for western blotting. For immunostaining, after a 10min/13000g centrifugation, the pellet is collected in a paraformaldehyde 4% - Sucrose 2% solution and spinned 30mins at 1300rpm – on a polylysine 0,01% coated – glass slide. After this operation, the capillaries are adherent to the slide.

12) *Statistical analysis*

Results were expressed as means \pm SD. All analyses were performed with appropriate software (GraphPAD Prism). Comparison of continuous variables between two groups was performed by an unpaired t-test and subsequently, if statistical significance was observed, by a non parametric Mann-Whitney test. A value of $p < 0.05$ was considered to be statistically significant.

B) Reagents

1) List of used antibodies

Antibody	Reference	Produced by	Western blot	Immuno-precipitation	Immuno - cytochemisty	Immuno - histochemisty*
HA	11583816001	Roche	1/1000	NO	1/200	NO
rab 5	sc 28570	Santa cruz	1/1000	NO	1/500	NO
v5	46-0705	Invitrogen	1/3000	1/1000	1/1000	ND
Myc	05-724	Milipore	1/3000	NO	1/1000	ND
PDZRN3	sc-99507	Santa Cruz	1/1000	1/1000	1/500	1/100
c-JUN	sc-45	Santa cruz	1/1000	1/1000	1/200	1/100
Active β catenin (8E7)	05-665	Milipore	1/1000	ND	1/500	ND
β catenin	C2206	Sigma	1/3000	ND	1/1000	1/500
α tubulin	B 5-1-2	Sigma	1/8000	ND	ND	ND
phosphorylated c-JUN	9261S	Cell signaling	1/1000	ND	ND	ND
Myc	05-419	Milipore	1/3000	1/1000	ND	ND
GFP	118144600001	Molecular probes	1/3000	1/1000	ND	ND
Clathrin	sc 6579	Santa cruz	1/3000	ND	1/1000	ND
rab11	sc 9020	Santa cruz	1/1000	ND	1/200	ND
Fzd4	AF 194	RandD	1/1000	NO	1/200	1/100
Ubiquitin	U5379-1vl	Sigma	1/3000	ND	1/500	ND
CD31	T-2001	BMA	ND	ND	1/500	1/100
ZO1	617300	Invitrogen	1/1000	1/1000	1/1000	1/200
Ve – cadherin	Sc 6458	Santa Cruz	1/1000	ND	1/500	1/200
Phosphotyrosine	05-1050	Milipore	1/3000	1/1000	ND	ND
c-Fos	Sc 52	Santa Cruz	1/1000	ND	1/500	1/100
MUPP1	104174	Abcam	1/1000	1/1000	ND	ND
Isolectin FITC	L2895	Sigma	ND	ND	1/100	1/100
Rhodamin Phalloidin	R415	Molecular probes	ND	ND	1/1000	1/1000
Collagen IV	Sc 113360	Santa Cruz	ND	ND	1/100	1/100

- Indicates that staining of cryosections / vibratome slices / *in toto* yolk sac works after paraformaldehyde 4% fixation of mouse samples ; ND = non determined

2) Chemical reagents

Reagents used for q RT-PCR

Reagent		Produced by
SYBR [®] Green [®] mix		Applied Biosystems
Isopropanol		BDH AnalAR
Chloroform		Sigma-Aldrich
GelRed [™]		Biotum
10mM dNTP mix		Invitrogen
TRIzol [®] Reagent		Invitrogen
1 kb DNA ladder		Invitrogen
Agarose		Fisher BioReagents
10x PCR buffer		Invitrogen
10x RT buffer		Roche
Glycogen		Invitrogen
DNase 10x buffer		Invitrogen

Reagents used for Western blotting

Reagent		Produced by
Protein G plus agarose		Santa Cruz
RIPA lysis buffer		
Protein ladder		Invitrogen
β -mercaptoethanol		Sigma
Tris		Sigma
Tween		Sigma
Sodium dodecyl sulfate		Sigma
TEMED		Sigma

Enzymes used for q RT – PCR

Reagent	Units	Produced by
RNase inhibitor	40U/ μ l	Roche
M-MLV Reverse Transcriptase (RT)	200U/ μ l	Roche
Taq DNA polymerase	200U/ μ l	Invitrogen
DNase	200U/ μ l	Invitrogen

Reagents used for immunostaining

Reagent		Produced by
Triton X100		Sigma
Trichloroacetic acid		Sigma
Saccharose		Sigma
Paraformaldehyde		Sigma
Bovine serum albumin		Sigma
Donkey serum		Sigma
Hemalun Eosin		Sigma
Glycerol		Sigma

Cell/ In vivo treatments

Reagent		Produced by
Ly72632	Rho kinase inhibitor	Santa Cruz
SP600125	JNK inhibitor	Santa Cruz
Dynasore	Dynamin I inhibitor	Santa Cruz
DMSO	Dimethylsulfoxyde	Sigma
Tamoxifen		Sigma
LiCl	Lithium Chloride	Sigma
FITC-Dextran	40kDA	Sigma

3) Equipments

Apparatus	Reference
Ultracentrifugator	Centrikon T2060
Spectrophotometer	Teccan Infinite M200 PRO
Robot for immunostaining	Ventana Discovery XT
Western Blot membrane imaging	Odyssey LICOR
Micro computer tomography	GE eXplore Locus SP
Time lapse imaging	Zeiss Axioobserver
Confocal imaging	Olympus FSV 100
Bright field imaging	Nikon Microphot FXE; Nikon SM 780800
Electrophoresis generator	Bio-Rad Power Pack 300
Vibratome slices	Leica VT1000S
Cryosections	Microm cryostat microtome
Paraffin sections	Reichert-Jung 2030 BioCut Rotary Microtome
Microcentrifugator	Eppendorf 5415 Microcentrifuge
Cell centrifugator	Jouan GR411
Cell incubator	Nuaire NU-5500E
Hybridization oven	Hybaid Shake n Stack
PCR machine	VWR Uno cycler
Tissue homogenizer	QIAGEN Tissue lyser
Shaker	Labover rotatest; Heidolph unimax 2010 agitator
UV Transilluminator	UVP
qPCR machine	Biorad DNA engine Opticon 2
Balance	Sartorius Scale LC 4201S

RESULTS

Article 1

Frizzled 4 regulates arterial network organization through noncanonical wnt/planar cell polarity signaling

Rationnel	<p>Frizzled4 est essentiel pour le développement vasculaire au niveau de la rétine et du cerveau. Ce travail a consisté à analyser le rôle de la protéine dans le développement vasculaire des organes périphériques dans un contexte physiologique et pathologique en tirant avantage d'un modèle de souris délétée pour <i>fzd4</i>. Le rôle de Fzd4 dans la régulation des fonctions endothéliales et dans la régulation des voies Wnt est aussi abordé.</p>
Résultats	<p>La souris délétée pour <i>fzd4</i> présente un phénotype vasculaire fort dans les organes périphériques. La structure 3D du réseau artériel a été étudiée par une stratégie de tomographie assistée par ordinateur après injection d'un produit de contraste. La souris KO pour <i>fzd4</i> présente une réduction du réseau artériel dans les cœurs et reins, avec perte des vaisseaux de petite taille.</p> <p>La délétion de <i>fzd4</i> par une stratégie de siRNA altère les fonctions de prolifération, de migration et de tubulogenèse des cellules endothéliales in vitro. Les cellules déplétées pour Fzd4 expriment moins de tubuline acétylée, et sont incapables de positionner le centre organisateur des microtubules (MTOC) correctement, ce qui explique le défaut de migration observé.</p> <p>La délétion de <i>fzd4</i> in vitro induit une altération des voies Wnt canoniques et non canoniques, indiquant un rôle majeur de la protéine dans l'équilibre entre les deux voies. Dans le même ordre d'idée, nous montrons que la protéine adaptatrice Dvl3 qui est normalement cytoplasmique est recrutée et activée à la membrane dans les cellules surexprimant Fzd4.</p> <p>Finalement, dans un modèle pathologique d'ischémique du membre inférieur, nous montrons que la délétion de <i>fzd4</i> fait que le réseau vasculaire néoformé 10 jours après ischémie est réduit et désorganisé.</p>
Conclusion	<p>Ces résultats mettent en évidence le rôle clé de Fzd4 dans le développement vasculaire des organes périphériques via une voie de signalisation Wnt /PCP.</p>

a) State of art

Fzd4 is a receptor for Wnt proteins. Binding of the Wnt ligands to the Fzd receptor lead to activation of disheveled proteins and activation of Wnt target genes. Fzd4 can activate both the canonical and the non canonical pathway depending of receptor context. In the canonical pathway, it promotes accumulation of β -catenin and stimulation of LEF/TCF-mediated transcriptional program. In the non canonical pathway, it induces activation of c-jun in a process that depends on PKC (Schulte et al. 2010).

The protein also plays a key role in retinal vascularization where it interacts with norrin. The exudative vitreoretinopathy is caused by mutations affecting the *fzd4* gene. This disease is characterized by a cessation of growth of retinal capillaries, leading to formation of an avascular region in the periphery of the retina. This leads to compensatory retinal neovascularization, which induces in some cases exudation and bleeding / or retinal detachment. Similar defects have been found in the *fzd4* knock-out mice where the retinal vasculature is massively reduced.

b) Hypothesis

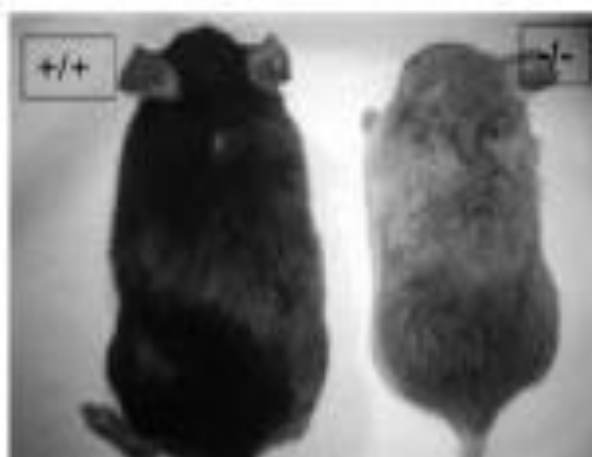


Figure 84: Phenotype of *fzd4*^{-/-} mice

This study was carried out on mice deleted of the *fzd 4* gene. *Fzd 4* deficient mice were smaller and died early (Fig 84). Many studies have shown that Fzd4 is implicated in vessel formation of the retina or

in the brain. The purpose of this study is to measure the role of Fzd4 in vessel formation in peripheral organs and after ischemia.

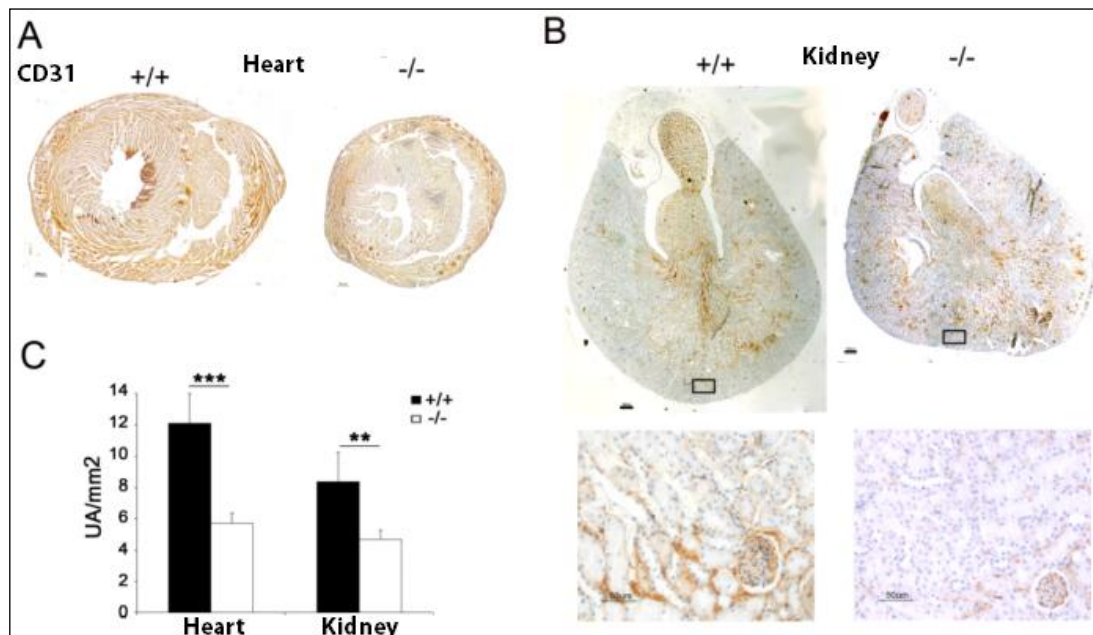


Figure 85: Effect of deletion of Fzd4 on vessel density

Deletion of Fzd4 was found to impact the vascularization of retina. In this study, we assessed if Fzd4 was required for vascularization of peripheral organs such as heart and Kidney (Fig 85).

c) Summary

This study identifies Fzd4 and Dvl3 as essential actors of vascular morphogenesis and remodeling after ischemia. The fact that both proteins modulate activation of the Wnt / non canonical pathway and are essential for the orientation of the endothelial cell *in vitro*; and for neovascularization to occur correctly, identifies for the first time the link between non canonical Wnt pathway and orientation/function of the endothelial cell.

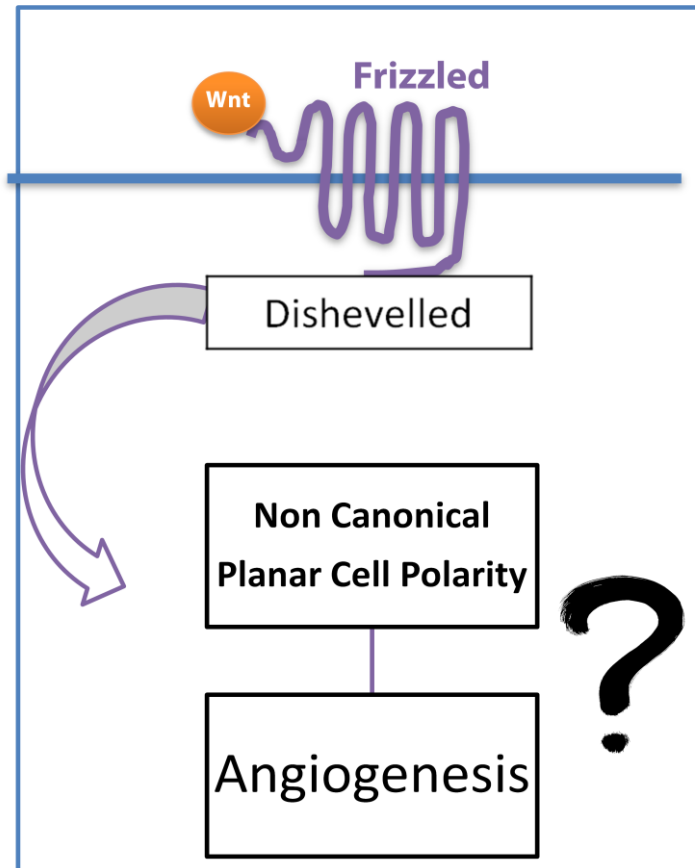


Figure 86: Interaction of Fzd4 and Dvl favor Wnt non canonical pathway to favor angiogenesis

No direct downstream effector of the Fzd/ Dvl complex has been identified yet. Identifying such proteins would be extremely interesting to understand the role of the Wnt non canonical pathway in angiogenesis.

Frizzled 4 Regulates Arterial Network Organization Through Noncanonical Wnt/Planar Cell Polarity Signaling

Betty Descamps, Raj Sewduth, Nancy Ferreira Tojais, Be´atrice Jaspard, Annabel Reynaud, Fabien Sohet, Patrick Lacolley, Ce´cile Allie`res, Jean-Marie Daniel Lamazie`re, Catherine Moreau, Pascale Dufourcq, Thierry Couffinhal, Ce´cile Dupla`a

Rationale: A growing body of evidence supports the hypothesis that the Wnt/planar cell polarity (PCP) pathway regulates endothelial cell proliferation and angiogenesis, but the components that mediate this regulation remain elusive.

Objective: We investigated the involvement of one of the receptors, Frizzled4 (Fzd4), in this process because its role has been implicated in retinal vascular development.

Methods and Results: We found that loss of *fzd4* function in mice results in a striking reduction and impairment of the distal small artery network in the heart and kidney. We report that loss of *fzd4* decreases vascular cell proliferation and migration and decreases the ability of the endothelial cells to form tubes. We show that *fzd4* deletion induces defects in the expression level of stable acetylated tubulin and in Golgi organization during migration. Deletion of *fzd4* favors Wnt noncanonical AP1-dependent signaling, indicating that Fzd4 plays a pivotal role favoring PCP signaling. Our data further demonstrate that Fzd4 is predominantly localized on the top of the plasma membrane, where it preferentially induces Dvl3 relocalization to promote its activation and -tubulin recruitment during migration. In a pathological mouse angiogenic model, deletion of *fzd4* impairs the angiogenic response and leads to the formation of a disorganized arterial network.

Conclusions: These results suggest that Fzd4 is a major receptor involved in arterial formation and organization through a Wnt/PCP pathway. (*Circ Res.* 2012;110:47-58.)

Key Words: blood vessels imaging ischemia transgenic mice vascular biology

During development, blood vessel formation ensures tissue Fzd4 is linked to sterility.¹⁰ We have previously demonstrated growth and organ function in the entire organism. Fzd4 impairs vascular cell proliferation and migration and performs this function through a noncanonical Wnt/PCP-dependent pathway altering golgi organization and tubulin acetylation. Among the Dvl members, we identified Dvl3 as a preferential target of Fzd4, because Fzd4 relocalizes and activates Dvl3 on the apical cell membrane. We report that Fzd4 expression is polarized in cells and organizes with Dvl3 to create a signaling platform favoring -tubulin recruitment and reorganization. Moreover, in postischemic neoangiogenesis, *fzd4* deletion impairs the angiogenic process. In control mice, after surgery, an arterial network is generated that extends directionally toward the extremity of the leg during the revascularization process, where as depletion of *fzd4* induces formation of a disorganized nondirectional and nonfunctional arterial network.

Results

Impairment of Arterial and Arteriolar Formation in the Absence of Fzd4

To elucidate the function of Fzd4 in postnatal development, we studied its vascular expression pattern in *fzd4^{LacZ}* mice, which allows visualization of Fzd4-expressing cells using the -galactosidase reporter driven by the *fzd4* promoter. Our results demonstrated differential expression in the adult vasculature with expression in the aorta, carotid artery, and other large arteries, and no expression in large veins (online Figure I). Frequent *fzd4* promoter activity was detected in the endothelial cell (EC) and smooth muscle cell (SMC) layers of small arterioles and in various vascular beds, including the heart, kidney, and skeletal muscle (online Figure I).

Microcomputed tomography three-dimensional quantitative analysis of the cardiac and renal vasculature was performed in *fzd4*^{-/-} mice. Comparison between *fzd4*^{-/-} and *fzd4*^{+/+} adult mice revealed a striking arterial phenotype with a quantitative reduction in arterial branching and density (Figure 1A, B). In the heart of *fzd4*^{-/-} mice, large coronary arteries enclose the heart and divide to give rise to an arterial network toward the apex that penetrates and perfuses the heart wall. In *fzd4*^{+/+} mice, the large coronary arteries were present, but the arterial network was severely reduced, most notably in the apex and interventricle septum. In the kidney of *fzd4*^{-/-} mice, the main renal artery courses in the renal hilum, dividing into segmental arteries that branch into the lobar arteries, supplying a dense capillary network in the cortex. In contrast, the kidney of *fzd4*^{+/+} mice showed a reduction of the smaller arteries, particularly in the renal cortex while the primary arterial architecture in the renal hilum was conserved. Quantitative polymerase chain reaction analysis of heart and kidney from *fzd4*^{-/-} and *fzd4*^{+/+} pups demonstrated a significant decrease in the arterial marker Ephrin B2 mRNA expression in both the heart (0.370.24-fold) and kidney (0.350.20-fold) of *fzd4*^{-/-} compared to *fzd4*^{+/+} pups (*P*0.05), whereas mRNA for the venous marker Eph B4 was not statistically different between these groups (Figure 1C). Western blot analysis of kidney and heart tissues also confirmed a significant decrease in expression of Ephrin B2 (Figure 1D). These data support the notion that Fzd4 is required for the development of arterioles and capillaries, but is not required for the formation of larger vessels.

Because the loss of *fzd4* induced an impressive vascular phenotype described, we next examined the functional impact of *fzd4*^{-/-} on cardiac and renal function. No difference in diastolic or systolic heart function was observed in any group (Tau and contractile index dP/dt minimum and maximum under basal or dobutamine treatment), and we did not identify any water, acid–base, or electrolyte imbalance when mice were studied under basal conditions (online Table I).

Loss of *fzd4* Altered Vascular Cell Proliferation and Migration

To gain further insight into the cell-autonomous function of Fzd4, we isolated ECs, SMCs, and murine embryonic fibroblasts (MEFs) from wild type and *fzd4*^{-/-} mice (Figure 2A, online Figure II). Primary *fzd4*^{-/-} EC, SMC, and MEF proliferation, analyzed by counting cells positive for BrdUrd, was significantly reduced compared to *fzd4*^{+/+} EC and MEF, respectively (Figure 2B, C, D). Consistent with these findings, *fzd4* knockdown (kd) of *fzd4*^{-/-} MEF and human microvascular EC reduced their proliferation as early as 2 days after culture, confirming an important impact of Fzd4 on EC and MEF proliferation (online Figure III). We next investigated the branching capability of *fzd4*^{-/-} EC in an in vitro three-dimensional matrigel assay. Consistent with results of the proliferation assay, *fzd4*^{-/-} EC had decreased ability to form branches in matrigel assay (Figure 2C). Additional comparisons showed that *fzd4*^{-/-} EC had a reduced migration compared to control EC using scratch and transwell assays under serum, vascular endothelial growth factor A, or fetal growth factor 2 activation (Figure 2F). These data suggest that Fzd4 controls cell migration under indistinct stimuli. Similarly, wounding assays demonstrated that *fzd4*^{-/-} SMC and MEF have a significantly reduced capacity to migrate compared to, respectively, that of *fzd4*^{+/+} SMC and MEF (Figure 2G, H).

Loss of *fzd4* Altered Microtubule Stabilization and Cell Polarization During Migration

Because cell proliferation and migration are affected by *fzd4* depletion, we analyzed the level of acetylated tubulin in MEF.

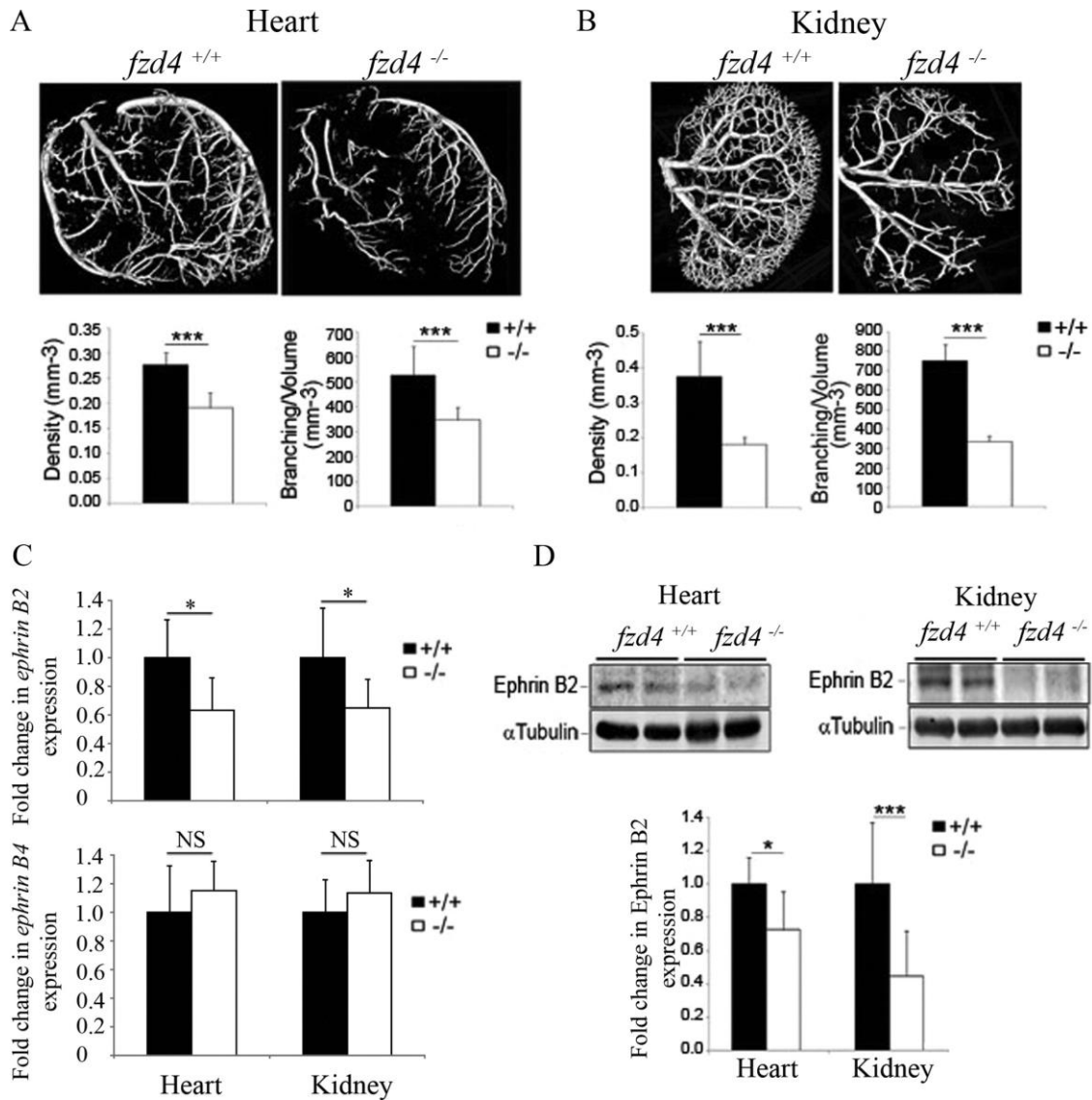


Figure 1. Loss of *fzd4* results in decrease in density and branching of small arteries in heart and kidney. Reconstructed microcomputed tomography images of *fzd4*^{-/-} and *fzd4*^{+/+} heart (A) and kidney (B). Bar graphs show arterial density and branching in heart (*fzd4*^{-/-}, n16; *fzd4*^{+/+}, n10; A) and in kidney (*fzd4*^{-/-}, n9; *fzd4*^{+/+}, n5; B). ***P<0.001. Loss of *fzd4* reduces *EphrinB2* expression. Fold difference (C) in expression (quantitative polymerase chain reaction) of *EphrinB2* and *EphB4* expressions in *fzd4*^{-/-} compared to *fzd4*^{+/+} heart and kidney. Values are meanSD (n4). *P<0.05 vs *fzd4*^{+/+}. D, Representative Western blot analysis of *EphrinB2* expression in two different samples of, respectively, wild-type control (*fzd4*^{+/+}) vs mutant (*fzd4*^{-/-}) heart and kidney. Alpha tubulin served as loading control. The graphs represent pooled data from three distinct experiments. Values are fold increase SD; n3. *P<0.05 and ***P<0.001 vs *fzd4*^{+/+}.

Cell extracts were examined by Western blotting. The absence of *fzd4* resulted in decreased α -tubulin acetylation without a change in the protein level of α -tubulin (Figure 3A). Because cell migration requires cell polarization, we directly measured cell polarity when stimulated by a directional stimulus by evaluating microtubule organization and by calculating the organization and volume of the Golgi in EC, SMC, and MEF migrating out of a wounded monolayer. The *fzd4*^{-/-} MEF display a filamentous network of α -tubulin oriented toward the wound healing. Suppression of Fzd4 decreased and altered the organization of the tubulin in migrating MEF (Figure 3B). Quantitative analysis of fixed immunostained samples showed that in migrating cells, Golgi assembled in front of the nucleus in a dense and compact structure (Figure 3C). We estimated the average labeling intensity of

the Golgi along the line crossing the center of the nucleus with the center of the Golgi and showed that the Golgi labeling intensity was reduced in the front of the nucleus in *fzd4*^{-/-} EC, SMC, and MEF compared to control wild-type cells (Figure 3C). Moreover, in *fzd4*^{-/-} cells, the volume of the Golgi was increased compared to control cells, revealing that the Golgi was less organized and largest at the front of the nucleus in *fzd4*^{-/-} cells compared to control cells (Figure 3).

Cooperation of Fzd4 With Dvl3 Is Required for Noncanonical Signaling Pathway

Because Dvl has been shown to play a role in cell polarity, we next investigated whether Fzd4 may shuttle Dvl away from the Wnt/catenin pathway to favor a noncanonical pathway. We found that in *fzd4*^{-/-} compared to *fzd4*^{+/+} MEF, the basal level in the active β -catenin fraction (ABC, the form of

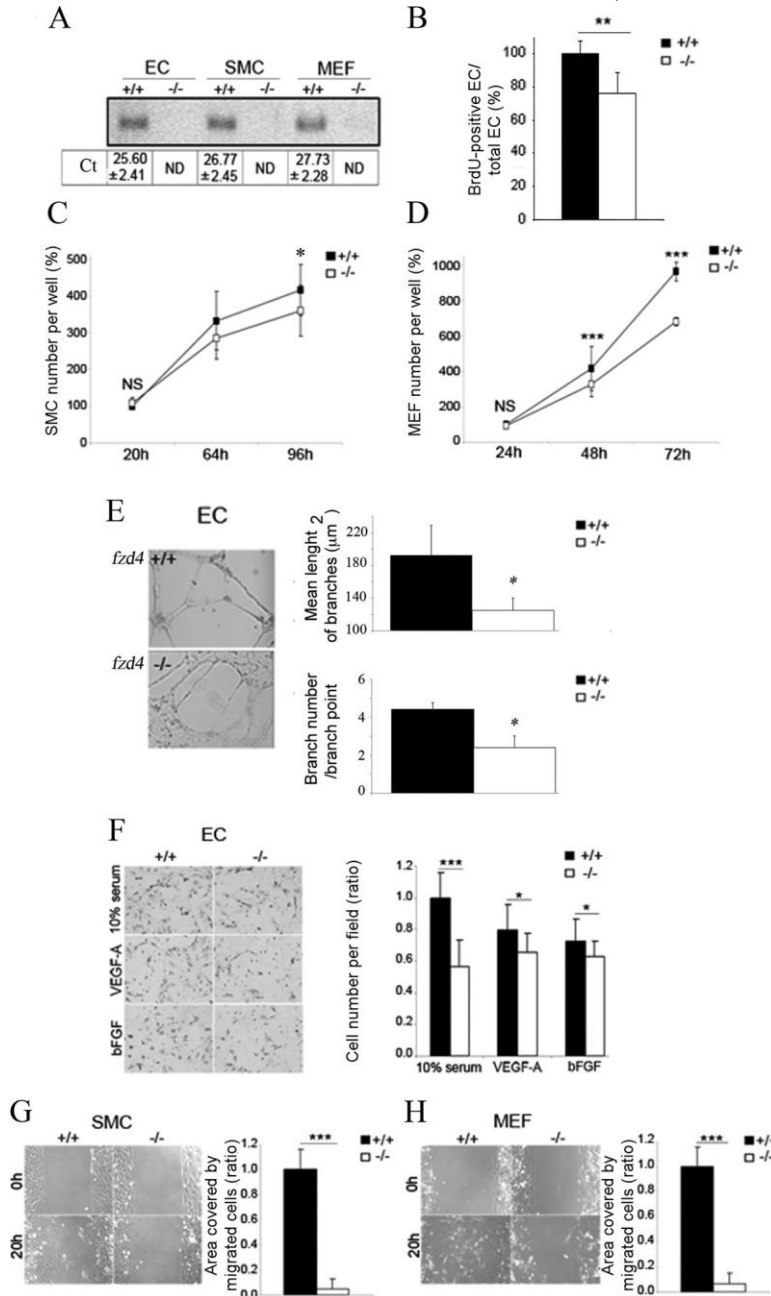


Figure 2. Effect of *fzd4* deletion on vascular cell proliferation and migration. **A**, Quantitative polymerase chain reaction analysis of *fzd4* expression in primary endothelial cells (ECs), smooth muscle cells (SMCs), and murine embryonic fibroblasts (MEFs) from *fzd4*^{+/+} and *fzd4*^{-/-} mice revealed by electrophoresis gel. Values represent control SD; n7. ND indicates not detected. Proliferation of primary *fzd4*^{+/+} compared to *fzd4*^{-/-} EC (n4) (**B**), SMC (n3; **C**), and MEF (n4; **D**) was analyzed respectively by BrdUrd incorporation assay or by cell count number at indicated times vs *fzd4*^{+/+} and *fzd4*^{-/-} compared to *fzd4*^{+/+} cells *P0.05, **P0.005, and ***P0.001 vs *fzd4*^{+/+}. NS indicates nonsignificant. **E**, Evaluation of *fzd4*^{+/+} vs *fzd4*^{-/-} EC differentiation in Matrigel. Branch numbers were quantified (phase contrast) at 6 hours after plating in the presence of vascular endothelial growth factor A (VEGFA) (*right*; n3). *P0.05 vs control. Branch numbers per branch point and mean length of branches (m²) were evaluated. **P0.01. **F**, Images represent chemotactic transwell migration of *fzd4*^{+/+} ECs in the presence in the lower chamber of 10% serum, VEGFA, or fetal growth factor 2 (FGF2) after 16 hours and quantification of cell number (%) in comparison to *fzd4*^{-/-} ECs (*right*; n4). *P0.05 and ***P0.001 vs *fzd4*^{+/+} and *fzd4*^{-/-} vs *fzd4*^{+/+}. **G**, SMC and MEF migration was quantified in a wound healing assay under FGF2 stimulation during 20 hours. Values represented in graph correspond to the percentage of migration per field SD; n3. ***P0.001 vs *fzd4*^{+/+}.

-catenin dephosphorylated on Ser37 and Thr41)¹⁵ was significantly increased; under Wnt3a activation, both *fzd4*^{-/-} and *fzd4*^{-/-} MEF were able to induce the active β -catenin fraction (Figure 4A). To determine if this increase in active β -catenin is associated with transcriptional activity, we transfected the cells with the topflash β -catenin construct. A significant increase in reporter activity was found in *fzd4*^{-/-} compared to *fzd4*^{-/-} MEF under basal condition or under Wnt3a activation (Figure 4B). These data suggest that Fzd4 might repress the canonical Wnt/ β -catenin signaling pathway. To test if Fzd4 can control the Wnt canonical pathway, we analyzed the modulation by Fzd4 of the top reporter activity. In HEK293T cells, we show that expression of Fzd4 alone represses Wnt3A activation of the topflash reporter. Dvl3 overexpression induces strong top reporter activity.

Coexpression of Fzd4 and Dvl3 blocks Dvl3-dependent activation of β -catenin transcriptional activity (Figure 4C).

We next addressed the requirement of Fzd4 to induce noncanonical signaling. We have previously demonstrated that in EC, sFRP1 via Fzd4 was able to induce a noncanonical pathway via a dependent activation of downstream components of the Wnt-PCP pathway such as GSK3 and Rac1.² Because it was reported that in Wnt/PCP signaling, Dvl activates JNK via a Rac-dependant pathway,¹⁶ we analyzed JNK signaling in *fzd4*^{-/-} and *fzd4*^{-/-} MEF transfected with an AP1-dependent transcriptional luciferase reporter and analyzed its activation under Wnt5A activation. We found an increase in AP1 reporter activity in *fzd4*^{-/-} MEF under Wnt5A stimulation after 6 hours but not in *fzd4*^{-/-} MEF (Figure 4D). Because Dvl proteins are central in the control of the PCP pathway, we sought to

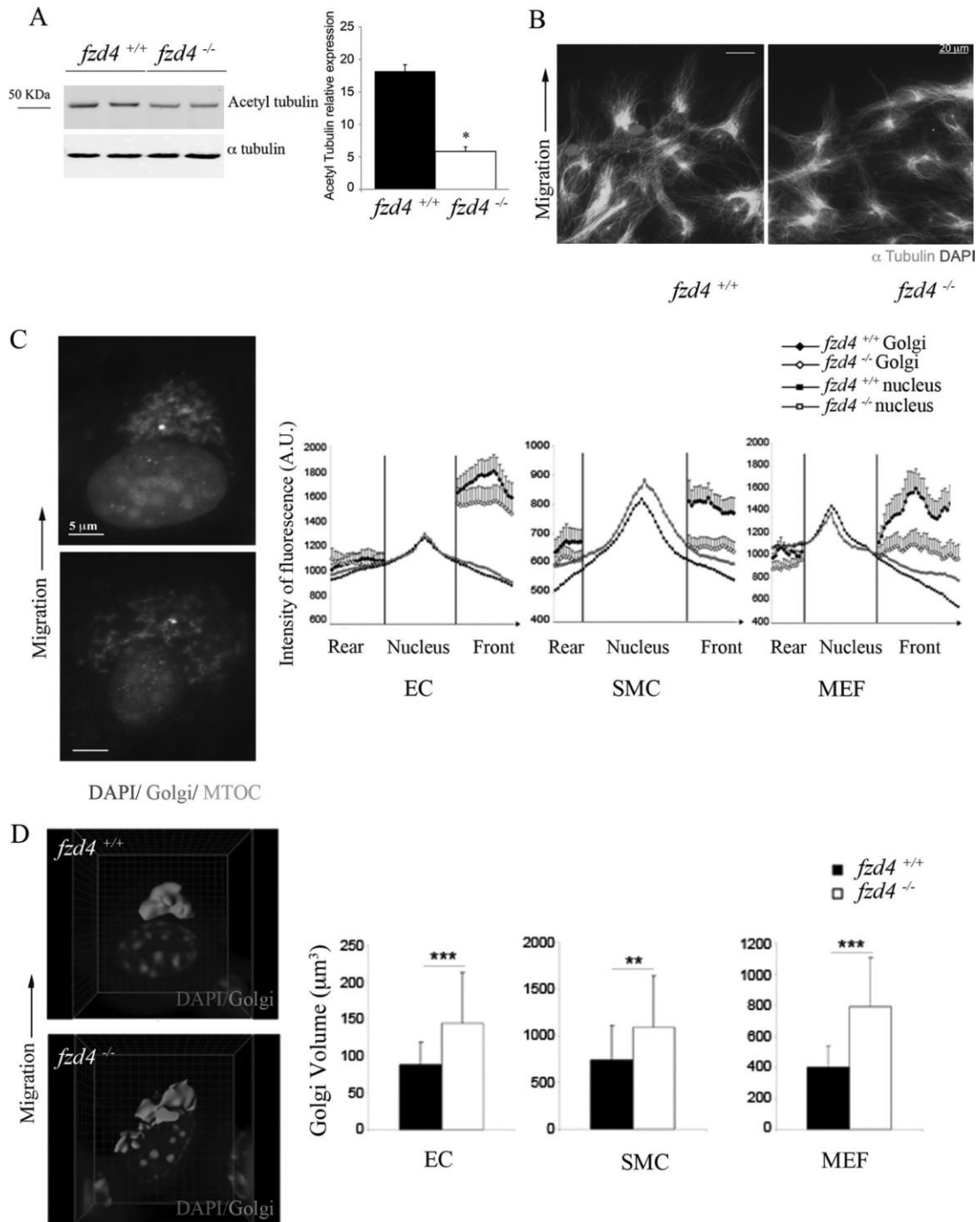


Figure 3. Loss of *fzd4* impairs vascular cell polarization. The *fzd4* deletion leads to decreased acetyl tubulin expression and organization. **A**, The *fzd4*^{-/-} and *fzd4*^{+/+} murine embryonic fibroblast (MEF) extracts were prepared and analyzed by Western blotting. The membranes were probed with antibodies recognizing β -tubulin either indiscriminately (β -tubulin) or only when in acetylated form (acetyl tubulin), and relative expression of acetyl tubulin was reported on the graph. ***P*0.01. **B**, Wound-edge *fzd4*^{-/-} and *fzd4*^{+/+} MEFs were stained with anti- β -tubulin to visualize the microtubule network. Loss of *fzd4* revealed an alteration of oriented tubulin organization. **C**, Golgi organization in migrating *fzd4*^{-/-} primary endothelial cells (ECs), smooth muscle cells (SMCs) and MEFs was established by measuring the fluorescence labeling of the Golgi (red) and the nucleus (DAPI; blue) along a line drawn through the nucleus toward the migrating edge and the volume in each cell (as shown in *fzd4*^{-/-} and *fzd4*^{+/+}

MEF image on the top). Note a marked flattened Golgi profile in front of *fzd4*^{-/-} cells (white dots) compared to *fzd4*^{+/+} cells (black dots) showing that *fzd4* deletion induces an altered Golgi organization in migrated cells. MTOC was labeled in green in front of the cell migration. Values represent intensity distribution of fluorescence (arbitrary units) SD (n50). The result of one of two representative experiments is shown. Migration direction was schematized by an arrow. **D**, To quantify the Golgi volume, the surface reconstruction of the Golgi was designed using Surpass software (Bitplane) as imaged with SMCs. For the three cell types, note a marked increase of Golgi volume in front of *fzd4*^{-/-} cells compared to *fzd4*^{+/+} cells, showing that *fzd4* deletion induces an altered Golgi organization in migrated cells. Values represent Golgi volumeSEM. ***P*0.005 and ****P*0.001 vs *fzd4*^{+/+}.

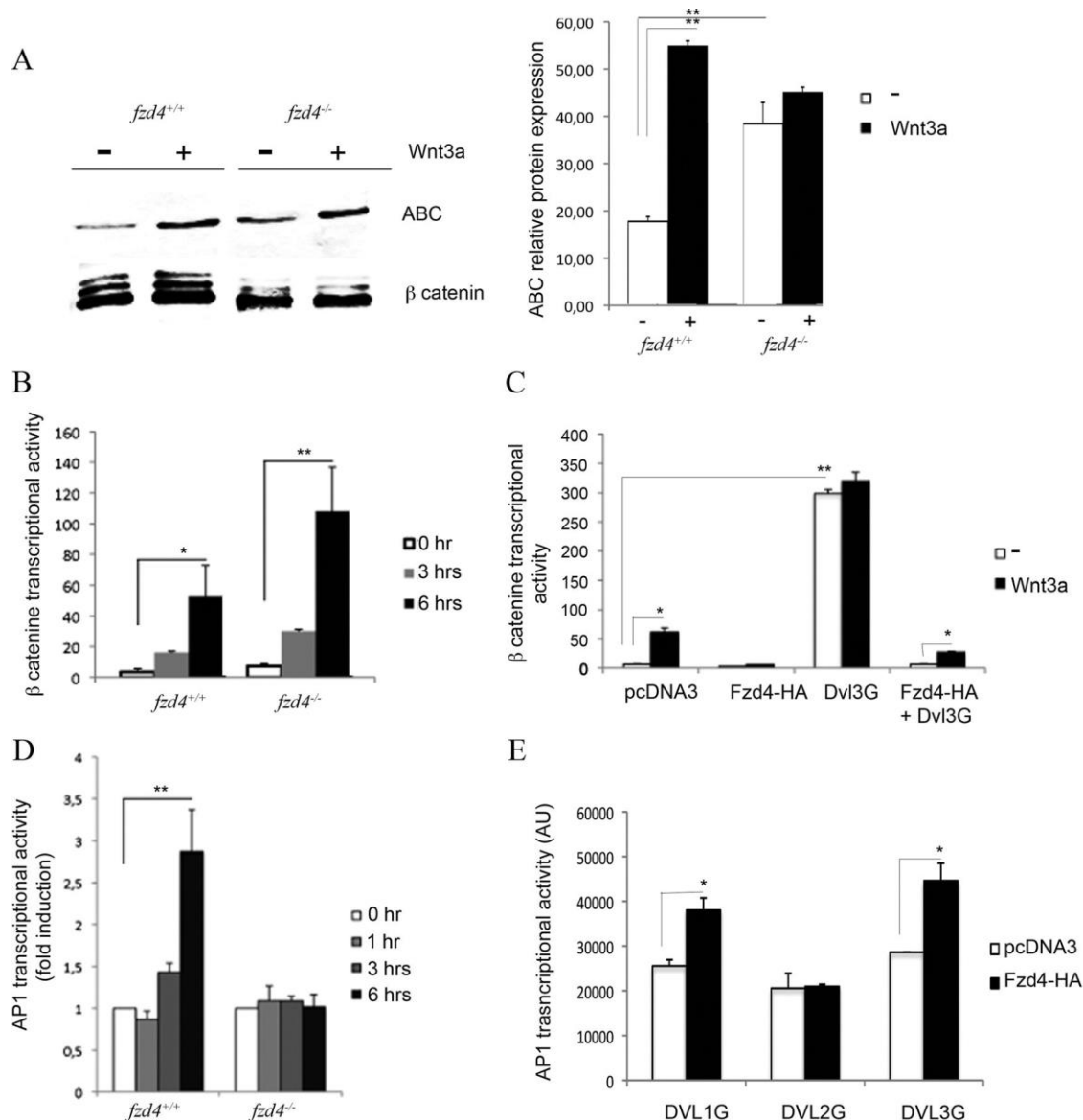


Figure 4. Fzd4 represses Wnt canonical pathway and favors Wnt noncanonical AP1-dependent pathway. Loss of *fzd4* favors activity of β -catenin. **A**, The *fzd4*^{+/+} and *fzd4*^{-/-} murine embryonic fibroblasts (MEFs) were cultured in the presence (+) or absence (-) of Wnt3A conditioned medium (Wnt3a CM) for 16 hours. Cell lysates were analyzed by Western blotting using an antidephosphorylated β -catenin (ABC) and anti- β -catenin (β -catenin) and relative expression of ABC was reported on the graph. Relative luciferase values are shown. Quantification of ABC levels without and after addition of Wnt3a CM was reported on graph. Error bars in this and subsequent figures shown as meanSE (n3). Probability values were determined by the two-tailed Student *t* test (paired).

****P0.01. B,** The *fzd4*^{-/-} and *fzd4*^{+/+} MEFs were transiently cotransfected with 8X top flash and -galactosidase reporter vectors. After culture in the presence of Wnt3a CM during 3 hours and 6 hours, activity of the -catenin signaling pathway was quantified by measuring the relative luciferase activity (RLU) normalized to -galactosidase activity. Relative luciferase values are shown. *P0.05. **C,** Fzd4 reduces -catenin-induced activity. HEK293T cells were cotransfected with 8X top flash and -galactosidase reporter plasmids with an empty vector (pcDNA3), with one plasmid encoding for either Fzd4-tagged HA (Fzd4-HA) or Dvl3-tagged green (Dvl3G), or with both the Fzd4 and Dvl3 plasmids. After culture in the presence of Wnt3a CM for 16 hours, cells were harvested for luciferase-based top flash assay of Wnt signaling. *P0.05, **P0.01. Fzd4 favors AP1 activity. **D,** Loss of *fzd4* inhibits AP1 activity. The *fzd4*^{-/-} and *fzd4*^{+/+} MEF were transiently cotransfected with AP1 and -galactosidase reporter vectors. After culture in the presence of Wnt5a CM for 1, 3, and 6 hours, AP1 signaling pathway activity was quantified by measuring the relative firefly luciferase activity normalized to -galactosidase activity. **P0.01. **E,** Fzd4 in presence of Dvl1 or Dvl3 induces a robust AP1 activity. AP1 and -galactosidase reporter plasmid transfected HEK293T cells were cotransfected with plasmid coding for either Dvl1, Dvl2, or Dvl3 tagged green (respectively, Dvl1G, Dvl2G, or Dvl3G) either with an empty vector (pcDNA3) or with a plasmid encoding Fzd4 (Fzd4-HA). AP1 signaling pathway activity was quantified by measuring the relative firefly luciferase activity normalized to -galactosidase activity (arbitrary units). *P0.05.

interrogate the ability of Fzd4 to interact preferentially with one of the Dvl isoforms to induce the Wnt noncanonical pathway. We transfected HEK293T cells with the AP1 luciferase reporter and measured activity of cells transfected with Dvl1, Dvl2, and Dvl3 in the absence or presence of Fzd4 (Figure 4E). Transfections with plasmid coding for either Dvl isoforms or Fzd4 alone do not activate the reporter. However, cotransfection with Fzd4 and Dvl1 or Fzd4 and Dvl3 lead to an activation of the AP1 reporter, which is not found when Fzd4 and Dvl2 are cotransfected.

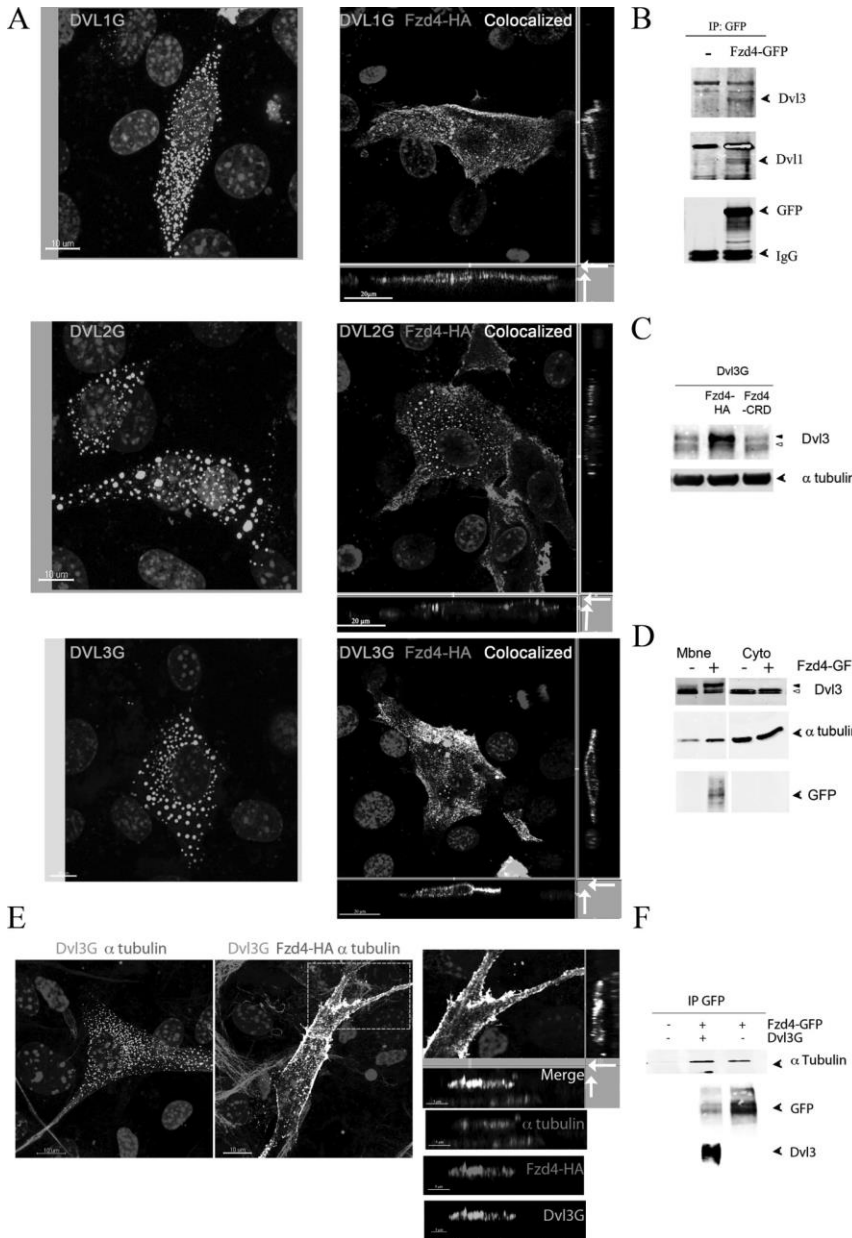


Figure 5. Fzd4 interacts with Dvl1 and Dvl3 and induces AP1 signaling pathway activation. **A**, Fzd4 induces a relocalization at the cytosolic membrane of Dvl1 and Dvl3. NIH 3T3 cells were cotransfected with plasmids coding for either Dvl1G, Dvl2G, or Dvl3G (green) alone or in the presence of plasmid coding for Fzd4 with a tag HA (Fzd4-HA) and immunostained for Fzd4 with an anti-HA (red). On coexpression with Fzd4, Dvl1 and Dvl3 green labeling in large punctates in the cytoplasm was decreased and associated with a plasma membrane pattern. Meanwhile, Dvl2G labeling remained in the cytoplasm in presence of Fzd4. **B**, Fzd4 interacts with endogenous Dvl1 and Dvl3. HEK293T were transiently transfected either with an empty vector () or with a plasmid coding for Fzd4 with a Tag GFP (Fzd4-GFP). Cell lysates were immunoprecipitated with anti-GFP antibody. The samples were analyzed by Western blotting with the indicated antibodies. Fzd4 induces Dvl3 activation. **C**, HEK293T cells were transiently cotransfected with a plasmid coding for Dvl3 tagged with a green epitope (Dvl3G) either with an empty vector () or with plasmids coding for Fzd4-HA or for Fzd4-CRD. Cell lysates were analyzed by

Western blotting with the indicated antibodies. **D**, HEK293T cells were transiently transfected either with an empty vector () or with plasmid coding for Fzd4 (Fzd4-GFP). After cell fractionation, Western blotting was performed on membrane (Mbne) and cytosolic (Cyto) fractions with indicated antibodies. *Open arrow* indicates Dvl3 unphosphorylated forms (78 and 80 kDa) and *black arrow* shows the phosphorylated (82 kDa) shifted form. Fzd4 polarizes Dvl3 expression at the edge of the cell with α -tubulin. **E**, NIH3T3 cells were transfected with plasmids coding for Dvl3-tagged green (Dvl3G; green) alone or in the presence of a plasmid coding for Fzd4 with a tag HA (Fzd4HA). Cells were immunostained for Fzd4 with anti-HA (purple) and for α -tubulin with anti- α -tubulin (red). Note that Dvl3 alone is expressed in large punctates, whereas, in the presence of Fzd4, it is redistributed and colocalized at the plasma membrane with α -tubulin. **F**, NIH 3T3 cells were transfected either with Fzd4-GFP or with Dvl3G plasmid. Lysates were immunoprecipitated with anti-GFP antibody and then analyzed by Western blotting with the indicated antibodies.

Fzd4 Preferentially Directs Relocalization and Activation of Dvl3 and, to a Lesser Extent, Dvl1

We examined, on a cell-by-cell basis, colocalization of Dvl isoforms with Fzd4. Transient expression of Dvl1, Dvl2, and Dvl3 tagged with green epitope (respectively, Dvl3G, Dvl2G, and Dvl3G) showed punctate staining

throughout the cytoplasm (Figure 5A), which correlates with large multiprotein complexes, as previously reported.^{17,18} Fzd4 tagged with the HA epitope (Fzd4-HA) showed preferential localization at the apical side of the cytoplasmic membrane. Cotransfection with Fzd4-HA revealed a major change in the distribution of Dvl3G and Dvl1G with relocalization to the cytoplasmic membrane and an even appearance throughout the cytoplasm in 95% and 70% of the cells, respectively. We did not find relocalization of Dvl2G when cotransfected with Fzd4-HA (Figure 5A). Quantification of Fzd4-induced relocalization of Dvl to the cytoplasmic membrane was performed by merging images and using Imaris software confocal image analysis. Through this method, we established that Fzd4-HA was able to preferentially relocalize Dvl3G to the membrane as compared to Dvl1G (28.4% of Dvl3G vs 2.7% of Dvl1G).

Together, these results imply that Fzd4 interacts preferentially with Dvl3 and, to a lesser extent, with Dvl1, but not with Dvl2 to induce the noncanonical Wnt pathway.

We confirmed the ability of Fzd4 to associate with the endogenous Dvl1 and Dvl3 isoforms from mammalian cell lysates by immunoprecipitation and immunoblotting assays. Cell extracts were prepared from HEK293T cells transfected with Fzd4-GFP fusion protein and immunoprecipitated with antibodies against GFP. Immunoprecipitation of Fzd4-GFP led to coprecipitation of endogenous Dvl1 and Dvl3 (Figure 5B). We next examined the capacity of Fzd4 to activate Dvl3 and found that cotransfection of HEK293T with Fzd4-HA and Dvl3G led to strong phosphorylation of Dvl3G, as shown by a mobility shift of the protein on SDS-PAGE (Figure 5C). To confirm that the observed signaling is specific to Fzd4, cells were cotransfected with a plasmid coding for the CRD domain of Fzd4 (Fzd4 CRD).⁸ Fzd4 CRD overexpression did not induce exogenous Dvl3G phosphorylation. Because we show that Fzd4 affects Dvl3 localization and interacts physically with Dvl3, we next wanted to confirm that the activation of Dvl3 was localized at the cytoplasmic membrane. HEK293T were transfected with a plasmid coding for Fzd4GFP; then, membrane and cytoplasmic fractions were separated using ultracentrifugation steps. Western blot analysis revealed that Fzd4-GFP was exclusively detected in the membrane fraction and not in the cytosolic fraction, although endogenous Dvl3 is evenly distributed in both fractions. These results indicate that Fzd4 leads to an endogenous Dvl3 shift in Fzd4 transfected cells, but not in control membrane fractions. In the cytosolic fractions, we did not detect any modification of endogenous Dvl3 profile both in Fzd4-GFP transfected and control conditions (Figure 5D).

We found that Fzd4 accumulates in a polarized way at the cytoplasmic membrane on the top of the cell (Figure 5A). When cells were transfected with Fzd4-GFP, we found an increase in α -tubulin in membrane fractions, although the overall level of α -tubulin detected in the cytoplasm was not modified in Fzd4 transfected versus control conditions (Figure 5D). Because Fzd4 affects tubulin organization (Figure 3B), we then investigated whether Fzd4-based molecular signals might drive the selective localization of Dvl3 and α -tubulin in polarizing migrating cells. When we overexpressed Fzd4-HA with Dvl3G and then visualized it with immunofluorescence, we found that both colocalized in an oriented manner driven partially by α -tubulin at the cytoplasmic membrane (Figure 5E). Using immunoprecipitation, we found that Fzd4-GFP interacts with α -tubulin, and when Fzd4-GFP and Dvl3G were cotransfected, Fzd4 and Dvl3G form a complex that enhances α -tubulin recruitment (Figure 5F).

We have performed experiments to analyze whether reexpression of Fzd4 with Dvl3 in *sifzd4*-treated EC might restore their ability to proliferate and form tubes. We show that double expression of Fzd4 along with Dvl3 was able to significantly rescue the impact of *fzd4* deletion on EC proliferation, but expression of Fzd4 or Dvl3 alone did not have this effect (Figure 6A). Tube formation assays revealed that *sifzd4* treatment reduced the ability of cells to form capillary networks and that Dvl3 with Fzd4 was able to rescue the *fzd4* deletion phenotype, significantly increasing branch lengths and branch numbers per branch point (Figure 6B). It is noteworthy that Dvl3 alone is able to significantly increase capillary network formation. Collectively, these results suggest that Fzd4 and Dvl3 interact to promote the Wnt-dependent pathway in vascular cells.

Our genetic analysis together with a biochemical analysis have identified Fzd4 with Dvl3, and to a lesser extent Dvl1, as crucial partners for PCP pathway induction in vascular cells. These results confirmed that Fzd4 expression is polarized in cells and organizes a platform with Dvl3 to enhance α -tubulin recruitment.

Dvl3 DEP Domain Is Crucial for Fzd4-Induced Relocalization

Next, we sought to identify the domain of Dvl3 that interacts with Fzd4. It has been previously shown that Dvl-mediated activation of the Wnt/-catenin or the Wnt/PCP signaling pathway is dependent of the availability of specific domains DIX, PDZ, and DEP.^{19,20} Although the DIX and PDZ domains are necessary for Wnt canonical signaling, the DEP domain is essential for PCP signaling²¹⁻²³ and linked to Rac 1 activation.^{20,24} To identify the Dvl domain necessary for Fzd4 interaction, we used myc-tagged truncated Dvl constructs lacking the DIX (DIX Dvl3), the PDZ (PDZ Dvl3), the DEP (DEP Dvl3), and a construct containing DEP domain (DEP). Distribution of the constructs was examined after transfection of HEK293T cells. Any one of the myc-tagged Dvl3 deleted constructs were detected in the cytoplasm in a punctate pattern mimicking the Dvl3-tagged myc pattern. It should be noted that the DEP Dvl3 construct also was detected in the nucleus (data not shown). The constructs were then cotransfected with a plasmid coding for HA-tagged Fzd4 in HEK293T cells. Only deletion of DEP domain impeded Dvl3 relocalization at the membrane. It is worth noting that DEP mutants strongly accumulate and colocalize with Fzd4 into the cytoplasmic membrane, confirming the major role of the DEP domain for interaction with Fzd4 (online Figure IV). In combination, these results indicate that Fzd4 regulates the phosphorylation and polarized cellular localization of Dvl3, and that Fzd4/Dvl3 interaction functions in noncanonical Wnt signaling.

Fzd4 Deletion Induces Arterial Disorganization in Ischemia-Induced Angiogenesis

To understand the importance of Fzd4 during vascular formation, we evaluated in vivo whether Fzd4 gene disruption impairs adult angiogenesis. It is noteworthy that under nonischemic conditions, quantitative analysis of the arterial network by microcomputed tomography showed a reduction in both arterial density and branching in the hind limb of *fzd4*^{-/-} compared to control mice (Figure 7 A, C, D). These results were confirmed with a lower capillary density in *fzd4*^{-/-} versus control mice, evaluated by immunohistochemistry (online Table I). We then explored the capacity of *fzd4*^{-/-} mice to restore a functional arterial network after ischemia using a femoral artery ligation model. Blood flow recovery in the hind limb was reduced in *fzd4*^{-/-} compared to control mice after 2 weeks (Figure 7B). This was consistent with a reduction in both the arterial density and branching in *fzd4*^{-/-} mice after ischemia, evaluated by quantitative analysis of microcomputed tomography images (Figure 7C, D). Interestingly, three-dimensional images revealed that in *fzd4*^{-/-} mice compared to controls, neovasculature structures were severely disorganized. In control mice, angiogenesis induces the formation of vascular structures oriented directionally toward the extremity of the hind limb. In *fzd4*^{-/-} mice, we found a modification of the organization with the formation of few clusters of

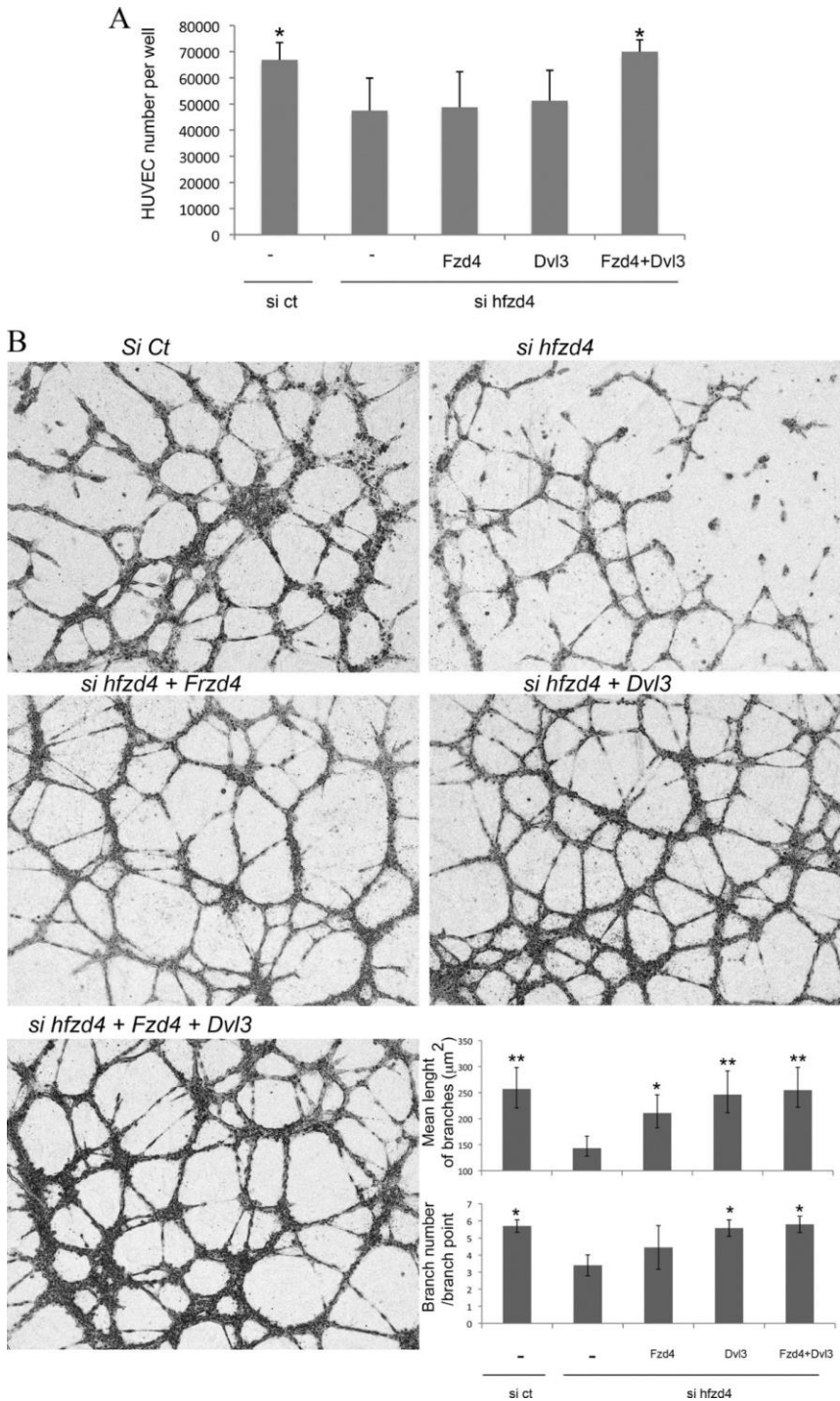


Figure 6. Re-expression of Fzd4 with Dvl3 in *sihfzd4*-treated endothelial cells (ECs) restored their ability to proliferate and form tube. **A**, ECs were transfected and after 48 hours were counted per well. The *sihfzd4*-treated ECs reduced their proliferation compared to control (siCt). Cotransfection with Fzd4-HA and Dvl3myc plasmids rescue significant *sihfzd4*-EC proliferation compared to Fzd4 or Dvl3 plasmid transfected cells. * $P < 0.05$, $n = 3$. **B**, ECs were seeded on matrigel after transfection with siRNA and plasmid as indicated. After 6 hours, ECs were fixed, photographed, and mean length and branch number per branch point were counted. The *sihfzd4* treatment reduced cell ability to form capillary network compared to siCt treatment. The *sihfzd4* EC transfection with Dvl3 plasmid alone (*sihfzd4*Dvl3) and with Dvl3 and Fzd4 plasmids (*sihfzd4*Dvl3Fzd4) significantly increased branch lengths and branch numbers per branch point compared to siCt conditions. * $P < 0.05$; ** $P < 0.001$, $n = 3$.

arterioles with a radial organization (Figure 7A). These data demonstrate that Fzd4 deletion impairs arterial formation and vessel-oriented branching in peripheral organ. These data support the concept that Fzd4 plays a role major in vessel organization via Wnt-dependent PCP polarity pathway.

Discussion

Fzd4 is expressed in different vascular beds throughout the organism. Genetic defects of *fzd4* have been linked to familial exudative vitreoretinopathy, a progressive retinal vascular disease.⁵ The *fzd4* deletion has been shown in mice to impair fertility,¹⁰ to alter vessel formation in the cerebellum,⁹ and to interact with Norrin to form retinal vessel network.⁸ In addition, our group has previously demonstrated that Fzd4 can interact with sFRP1, a potent angiogenic factor.² All these data taken together indicate that Fzd4 signaling may play an important role in

vascular formation. In this article, we extend and strengthen this notion by providing evidence that Fzd4 is required for formation and branching of the vascular arterial network in peripheral organs (with regard to their vascular system) through a noncanonical Wnt/PCP-dependent mechanism.

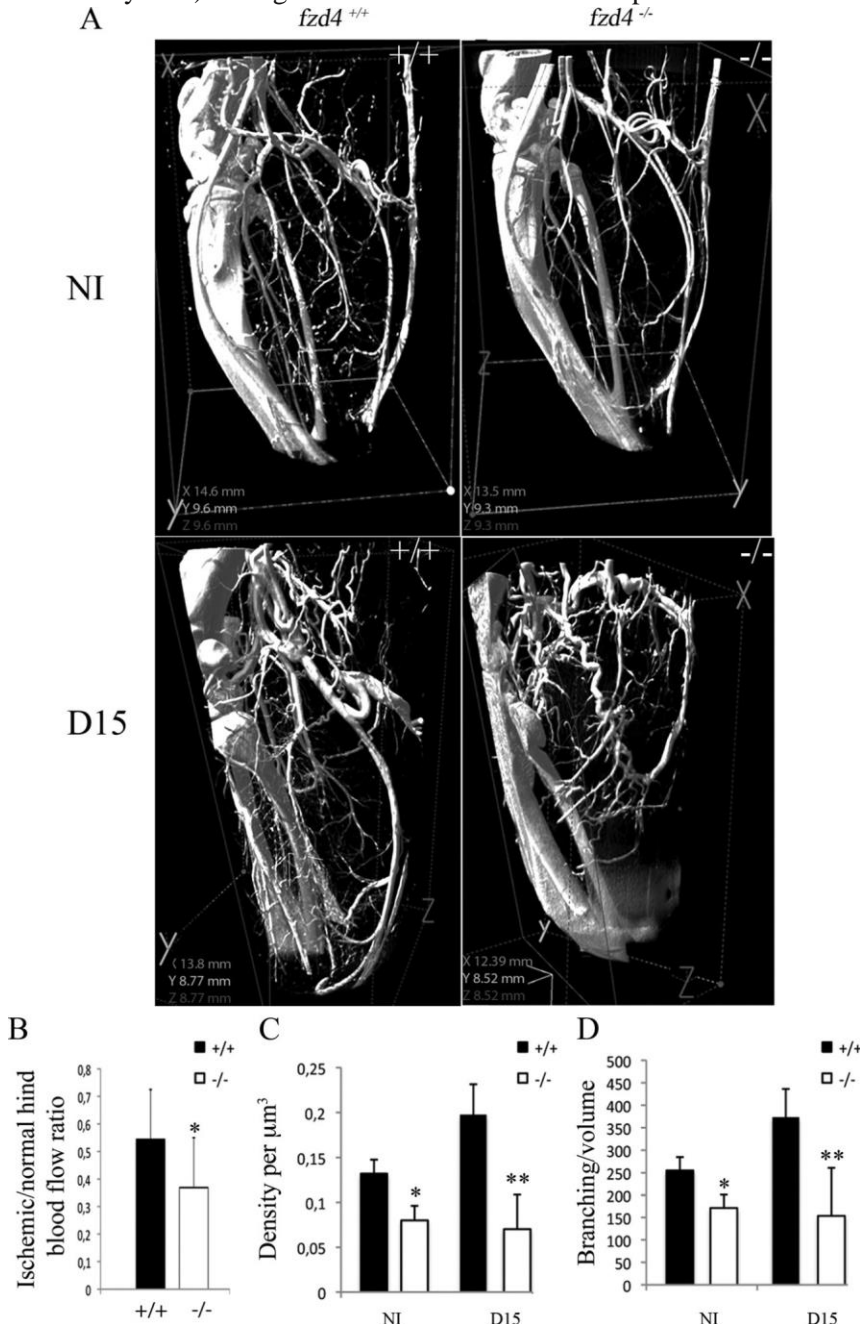


Figure 7. The *fzd4* deletion impairs the angiogenic response. **A**, Reconstructed microcomputed tomography images representative in *fzd4*^{+/+} (l) and *fzd4*^{-/-} (r) hind limb mice before (NI) and after ischemia at D15. **B**, Quantitative analysis of hind limb blood flow was performed by calculating ischemic/normal limb perfusions ratios after the induction of hind limb ischemia. Note a decrease (**C**) in vessels number and (**D**) in branching/connectivity in *fzd4*^{+/+} (l) and *fzd4*^{-/-} (r) hind limb in nonischemic (NI) conditions and 15 days after ischemia (D15). **P*0.05.

Fzd4 Deletion Selectively Impairs Small Artery and Capillary Formation in Peripheral Organs

We have demonstrated that Fzd4 is expressed throughout the vasculature, and in EC and SMC of arteries, small arterioles, and capillaries, but not in large veins, and that *fzd4* depletion results in a drastic reduction in the number of small-caliber arteries and in their branching. This defective vessel development is restricted to the arterial system consistent with the observation of reduced arterial, but not venous, marker expressions. Collectively, these data suggest the importance of properly regulating Fzd4 activity during arterial development because Fzd4 controls induction and branching of small arterioles and capillary beds at the distal end of tissue. Despite these

marked arterial defects and a reduction in body size, other aspects of heart and kidney vascular development, such as formation and branching of large arteries, are not affected.

The formation of new vessels requires both vascular cell proliferation and migration to enable sprout growth and the formation of a branched network. We have demonstrated that reducing expression of Fzd4 mitigated EC and SMC proliferation, migration, and EC tube formation. In a wound model, the Golgi is oriented in front of the nucleus²⁵ around the centrosome, the organizing center for cytoplasmic microtubules.²⁶ In this model, we showed that *fzd4* deletion impairs both tubulin and Golgi reorganization and capillary-like network formation *ex vivo*, which support a critical role of Fzd4 in vessel branching. Thus, we hypothesize that Fzd4 can control vascular formation by a noncanonical-dependent mechanism in peripheral organs.

How Is the Wnt/Frizzled Signaling Pathway Involved in the Vascular System?

In vitro studies have demonstrated a functional role of the canonical β -catenin-dependent pathway in EC.²⁷ It has been proposed that during development, the Wnt/ β -catenin pathway was only functional during angiogenesis in the central nervous system but not in peripheral tissue as in heart and kidney²⁸; after birth, the activation of the Lef/Tcf Wnt reporter system is only restricted to a few vascular beds in the central nervous system.²⁹ Analysis of β -catenin conditional depletion demonstrated a major role of β -catenin in blood–brain barrier maturation.³⁰ Consistent with these findings, in responder top gal transgenic mice, we could not detect any β -gal-positive EC, outside of the central nervous system, in heart and kidney at postnatal day 5 or in adults (data non shown). Additionally, we have demonstrated that sFRP1 was also able to activate a noncanonical Rac1-dependant signaling pathway in EC.² Recent studies demonstrated a role of PCP in endothelial cells through Daam1-forming family members. Daam1 has been shown to be involved in polarity of embryonic development in *Xenopus* and *Drosophila* acting downstream of frizzled receptors via an interaction with Dvl.²³ In EC, activated Daam1 would control proliferation and migration,³ affecting both cell polarity and cell movement,³¹ regulating the microtubule network.³²

Our data corroborate the role of PCP in EC and disclose the role of Fzd4 in vascular cells in Wnt/PCP signaling pathway, because we showed that Fzd4 regulates microtubule network. Using *in vitro* assays, we report that Fzd4 was able to repress the Wnt canonical pathway and activate the noncanonical pathway. These results demonstrate that Fzd4 is localized in a polarized manner on the top of the cell membrane, and it is able to recruit and preferentially activate DV13. Three isoforms of Dvl proteins have been identified and share high-sequence homology. Genetic approaches have previously shown that *Dvl* has been involved in PCP signaling during gastrulation and that it has a functionally redundant role during development.^{33,34} Interestingly, Dvl3 mutants exhibited craniorachischisis, which is often associated with PCP signaling disruption. Our data further demonstrate that Fzd4 is one of the major receptors of the Wnt/PCP pathway in angiogenesis and facilitates cell polarization through tubulin network reorganization.

Fzd4 and Pathogenesis

Our results suggest that absence of Fzd4 leads to impaired vascular cell polarization. To test the impact of Fzd4 deletion on angiogenesis, we used a mouse model of vessel formation after hind limb ischemia. These data revealed that the absence of Fzd4 impairs adult neoangiogenesis and results in the formation of a disorganized network. Given the fact that the noncanonical Wnt cascade is involved in the growth and guidance of neurons,³⁵ it may be speculated that the directional growth of the peripheral vascular network is a feature of PCP signaling involving Fzd4 receptors.

This study extends our understanding of the role of Fzd4 in adult peripheral organs and during postischemic angiogenesis, and implicates Fzd4 as an important regulator in the directional development and branching morphogenesis of small-caliber arteries and arterioles through a Wnt/PCP pathway in vascular cells.

Acknowledgments

The authors thank Jerome Guignard for assistance in mouse breeding.

Sources of Funding

This work was supported by ANR grant (ANR-2010-BLAN-113501), Aquitaine Region grant (20101301039MP), Communauté de Travail Pyrénéenne, and from the Fondation pour la Recherche Médicale (DCV20070409258). B.D. was a recipient of a fellowship from Fondation pour la Recherche Médicale. R.S. was a recipient of a fellowship from Aquitaine Region and Inserm.

Disclosures

None.

References

1. Masckauchan TN, Agalliu D, Vorontchikhina M, Ahn A, Parmalee NL, Li CM, Khoo A, Tycko B, Brown AM, Kitajewski J. Wnt5a signaling induces proliferation and survival of endothelial cells in vitro and expression of MMP-1 and Tie-2. *Mol Biol Cell*. 2006;17:5163–5172.
2. Dufourcq P, Leroux L, Ezan J, Descamps B, Lamaziere JM, Costet P, Basoni C, Moreau C, Deutsch U, Couffinhal T, Duplaa C. Regulation of endothelial cell cytoskeletal reorganization by a secreted frizzled-related protein-1 and frizzled 4- and frizzled 7-dependent pathway: role in neovessel formation. *Am J Pathol*. 2008;172:37–49.
3. Ju R, Cirone P, Lin S, Griesbach H, Slusarski DC, Crews CM. Activation of the planar cell polarity formin DAAM1 leads to inhibition of endothelial cell proliferation, migration, and angiogenesis. *Proc Natl Acad Sci U S A*. 2010;107:6906–6911.
4. Stenman JM, Rajagopal J, Carroll TJ, Ishibashi M, McMahon J, McMahon AP. Canonical Wnt signaling regulates organ-specific assembly and differentiation of CNS vasculature. *Science*. 2008;322: 1247–1250.
5. Robitaille J, MacDonald ML, Kaykas A, Sheldahl LC, Zeisler J, Dube MP, Zhang LH, Singaraja RR, Guernsey DL, Zheng B, Siebert LF, Hoskin-Mott A, Trese MT, Pimstone SN, Shastry BS, Moon RT, Hayden MR, Goldberg YP, Samuels ME. Mutant frizzled-4 disrupts retinal angiogenesis in familial exudative vitreoretinopathy. *Nat Genet*. 2002;32: 326–330.
6. Toomes C, Bottomley HM, Jackson RM, Towns KV, Scott S, Mackey DA, Craig JE, Jiang L, Yang Z, Trembath R, Woodruff G, Gregory-Evans CY, Gregory-Evans K, Parker MJ, Black GC, Downey LM, Zhang K, Inglehearn CF. Mutations in LRP5 or FZD4 underlie the common familial exudative vitreoretinopathy locus on chromosome 11q. *Am J Hum Genet*. 2004;74:721–730.
7. Ai M, Heeger S, Bartels CF, Schelling DK, Osteoporosis-Pseudoglioma Collaborative Group. Clinical and molecular findings in osteoporosis pseudoglioma syndrome. *Am J Hum Genet*. 2005;77:741–753.
8. Xu Q, Wang Y, Dabdoub A, Smallwood PM, Williams J, Woods C, Kelley MW, Jiang L, Tasman W, Zhang K, Nathans J. Vascular development in the retina and inner ear: control by Norrin and Frizzled-4, a high-affinity ligand-receptor pair. *Cell*. 2004;116:883–895.
9. Ye X, Wang Y, Cahill H, Yu M, Badea TC, Smallwood PM, Peachey NS, Nathans J. Norrin, frizzled-4, and Lrp5 signaling in endothelial cells controls a genetic program for retinal vascularization. *Cell*. 2009;139: 285–298.
10. Hsieh M, Boerboom D, Shimada M, Lo Y, Parlow AF, Luhmann UF, Berger W, Richards JS. Mice null for Frizzled4 (*Fzd4*^{-/-}) are infertile and exhibit impaired corpora lutea formation and function. *Biol Reprod*. 2005;73:1135–1146.
11. Dufourcq P, Couffinhal T, Ezan J, Barandon L, Moreau M, Daret D, Duplaa C. FrzA, a secreted frizzled related protein, induced angiogenic response. *Circulation*. 2002;106:3097–3103.
12. Zhang Y, Yeh JR, Mara A, Ju R, Hines JF, Cirone P, Griesbach HL, Schneider I, Slusarski DC, Holley SA, Crews CM. A chemical and genetic approach to the mode of action of fumagillin. *Chem Biol*. 2006; 13:1001–1009.

13. Cirone P, Lin S, Griesbach HL, Zhang Y, Slusarski DC, Crews CM. Arole for planar cell polarity signaling in angiogenesis. *Angiogenesis*. 2008;11:347–360.
14. Liu W, Sato A, Khadka D, Bharti R, Diaz H, Runnels LW, Habas R. Mechanism of activation of the Formin protein Daam1. *Proc Natl Acad Sci U S A*. 2008;105:210–215.
15. van Noort M, Meeldijk J, van der Zee R, Destree O, Clevers H. Wnt signaling controls the phosphorylation status of beta-catenin. *J Biol Chem*. 2002;277:17901–17905.
16. Wong CK, Luo W, Deng Y, Zou H, Ye Z, Lin SC. The DIX domain protein coiled-coil-DIX1 inhibits c-Jun N-terminal kinase activation by Axin and dishevelled through distinct mechanisms. *J Biol Chem*. 2004;279:39366–39373.
17. Schwarz-Romond T, Merrifield C, Nichols BJ, Bienz M. The Wnt signalling effector Dishevelled forms dynamic protein assemblies rather than stable associations with cytoplasmic vesicles. *J Cell Sci*. 2005;118:5269–5277.
18. Smalley MJ, Signoret N, Robertson D, Tilley A, Hann A, Ewan K, Ding Y, Paterson H, Dale TC. Dishevelled (Dvl-2) activates canonical Wnt signalling in the absence of cytoplasmic puncta. *J Cell Sci*. 2005;118:5279–5289.
19. Gao C, Chen YG. Dishevelled: The hub of Wnt signaling. *Cell Signal*. 2010;22:717–727.
20. Boutros M, Mlodzik M. Dishevelled: at the crossroads of divergent intracellular signaling pathways. *Mech Dev*. 1999;83:27–37.
21. Kishida S, Yamamoto H, Hino S, Ikeda S, Kishida M, Kikuchi A. DIX domains of Dvl and axin are necessary for protein interactions and their ability to regulate beta-catenin stability. *Mol Cell Biol*. 1999;19:4414–4422.
22. Li L, Yuan H, Xie W, Mao J, Caruso AM, McMahon A, Sussman DJ, Wu D. Dishevelled proteins lead to two signaling pathways. Regulation of LEF-1 and c-Jun N-terminal kinase in mammalian cells. *J Biol Chem*. 1999;274:129–134.
23. Habas R, Kato Y, He X. Wnt/Frizzled activation of Rho regulates vertebrate gastrulation and requires a novel Formin homology protein Daam1. *Cell*. 2001;107:843–854.
24. Axelrod JD, Miller JR, Shulman JM, Moon RT, Perrimon N. Differential recruitment of Dishevelled provides signaling specificity in the planar cell polarity and Wingless signaling pathways. *Genes Dev*. 1998;12:2610–2622.
25. Kupfer A, Louvard D, Singer SJ. Polarization of the Golgi apparatus and the microtubule-organizing center in cultured fibroblasts at the edge of an experimental wound. *Proc Natl Acad Sci U S A*. 1982;79:2603–2607.
26. Thyberg J, Moskalewski S. Role of microtubules in the organization of the Golgi complex. *Exp Cell Res*. 1999;246:263–279.
27. Goodwin AM, D'Amore PA. Wnt signaling in the vasculature. *Angiogenesis*. 2002;5:1–9.
28. Daneman R, Agalliu D, Zhou L, Kuhnert F, Kuo CJ, Barres BA. Wnt/beta-catenin signaling is required for CNS, but not non-CNS, angiogenesis. *Proc Natl Acad Sci U S A*. 2009;106:641–646.
29. Liebner S, Corada M, Bangsow T, Babbage J, Taddei A, Czupalla CJ, Reis M, Felici A, Wolburg H, Fruttiger M, Taketo MM, von Melchner H, Plate KH, Gerhardt H, Dejana E. Wnt/beta-catenin signaling controls development of the blood-brain barrier. *J Cell Biol*. 2008;183:409–417.
30. Cattelino A, Liebner S, Gallini R, Zanetti A, Balconi G, Corsi A, Bianco P, Wolburg H, Moore R, Oreda B, Kemler R, Dejana E. The conditional inactivation of the beta-catenin gene in endothelial cells causes a defective vascular pattern and increased vascular fragility. *J Cell Biol*. 2003;162:1111–1122.
31. Ang SF, Zhao ZS, Lim L, Manser E. DAAM1 is a formin required for centrosome re-orientation during cell migration. *PLoS One*. 2010;5.
32. Wen Y, Eng CH, Schmoranzler J, Cabrera-Poch N, Morris EJ, Chen M, Wallar BJ, Alberts AS, Gundersen GG. EB1 and APC bind to mDia to stabilize microtubules downstream of Rho and promote cell migration. *Nat Cell Biol*. 2004;6:820–830.

33. Wang J, Hamblet NS, Mark S, Dickinson ME, Brinkman BC, Segil N, Fraser SE, Chen P, Wallingford JB, Wynshaw-Boris A. Dishevelled genes mediate a conserved mammalian PCP pathway to regulate convergent extension during neurulation. *Development*. 2006;133: 1767–1778.
34. Etheridge SL, Ray S, Li S, Hamblet NS, Lijam N, Tsang M, Greer J, Kardos N, Wang J, Sussman DJ, Chen P, Wynshaw-Boris A. Murine dishevelled 3 functions in redundant pathways with dishevelled 1 and 2 in normal cardiac outflow tract, cochlea, and neural tube development. *PLoS Genet*. 2008;4:e1000259.
35. Wang Y, Nathans J. Tissue/planar cell polarity in vertebrates: new insights and new questions. *Development*. 2007;134:647–658.
36. Oses P, Renault MA, Chauvel R, Leroux L, Allieres C, Seguy B, Lamaziere JM, Dufourcq P, Couffignal T, Duplaa C. Mapping 3-dimensional neovessel organization steps using micro-computed tomography in a murine model of hindlimb ischemia-brief report. *Arterioscler Thromb Vasc Biol*. 2009;29:2090–2092.

DETAILED METHODS

Experimental Animals *fzd4^{+/-LacZ}* heterozygous knock-in-mice were bred in C57BL6 (8 backcross) and CBA (7 backcross) background and then interbred to generate *fzd4^{-/-}* and control (wild-type) littermate mice. Genotyping of *fzd4* mutant mice were performed as previously described¹. A description of the hindlimb ischemia model and laser Doppler perfusion imaging can be found

in the Supplemental section.fzd4

We produced *fzd4^{+/-}* hets during the breeding as *fzd4^{-/-}* mice are sterile and could only be generated using *fzd4^{+/-}* mice crossbreeding. The *fzd4^{+/-}* mice are healthy and fertile and are grossly indistinguishable from their littermate wild-type. They displayed no gross alteration in the morphology (there is no significant differences in weight and size compared to wild type littermate). However a careful examination showed that *fzd4^{+/-}* mice have a vascular phenotypic alteration of the arterial network in the hindlimb after ischemia, compared to wildtype littermates but not likely at the *fzd4^{+/-}* level.

For microCT scanning

The vasculature was imaged with a high-resolution micro-CT imaging system (GE eXplore Locus SP), set to a 0.016-mm effective detector pixel size as previously described⁷. The apparatus used for imaging the vessels was the eXplore Locus Micro-CT scanner from General Electric Healthcare® with spatial resolutions of 36 to 7 μm, and used with the 3D image reconstruction software (Digisens®). Data were acquired in an axial mode covering a single hindlimb as described⁸. The quantification parameters were obtained using the Microview ABA® program. Bones of the hindlimb were delimited and digitally deleted and the density of contrast medium was used as a reference for the program.

Immunohistochemistry

Staining with 5-bromo-4-chloro-3-indolyl- β -D-galactopyranoside (X-Gal) was performed with heart, kidney, skeletal muscle and large arteries and veins as described². Tissues were then embedded in paraffin and sectioned. Nuclear counterstaining was carried out with nuclear red.

Five-micron, paraffin-embedded sections were cut transversely from the mouse muscle. After immunolabelling with antibodies against CD-31 (BMA biomedical), the capillary density was recorded as the number of CD31 positive capillaries per mm² as described⁷. A minimum of 30 randomly chosen pictures were recorded at 40X magnification under a microscope for each animal at each time point with a camera connected to a PC. Positive cells were manually counted on captured images and the data were analyzed with the help of Sigma Plot software.

All analysis was performed by an investigator blinded to treatment groups.

Cell isolation from mutant and wild-type mice:

Primary endothelial cells (EC) and smooth muscle cells (SMC) from adult mouse kidneys and aorta, were isolated as previously described^{3 4}. MEF were isolated from 12.5 day post coitum mouse embryo⁵.

- Primary Renal Endothelial Cell Isolation

Mice were sacrificed, and kidneys were removed, minced in slices and incubated with collagenase (Type I, 2mg/ml; Sigma) for 45 min at 37°C with agitation. The suspensions were triturated with a canule and filtered with 70 μ m filters (BD) followed by a second filtration with 30 μ m filters (Miltenyi). After centrifugation and washings, the pellets were resuspended and plated in growth media (MEM supplemented with D-valine). After five days, cells were trypsinized and incubated with 12.5 μ g/ml of anti-CD31 antibody (Pharmingen) and 5 μ g/ml of anti-endoglin antibody (Santacruz) for 30min at room temperature. Next, the cell solution was incubated with 20 μ l of Goat anti-rat IgG microbeads (Miltenyi) for 15min, at 4°C. After washing, magnetic separation

with MS MACS columns (Miltenyi) was performed and isolated cells were plated in growth media (EBM-2). Greater than 85% of the cells stained positively for CD31.

- Primary Aortic Smooth Muscle Cells Isolation

Aortas were removed and dissected away from fat and extraveneous tissue in sterile, ice-cold, phosphate-buffered saline (PBS) plus $\text{CaCl}_2/\text{MgCl}_2$ (Gibco). Each aorta was incubated in dissecting media consisting of PBS plus $\text{CaCl}_2/\text{MgCl}_2$, 1mg/ml collagenase (Type IV, Sigma), and 125 $\mu\text{g}/\text{ml}$ elastase (Sigma), for 30 min at 37°C. After removal of the adventitia, aortas were minced and shaken gently at 37°C for 2h in dissecting media. The dissociated tissues were subsequently rinsed with PBS plus $\text{CaCl}_2/\text{MgCl}_2$, centrifuged, resuspended and plated in growth media. Greater than 95% of the cells stained positively for α -smooth muscle actin, and myosin heavy chain. All assays were performed with cells before passage four.

- Mouse Embryonic Fibroblast (MEF) Isolation

Primary MEFs were derived from 13.5-day-old embryos. Following removal of the head and organs, embryos were rinsed with PBS, minced, and digested with trypsin (0.05% solution containing 25 $\mu\text{g}/\text{ml}$ DNase) for 90 min at 37°C. Trypsin was inactivated by addition of 100% FBS and cells were plated in growth media. All assays were performed with cells before passage five.

Proliferation assay

Standard procedures were employed. The bromodeoxyuridine (BrdU) assay was conducted as follows, cells were grown on glass slides (Labtek-II system, Nalge Nunc International Corp) and incubated with a BrdU solution (10 μM , Sigma) for 30 min, and revealed with an antiBrdU antibody (Oxford Biotechnologies) after incubation with hydrochloric acid and neutralization using sodium tetraborate as described ⁶. Nuclei cells were stained with Vectashield mounting medium with DAPI (Vector). BrdU labelling cells were counted, and a ratio BrdU labelling /total cell per field was expressed.

Migration (Wound) Assay

To study cell migration, we used Culture-Inserts (Ibidi). Cells were plated on each well of Culture-Inserts and allowed to reach confluence. Cells were serum starved for 24h, then Culture-Inserts were gently removed, and cells were stimulated or not with FGF2 (20ng/ml). The subsequent gaps were imaged at baseline and 20 hr later.

Chemotaxis Assay

Transwell cell culture chambers containing polycarbonate membrane with 8- μ m pore size (Becton Dickinson.) were coated with 0.2% gelatin for MEF and 2% for endothelial cells. Primary and siRNA treated cells were serum starved for 24 hr then trypsinized and plated at 10^5 cells/insert in a Transwell chamber. After 2 hr, the bottom compartment was filled with 800 μ l DMEM plus 1% or 10% FBS, or DMEM plus FGF2 (20ng/ml) or VEGF-A (40ng/ml), and the assembly was incubated at 37°C for 16 h, to allow cell migration. In the negative controls, bottom chambers were filled with DMEM serum-free. After incubation, the membranes were washed with PBS, and cells were fixed in 2% paraformaldehyde, permeabilized with 0.2% Triton X-100 and stained with Mayer's Hematoxylin solution (Merck) according to the manufacturer's protocols. Cells, that did not migrate, were gently removed from the top surface, and cells, that had migrated to the bottom of the membrane, were counted in seven random fields using a Nikon inverted microscope.

Capillary-like tube formation on Matrigel

Tube formation assays were set up using \square -slide angiogenesis (Ibidi) following manufacturer instructions. Human Umbilical Vein cells (HUVEC), purchased from Lonza, were transfected with scramble siRNA or anti-*hfzd4* siRNA (si *hfzd4*) (30 nM) and transfected either with control plasmid or with plasmids coding for Dvl3 tagged myc or Fzd4 tagged HA. 48 hours after

transfection, 15,000 cells per well were plated on top of Matrigel® (Becton Dickinson) in growth medium (EBM-2). After 6 hr at 37 °C, tube formation was examined under an inverted light microscope (Olympus,). Branch lengths were measured and branch numbers per branch point were counted. siRNAs were transfected using Interferin (Ozyme) and plasmid with jetprime (Ozyme), following the manufacturer's protocol. The oligonucleotides used were either a validated negative control (Eurogentec) or designed by Qiagen for *hfzd4*: 5'-

GAA UGA UAG UGC CUU UAA Att -3' (#SI02639105) and Ambion for *mfzd4*: 5'- GGA UGU GCA AUA AUU UUC Utt -3' (#61777). The plasmids encoding for Dvl3 tagged myc were generated in the laboratory and for Fzd4 tagged HA were kindly provided by Tomas Kirchhausen (CBR Institute for biomedical research, Boston).

Golgi polarization assay

This assay was conducted in a migration assay using Culture-Inserts (Ibidi) (see above). 24hrs before experiments, confluent monolayers were serum starved and then activated with FGF2 (20ng/ml). Anti-Golgin97 antibody (Invitrogen), pericentrine and FITC phalloidin (Sigma) were used to stain the Golgi, Microtubule Organizing Center (MTOC) and actin cytoskeleton, respectively.

For the analysis, all images were taken with the same intensity parameters and only cells located in the first row of the wound edge were measured. For determination of the Golgi profile, a line was drawn along the cell and passing by the nucleus, in the direction of the migration edge. For each fluorochrome, the intensity profile was measured along this line using the Axiovision 4.7 program. To quantify Golgi volume, golgi and nucleus surface reconstructions were assigned and cell surface area/cell volume analysis was performed using the Surpass program (Imaris) after 3D deconvolution with autoQuant deconvolution

(Mediacybernetics). For each cellular type, at least 50 cells were examined.

Cell culture

Wnt3a and Wnt5a producing mouse L cells (American Type Culture Collection ATCC) were cultured in DMEM medium, 10% fetal bovine serum (FBS) and penicillin-streptomycin. Conditioned medium was harvested as described in ATCC protocol. Primary renal endothelial cells were cultured in MEM supplemented with 100 μ g/ml Heparin, 50 μ g/ml ECGF, 3.5g/L Glucose, 50mg/L D-valine, 20% FBS (Hyclone) and penicillin-streptomycin, and plated on a 0.2% gelatin-coated dish. After purification, they were cultured in EBM-2 complete medium with EGM2 single coat (Clonetics), and plated on a 5 μ g/ml fibronectin-coated dish. Mouse smooth muscle cells, embryonic fibroblasts (MEF), NIH3T3 and HEK293T were cultured in DMEM supplemented with 10% FBS (Hyclone) and penicillin-streptomycin, and plated on a 0.1% gelatin-coated dish. Human microvascular endothelial cells (HMEC-1) were cultured in EBM complete medium with EGM-MV single coat (Clonetics), and plated on a 2% gelatincoated dish. All cells were serum starved with DMEM plus 1% FBS/0.25% BSA.

Analysis of mRNA expression by quantitative reverse transcriptase-polymerase chain reaction (qRT-PCR)

For RT-PCR analysis 1 μ g of total RNA from mouse tissue or cell extracts was reverse-transcribed: PCR was performed using IQ SYBR Green supermix (Bio-Rad) ². An MJ Research Opticon and the following parameters were used for real-time PCR: 95°C for 5 minutes followed by 34 cycles of 95°C for 30 seconds, 60°C for 1 minute, 72°C for 30 seconds, 76°C for 1 minute and 80°C for 1 minute. Negative controls without RT were prepared in parallel for each RNA sample. All experiments were performed in triplicate and differences in cDNA input were compensated by normalization to expression of P0 or β -actin.

qPCR Primer list

Primers used are as follows: P0 forward primer: 5'-GCGACCTGGAAGTCCAAC-3', and P0 reverse primer: 5'-CCATCAGCACCCACAGCCTTC-3', beta-actin forward primer: 5'-GGAGGAAGAGGATGCGGCA-3', and beta-actin reverse primer: 5'-GAAGCTGTGCTATGTTGCTCTA-3'; ephrinB2 forward primer: 5'-AAGCCAAAGGTCAAACAGG-3', and ephrinB2 reverse primer: 5'-CACGGCCATAAACCAAAAAC-3'; ephB4 forward primer: 5'-AATGCCACAGCCTTAGACAG-3', and ephB4 reverse primer: 5'-AGAATCCCCTTCCAAGCAC-3'; mfzd4 forward primer: 5'-TGACAACCTTTCACGCCGCTC-3', and mfzd4 reverse primer: 5'-TACAAGCCAGCATCGTAGCCACAC-3'; hfzd4 forward primer: 5'-GCTGACAACCTTTCACACCGCTC-3', and hfzd4 reverse primer: 5'-AAGGGCACCTCTTCATCACCTG-3'.

Western Blot analysis and immunoprecipitation

Organ tissues or cells were lysed for 30 minutes in RIPA buffer (1% Nonidet P-40, 0.5% deoxycholate, 0.1% sodium dodecyl sulphate, 50mmol/L Tris, pH 8.0, 2µg/ml aprotinin, 10µg/ml leupeptin, 200µM AEBSF, 1mM benzamide, 1µM orthovanadate). Cell lysates were cleared by centrifugation at 14,000 g for 20 min. Supernatant fractions were used for Western blot or immunoprecipitation. For Western blot analysis, cell lysates were resolved by SDS-PAGE and probed with indicated antibodies. For immunoprecipitation analysis, 500 µg of lysates were incubated overnight with the primary antibody at +4°C with gentle agitation. After this 20 µl of protein G-Sepharose slurry was added and samples were incubated for 1 hr at +4°C. Beads were washed three times and subsequently resuspended and boiled in 20 µl of loading buffer for SDS-PAGE, followed by western blotting.

Antibodies used were: anti EphrinB2 and EphB4 antibodies from Santa Cruz, anti phosphorylated β -catenin (anti-ABC) clone 8E7 monoclonal antibody from Upstate, anti β catenin, acetylated tubulin and α tubulin from sigma, anti Dvl3 and Dvl1 from Santa Cruz, anti GFP from Molecular probes and anti HA from Roche. Binding of antibodies to the blots was detected using Odyssey Infrared Imaging System (LI-COR Biosciences).

Luciferase reporter assay

For the canonical pathway, MEF and HEK 293T cells grown in 24-well culture plates were transiently transfected at 60-70% confluence with 0.2 μ g of 8XTOPflash reporter, 0.1 μ g of β galactosidase reporter (to evaluate efficiency of transfection) and various plasmids as indicated for individual experiments. The total quantity of DNA in the transfection mixes was adjusted to equal amounts with empty vector. 24 hr after transfection, cells were activated with Wnt3a or Wnt5a conditioned medium as indicated. Luciferase activity was measured using the Luciferase Reporter Assay system (Promega) and a luminometer according to the manufacture's specifications. The firefly luciferase activity was normalized to β galactosidase activity.

For the non canonical pathway, MEF and HEK 293T cells were transiently transfected with 0.2 μ g of AP1 reporter, 0.1 μ g of β galactosidase reporter (to evaluate efficiency of transfection) and various plasmids as indicated for individual experiments.

Immunofluorescence microscopy

For tubulin staining, cells were fixed in and stained with monoclonal anti α tubulin. For Fzd4 and Dvl3 co-localization, HA-tagged Frizzled 4 was detected using anti-HA antibodies (Roche) followed by Alexa Fluor 568 conjugated goat anti-mouse IgG. The DNA was counterstained by 4',6-diamidino-2-phenylindole (DAPI). For co-localization studies, cells were analyzed with a Nikon laser scanning confocal microscope using multichannel scanning

(Nikon PCM 2000) using a 60x/1.4 ApoPlan oil immersion objective, and EZ200 software (Nikon). Single XY scans had an optical slice thickness of 0.4 μ m. Three-dimensional projections were digitally reconstituted from stacks of confocal optical slices by Imaris software (Bitplane).

Mouse model of unilateral hind limb ischemia

Unilateral hind limb ischemia was operatively induced as previously described with the excision of the femoral and saphenous arteries ⁶. This study was conducted in accordance with both institutional guidelines and those in force in the European community for experimental animal use (L358-86/609/EEC). Seven days after the surgery, perfusion using Laser Doppler perfusion imaging (LPDI) vascular density was used to record serial blood flow measurements, and connectivity was analyzed using microCT analysis on serial tissue sections.

Statistical analysis

Results are expressed as means \pm SD. All analyses were performed with appropriate software (Statview 5-1, Abacus). Comparison of continuous variables between two groups was performed by a one-way ANOVA and subsequently, if statistical significance was observed, by a two-sided paired *t* test. A value of $p < 0.05$ was considered to be statistically significant.

SUPPLEMENTAL REFERENCES

1. Xu Q, Wang Y, Dabdoub A, Smallwood PM, Williams J, Woods C, Kelley MW, Jiang L, Tasman W, Zhang K, Nathans J. Vascular development in the retina and inner ear: control by Norrin and Frizzled-4, a high-affinity ligand-receptor pair. *Cell*. 2004; 116:883-895.
2. Dufourcq P, Leroux L, Ezan J, Descamps B, Lamaziere JM, Costet P, Basoni C, Moreau C, Deutsch U, Couffinhal T, Duplaa C. Regulation of endothelial cell cytoskeletal reorganization by a secreted frizzled-related protein-1 and frizzled 4- and frizzled 7-dependent pathway: role in neovessel formation. *Am J Pathol*. 2008; 172:37-49.
3. Marelli-Berg FM, Peek E, Lidington EA, Stauss HJ, Lechler RI. Isolation of endothelial cells from murine tissue. *J Immunol Methods*. 2000; 244:205-215.

4. Bradshaw AD, Francki A, Motamed K, Howe C, Sage EH. Primary mesenchymal cells isolated from SPARC-null mice exhibit altered morphology and rates of proliferation. *Mol Biol Cell*. 1999; 10:1569-1579.
5. Kamijo T, Zindy F, Roussel MF, Quelle DE, Downing JR, Ashmun RA, Grosveld G, Sherr CJ. Tumor suppression at the mouse INK4a locus mediated by the alternative reading frame product p19ARF. *Cell*. 1997; 91:649-659.
6. Ezan J, Leroux L, Barandon L, Dufourcq P, Jaspard B, Moreau C, Allieres C, Daret D, Couffinhal T, Duplaa C. FrzA/sFRP-1, a secreted antagonist of the Wnt-Frizzled pathway, controls vascular cell proliferation in vitro and in vivo. *Cardiovasc Res*. 2004; 63:731-738.
7. Oses P, Renault MA, Chauvel R, Leroux L, Allieres C, Seguy B, Lamaziere JM, Dufourcq P, Couffinhal T, Duplaa C. Mapping 3-dimensional neovessel organization steps using micro-computed tomography in a murine model of hindlimb ischemia: brief report. *Arterioscler Thromb Vasc Biol*. 2009; 29:2090-2092.
8. Tirziu D, Moodie KL, Zhuang ZW, Singer K, Helisch A, Dunn JF, Li W, Singh J, Simons M. Delayed arteriogenesis in hypercholesterolemic mice. *Circulation*. 2005; 112:2501-2509.

Article 2

The ubiquitin ligase PDZRN3 is required for vascular morphogenesis through Wnt/planar cell polarity signaling

Rationnel	<p>La signalisation Wnt est importante durant la morphogénèse et le remodelage vasculaire. Cependant, les partenaires en aval de cette voie dans ce processus restent méconnus. Des études récentes suggèrent que l'endocytose des récepteurs Fzd et l'ubiquitination des protéines Dvl seraient essentielles dans la transduction du signal dans les voies Wnt.</p>
Résultats	<p>Grâce à une stratégie de double Hybride, nous avons identifié des nouveaux partenaires de Dvl, dont l'E3 ubiquitine ligase, PDZRN3. Des mutants murins délétés pour le gène <i>Pdzrn3</i> ont été créés et croisés avec des souris <i>Ubc-iCre</i> et <i>PDGF-iCre</i>, permettant la délétion de <i>Pdzrn3</i> de façon ubiquitaire ou spécifiquement dans les cellules endothéliales respectivement. La délétion ubiquitaire de <i>Pdzrn3</i> induit une létalité embryonnaire précoce due à un défaut de vascularisation du placenta et du sac amniotique. La délétion de <i>Pdzrn3</i> dans les cellules endothéliales avant vascularisation de la rétine induit un retard et une désorganisation des différents plexus.</p> <p>La répression de <i>Pdzrn3</i> réduit la migration des cellules endothéliales et la formation de tubes endothéliaux dans un modèle de culture en 3D sous activation Wnt. PDZRN3 modulerait l'activité du complexe Fzd/Dvl à la surface des cellules endothéliales. PDZRN3, en induisant la prise en charge de Fzd4 par les voies d'endocytose, favoriserait l'activation de la voie Wnt dans les cellules endothéliales. Ainsi, PDZRN3 ubiquitinerait Dvl, ce qui favoriserait le recrutement de Fzd4 dans les vésicules d'endocytose.</p>
Conclusion	<p>Nous proposons un mécanisme par lequel la protéine PDZRN3 favoriserait l'activation de la voie Wnt non canonique au cours de la morphogénèse vasculaire.</p>

a) State of art

PDZ domains are described in scaffolding proteins. PDZ-containing scaffolds assemble proteins in large molecular complex at defined localizations in the cell. It is the case of PSD-95 that organizes glutamate receptors in synapse. PDZ scaffolds can also modulate trafficking of cargo proteins via vesicles. PDZRN3 is remarkable as it possesses PDZ domains/ PDZ binding domains and a RING domain. The RING domain is functional and identifies PDZRN3 as an ubiquitin ligase, a protein that gives the specificity to the reaction of ubiquitylation.

As downstream effectors of Fzd4 and Dvl3 are not known well, a strategy of Yeast two hybrid was set up. Dvl proteins are composed of various domains such as the Dix domain, essential for the interaction with β -catenin and for activation of the canonical pathway. The PDZ and DEP domains are essential for Dvl interaction with Fzd proteins.

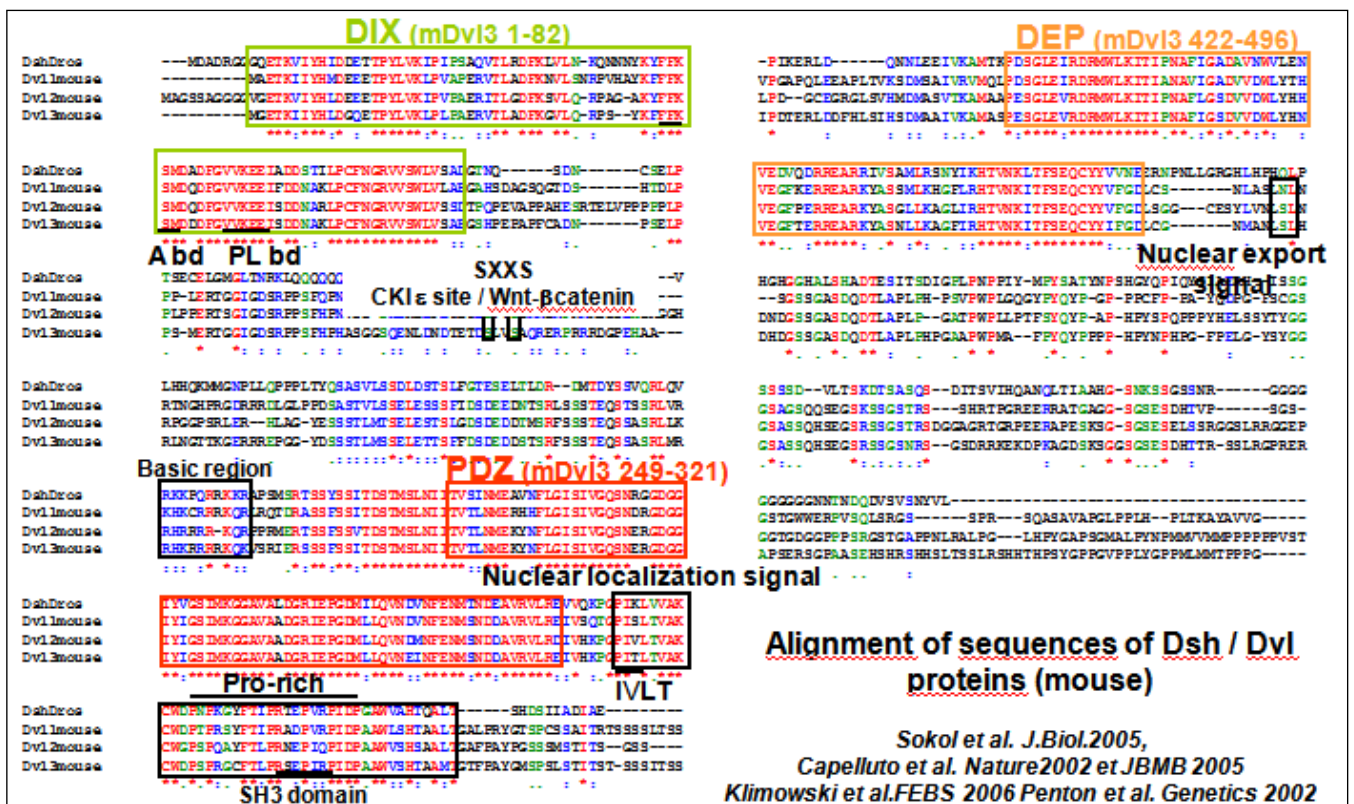


Figure 87: Alignment of the Dvl1/ 2 and 3 sequences

b) Hypothesis

We hypothesize that Dvl interacts via its PDZ/ DEP domains with partners involved in the non canonical pathway.

c) Strategy

As the DIX domain of Dvl is essential for signal transduction in the canonical pathway, a Dvl3 construct deleted from the DIX domain was chosen as bait for the yeast two hybrid. A bank of cDNAs from mouse embryo day post coitum 12.5 was chosen as prey, because Wnt signaling is important during development (Fig 88). Using this strategy, we were able to identify many targets implicated in cell cycle/ proteasome and microtubules rearrangement (Fig 89).

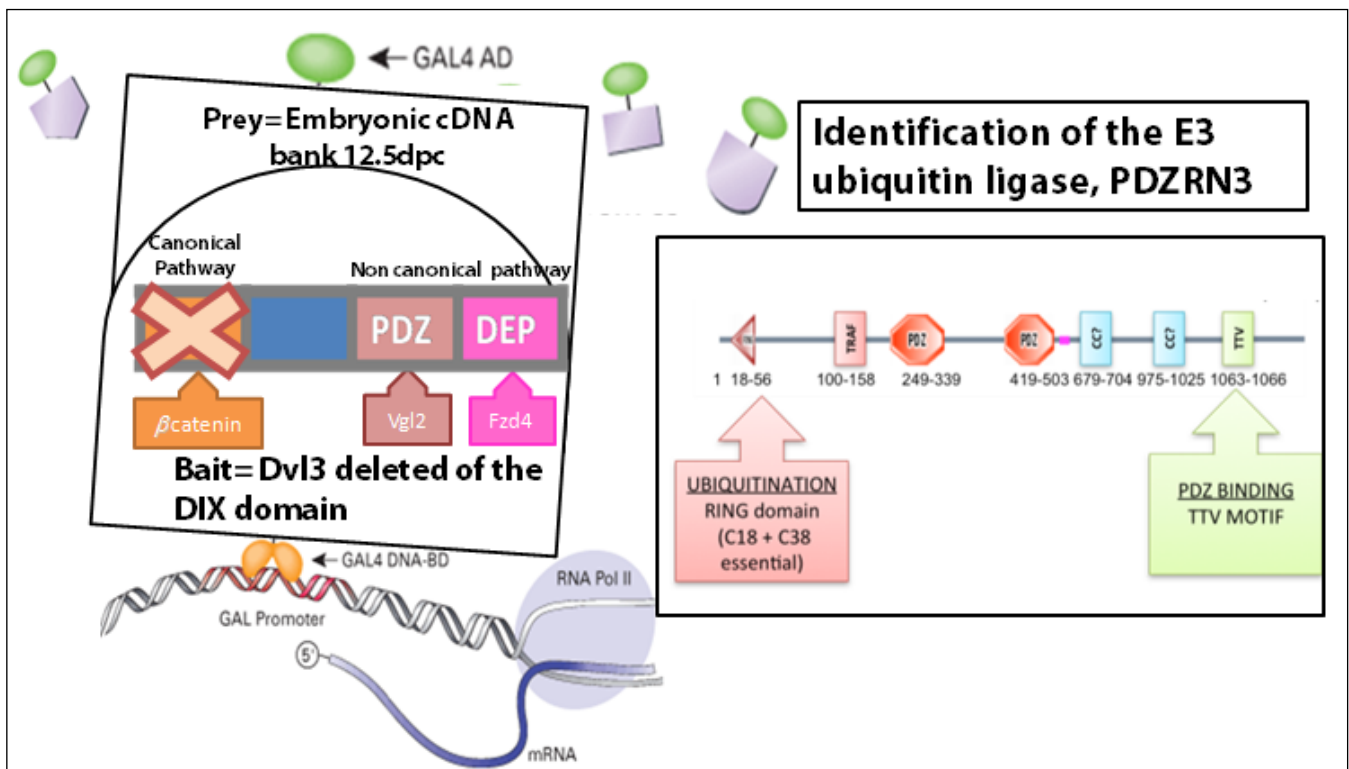


Figure 88: Yeast two Hybrid Strategy and Structure of the PDZR3 protein

d) Preliminary Results

cell division cycle associated 8 (Cdca8)	microtubule associated serine/threonine kinase 2 (Mast2)	Niemann Pick type C2 (Npc2)	proteasome 26S subunit, non-ATPase, 8 (Psm8)	large tumor suppressor (Lats1)
Notch gene homolog 1 (Notch1)	homeodomain interacting protein kinase 1 (Hipk1)	La ribonucleoprotein domain family, member 2 (Larp2)	E2F transcription factor 7 (E2f7)	DNA-damage regulated autophagy modulator 2 (Dram2)
dapper homolog 1, antagonist of beta-catenin (Dact1)	syntaxin 8 (Stx8)	elastin microfibril interfacier 1 (Emilin1)	von Hippel-Lindau binding protein 1 (Vbp1)	stathmin-like 2 (Stmn2)
vang-like 2 (van gogh, Drosophila) (Vangl2)	topoisomerase (DNA) III beta (Top3b)	LIM domain only 4 (Lmo4),	kinesin family member 26B (Kif26b)	Jun-B oncogene (Junb)

Figure 89 A few of the proteins found to be interacting with Dvl3 Dix using the screening

A few proteins were chosen for characterization. We performed quick assays on each candidate (Larp1b; Lmo4; Kif26b; Pdzn3; Dram2). In this screening, we evaluated whether the candidate was expressed in endothelial cells, regulated properties of EC such as migration or tubulogenesis and finally, whether they modulated Wnt pathway. The E3 ubiquitin ligase PDZRN3 was one of the more interesting candidates. The protein is composed of a RING domain essential for its activity of ubiquitin ligase, two PDZ domains and one PDZ binding motif (thr-thr-valine motif)(Fig88). This domain is rare and is required for binding of proteins containing PDZ domains.

To study PDZRN3, we asked for the plasmid coding for the protein to Dr. Yamamoto that was tagged with a V5 cassette (Ji-Ae Ko 2006, Honda et al. 2010). We expressed the plasmid in Hela cells and assessed the localization of the tagged protein. PDZRN3 –V5 was found in cytoplasmic puncta.

These puncta colocalized with markers of clathrin mediated endocytosis such as Rab5 and Rab11; but also with endogenous ubiquitin (Fig 90).

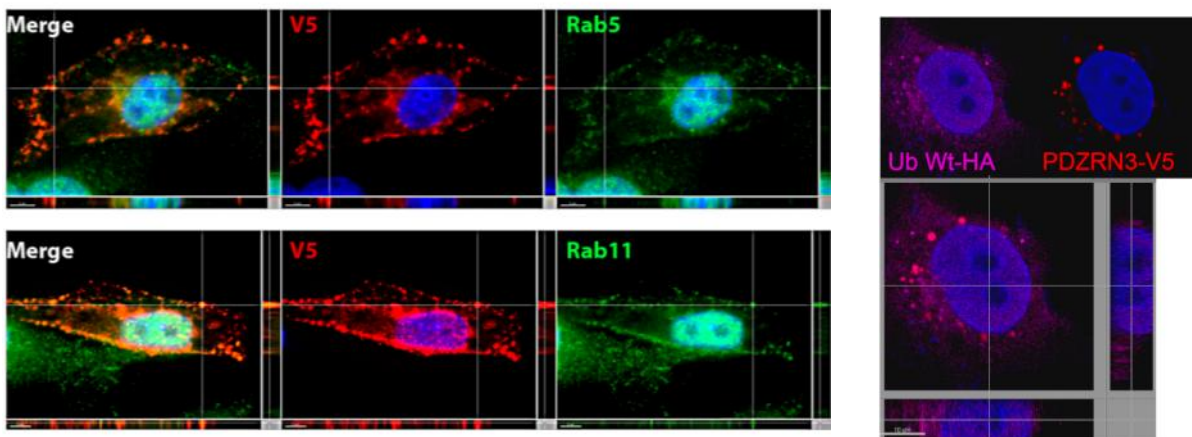


Figure 90 PDZRN3 (V5) colocalizes with clathrin, Rab5 and Rab11; wth ubiquitin

We also purchased siRNA directed against the gene coding for human form of *Pdzrn3*. We performed basic tests on HUVECs to assess if depletion of *Pdzrn3* impacts their properties. Depletion of *Pdzrn3* reduced endothelial migration in an Ibidi 2D migration assay (Fig 91).

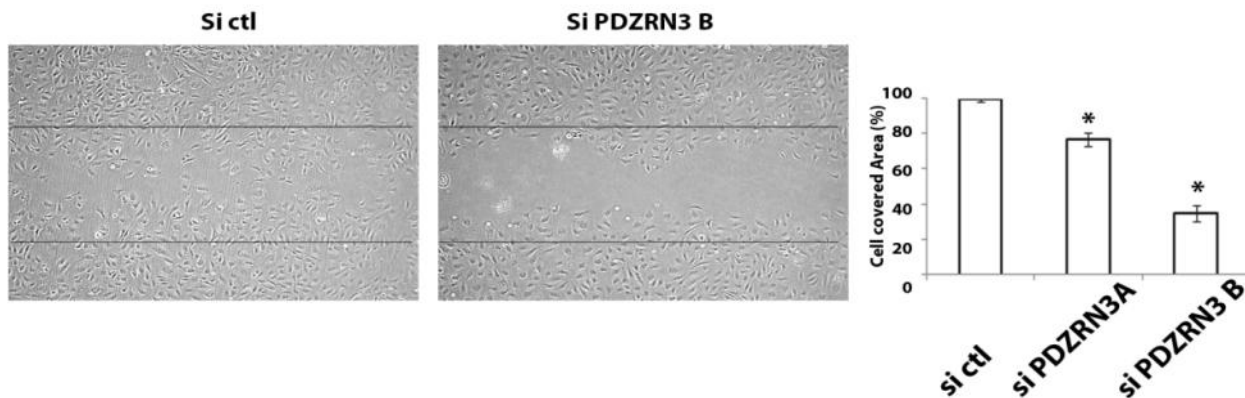


Figure 91 Depletion of *Pdzrn3* using two siRNAs reduces migration of endothelial cells

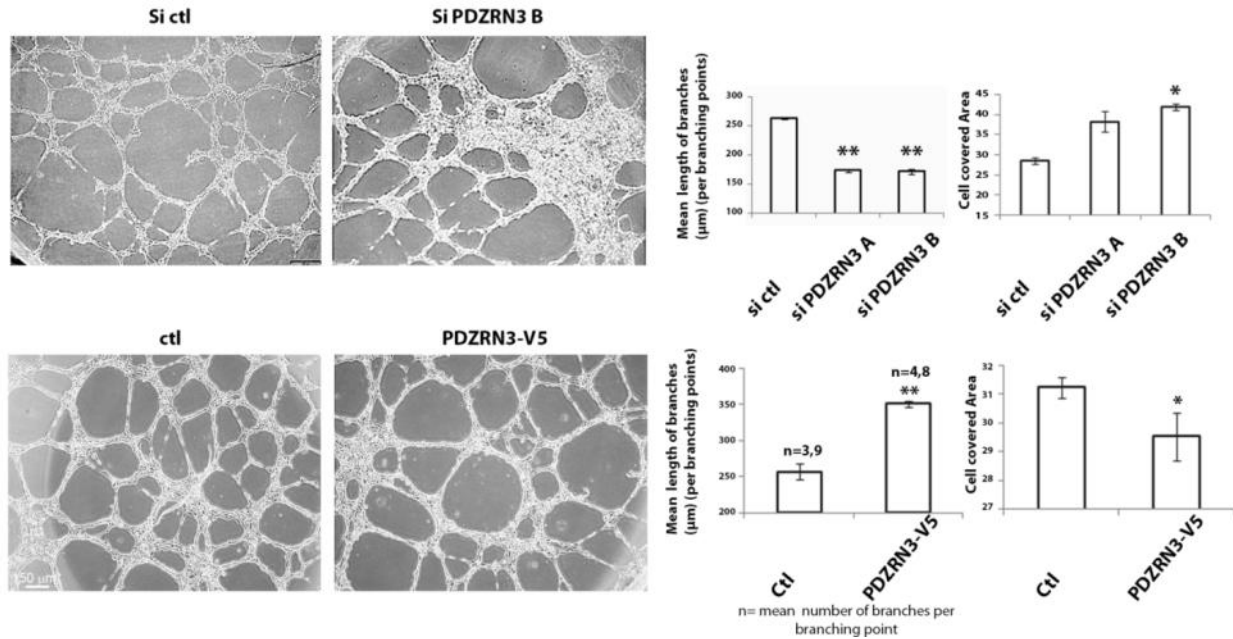


Figure 92 Loss of *Pdzn3* modifies the ability of endothelial cells to form tubes

In a similar manner, we were able to show that depletion of *Pdzn3* would also reduce the ability of EC to form tubular structures in a 2D tubulogenesis assay. These assays indicated a role of the protein in endothelial function and the localization of the protein to clathrin mediated vesicles suggested a role of PDZRN3 in vesicular trafficking. That's why we decided to process with a complete study of the role of PDZRN3 in Wnt non canonical signaling.

e) Summary

This work identifies PDZRN3 as a switch between Wnt non canonical and canonical pathways. PDZRN3 ubiquitinylates Dvl3. This promotes clathrin-mediated endocytosis of the Fzd4/Dvl3 complex; and enables signal transduction from the early endosome, a mechanism similar to the one described with TLR signaling (Dobrowolski and De Robertis 2011). This process takes off the Fzd/ Dvl complex from the canonical Wnt pathway signal transduction that probably uses caveolin-mediated endocytosis for signal transduction. Non canonical pathway is essential for vascular morphogenesis (migration of EC, remodeling) while canonical is required for proliferation and differentiation. PDZRN3 would activate angiogenesis by inducing non canonical pathway and blocking the canonical pathway.

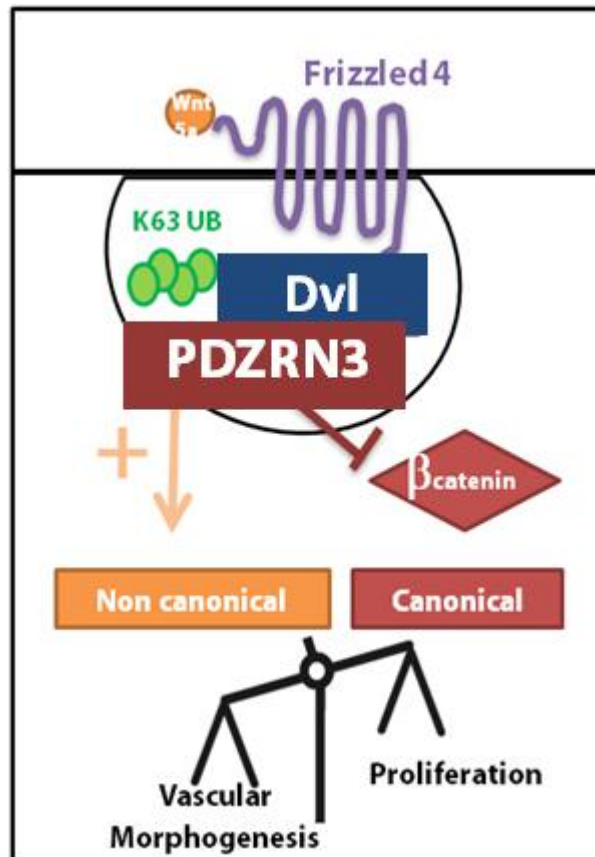


Figure 93: Role of PDZRN3 for transduction of Wnt signaling and vascular morphogenesis

The ubiquitin ligase PDZRN3 is required for vascular morphogenesis through Wnt/Planar cell polarity signaling

Raj N. Sewduth¹, Béatrice Jaspard-Vinassa^{1,2}, Claire Peghaire¹, Aude Guillabert¹, Nathalie Franzl¹, Catherine Moreau¹, Markus Fruttiger³, Pascale Dufourcq^{1,2}, Thierry Couffinhal^{1,2,4}, Cécile Dupl a^{1,2}.

1 INSERM, Adaptation cardiovasculaire   l'isch mie, U1034, F-33600 Pessac, France

2 Univ. Bordeaux, Adaptation cardiovasculaire   l'isch mie, U1034, F-33600 Pessac, France

3 UCL Institute of Ophthalmology, London EC1V 9EL, UK

4 CHU de Bordeaux, Service des Maladies Cardiaques et Vasculaires, F-33000 Bordeaux, France

Contact: C cile Dupl a M : cecile.dupl a@inserm.fr

Summary

Development and stabilization of a vascular plexus requires the coordination of multiple signaling processes. Wnt Planar cell polarity (PCP) signaling is critical in vertebrates for diverse morphogenesis events, which coordinate cell orientation within a tissue specific plane. However, its functional role in vascular morphogenesis is not well understood. Here we identify PDZRN3, an ubiquitin ligase, and report that *Pdzrn3* deficiency impairs embryonic angiogenic remodeling and post natal retinal vascular patterning with a loss of 2D polarized orientation of the intermediate retinal plexus. Using *in vitro* and *ex vivo* *Pdzrn3* loss-of-function and gain-of-function experiments, we demonstrate a key role of PDZRN3 in endothelial cell directional and coordinated extension. PDZRN3 ubiquitinates Dishevelled 3 (Dvl3), to promote endocytosis of the Frizzled/Dvl3 complex, for PCP signal transduction. These results highlight the role of PDZRN3 to direct Wnt PCP signaling, and broadly implicate this pathway in the planar orientation and highly branched organization of vascular plexuses.

Introduction

During development or tissue regeneration, vascular growth is a complex process that can be schematically divided in two dynamic steps. First a highly unstable vascular plexus is developed, with vessels expanding and collapsing at a high rate. Then, the newly formed vascular system is remodeled to ensure the transition toward a stable and functional network (Herbert and Stainier, 2011). Evolution toward a structured vascular system is characterized by the formation of a 3 dimensional (3D) hierarchically branched and organized vascular network (Fruttiger, 2007), suggesting that vascular cells

or groups of vascular cell, are instructed to be oriented within stable functional tubes. Recently, several groups, including our own, have provided evidence to underscore the importance of Wnt/Frizzled/planar cell polarity (Wnt/PCP) signaling in vascular system morphogenesis and remodeling (Cirone et al., 2008; Ju et al., 2010).

Evidence has previously linked the Wnt canonical pathway to vascular formation. Mutations of Norrin (Ndp), Frizzled4 (Fzd4), Tetraspanin-12 (TSPAN12) or LRP5, led to ocular syndromes, such as exudative vitreoretinopathy (EVR) (Junge et al., 2009; Nikopoulos et al., 2010; Poulter et al., 2010; Xu et al., 2004; Ye et al., 2010). In *ndp*, *fzd4*, *lrp5* and *tspan12* loss-of-function mice, development of the superficial retinal plexus has been shown to be altered, with a lack of the deep and intermediate vascular plexuses (Junge et al., 2009; Xia et al., 2010; Xu et al., 2004; Zuercher et al., 2012), linking the Wnt canonical signaling complex to vascular formation in the retina. However, the role of the non-canonical PCP pathway is not yet well understood during vessel development and the mechanisms by which the endothelial Wnt/PCP pathway regulates vessel morphogenesis remain elusive.

The conserved Wnt/PCP signaling is involved in patterning, by instructing cell polarity within a tissue (Wu and Mlodzik, 2009). First observed in insects, where it regulates the orientation of hair on wings and facets on the eye, Fzd/PCP is now known to be involved in regulating gastrulation and sensory cell orientation in vertebrates (Wang and Nathans, 2007). PCP signaling controls basic mechanisms including cell migration, axonal guidance, asymmetric cell division, as well as hair and cilia orientation (Devenport and Fuchs, 2008; Seifert and Mlodzik, 2007). PCP signaling in insects and vertebrates, shares a core pathway that includes members of the dishevelled (Dvl1-3 members) (Etheridge et al., 2008) and *fzd* gene families, but is distinct from the β -catenin-dependent canonical Wnt pathway (Montcouquiol et al., 2006). Dvl proteins are the relays between the Fzd receptor and Wnt downstream signaling pathways (Gao and Chen, 2010). To regulate all of these functions, Dvl has to associate with different protein partners and induce PCP signaling cascades that involve activation of c-jun, a hallmark for PCP signaling and the small GTPases Rho and Rac (Park et al., 2005).

Interestingly, among Dvl members, Dvl3 could be an important relay for Wnt/PCP signaling. Indeed, Dvl3 has a unique function compared to that of the other isoforms in analyzing genetic Dvl1-3 mutant phenotypes (Etheridge et al., 2008). In vitro studies showed that Dvl3 compared to Dvl1 and Dvl2 potentiated non canonical Dab2-dependent activity (Hocevar et al., 2003). Recently, our group has identified an important role for Dvl3 in PCP signaling induction in endothelial cells (Descamps et al., 2012). To further elucidate the molecular mechanisms regulating the activity of Dvl3 in the PCP pathway, we performed a yeast-two hybrid screening to search for novel Dvl3-interacting proteins. Among these we identified the E3 ubiquitin ligase PDZ domain-containing RING finger protein 3 (PDZRN3). Whereas previously published studies have revealed the role of PDZRN3 in skeletal muscle (Ko et al., 2006) and osteoblast differentiation acting as an inhibitor of Wnt/b catenin signaling (Honda et al., 2010), its role in Wnt signaling is poorly understood.

We report that PDZRN3 is expressed in endothelium and using a gene-targeting strategy, we explored the *in vivo* role of *Pdzrn3* during angiogenesis. First, we deleted *Pdzrn3* during angiogenic gestational steps from E7.5, taking advantage of the inducible Ubc Cre^{ERT2} mice. We report that embryos died very early *in utero* at E11.5, exhibiting defects in large vitelline vessel morphogenesis in the yolk sac, and impairment of embryonic capillary invasion in the placenta leading, to severe growth retardation. Next, we showed that conditional deletion of *Pdzrn3* in EC, in neonates induced a defect in branch extension with excessive vessel regression of the superficial retinal vascular plexus, and ultimately a global mis-orientation of polarized capillaries in the intermediate plexus. *In vitro* and *ex vivo* gain and loss of *Pdzrn3* expression experiments, revealed a role of PDZRN3 in EC coordinated extension, polarization and tubular plexus formation. Mechanistically, we present evidence that PDZRN3 acts as a new partner of Dvl3 and could promote Dvl3 ubiquitylation, to mediate PCP signaling activation in EC. Taken together, our data reveals a novel and crucial role of Wnt PCP signaling via the ubiquitin ligase PDZRN3 during vascular plexus directional extension and planar organization.

Results

PDZRN3 gene deletion induces vascular defects in the yolk sac and placenta

A yeast two-hybrid screen was conducted on an 11.5 dpc mouse embryonic library, with Dvl3 as bait in which the DIX domain was deleted-(Dvl3 Δ DIX) as bait. The DIX domain has been shown to favor the canonical pathway over the PCP pathway (Kishida et al., 1999; Liu et al., 2011; Wong et al., 2004). We identified PDZRN3, an E3 ubiquitin-protein ligase, shown to negatively regulate Wnt signaling during osteoblast differentiation. As it is widely expressed in various adult mouse tissues (Ko et al., 2006) (Supplementary Fig 1), we asked if PDZRN3 was expressed in a common structure, the endothelium. We first performed real time RT/PCR experiments on distinct mouse and human primary and cultured endothelial cells and showed that it is expressed at a high level (Supplementary Fig 1a-c). Then we showed that its expression during angiogenic processes, co-localized predominantly with CD31+ vessels in E12.5 yolk sac, E14.5 brain and, postnatally at day 7 (P7), in retinal EC and aortic EC, providing support for a potential role during angiogenesis (Supplementary Fig 1d). To investigate the role of PDZRN3 in blood vessel development, we created mice with targeted deletions of *Pdzrn3*, by crossing a homozygous LoxP-flanked *Pdzrn3* allele with Cre expression driven by Ubc-cre^{ERT2}, a potent ubiquitous promoter (Ruzankina et al., 2007). Pregnant mice were treated daily with tamoxifen injections from E7.5 to E9.5, to inactivate *Pdzrn3* during earlier angiogenesis phases. We verified that PDZRN3 expression at E10.5 was significantly reduced in embryonic brain lysates by Western blot (Fig 1a). The Ubc-Cre^{ERT2} + *Pdzrn3*^{ff} genotype had retarded growth from E9.5 and died between E11.5 - E12.5 (Fig 1b-c). In whole-mount, the pattern of vascularization of Ubc-Cre^{ERT2}; *Pdzrn3*^{ff} embryos yolk sacs from E9.5 through E10.5 appeared altered-compared to that in their wild-type littermates, suggesting a defect in circulation (Fig 1c). At E9.5, all Ubc-Cre^{ERT2}+; *Pdzrn3*^{ff} mutant yolk sacs showed an altered pattern of distribution compared to wild type, associated with an increase of vitelline artery diameter, while at E10.5, disorganization of the vascular network was more apparent suggesting an inability to complete angiogenic remodeling (Fig 1c). It is worth noting that tamoxifen treatment of pregnant mice from E10.5 to E12.5, did not induce lethality (Fig 1b), indicating a key role for *Pdzrn3* in the early angiogenic phases. Histological analysis of the placenta from E9.5 and E10.5 mutant embryos, revealed that while chorio-allantoic fusion had occurred, the labyrinth layer was reduced and fetal capillaries invading the labyrinth

were absent. Comparatively, in wild-type embryos, fetal vessels were evenly distributed throughout the labyrinth (Fig 1d). Ubc-Cre^{ERT2} *Pdzn3*^{f/f} embryo vasculature, revealed by whole mount PECAM staining, appeared altered with reduction of the brain vasculature (Fig 1e). Taken together, our results suggest that severe growth retardation and embryonic death, at mid gestation in Ubc-Cre^{ERT2}+ *Pdzn3*^{f/f} mice, could be caused by defective yolk sac circulation and/or placenta function.

Furthermore, we created mice with targeted deletions of *Pdzn3*, by crossing a LoxP-flanked *Pdzn3* gene with Cre expression driven by a *Pdgf* tamoxifen-inducible promoter which targets ECs (Claxton et al., 2008). We then analyzed *Pdgf*^{cre} *Pdzn3*^{f/f} embryo mutants (iEC KO) between E9.5 and E11.5 versus *Pdzn3*^{f/f} embryo controls (iEC WT) (Supplementary Fig. 2). We observed an altered pattern of vessel organization in the yolk sacs of the iEC KO embryos similar to that reported for the Ubc-CreERT2 + *Pdzn3*^{f/f} mutants (Supplementary Fig. 2a). Moreover, histological analysis of mutant placenta at E10.5, revealed a statistical decrease in the number of embryonic vessels that invade the labyrinth layer (Supplementary Fig. 2b). However, it is noteworthy that the alterations of the embryo vascular network, either in yolk sacs or placenta, were milder than the one found under Ubc-Cre^{ERT2} depletion and only 25% of the iEC KO embryos had growth retarded at E11.5. In conclusion, this complementary genetic approach strongly supports a direct role for *Pdzn3* on vascular yolk sac organization and the development of the embryonic vascular labyrinth structure in placenta.

PDZRN3 gene deletion in ECs induces vascular defects

Next, we analyzed the effects of PDZRN3 deficiency on vessel morphogenesis postnatally, in the mouse retina. Western blots on wild-type whole retinal lysates from P3 to P21 showed that PDZRN3 is expressed in EC, with peak expression at P12, which coincides with intense vascular remodeling (Fig 2a). Post natal recombination efficiency was evaluated by crossing mT/mG *Pdzn3*^{f/f} reporter mice with *Pdgf*^{cre} + *Pdzn3*^{f/f} mice. Depletion of *Pdzn3* was verified by Western blot, in *Pdzn3*^{iECKO} versus littermate control (*Pdzn3*^{iECWT}) retina lysates (Fig 2b). Retina from *Pdzn3*^{iECKO} mice had delayed vascularization of the superficial retinal plexus (SRVP) at P7 compared to control *Pdzn3*^{iECWT} mice, with reduced vascular density and a decrease in the number of branch points, while EC proliferation was

significantly increased in tip cells and in the plexus as revealed after BrdU injection. *Pdzrn3*^{iECKO} vessels appeared to be unstable, with an increase in the number of empty Collagen IV positive/ isolectin B4 negative “sleeves” in the central areas (Fig 2c). The number of tip cells was not affected. At P12, the SVRP still displayed excessive capillary regression (Fig 2d). Interestingly, in control retinas the deep capillary plexus displayed a complex hexagonal pattern, reminiscent of honey comb structures, while in mutant retinas the capillary network was abnormal and massively reduced. To test whether *Pdzrn3* deletion could alter plexus formation via the PCP pathway, we analyzed the planar polarized organization of the intermediate capillary network, which forms bridges between the parent apical plexus (superficial retinal vascular plexus, SRVP) and the parallel basal deep plexus (deep retinal vascular plexus, DRVP). This intermediate network emerged in a two-dimensional sheet, orthogonal to the axis of the SRVP (Fig 2d). We collected confocal images and extracted capillary skeletons in this plane, which revealed that the pattern of vessel organization from SRVP to DRVP, was altered. In mutants, capillaries that initiated from the SRVP, subsequently pointed in inappropriate directions in the deepest plexus compared to that of the well-organized polarized network in control mice (Fig 2e). These data demonstrate that *Pdzrn3* deletion alters vessel remodeling and stabilization during retinal angiogenesis, and impairs polarized capillary structure formation during tertiary plexus formation.

PDZRN3 silencing impairs directional migration and favors sprout regression in vitro

We then explored whether the observed angiogenic phenotype in *Pdzrn3* mutants was due to EC motility defects. First we analyzed the role of PDZRN3 on EC migration under Wnt induction. Cell tracking of migrating EC revealed that Wnt5a enhanced the distance of EC migration compared to control conditions (Fig 3a). We then showed that *Pdzrn3* depletion, using siRNA, impairs Wnt5a-induced EC migration and that conversely, lentiviral *Pdzrn3* transduction markedly enhanced EC migration in Wnt5a-treated conditions. Importantly, *Pdzrn3* depleted cells lost their ability to migrate in a directional manner while *Pdzrn3* lentivirus transduced EC migrated primarily in a straight path, in Wnt5a conditions (Fig 3a).

Next, we assessed whether PDZRN3 is required for sprouting extension using an assay for collective EC migration, where HUVECs form sprouts in a fibrin gel (Fig 3b). In this assay, we first

confirmed that Wnt5a enhanced angiogenic sprout lengths, by showing that Wnt5a-transfected fibroblasts layered on top of the gel enhanced EC tube length significantly, compared to control fibroblasts. Ninety-six hours after plating, silencing of *Pdzrn3* blocked cells from leaving the beads in response to basal or Wnt5a conditions. *Pdzrn3*-silenced EC did not migrate collectively and could not form long, multi-nuclei branched structures, while PDZRN3 lentiviral transduction of *Pdzrn3*-silenced HUVECs restored 3D EC migration in response to basal or Wnt5a conditions (Fig 3b). The analysis of the duration of tube-like structure on recorded time lapse images, revealed that sprouts are dynamically formed over the course of 16 hours, while *Pdzrn3*-silenced EC were incapable of maintaining sprouts. This data demonstrates the role of PDZRN3 in favoring capillary like structure formation and stabilization (Fig 3c).

***Pdzrn3* regulates Dvl3 ubiquitinylation**

We then explored mechanistically, the role of PDZRN3 in endothelial morphogenetic events. First, we confirmed that at endogenous levels Dvl interacts with PDZRN3. In *Pdzrn3*^{iECWT} lung lysates, co-immunoprecipitation of endogenous Dvl3 using anti Dvl3 antibody, co-precipitated PDZRN3, which included several ubiquitin chains, whereas in *Pdzrn3*^{iECKO} lung extracts, the Dvl3-PDZRN3 interactions and Dvl3 ubiquitinylation were markedly reduced (Fig 4a).

We further investigated whether Dvl3 was a substrate of PDZRN3-mediated ubiquitinylation. We co-expressed either Ub WT-HA or Ub^{K48only}-HA and Ub^{K63only}-HA, in which all the lysine residues are mutated to arginine except Lys48 or Lys63, respectively, with Dvl3-myc. PDZRN3-V5 was able to induce Dvl3 ubiquitinylation in the presence of either Ub WT-HA or Ub^{K63only}-HA, but not with HA-Ub^{K48only}. As Lys63 is the major site for PDZRN3 mediated polyubiquitinylation of Dvl3, our data suggests that ubiquitinylation of Dvl3 by PDZRN3 is an intracellular signal promoting Dvl3 trafficking (Fig 4b). Since Dvl proteins are known to be involved in endocytosis during Wnt/PCP signaling (Chen et al., 2003; Kim et al., 2008; Kishida et al., 2007; Yu et al., 2007), we hypothesized that PDZRN3 may facilitate endocytosis of the Dvl3 complex, in order to induce non-canonical PCP signaling. To test this hypothesis, we followed Dvl3 ubiquitinylation under Wnt/PCP activation. Incubation with Wnt5a conditioned medium (CM) for 1 hour, induced ubiquitinylation of Dvl3-Myc in HEK293T cells co-

transfected with Ub^{K63only}-HA and Dvl3-Myc (Fig 4c). However, Wnt5a failed to induce Dvl3-Myc ubiquitinylation in *Pdzn3* depleted cells using siRNA. These results demonstrate that PDZRN3 is required for Wnt5a mediated ubiquitinylation of Dvl3-Myc.

To understand how Dvl3 interacts with PDZRN3, we sought to identify the domains in Dvl3 and PDZRN3 that are important for their interaction and for PDZRN3 ubiquitinylation activity (Fig 4d). When PDZRN3-V5 was co-transfected with Dvl3-myc and HA-tagged Ubiquitin (Ub Wt-HA) in HeLa cells, Dvl3 ubiquitinylation was detected as a smear of bands in the anti-myc immunoprecipitate with anti-HA. Interestingly, PDZRN3 could not induce ubiquitinylation of Dvl3 Δ DIX in the presence of Ub-HA, suggesting that PDZRN3 ubiquitinylates Dvl3 on its DIX domain. We identified the domains of PDZRN3 required for interaction with Dvl3. As the Thr-Thr-Val-COOH motif (TTV motif) has previously been characterized as a PDZ binding domain (PDZB) (Torres et al., 1998; Valiente et al., 2005), we co-expressed Dvl3-myc with PDZRN3 deleted from the C terminal TTV motif (PDZRN3 Δ PDZB). Dvl3-myc was unable to precipitate PDZRN3 Δ PDZB, demonstrating that the PDZ binding motif (TTV) of PDZRN3 is required for PDZRN3 binding to Dvl3. Next, we mapped the PDZRN3-interacting domain of Dvl3 using various myc-tagged Dvl3 constructs (Descamps et al., 2012). Deletion of PDZ (Dvl3 Δ PDZ), but not the DIX (Dvl3 Δ DIX) domain, impaired Dvl3 immunoprecipitation of PDZRN3 (Fig 4d). This data shows that the interaction between PDZRN3 and Dvl3 is mediated by the C-terminal PDZRN3 PDZ binding domain and the PDZ domain of Dvl3.

***Pdzn3* silencing impairs Frizzled/Dvl3 endocytosis in the Rab5 positive compartment**

We previously demonstrated that Fzd4 recruits Dvl3 at the cell membrane to induce PCP signaling. Here we analyzed whether PDZRN3 could be recruited to the Fzd4/Dvl3 complex at the cell membrane. Examination of sub-cellular distribution of the three partners (PDZRN3, Fzd4 and Dvl3) showed that in Fzd4-HA-transfected HeLa cells, PDZRN3-V5 and Dvl3-Myc re-localized from the cytoplasm to the cell membrane, co-localizing with Fzd4-HA (Supplementary Fig 3). In the presence of Dvl3 Δ PDZ-Myc and PDZRN3-V5, only Dvl3 Δ PDZ-Myc was re-localized to the cell membrane with Fzd4-HA, while PDZRN3-V5 stayed in the cytoplasm (Supplementary Fig 3). This result supports the notion that the

interaction between PDZRN3 and Dvl3, via the PDZ domain of Dvl3, is required for recruitment of PDZRN3 toward Fzd4.

Next, we examined the role of PDZRN3 in endocytosis of the Fzd4/Dvl3 complex upon activation of Wnt5a, using *in vitro* models. Immunoprecipitation assays demonstrated that Wnt5a treatment induces Fzd4/Dvl3 re-localization in the Rab5 positive compartment, and its effects are impaired under conditions of *Pdzrn3* depletion. (Fig 5a). Using cell fractionation approaches, we confirmed that Wnt5a treatment induces re-localization of the Fzd4/Dvl3 complex from the cytosolic membrane, to early endosome fractions. Treatment with either the inhibitor of dynamin, Dynasore, or depletion of *Pdzrn3*, blocked Fzd4/Dvl3 re-localization (Fig 5b). Using confocal imaging, we next demonstrated that Fzd4 accumulates at the cell membrane in HeLa cells transiently transfected with HA-tagged Fzd4, while 30 minutes of exposure to Wnt5a induces re-localization of Fzd4 in the intracellular compartment. PDZRN3 is required for the process, as internalization of Fzd4 was efficiently blocked when *Pdzrn3* was depleted with siRNA (Fig 5c). Fzd4 was detected in intracellular Rab5-positive early endosome vesicles after incubation with Wnt5a conditioned medium, as shown by an overlapping punctate staining pattern of HA-Fzd4 with Rab5. *Pdzrn3* depletion via siRNA transfection or treatment with the inhibitor of dynamin, dynasore, abolished Fzd4 co-localization with Rab5 in intracellular cargos under Wnt5a activation. Co-localization of Fzd4 with Rab5 was quantified in each condition (Fig 5c).

PDZRN3 promotes the non-canonical Wnt/PCP pathway while repressing Wnt canonical signaling in endothelial cells *ex vivo* and *in vitro*

We investigated whether PDZRN3 could regulate the Wnt signaling pathway using Western blot. We evaluated active beta catenin (ABC) and p-c jun levels, as markers of canonical and PCP Wnt pathways, respectively (Fig 6a). There was significant up regulation of ABC expression with a down regulation of p-c jun in EC isolated from *Pdzrn3*^{iECWT} versus *Pdzrn3*^{iECKO} lungs at P7, suggesting that PDZRN3 is required to attenuate the Wnt/ β catenin canonical signal transduction and to promote the Wnt/PCP pathway in postnatal EC, confirming previous work on cultured osteoblast differentiation (Honda et al., 2010). To test this hypothesis, we followed β catenin activation in cultured EC under

Wnt3a activation. Our data showed that, under basal conditions and after Wnt3a stimulation, β catenin and ABC expression were significantly elevated in *Pdzrn3*-depleted EC versus control EC (Fig 6b). Interestingly, upregulation of p-c jun by Wnt5a was impaired in *Pdzrn3*-depleted cells (Fig 6c). Next, β catenin transcriptional activity was measured using the Top-Flash/luciferase reporter construct. Again, we observed that under basal conditions and after Wnt3a stimulation, the Top flash reporter was more robustly activated in EC depleted of *Pdzrn3* with siRNA versus control, and reduced in *Pdzrn3* lentiviral transduced EC (Fig 6d). Conversely, we monitored c-jun-dependent gene transcription using an AP1-responsive luciferase-based reporter, and observed that Wnt5a induction of luciferase reporter gene expression was repressed in *Pdzrn3*-depleted EC and induced in *Pdzrn3* lentiviral transduced conditions (Fig 6e). Taken together, these data support our hypothesis that PDZRN3 favors Dvl3 re-routing from the Wnt canonical pathway toward the PCP signaling pathway.

Endocytosis blockade delays endothelial sprouting *in vivo* and *ex vivo*

Next, we asked whether PDZRN3-induced endocytosis is a mechanism that drives angiogenic morphogenetic events. We tested endocytosis blockade, for its effect *in vivo* and *ex vivo* on sprouting endothelial cells. Intravitreal injection of dynasore or vehicle was performed in P3 neonatal pups to compare the extent of primary plexus at P5 in the control eye, and in the dynasore-injected eye of the same animal (Fig 7a). Radial extension of the primary plexus in dynasore injected eyes was significantly reduced and vessel regression was greater, demonstrated by an increase in the number of empty collagen IV sleeves without ECs, as compared to those injected with vehicle only (Fig 7a). Similar results were obtained when dynasore was added *ex vivo* to mouse aortic ring cultures. Aortic rings were obtained from either P7 *Pdzrn3^{iECKO}* or *Pdzrn3^{iECWT}* neonatal pups. *Pdzrn3^{iECKO}* and *Pdzrn3^{iECWT}* treatment with dynasore led to the formation of fewer sprouts compared to *Pdzrn3^{iECWT}* control conditions (Fig 7b). Interestingly, incubation of the *Pdzrn3^{iECKO}* aortic rings with *Pdzrn3* lentivirus, restored their ability to form sprouts (Fig 7b). We then examined whether impairment of endocytosis could impair Wnt signaling by Western blot, using retina lysates. At P5, *Pdzrn3^{iECKO}* versus *Pdzrn3^{iECWT}* induced repression of p-c-jun and an increase of ABC expression (Fig 7c) while intravitreal injection of dynasore, decreased p-c jun level but

did not affect ABC expression, suggesting that dynasore treatment partially mimics the *Pdzrn3* deletion phenotype (Fig 7d). We can not exclude the possibility that the vascular morphogenetic impairment under dynasore treatment might reflect an accumulative effect on targets other than endothelial cells, such as myeloid cells.

Discussion

Understanding the molecular mechanisms required for coordinating and orienting cell movements to shape vascular networks in a precise and tightly regulated pattern, is an important question in developmental biology. In this study, we used mouse loss-of-function experiments to demonstrate that the loss of E3 ubiquitin ligase *Pdzrn3* activity, leads to disorganization of the vascular vitelline network during embryogenesis and defects in retinal vascular branching. We have also identified Dvl ubiquitinylation as a physiological target of PDZRN3 signaling as it is strongly reduced in the absence of *Pdzrn3* *in vivo* and *in vitro*. We further demonstrate an important and unexpected role for PDZRN3, inducing PCP signaling and directing endothelial cell movements, in an autonomous Fzd/Dvl dependent manner.

We then designed an *in vivo* study, to conditionally block *Pdzrn3* expression within a narrow time window, when earlier vasculogenesis would not be affected. We induced *Pdzrn3* excision after the formation of the primary vascular plexus, by injection of tamoxifen in pregnant mice at E7.5 and 8.5. By E9.5, vascular remodeling has already started in the yolk sac with large vitelline vessels and at E10.5, an intricate, orderly arrangement of large vitelline arteries and veins branching in a fractal pattern to smaller vessels can be seen. Deletion of *Pdzrn3* did not impair vitelline vessel formation but did effect the pattern of hierarchically organized, vitelline vessel architecture throughout the yolk sac. At E10.5 the mutant vascular network degenerated with numerous small disorganized vitelline vessels, evenly distributed throughout the yolk sac. Moreover, embryonic vessels did not invade into the labyrinth placenta layer. Based on this data, we conclude that mutant embryos may die from failure to establish a functional placenta, which is required for embryo nutrition. The identification of PDZRN3 as a physiological target

of Wnt signaling is consistent with previous loss-of-function analyses of Wnt signaling components in mice, reporting their involvement in different steps of placental development (Aoki et al., 2007; Cross et al., 2006; Galceran et al., 1999; Parr et al., 2001). Interestingly, embryos deficient in *Wnt2* and *fzd5* share similar vascular defects. *Wnt2* mutants have poorly developed labyrinth layers with reduced fetal vasculature (Monkley et al., 1996), while *fzd5* deficient embryos die *in utero* with early defects in the yolk sac, and placental angiogenesis with degeneration of large vitelline vessels (Ishikawa et al., 2001). Recently, GCM1, a key transcription factor involved in placental branching morphogenesis, was identified as a novel target of Wnt- β catenin signaling. Its expression was decreased in *BCL9-Like*, *fzd5* and *R-spondin3* deficient mice, which all display placental defects (Matsuura et al., 2011).

To confirm a functional role of PDZRN3 in angiogenesis, we specifically deleted *Pdzrn3* in EC using a *Pdgf^{cre}* mutant. Mutants had an increase in vascular regression/remodeling of the superficial plexus, but no effect on tip cells, and a planar mis-orientation of the intermediate plexus in the plane orthogonal to the axis of the apical plexus, which leads to an incomplete and disorganized deep plexus. The Wnt signaling components and canonical signaling pathway have been involved in the control of hyaloid regression and primary plexus extension (Junge et al., 2009; Phng et al., 2009; Richter et al., 1998; Xia et al., 2010; Xu et al., 2004). Recently, Wnt non canonical signaling was shown to control the deeper, retinal layer branching. Stefater *et al.* have shown that resident myeloid cells, via Wnt5a-dependent non canonical signaling, can secrete sFlt1 to regulate VEGF-stimulated angiogenesis (Stefater et al., 2011). Here, we propose a novel, autonomous role of Wnt non canonical signaling to regulate endothelial cell morphogenetic movements mainly for deeper plexus architecture.

These *in vivo* data demonstrate that PDZRN3 signaling is required for the oriented branching architecture in vessels. Vascular maturation is a tightly regulated process, controlled by a balance of angiogenic signaling. Several recent reports have involved Wnt PCP in vascular morphogenesis (Cirone et al., 2008; Ju et al., 2010; Tatin et al., 2013). Wnt PCP signaling, controls large mechanisms such as; cells migration, axonal guidance, asymmetric cell division, hair or cilia orientation (Seifert and Mlodzik, 2007; Wu and Mlodzik, 2009; Zallen, 2007) as well as mammalian wound healing repair (Caddy et al., 2010). Manifestation of planar polarity features, depends on tissue context, and as such we sought to

examine the role of the PCP pathway in control of endothelial cell migration and polarity and *in fine* vessel morphogenesis. In vertebrate, the PCP pathway was shown to require a core of conserved proteins, including Frizzled receptors, disheveled (Dvl) 1/2/3, prickle1/2, diversin, Celsr1/2/3, Vangl2 and Daam1 (Ju et al., 2010; Montcouquiol et al., 2006). Here, we identified *Pdzn3* as a novel PCP gene required for EC directional migration, using loss and gain of function approaches in *in vitro* and *ex vivo* models. It is not yet clear how Wnt activates the PCP pathway after binding to the Fzd receptor, to impart information to EC during vascular remodeling. Fzd4 has attracted considerable attention, due to its major role in retinal vascular plexus formation, through Wnt canonical signaling involving the receptor complex Tetraspanin-12 and LRP5 (Junge et al., 2009 ; Wang et al., 2012). We recently reported that Fzd4 was also involved in the Wnt/PCP pathway and proposed its role in vascular morphogenesis in *fzd4* KO mice (Descamps et al., 2012). Endocytic mechanisms have emerged to control either β catenin Wnt-dependent signaling (Blitzer and Nusse, 2006; Jiang et al., 2012; Seto and Bellen, 2006) or PCP signaling (Chen et al., 2003; Kim and Han, 2007; Yu et al., 2007). Importantly, endothelial cell depletion of *Pdzn3*, modified the Wnt canonical versus non canonical balance, as we found an ABC accumulation, coupled with a blockade of c-jun phosphorylation, in mutant versus control EC *ex vivo* and *in vitro* under Wnt5a stimulation. Similarly, it has been reported that Wnt5a signals through the receptor Ror2 to inhibit the β catenin dependent canonical Wnt signaling pathway and activate c-Jun N-terminal kinase (JNK) *in vitro* (Mikels and Nusse, 2006; Oishi et al., 2003). Our demonstration that Dvl ubiquitinylation is a consequence of PDZRN3 activity, raises the possibility that the ubiquitinated form of Dvl could be a molecular switch to specify non canonical versus canonical functionality. However, we cannot exclude the possibility that PDZRN3 may have other still unknown substrates, which may participate in the vascular function of PDZRN3. This, then raises the possibility that part of the vascular phenotype induced under *Pdzn3* depletion may be independent of Dvl3 trafficking.

It has been proposed that Wnt responsiveness is controlled by Fzd receptor levels at the cell surface via interplay between E3 ubiquitin and deubiquitine ligase (Hao et al., 2012; Mukai et al., 2010). Here we proposed that Dvl3-K63 polyubiquitination could act as a cargo selection signal required to induce Fzd/Dvl complex internalization and activation of the Wnt/PCP signaling. Indeed we report that

PDZRN3 would preferentially adds K63 ubiquitin chain to Dvl3 versus K48 ubiquitin.. A recent study combining genetic and quantitative proteomic approaches proposed that K63 Ub linkages is a non-degradative form of ubiquitination (Xu et al., 2009) and as such, could allow various proteasome-independent biological outcomes. For example, in a yeast model K63 ubiquitination is involved in DNA repair (Spence et al., 1995); and parkin-mediated K63 ubiquitination is involved in NFκB signaling (Henn et al., 2007). As it was proposed that the routing of receptor in intracellular organelles could be an active process for signaling transduction (Dobrowolski and De Robertis, 2012), here we provide evidence that internalization of active Fzd receptor is required for signal transduction, bringing active Fzd/Dvl complex to the intracellular compartment.

Given its expression in distinct tissues, and the presence of PDZ domains that mediate protein clustering to regulate the signaling network, this indicates a broader role of PDZRN3. As a large number of cancers have been linked to deregulation of the Wnt pathway, we searched for PDZRN3 expression in high-throughput cancer profiling databases. In a human breast cancer microarray database, PDZRN3 was co-expressed with other Wnt genes such as DKK3, TCF4, netrin receptor Unc5B that is involved in EC guidance (Lu et al., 2004) and Col4A1 that is associated with autosomal dominant hereditary angiopathy (Lanfranconi and Markus, 2010) (OncoPrint™, Compendia Bioscience, Ann Arbor, MI). In a multi cancer database, PDZRN3 expression was linked with a large number of EC markers, suggesting that PDZRN3 could be a novel Wnt signaling regulator in human cancer pathologies linked to vascular disorders.

This study provides a novel molecular partner that could fine-tune Wnt complex signaling pathways to control of EC behavior. In collectively regulating EC migration and polarity, PDZRN3 induces PCP signaling which is critical for vascular morphogenesis.

Methods

Author contributions

R.N.S. performed all the experiments; B. J.V. performed yeast two-hybrid screen and cloned the constructs; C.P., A.G., N. F. and P.D. were involved in study design. T.C. and C. D. analyzed data; R.N.S and C.D. wrote the paper. All authors discussed the results and commented on the manuscript.

Acknowledgements

We thank Dr Jerome Ezan and Dr Martin Hagedorn for reading of the manuscript and discussions. We thank the excellent technical support of the U1034 laboratory by Jerome Guignard for assistance in animal breeding and by Myriam Petit for assistance in placenta histological analysis . This work was supported by grants from the Agence Nationale de la Recherche (ANR-2010-Blanc-1135-01), from Region Aquitaine (20101301039MP). R.N.S is supported by grant from the Fondation pour la Recherche Médicale (FDT20130928208).

Competing Financial Interests

References

- Aoki, M., Mieda, M., Ikeda, T., Hamada, Y., Nakamura, H., and Okamoto, H. (2007). R-spondin3 is required for mouse placental development. *Dev Biol* *301*, 218-226.
- Blitzer, J.T., and Nusse, R. (2006). A critical role for endocytosis in Wnt signaling. *BMC Cell Biol* *7*, 28.
- Caddy, J., Wilanowski, T., Darido, C., Dworkin, S., Ting, S.B., Zhao, Q., Rank, G., Auden, A., Srivastava, S., Papenfuss, T.A., *et al.* (2010). Epidermal wound repair is regulated by the planar cell polarity signaling pathway. *Dev Cell* *19*, 138-147.
- Chen, W., ten Berge, D., Brown, J., Ahn, S., Hu, L.A., Miller, W.E., Caron, M.G., Barak, L.S., Nusse, R., and Lefkowitz, R.J. (2003). Dishevelled 2 recruits beta-arrestin 2 to mediate Wnt5A-stimulated endocytosis of Frizzled 4. *Science* *301*, 1391-1394.
- Cirone, P., Lin, S., Griesbach, H.L., Zhang, Y., Slusarski, D.C., and Crews, C.M. (2008). A role for planar cell polarity signaling in angiogenesis. *Angiogenesis* *11*, 347-360.
- Claxton, S., Kostourou, V., Jadeja, S., Chambon, P., Hodivala-Dilke, K., and Fruttiger, M. (2008). Efficient, inducible Cre-recombinase activation in vascular endothelium. *Genesis* *46*, 74-80.
- Cross, J.C., Nakano, H., Natale, D.R., Simmons, D.G., and Watson, E.D. (2006). Branching morphogenesis during development of placental villi. *Differentiation* *74*, 393-401.
- Descamps, B., Sewduth, R., Ferreira Tojais, N., Jaspard, B., Reynaud, A., Sohet, F., Lacolley, P., Allieres, C., Lamaziere, J.M., Moreau, C., *et al.* (2012). Frizzled 4 regulates arterial network organization through noncanonical Wnt/planar cell polarity signaling. *Circ Res* *110*, 47-58.
- Devenport, D., and Fuchs, E. (2008). Planar polarization in embryonic epidermis orchestrates global asymmetric morphogenesis of hair follicles. *Nat Cell Biol* *10*, 1257-1268.
- Dobrowolski, R., and De Robertis, E.M. (2012). Endocytic control of growth factor signalling: multivesicular bodies as signalling organelles. *Nat Rev Mol Cell Biol* *13*, 53-60.
- Etheridge, S.L., Ray, S., Li, S., Hamblet, N.S., Lijam, N., Tsang, M., Greer, J., Kardos, N., Wang, J., Sussman, D.J., *et al.* (2008). Murine dishevelled 3 functions in redundant pathways with dishevelled 1 and 2 in normal cardiac outflow tract, cochlea, and neural tube development. *PLoS Genet* *4*, e1000259.
- Fruttiger, M. (2007). Development of the retinal vasculature. *Angiogenesis* *10*, 77-88.
- Galceran, J., Farinas, I., Depew, M.J., Clevers, H., and Grosschedl, R. (1999). Wnt3a^{-/-}-like phenotype and limb deficiency in Lef1^(-/-)Tcf1^(-/-) mice. *Genes Dev* *13*, 709-717.
- Gao, C., and Chen, Y.G. (2010). Dishevelled: The hub of Wnt signaling. *Cell Signal* *22*, 717-727.
- Hao, H.X., Xie, Y., Zhang, Y., Charlat, O., Oster, E., Avello, M., Lei, H., Mickanin, C., Liu, D., Ruffner, H., *et al.* (2012). ZNRF3 promotes Wnt receptor turnover in an R-spondin-sensitive manner. *Nature* *485*, 195-200.
- Henn, I.H., Bouman, L., Schlehe, J.S., Schlierf, A., Schramm, J.E., Wegener, E., Nakaso, K., Culmsee, C., Berninger, B., Krappmann, D., *et al.* (2007). Parkin mediates neuroprotection through activation of IκappaB kinase/nuclear factor-kappaB signaling. *J Neurosci* *27*, 1868-1878.
- Herbert, S.P., and Stainier, D.Y. (2011). Molecular control of endothelial cell behaviour during blood vessel morphogenesis. *Nat Rev Mol Cell Biol* *12*, 551-564.
- Hocevar, B.A., Mou, F., Rennolds, J.L., Morris, S.M., Cooper, J.A., and Howe, P.H. (2003). Regulation of the Wnt signaling pathway by disabled-2 (Dab2). *EMBO J* *22*, 3084-3094.
- Honda, T., Yamamoto, H., Ishii, A., and Inui, M. (2010). PDZRN3 negatively regulates BMP-2-induced osteoblast differentiation through inhibition of Wnt signaling. *Mol Biol Cell* *21*, 3269-3277.
- Ishikawa, T., Tamai, Y., Zorn, A.M., Yoshida, H., Seldin, M.F., Nishikawa, S., and Taketo, M.M. (2001). Mouse Wnt receptor gene Fzd5 is essential for yolk sac and placental angiogenesis. *Development* *128*, 25-33.

- Jiang, Y., He, X., and Howe, P.H. (2012). Disabled-2 (Dab2) inhibits Wnt/beta-catenin signalling by binding LRP6 and promoting its internalization through clathrin. *EMBO J* **31**, 2336-2349.
- Ju, R., Cirone, P., Lin, S., Griesbach, H., Slusarski, D.C., and Crews, C.M. (2010). Activation of the planar cell polarity formin DAAM1 leads to inhibition of endothelial cell proliferation, migration, and angiogenesis. *Proc Natl Acad Sci U S A* **107**, 6906-6911.
- Junge, H.J., Yang, S., Burton, J.B., Paes, K., Shu, X., French, D.M., Costa, M., Rice, D.S., and Ye, W. (2009). TSPAN12 regulates retinal vascular development by promoting Norrin- but not Wnt-induced FZD4/beta-catenin signaling. *Cell* **139**, 299-311.
- Kim, G.H., and Han, J.K. (2007). Essential role for beta-arrestin 2 in the regulation of *Xenopus* convergent extension movements. *EMBO J* **26**, 2513-2526.
- Kim, G.H., Her, J.H., and Han, J.K. (2008). Ryk cooperates with Frizzled 7 to promote Wnt11-mediated endocytosis and is essential for *Xenopus laevis* convergent extension movements. *J Cell Biol* **182**, 1073-1082.
- Kishida, S., Hamao, K., Inoue, M., Hasegawa, M., Matsuura, Y., Mikoshiba, K., Fukuda, M., and Kikuchi, A. (2007). Dvl regulates endo- and exocytotic processes through binding to synaptotagmin. *Genes Cells* **12**, 49-61.
- Kishida, S., Yamamoto, H., Hino, S., Ikeda, S., Kishida, M., and Kikuchi, A. (1999). DIX domains of Dvl and axin are necessary for protein interactions and their ability to regulate beta-catenin stability. *Mol Cell Biol* **19**, 4414-4422.
- Ko, J.A., Kimura, Y., Matsuura, K., Yamamoto, H., Gondo, T., and Inui, M. (2006). PDZRN3 (LN3, SEMCAP3) is required for the differentiation of C2C12 myoblasts into myotubes. *J Cell Sci* **119**, 5106-5113.
- Lanfranconi, S., and Markus, H.S. (2010). COL4A1 mutations as a monogenic cause of cerebral small vessel disease: a systematic review. *Stroke* **41**, e513-518.
- Liu, Y.T., Dan, Q.J., Wang, J., Feng, Y., Chen, L., Liang, J., Li, Q., Lin, S.C., Wang, Z.X., and Wu, J.W. (2011). Molecular basis of Wnt activation via the DIX domain protein Ccd1. *J Biol Chem* **286**, 8597-8608.
- Lu, X., Le Noble, F., Yuan, L., Jiang, Q., De Lafarge, B., Sugiyama, D., Breant, C., Claes, F., De Smet, F., Thomas, J.L., *et al.* (2004). The netrin receptor UNC5B mediates guidance events controlling morphogenesis of the vascular system. *Nature* **432**, 179-186.
- Matsuura, K., Jigami, T., Taniue, K., Morishita, Y., Adachi, S., Senda, T., Nonaka, A., Aburatani, H., Nakamura, T., and Akiyama, T. (2011). Identification of a link between Wnt/beta-catenin signalling and the cell fusion pathway. *Nat Commun* **2**, 548.
- Mikels, A.J., and Nusse, R. (2006). Purified Wnt5a protein activates or inhibits beta-catenin-TCF signaling depending on receptor context. *PLoS Biol* **4**, e115.
- Monkley, S.J., Delaney, S.J., Pennisi, D.J., Christiansen, J.H., and Wainwright, B.J. (1996). Targeted disruption of the Wnt2 gene results in placentation defects. *Development* **122**, 3343-3353.
- Montcouquiol, M., Sans, N., Huss, D., Kach, J., Dickman, J.D., Forge, A., Rachel, R.A., Copeland, N.G., Jenkins, N.A., Bogani, D., *et al.* (2006). Asymmetric localization of Vangl2 and Fz3 indicate novel mechanisms for planar cell polarity in mammals. *J Neurosci* **26**, 5265-5275.
- Mukai, A., Yamamoto-Hino, M., Awano, W., Watanabe, W., Komada, M., and Goto, S. (2010). Balanced ubiquitylation and deubiquitylation of Frizzled regulate cellular responsiveness to Wg/Wnt. *EMBO J* **29**, 2114-2125.
- Nikopoulos, K., Gilissen, C., Hoischen, A., van Nouhuys, C.E., Boonstra, F.N., Blokland, E.A., Arts, P., Wieskamp, N., Strom, T.M., Ayuso, C., *et al.* (2010). Next-generation sequencing of a 40 Mb linkage interval reveals TSPAN12 mutations in patients with familial exudative vitreoretinopathy. *Am J Hum Genet* **86**, 240-247.
- Oishi, I., Suzuki, H., Onishi, N., Takada, R., Kani, S., Ohkawara, B., Koshida, I., Suzuki, K., Yamada, G., Schwabe, G.C., *et al.* (2003). The receptor tyrosine kinase Ror2 is involved in non-canonical Wnt5a/JNK signalling pathway. *Genes Cells* **8**, 645-654.
- Park, T.J., Gray, R.S., Sato, A., Habas, R., and Wallingford, J.B. (2005). Subcellular localization and signaling properties of dishevelled in developing vertebrate embryos. *Curr Biol* **15**, 1039-1044.
- Parr, B.A., Cornish, V.A., Cybulsky, M.I., and McMahon, A.P. (2001). Wnt7b regulates placental development in mice. *Dev Biol* **237**, 324-332.

Phng, L.K., Potente, M., Leslie, J.D., Babbage, J., Nyqvist, D., Lobov, I., Ondr, J.K., Rao, S., Lang, R.A., Thurston, G., *et al.* (2009). Nrarp coordinates endothelial Notch and Wnt signaling to control vessel density in angiogenesis. *Dev Cell* *16*, 70-82.

Poulter, J.A., Ali, M., Gilmour, D.F., Rice, A., Kondo, H., Hayashi, K., Mackey, D.A., Kearns, L.S., Ruddle, J.B., Craig, J.E., *et al.* (2010). Mutations in TSPAN12 cause autosomal-dominant familial exudative vitreoretinopathy. *Am J Hum Genet* *86*, 248-253.

Richter, M., Gottanka, J., May, C.A., Welge-Lussen, U., Berger, W., and Lutjen-Drecoll, E. (1998). Retinal vasculature changes in Norrie disease mice. *Invest Ophthalmol Vis Sci* *39*, 2450-2457.

Ruzankina, Y., Pinzon-Guzman, C., Asare, A., Ong, T., Pontano, L., Cotsarelis, G., Zediak, V.P., Velez, M., Bhandoola, A., and Brown, E.J. (2007). Deletion of the developmentally essential gene ATR in adult mice leads to age-related phenotypes and stem cell loss. *Cell Stem Cell* *1*, 113-126.

Seifert, J.R., and Mlodzik, M. (2007). Frizzled/PCP signalling: a conserved mechanism regulating cell polarity and directed motility. *Nat Rev Genet* *8*, 126-138.

Seto, E.S., and Bellen, H.J. (2006). Internalization is required for proper Wingless signaling in *Drosophila melanogaster*. *J Cell Biol* *173*, 95-106.

Spence, J., Sadis, S., Haas, A.L., and Finley, D. (1995). A ubiquitin mutant with specific defects in DNA repair and multiubiquitination. *Mol Cell Biol* *15*, 1265-1273.

Stefater, J.A., 3rd, Lewkowich, I., Rao, S., Mariggi, G., Carpenter, A.C., Burr, A.R., Fan, J., Ajima, R., Molkenin, J.D., Williams, B.O., *et al.* (2011). Regulation of angiogenesis by a non-canonical Wnt-Flt1 pathway in myeloid cells. *Nature* *474*, 511-515.

Tatin, F., Taddei, A., Weston, A., Fuchs, E., Devenport, D., Tissir, F., and Makinen, T. (2013). Planar cell polarity protein *Celsr1* regulates endothelial adherens junctions and directed cell rearrangements during valve morphogenesis. *Dev Cell* *26*, 31-44.

Torres, R., Firestein, B.L., Dong, H., Staudinger, J., Olson, E.N., Haganir, R.L., Bredt, D.S., Gale, N.W., and Yancopoulos, G.D. (1998). PDZ proteins bind, cluster, and synaptically colocalize with Eph receptors and their ephrin ligands. *Neuron* *21*, 1453-1463.

Valiente, M., Andres-Pons, A., Gomar, B., Torres, J., Gil, A., Tapparel, C., Antonarakis, S.E., and Pulido, R. (2005). Binding of PTEN to specific PDZ domains contributes to PTEN protein stability and phosphorylation by microtubule-associated serine/threonine kinases. *J Biol Chem* *280*, 28936-28943.

Wang, Y., and Nathans, J. (2007). Tissue/planar cell polarity in vertebrates: new insights and new questions. *Development* *134*, 647-658.

Wang, Y., Rattner, A., Zhou, Y., Williams, J., Smallwood, P.M., and Nathans, J. (2012). Norrin/Frizzled4 signaling in retinal vascular development and blood brain barrier plasticity. *Cell* *151*, 1332-1344.

Wong, C.K., Luo, W., Deng, Y., Zou, H., Ye, Z., and Lin, S.C. (2004). The DIX domain protein coiled-coil-DIX1 inhibits c-Jun N-terminal kinase activation by Axin and dishevelled through distinct mechanisms. *J Biol Chem* *279*, 39366-39373.

Wu, J., and Mlodzik, M. (2009). A quest for the mechanism regulating global planar cell polarity of tissues. *Trends Cell Biol* *19*, 295-305.

Xia, C.H., Yablonka-Reuveni, Z., and Gong, X. (2010). LRP5 is required for vascular development in deeper layers of the retina. *PLoS One* *5*, e11676.

Xu, P., Duong, D.M., Seyfried, N.T., Cheng, D., Xie, Y., Robert, J., Rush, J., Hochstrasser, M., Finley, D., and Peng, J. (2009). Quantitative proteomics reveals the function of unconventional ubiquitin chains in proteasomal degradation. *Cell* *137*, 133-145.

Xu, Q., Wang, Y., Dabdoub, A., Smallwood, P.M., Williams, J., Woods, C., Kelley, M.W., Jiang, L., Tasman, W., Zhang, K., *et al.* (2004). Vascular development in the retina and inner ear: control by Norrin and Frizzled-4, a high-affinity ligand-receptor pair. *Cell* *116*, 883-895.

Ye, X., Wang, Y., and Nathans, J. (2010). The Norrin/Frizzled4 signaling pathway in retinal vascular development and disease. *Trends Mol Med* *16*, 417-425.

Yu, A., Rual, J.F., Tamai, K., Harada, Y., Vidal, M., He, X., and Kirchhausen, T. (2007). Association of Dishevelled with the clathrin AP-2 adaptor is required for Frizzled endocytosis and planar cell polarity signaling. *Dev Cell* *12*, 129-141.

Zallen, J.A. (2007). Planar polarity and tissue morphogenesis. *Cell* *129*, 1051-1063.

Zuercher, J., Fritzsche, M., Feil, S., Mohn, L., and Berger, W. (2012). Norrin stimulates cell proliferation in the superficial retinal vascular plexus and is pivotal for the recruitment of mural cells. *Hum Mol Genet* *21*, 2619-2630.

Figure legends

Fig 1. *Ubc^{creERT2} Pdzn3^{ff}* embryos displayed defects in yolk-sac and placental angiogenesis

- a. Level of *Pdzn3* depletion in *Ubc^{creERT2} Pdzn3^{ff}* versus *Pdzn3^{ff}* mice was evaluated by Western blot on E10.5 embryo brain lysates after tamoxifen treatment of pregnant mothers at E7.5. Normalization was done using the expression of α tubulin.
- b. Survival rate of *Ubc^{creERT2} Pdzn3^{ff}* embryos was measured after gene deletion induced by daily tamoxifen treatment (tmx) of pregnant mothers at E7.5 (red arrowhead) (n=214) or at E10.5 (blue arrowhead) (n=44). *Pdzn3* deletion at E7.5 leads to growth retardation and early embryo lethality from E11.5 to E12.5 (n=79).
- c. Deletion of *Pdzn3* coding gene by tamoxifen injection at E7.5 leads to severe growth retardation as observed at E9.5 and E10.5. *Ubc^{creERT2} Pdzn3^{ff}* embryos were significantly smaller and exhibited abnormal vascularization of the yolk sac (scale bar=500 μ m). Whole-mount visualization of *Ubc^{creERT2} Pdzn3^{ff}* versus *Pdzn3^{ff}* yolk sac demonstrated an organized and ordered vitelline architecture in control mice, while this network was disorganized in mutant embryos at E9.5 and E10.5. Scale bar= 500 μ m in the Inset and 200 μ m at higher magnification.
- d. Placental vasculature was examined in hematoxylin/Eosin-stained sections of control and mutant placentas at E9.5, revealing a reduced labyrinth layer in *Ubc^{creERT2} Pdzn3^{ff}* mutant embryos (scale bar=100 μ m). In a higher magnification, embryonic vessels (arrowhead), as defined by the presence of nucleated red cells are evenly distributed in the labyrinth in *Pdzn3^{ff}* control placenta while in mutant placentas they are missing (scale bar=50 μ m). Embryonic vessels are close to maternal vessels (arrow) in control embryos indicating that maternal-fetal exchanges occur in control but not in mutant embryos. MD: maternal deciduas; GT: Giant trophoblasts; L: labyrinth; YS: yolk sac.
- e. Whole-mount of CD31 of *Ubc^{creERT2} Pdzn3^{ff}* mutant and *Pdzn3^{ff}* control embryos. Vessel network of the brain, but not of the somites is altered in mutants compared to controls at E10.5 (scale bar = 500 μ m; 300 μ m in insets). The mutant embryo showed fewer vessels and branches in the brain.

Fig2. PDZRN3 is essential in EC for capillary extension/ stabilization and 2D directional angiogenesis during retina vascular development

- a. Wild-type retina protein extracts, evaluated by Western blot, revealed that PDZRN3 levels peak at P12; normalization was done using Ve-cadherin and α tubulin.

- b. Post-natal tamoxifen treatment induced PDZRN3 ablation in *Pdzrn3*^{iECKO} (iEC KO) versus *Pdzrn3*^{iECWT} (iEC WT) retinal protein extracts at P12. Normalization was done using Ve-cadherin and α tubulin.
- c. Confocal images of isolectin-B4 (green)/collagen IV (red) retina showing a reduced area of vascularization, of the number of branch points in iEC KO versus iEC WT retinal vasculature at P7 and an increase in regressing isolectin-B4⁻/collagen IV⁺ branches (arrow). Scale bars=500 μ m and 50 μ m respectively. Regression was quantified by the ratio of isolectin-B4⁻/collagen IV⁺ branches to total branches. Box denotes first and third quartiles; band inside the box represents the median; Whiskers denote min to max. Proliferation is increased in iEC KO versus iEC WT vasculature in both tip and plexus areas as indicated by quantification of BrdU (red) isolectin-B4 (green) positive nuclei related to the vessel surface, indicating that the defect of vascularization cannot be correlated to a defect of proliferation. Mean and standard deviation n= 6 for iEC KO; n=6 for iEC WT. Unpaired t test. Scale bars=50 μ M.
- d. At P12, formation of the intermediate and deep plexus is altered in *Pdzrn3*^{iECKO} compared to that in *Pdzrn3*^{iECWT} mice. The number of branch points after isolectin-B4 (green) staining in the deep plexus was decreased from iEC KO vs iEC WT. The intermediate plexus is severely disorganized in iEC KO mice. Transverse reconstruction of retinal images obtained by confocal microscopy shows the intermediate plexus organization linking the superficial (SP) to the deep (DP) retinal vascular plexus in a 2D orthogonal plane. n= 6 for iEC KO; n=6 for iEC WT. Unpaired t test. Box denotes first and third quartiles; band inside the box represents the median; Whiskers denote min to max. Scale bar=100 μ m.
- e. 3-dimensional projected Z stacks views of the intermediate plexus revealed a disorganization of the plexus capillary network when retinas from iEC KO are compared to iEC WT retinas. The orientation of the branches of the intermediate plexus was represented by vectors indicating their direction between two Z planes in the x and y axis plane. In the intermediate plexus of iEC WT mice, all capillaries are parallel and directionally oriented from superficial (SP) to deep (DP) and point to the same direction as indicated by the graph and the angle distribution. In iEC KO mice, branches are disorganized and are not able to follow the same direction, leading to alteration of the organization of the deep plexus. Scale bar=100 μ m. Circular variance that indicates how much orientations deviate from the mean was increased in iEC KO mice, confirming the branch disorganization in these mice. Box denotes first and third quartiles; band inside the box represents the median; Whiskers denote min to max, n= 10 iEC KO; 10 iEC WT. Unpaired t test.

Fig3. PDZRN3 regulates EC migration and tube formation in a Wnt5a dependent manner

- a. PDZRN3 regulates migration of HUVEC under Wnt5a activation. Migration is repressed after si *Pdzrn3* treatment and activated after *Pdzrn3* transduction (*lenti Pdzrn3*). The migration distance was

followed by time laps and calculated based upon recorded images taken 6 hrs after Wnt5a activation for 10 hrs; quantification is provided in the graph. Migration plot analysis shows the direction of migration of EC. Quantification of the distance of migration using Imaris is shown. Circular variance that indicates how much the orientation deviates from the directional mean is low in control cells and increased in *Pdzrn3* depleted cells, confirming that both the control and lenti *Pdzrn3* transduced EC migrate in a Wnt5a dependent context while si *Pdzrn3* EC do not migrate directionally, indicating that PDZRN3 is required for signal transduction upon Wnt5a binding to its receptor. Box denotes first and third quartiles; band inside the box represents the median; Whiskers denote min to max. Experiments were performed in triplicate, error bars denote standard deviation, n=3; Unpaired t test on average measure of three independent experiments – approximately 20 tracks analyzed per field.

b. PDZRN3 regulates 3D tubulogenesis of HUVEC. A suspension of HUVEC-coated cytodex beads were embedded in fibrin gels, in the presence of fibroblasts transfected to express Wnt5a (with Wnt5a) or not (W/O). Nuclei were stained with Hoechst dye and images were acquired 96 hours after plating. For each experiment, sprout length after 96 hours was measured. In the presence of Wnt5a, sprout formation was enhanced. si *Pdzrn3* treated HUVEC exhibited impaired sprout formation as compared to control treated HUVEC in both W/O or with Wnt5a conditions. Transduction of *Pdzrn3* was able to reverse *Pdzrn3* siRNA impairment of sprout formation and response to Wnt5a. Experiments performed in triplicate, bars denote min to max, n=3, 5 beads were analyzed per condition. Box denotes first and third quartiles; band inside the box represents the median; Whiskers denote min to max. Unpaired t test on the average values obtained in 3 independent experiments. Scale bars= 50 μ M.

c. *Pdzrn3* regulates stability of tube-like structures in the 3D tubulogenesis assay. The cytodex preparation was subjected to time-lapse imaging between 48 (48H + T0H) and 64 (48H + T16H) hours after plating with an acquisition each 30 min. In control conditions, the majority of sprouts were stable and extending (green arrows) during the whole acquisition (16 hrs) while in *Pdzrn3* depleted conditions, most of the sprouts were unstable, as indicated by the large number of regressing sprouts (red arrows). Scale bars=50 μ m The number of stable sprouts at the different time points was quantified. Experiments performed in triplicate, bars denote standard deviation, n=3, 5 beads were analyzed per condition, Unpaired t test on the average values obtained in 3 independent experiments.

Fig4. PDZRN3 regulates Dvl3 ubiquitylation

a. Dvl3 ubiquitylation required PDZRN3 activity. Lung homogenates from *Pdzrn3*^{iECKO} (iEC KO) compared to that in *Pdzrn3*^{iECWT} mice vs (iECWT) mice were subjected to immunoprecipitation with anti Dvl3 or non immune (IgG) antibodies, followed by anti-PDZRN3 and anti-ubiquitin immunoblotting.

- b. PDZRN3 induces Dvl3 ubiquitinylation preferentially with K63 dependent ubiquitin chains. Ubiquitinylation of Dvl3 is induced in HEK293 cells transfected with PDZRN3-V5 in the presence of either UB wt-HA or UB^{K63 only}-HA, but not in the presence of UB^{K48 only}-HA.
- c. PDZRN3 ubiquitinylates Dvl3 in a Wnt dependent manner. Depletion of *Pdzm3* in HeLa cells (si *Pdzm3*) inhibits Ub^{K63}-dependent ubiquitinylation of Dvl3 induced by Wnt5a CM. Ubiquitinylation of the Dvl3 is indicated by co-precipitation of Dvl3-Myc with HA tagged polyubiquitin chains.
- d. Co-precipitation of Dvl3 and PDZRN3 requires the PDZ domain of Dvl3 and the PDZB (PDZ binding) domain of PDZRN3. PDZRN3 – V5 but not PDZRN3 Δ PDZB-V5 induces co-precipitation of Dvl3- Myc; PDZRN3 – V5 cannot co-precipitate Dvl3 Δ PDZ-Myc. PDZRN3 – V5 induces co-precipitation of Dvl3-Myc but not Dvl3 Δ DIX-Myc with HA tagged polyubiquitin chains, suggesting that the DIX domain of Dvl3 is required for ubiquitinylation by PDZRN3.

Fig5. PDZRN3 is required for Fzd4 endocytosis upon Wnt5a activation

- a. PDZRN3 is required for Wnt5a mediated internalization of Fzd4, as indicated by co-precipitation of Fzd4-GFP and Dvl3-myc with Rab5 in HEK293 cells after incubation with Wnt5a CM, but not in si *Pdzm3* treated cells. Wnt5a treatment induces co-precipitation of Fzd4 and Dvl3 in a phosphorylated (activated) form, as indicated by the shift of mobility (arrow head).
- b. Wnt5a induces recruitment of Fzd4-GFP and Dvl3 to the early endosome fraction, in a PDZRN3 dependent manner. In HeLa cells, transfected Fzd4-GFP and Dvl3-myc are detected mostly in the membrane fraction. After Wnt5a treatment, levels of Fzd4-GFP and Dvl3 are reduced in the membrane fraction, and are partially re-located to the early-endosome fraction. Treatment with an endocytosis inhibitor, Dynasore, or with si *Pdzm3*, block Wnt5a-mediated Fzd4/Dvl3 recruitment to the endosome. The membrane fraction was normalized using paxillin; the early endosome using Rab5 and the lysate with tubulin.
- c. Depletion of *Pdzm3* in HeLa cells inhibits Wnt5a dependent re-localization of Fzd4 to Rab5-positive vesicles. Immunofluorescence analysis detected Rab5 (green) in cytoplasmic vesicles and Fzd4-HA (red) at the cell membrane in control CM treated cells (W/O, Control). Merged image of Fzd4-HA and Rab5 and magnification view of insets shows that Fzd4 is relocated to Rab5-positive cytoplasmic punctates in HeLa cells exposed to Wnt5a CM treatment as indicated by co-localization (yellow) but not in *Pdzm3* depleted cell (si *Pdzm3*) or those treated with Dynasore. Scale bar=20 μ m. Experiments were performed in triplicate, bars denote min to max, n=3. Unpaired t test on the average values obtained in 3 independent experiments.

Fig6. PDZRN3 regulates the balance between non-canonical Wnt/PCP and Wnt canonical signaling in endothelial cells

- a. The Wnt canonical pathway is activated constitutively and the c-Jun dependent/PCP pathway repressed, in lung lysates from P7 mice when *Pdzrn3* was silenced in endothelial cells (iEC KO) compared to lysates from control littermate mice (iEC WT) as indicated by anti-active β catenin (ABC) and anti p-c Jun immunoblot analysis. PDZRN3 expression was evaluated. Normalization was done using the expression of α tubulin.
- b. siRNA depletion of *Pdzrn3* enhanced the accumulation of cytoplasmic β catenin in HUVEC after treatment with Wnt3a CM; quantification of cytoplasmic β catenin and ABC are normalized with cytoplasmic α tubulin after cell fractionation.
- c. The phosphorylation of c-Jun in HUVEC is indicative of activation of the PCP pathway, as a 30-min incubation with Wnt5a CM activates phosphorylation of c-Jun. Depletion of *Pdzrn3* blocks Wnt mediated phosphorylation of c-Jun. quantification of c-Jun was normalized with α tubulin.
- d. Depletion of *Pdzrn3* (si *Pdzrn3*) increases the activation of the TOP luciferase reporter system while lentivirus *Pdzrn3* (lenti *Pdzrn3*) transduction blocks the activation of a Lef/Tcf luciferase reporter system (Top reporter) after incubation with Wnt3a CM in HUVEC; experiments were performed in triplicate, error bars denote standard deviation, n=3.
- e. Depletion of *Pdzrn3* (si *Pdzrn3*) blocks activation of the AP1 luciferase reporter system after incubation with Wnt5a CM while lentivirus *Pdzrn3* (lenti *Pdzrn3*) transduction activates the AP1 luciferase reporter moderately in HUVEC; experiments were performed in triplicate, error bars denote standard deviation, n=3. Unpaired t test on the average values obtained in 3 independent experiments.

Fig7. Endocytosis is essential for activation of the PCP pathway and stability of vessels during retinal vascularization

- a. Blockade of endocytosis by Dynasore intraocular injection at P3, induces retinal vasculature regression quantified at P5. The number of branch points after Isolectin FITC staining, in the superficial plexus was decreased and capillary regression was increased in retinas injected with Dynasore when compared to retinas injected with DMSO (control), as quantified by the ratio of collagen IV positive/ isolectin FITC negative branches to total branches. Whiskers denote min to max, n= 6 DMSO injected; n=6 Dynasore injected. Unpaired t test. Scale bars=100 μ m
- b. Aortic rings were implanted in Matrigel and the area of sprouting was quantified 72 hrs after plating. Aortic rings from P7 *Pdzrn3*^{iECKO} (iEC KO) mice produce significantly smaller and less organized sprouts, as compared to aortic rings from *Pdzrn3*^{iECWT} (iEC WT) mice. Treatment of wild-type

rings with Dynasore reduced the number and length of sprouts while treatment of iEC KO rings with *Pdzn3* lentivirus (lenti *Pdzn3*) restores their ability to form longer sprouts; n= 7 iEC KO; n=7 iEC WT, sprouting surface area was measured per aorta. Whiskers denote min to max. Unpaired t test. Scale bars=50µm

c. At P5, the Wnt canonical pathway is activated constitutively and the c-Jun dependent/ PCP pathway repressed, in iEC KO retina compared to iEC WT retina, as indicated by anti- active β catenin (ABC) and anti p-c Jun immunoblot analysis in retina lysates.

d. The level of the active form of c-Jun is downregulated at P5 by blockade of endocytosis by intraocular injection of Dynasore at P3, indicating that endocytosis is an important step for activation of the planar cell polarity signaling during retinal vascularization. The level of p c-Jun was normalized using tubulin. Expression of active beta catenin (ABC) and PDZRN3 was unchanged under Dynasore treatment in contrast to that in *Pdzn3* knockdown (iEC KO vs iEC WT) conditions.

Supplementary figures

Supplementary Fig 1: PDZRN3 is expressed in the vasculature in embryo and during development

a. Quantitative RT-PCR revealed that mouse *Pdzn3* transcript is detected at a high level in several mouse tissues such as aorta, heart and kidney. Interestingly, PDZRN3 expression levels are regulated in the retina during its vascularization (between P5 and P21). N=3 for each condition. Unpaired t test.

b,c. Quantitative RT-PCR revealed that the *Pdzn3* transcript is expressed in a large number of cell lines, including C2C12 cell lines (mouse cardiomyocytes) but is only detected in small amounts in fibroblasts. *Pdzn3* is detected in different murine (MS1, H5V and primary EC) and human (HUVEC, HMVEC) endothelial cell lines and tumoral cell (HeLa). N=3 for each condition. Unpaired t test.

d. Co -immunostaining with an anti-PDZRN3 (green) and anti CD31 (red) antibodies was performed on whole-mount E10.5 yolk sacs, E12.5 brain tissue sections, eye tissue sections at P7 and *en face* aorta tissue at P7. In merged images yellow staining indicates co-localization of PDZRN3 and CD31 in EC. Scale bars= 50, 100, 30 & 20 µm respectively.

Supplementary Fig 2: *PDGF α ^{cre} Pdzn3^{fl/fl}* embryos displayed defects in yolk sac and placenta angiogenesis

a. Deletion of the *Pdzn3* coding gene by tamoxifen injection (iEC KO) at E7.5 leads to abnormal vascularization of the yolk-sac compared to control (iEC WT) embryos. Scale bar= 1mm

b. Placenta vasculature was examined in hematoxylin/eosin-stained sections of control and mutant placenta at E10.5. A higher magnification of the labyrinth layer revealed a reduced number of embryonic vessels as defined by the presence of nucleated red cells in iEC KO mutant versus iEC WT control embryos. Scale bar = 200µm for the left panel and 50µm for the right panel. The vascular embryonic

surface delineated by nucleated red cells (%) was quantified (n=4 in iEC KO vs iEC WT from 3 distinct litters, p<0.05). MD: maternal decidua; GT: giant trophoblasts; L: labyrinth. n= 5 for iEC KO; n=6 for iEC WT. Unpaired t test.

Supplementary Fig 3: Dvl3 is required for the recruitment of PDZRN3 to Fzd4 at the membrane

Fzd4 induces PDZRN3 and Dvl3 re-localization from the cytoplasm to the cell membrane. Hela cells were transfected with Dvl3-myc and PDZRN3-V5 either with or without Fzd4-HA. Con-focal images of anti-HA(violet), anti-Myc(green) and anti-V5(red) were merged to show regions of co-localization (yellow) in the presence of Fzd4-HA; Scale bars= 15µM. Dvl3 mutant (Dvl3ΔPDZ) is recruited to the membrane in the presence of Fzd4-HA while re-localization of PDZRN3-V5 is impaired, indicating that the interaction between the PDZ domain of Dvl3 and PDZRN3 is required for recruitment of PDZRN3 to the Fzd4/ Dvl3 complex at the membrane.

Methods

Yeast Two Hybrid experiment

mDvl3 lacking the DIX domain {Descamps, 2012 #365} was subcloned into pGBTK7 in-frame with the DNA binding domain of galactosidase-4 (GAL4). Yeast two-hybrid screening and assays were performed as described in the Clontech protocol (MatchMaker GAL4 Two-Hybrid Sstem3, Clontech, K1612-1). AH109 cells expressing GAL4–Dvl3ΔDIX were combined with Y187 cells expressing the mouse E11 embryo cDNA library (Clontech, 638868). The mating mixture was plated on SD/ -TRY, -LEU, -HIS, -ADE, X-α-gal plates. From colonies obtained after transformation, more of 500 colonies tested were His positive/MEL1 positive. The library plasmids from those colonies were rescued, amplified by PCR, and sequenced.

Expression constructs

mDvl3, Dvl3ΔDIX and Dvl3ΔPDZ cDNA sequences ¹ were PCR amplified and sub cloned in frame in pcDNA3.1-myc his . Vector coding for Fzd4-HA was provided by Dr. Tomas Kirchhausen ² and for Fzd4-GFP by Dr. M. Montcouquiol. From Human PDZRN3 cDNA provided by Dr.Makoto Inui ³,the full sequence and the sequence of PDZRN3 excluding the PDZ binding motif TTV were PCR amplified and subcloned in frame into the pcDNA3.1-V5-His plasmid (Invitrogen), to generate PDZRN3-V5 and PDZRN3ΔPDZB-V5. Dvl3-green ¹ and PDZRN3–V5 sequence were subcloned into the lentiviral vectorpRRLsin-MND-MCS-WPRE. Lentivirus preparations were produced at the Bordeaux 2 lentivirus platform.

Generation of conditional *Pdznr3* knock-out mice

All mice used in this study were bred and maintained at the institute. This study was conducted in accordance with both institutional committee guidelines and those in force in the European community for experimental animal use (L358-86/609/EEC).

Floxed *Pdznr3* mice (stock 01750, Riken institute) were generated by Dr Y. Saga (National Institute of Genetics, Japan). The neomycin cassette was subsequently removed by flippase-mediated recombination by breeding with *Flp* mice. Floxed *Pdznr3* (*PDZRN3^{fl/+}*) mice were subsequently backcrossed on C57BL6/J background. Interbred, homozygous *Pdznr3^{fl/fl}* mice exhibit apparently normal development, and are viable and fertile. Two lines of Cre mice, *Ubc^{creERT2}* (B6;129S-Tg(UBC-cre/ERT2)1Ejb/J, Jackson Lab) and *PDGFb^{icre}* transgenics were bred with *Pdznr3^{fl/fl}* females to generate *Pdznr3^{fl/fl}; Ubc^{creERT}* and *Pdznr3^{fl/fl}; Pdgf PDGFb^{icre}* or to simplify *Pdznr3^{iECKO}* (iEC KO) respectively. Cre negative littermates were used as controls. To verify the efficiency of Cre recombination, Cre mice were mated with the reporter transgenic line mTmG ((ROSA)26Sor^{tm4(ACTB-tdTomato,-EGFP)Luo}/J, Jackson Lab). For yolk sac vascularization analysis, gene inactivation was induced by tamoxifen injection (100µl of a 10 mg.ml⁻¹ solution, corn oil) intraperitoneally in pregnant mother daily from d7.5 to d9.5 or from d10.5 to d12.5 and pups were analyzed respectively starting from d10.5 and d13.5. For pups, tamoxifen was administered by i.p. injection at 50µl of a 1 mg.ml⁻¹ solution at P1 P3. The phenotypes of the mutant mice were analyzed at the reported time. Tails of pups were genotyped by PCR using the P1/P2 primer set for the wild-type allele and for the Flox allele and the P3/P4 primer set for the KO allele: P1: 5' cgaccacttgctccagtaaccggaaag -3'; P2: 5'-gaggctgacataattcccgatcagc -3'; P3: 5' - TCTGGCCTGTCCCATCCAGACAGCTGGAG - 3'; P4: 5'- GGAGATGTTTTAATTCAAGGAGGCTATCAC - 3'. For PDGF Cre-recombinase, forward primer: 5' - CCAGCCGCCGTCGCAACT - 3', and reverse primer: 5' - GCCGCCGGGATCACTCTCG- 3' {Claxton, 2008 #1352} were used.

Histology and Immunohistochemistry

For whole mount or tissue section histologic and immunohistologic analysis, embryos and yolk sacs were fixated in 80% Methanol / 20% DMSO overnight, treated with 3% H₂O₂ for 5 hours to block endogenous peroxidases then rehydrated in 50% Methanol/ 50% PBS for analysis. Brains from embryos (E14.5) were fixed in PFA 4%-PBS, frozen in OCT and cryosectioned. For en face aorta staining, aorta were removed from P7 pups and fixed in PFA 4%-PBS for 30 mins. Placentas were fixed in PFA 4%-PBS then paraffin embedded and sections were stained with hematoxylin/eosin for morphologic evaluation. Briefly, immunohistochemical staining was performed in PBS supplemented with 1% Donkey Serum with the following antibodies: anti CD31 (BMA Pharmingen, T-2001, 1/50), anti PDZRN3 (Santa cruz, sc-99507, 1/50).

RNA preparation and Q-PCR

Mouse tissues or cells were homogenized in TRI-REAGENT™ (Euromedex) and RNA were extracted according to the manufacturer's instructions and reverse transcribed using the M-MLV Reverse Transcriptase (Promega). Q-PCR was performed on a Biorad Opticon using the Sybrgreen reagent (Life Technologies).

Primer sequences are as follows: Mouse beta-actin forward primer (NM_007393): 5'-ATTTCTTTTGGACTTGCGGGC -3', and reverse primer: 5'- GGAGGAGCTGGAAGCAGCC -3'; Mouse PDZRN3 forward primer (NM_018884.2): 5'- CTGACTCTTGTCCTGCATCGGGACTC -3', and reverse primer: 5'- ATGGGCTCCTTGGCTGTCTTGAAAGC -3'. Human beta-actin forward primer (NM_001101): 5'- ATTTCTTTTGGACTTGCGGGC -3', and reverse primer: 5'- GGAGGAGCTGGAAGCAGCC -3'; Human PDZRN3 forward primer (NM_015009.1): 5' – ATTATTGAGGTCAACGGCAG -3', and reverse primer: 5'- AGGGCCATGATATGTTCAAAG -3'.

Mouse retina analysis

Mouse eyes at postnatal stage were dissected and stained with Isolectin B4 (Sigma, L2895, 1/100) or Collagen IV (Santa Cruz, sc-113360, 1/100) in PBS supplemented with 5% BSA. Retinal vasculatures were imaged with a fluorescent microscope (Apo-observer, Zeiss) and vascularized retinal areas quantified with axiovision software (Zeiss). The number of branch points was quantified after skeletonization (Cell profiler) in an area of 0,25mm² (8 fields per retina). To assess blood vessel regression, the ratio of the number collagen IV-positive/Isolectin-negative to the total number of capillary segments was assessed (8 fields per retina). The retinal vascularization at P12 was imaged with a confocal microscope (Olympus FV 1000) and analyzed using Imaris (Bitplane). The organization of the secondary plexus was analyzed using Image J (tracking plugin) and the Chemotaxis and Migration tool (Ibidi). BrdU staining of retina was performed as described before⁵. Counts of BrdU+ nuclei on or near vessels per field were normalized to the densities of the vessels of the field. Intraocular injection was performed using the injector from World precision instruments. 0.5µl of Dynasore (200 µM in 6% DMSO; 94 % Ethanol) was injected in one eye of the animal at the speed of 50nl/sec; the other control eye was injected with a solution of 6% DMSO; 94% Ethanol.

Cell culture/ DNA transfection and drug treatments

HEK293-Tq cells (ATCC, CRL-1573) were cultured in DMEM supplemented with 10% FBS (Hyclone) and penicillin-streptomycin. HeLa and MS1 (mouse pancreatic islet endothelial cell line) cells were cultured in RPMI supplemented with 10% FBS and penicillin-streptomycin. Human umbilical vein endothelial cells (HUVEC) and human microvascular endothelial cells (HMVEC)(ATCC, CRL-1730 &

CRL-4025) were cultured in EGM-2 media (Lonza, CC-3156) supplemented with EGM-2 Single Quots (Lonza, CC-4176). All these cells were serum starved with DMEM plus 1% FBS/0.25%BSA.

Conditioned medium (CM) from Wnt3a and Wnt5a producing mouse L cells (American Type Culture Collection ATCC) was harvested as described in ATCC. Cells were activated either with Wnt3a CM, and with Wnt5a CM.

Plasmids were transfected using jetPRIME™ (Polyplus) following the manufacturer's protocol (final concentration of 1.5 µg/ml for HEK293 cells, 0.5µg/ml for HeLa cells). SiRNA were transfected using INTERFERin™ (Polyplus) at a final concentration of 30nM. The oligonucleotides used were designed by Origene for h-pdzrn3: SR307944A SR307944B and SR307944C. Lentivirus were transduced at a multiplicity of infection of 20 (MOI). Ly.72632 (Sigma) was used at 10µM (Sigma). Dynasore (Santa Cruz) was used at 40µM *in vitro* and *ex vivo*.

***In vitro* assays on endothelial cells**

Chemotaxis assay was carried out by plating Hoechst pre-treated HUVEC cells in µ-Slide Chemotaxis 2D slides (Ibidi). After 6 hours, 90 µl of control CM was added to one of the chemotactic chamber and 90 µl of Wnt5a CM (diluted 1/20) to the other chamber, creating a gradient of Wnt factors in the capillary. The capillary was then filled with fresh medium and the slide placed for 6 hours under an inverted microscope (AxioObserver, Zeiss). Nuclei of each cell were tracked during time and surfaced using Imaris software (Bitplane).

For 3D tubulogenesis assay, HUVECs were transduced with control or *Pdzrn3* expressing lentivirus and transfected with various siRNAs and nuclei labeled by supplementation with Hoechst (5µg/ml) for 30mins. Cells were then incubated with Gelatin-coated microcarrier beads (Cytodex 3; Sigma) for 5 to 6 hours. When the cells reached confluence, equal numbers of HUVECs-coated beads were embedded in fibrin gels in a µ-slide angiogenesis plate (Ibidi). The fibrin gel was prepared by dissolving bovine fibrinogen (2.5 mg/mL; Sigma) in EBM2 medium supplemented with Aprotinin (0.05 mg/mL; Sigma). Clotting was induced by the addition of thrombin (1.2 U/mL) (Sigma). After 60 min, control or Wnt5a transfected human fibroblasts were plated on the top of gel and EBM2 medium added. The formation of tube-like structure was imaged by time-lapse videomicroscopy (in fluorescence) for 12 h under an inverted microscope (AxioObserver, Zeiss) 48h after plating for quantification. The number of sprouts per bead, length of sprout and number of nuclei per sprout was quantified at 96h after plating.

Luciferase reporter assay

Transactivation analysis of TopFlash and AP1 reporter plasmids were performed in HUVEC cells. Briefly, the cells grown in 48-well culture plates were transiently transduced at 60-70% confluence with

the 8XTOPflash reporter (Nusse lab), and a β galactosidase reporter for normalization. . Cells were activated 24h after transfection with Wnt3a, Wnt5a or control CM.

Western blot, immunoprecipitation, ubiquitinylation analysis and *in vitro* Pull-Down Assay

For cell fractionation, cells lysates were potterized and centrifuged at 1,000g to obtain the pellet and the supernatant. The pellet from the cell lysate was then resuspended and loaded on cushions of Sucrose 40%; Sucrose 30%; Sucrose 20%; Sucrose 16%; after a 60,000g centrifugation, the interface between the Sucrose 30% and Sucrose 20% phases was collected, resuspended; finally after a spinning at 100,000, the pellet obtained corresponded to the early endosome. The supernatant from the cell lysate was centrifuged at 100,000g and the pellet obtained was resuspended in the TRIS buffer + 1% triton and spinned again for 10min at 13,000g. The supernatant was then collected and identified as the membrane fraction. For ubiquitinylation assay, cells were transfected with the following vectors: pRK5-HA-UB-wt, pRK5-HA-UB^{K48 only}, which codes for lysine 48-only-ubiquitin or pRK5-HA-UB^{K63 only} which codes for lysine-63-only ubiquitin (Addgene). HEK293 were cotransfected with Dvl3-myc (0.5 μ g/ml), one of the ubiquitin coding plasmids (0.5 μ g/ml) and PDZRN3-V5 or empty control plasmid (0.5 μ g/ml). For immunoprecipitation, lysates were incubated with primary antibody at +4°C followed by incubation with protein G-Sepharose slurry . Immunoprecipitation was carried out using the following antibodies at 2 μ g for 500 μ g of protein lysate: anti Dvl3 (Santa Cruz, sc 8027) and anti myc (9E10, Millipore, 05-724).

Proteins were then resolved by SDS-PAGE and blotted with the following antibodies: anti HA (Cell signaling, 3724, 1/1000), anti rab 5 (Santa cruz, sc-9020, 1/1000), anti V5 (Invitrogen, 46-0705, 1/3000), anti PDZRN3 (Santa Cruz, sc-99507, 1/500), anti c-JUN (Upstate, 06-225, 1/500), anti activated β catenin (anti-ABC, clone 8E7, Millipore, 05-665, 1/1000), anti β catenin (Sigma, C2206, 1/3000), α -tubulin (Sigma, T5168, 1/5000), anti phosphorylated c-Jun (Cell signaling, 9261S, 1/500), anti myc (9E10, Millipore, 05-724, 1/3000), anti GFP (Molecular probes, 11-814-460-001, 1/3000), anti Ve-cadherin (Santa Cruz, sc 6458, 1/1000), anti Ubiquitin (Sigma, U5379, 1/1000), anti Paxillin (Santa Cruz, sc-5574, 1/1000), and anti Dvl3 (Santa Cruz, sc 8027, 1/500). Binding of antibodies to the blots was detected using Odyssey Infrared Imaging System (LI-COR Biosciences).

Immunocytochemistry

Immunofluorescence analyses were realized on HeLa or HUVECs cells. The cells were fixed in formalin 4% and stained with anti HA (Cell signaling, 3724, 1/200), anti rab 5 (Santa cruz, sc-9020, 1/100), anti V5 (Invitrogen, 46-0705, 1/200), anti myc (Millipore, 05-724, 1/200), and anti ubiquitin (Sigma U5379, 1/100). Cells were imaged using a fluorescent microscope (AxioObserver, Zeiss) and analyzed using Axiovision imaging software (Zeiss). For colocalization studies, cells were analyzed with a confocal

microscope (Olympus FV 1000). Visualisation was obtained after digitized image multichannel deconvolution by Autodeblur (Media Cybernetics Inc., MD 20910 USA) and three-dimensional projections were digitally reconstituted from stacks of confocal optical slices by Imaris software (Bitplane) (Bitplane AG, Zurich, Switzerland).

Aortic endothelial cell sprouting assay

Thoracic aorta were removed from mice P7 (males) and cut into 1mm rings. The aortic rings were embedded in Growth factor-reduced Matrigel® (Becton Dickinson) on a μ -slide angiogenesis plate (Ibidi), incubated in EBM2 medium for 72h and imaged using an Olympus inverted microscope after incorporation of Hoechst (5 μ g/ml in medium for 30mins). The aorta rings were transduced with *Pdzrn3* lentivirus or control lentivirus mixed in matrigel (10⁶ particles / 100 μ l of gel). The sprouting area was then quantified after surfacing using Imaris (Bitplane).

Isolation of primary endothelial cells from mouse kidney or lung

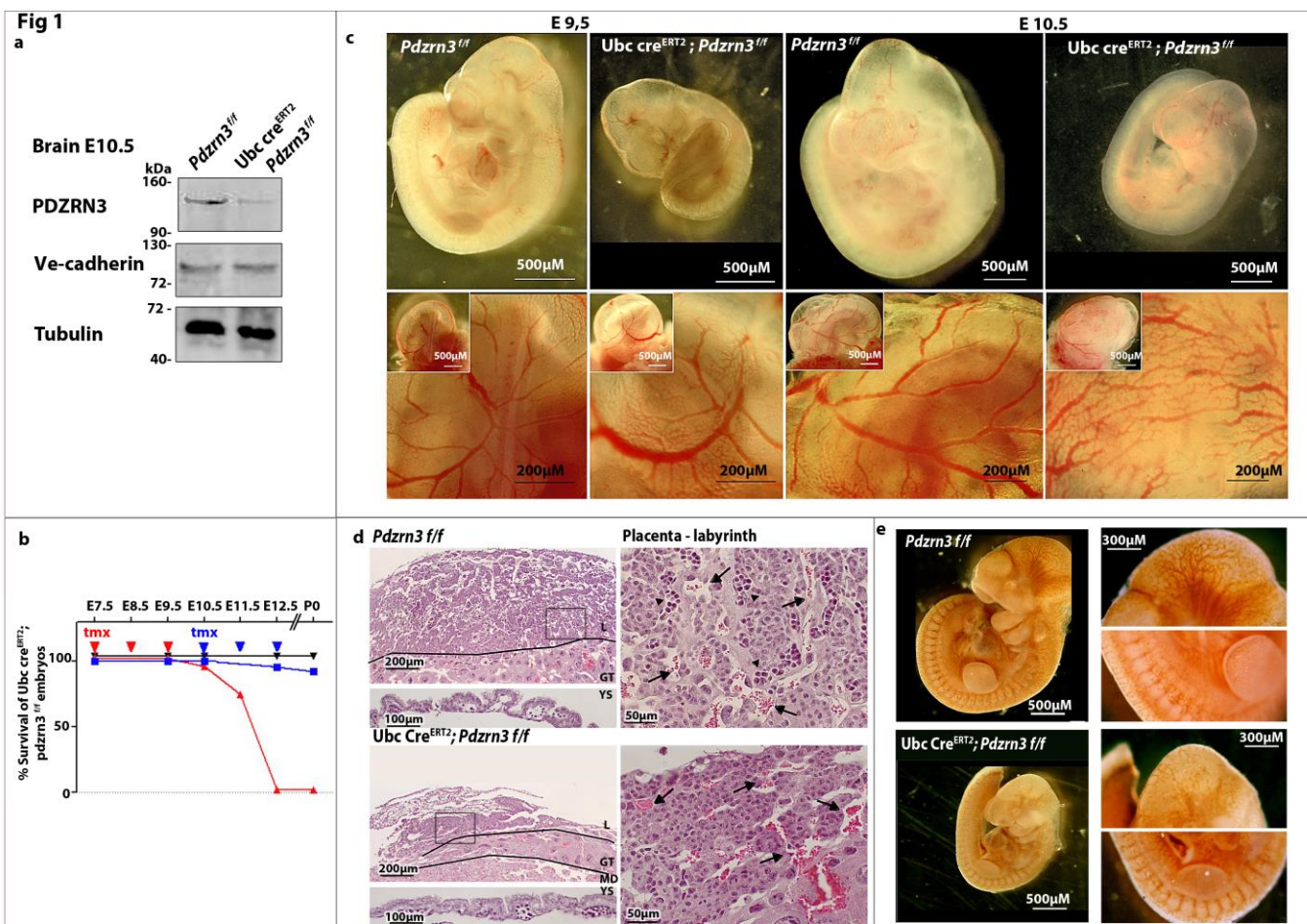
Lungs were removed in PBS-containing CaCl₂ and MgCl₂ (Gibco), and endothelial cells were isolated after incubation with anti-CD31 (Pharmingen) and anti-endoglin (Santacruz) antibodies using microbeads (Miltenyi) as reported ¹.

Statistical analysis

Results were expressed as mean \pm SD or mean \pm min to max. All analyses were performed with appropriate software (Graphpad PRISM). Comparison of continuous variables between two groups was performed by a one-way ANOVA and subsequently, if statistical significance was observed, by an unpaired *t* test. A value of *p* <0.05 was considered to be statistically significant.

References

- 1 Descamps, B. *et al. Circ Res* **110**, 47-58, (2012).
- 2 Yu, A. *et al. Dev Cell* **12**, 129-141, (2007).
- 3 Ko, J. A. *et al. J Cell Sci* **119**, 5106-5113, (2006).
- 4 Claxton, S. *et al. Genesis* **46**, 74-80, (2008).
- 5 Phng, L. K. *et al. Dev Cell* **16**, 70-82, (2009).
- 6 Stasyk, T. *et al. Electrophoresis* **26**, 2850-2854, (2005).



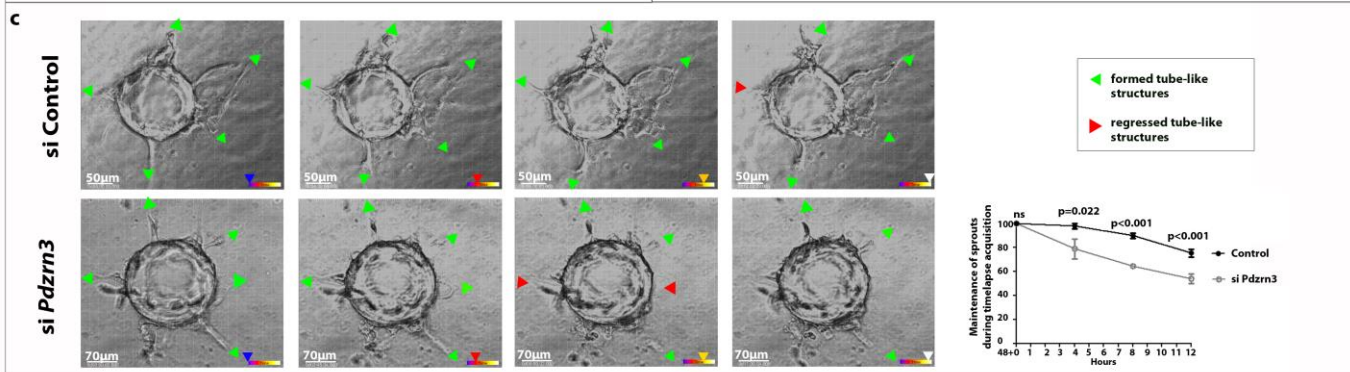
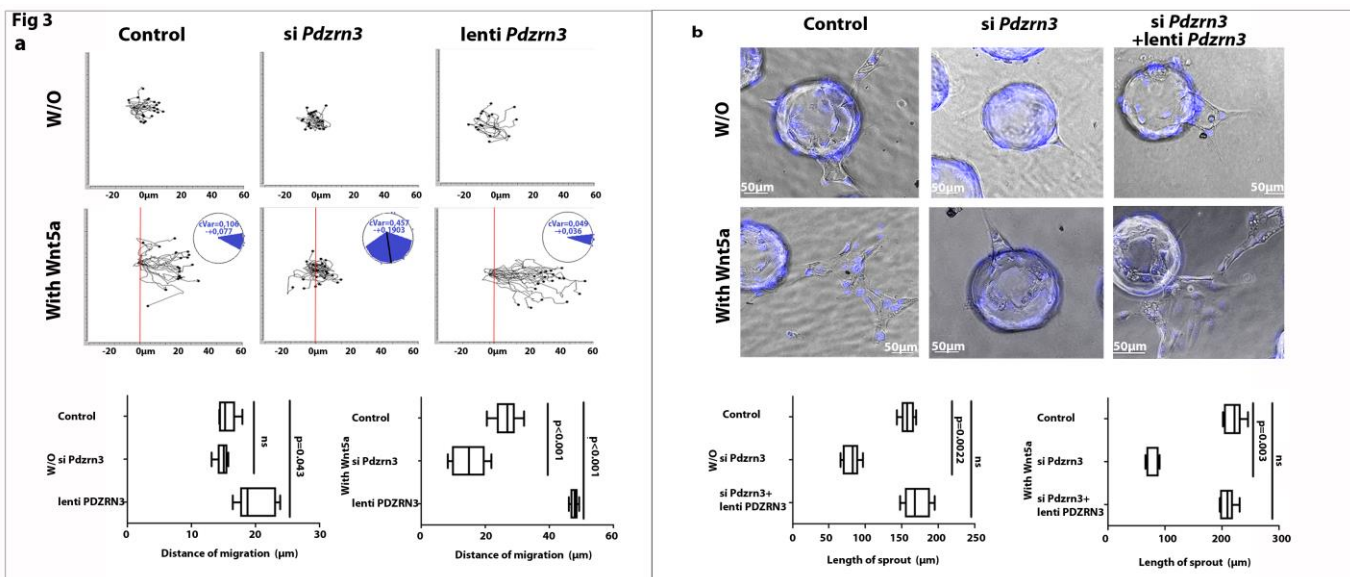
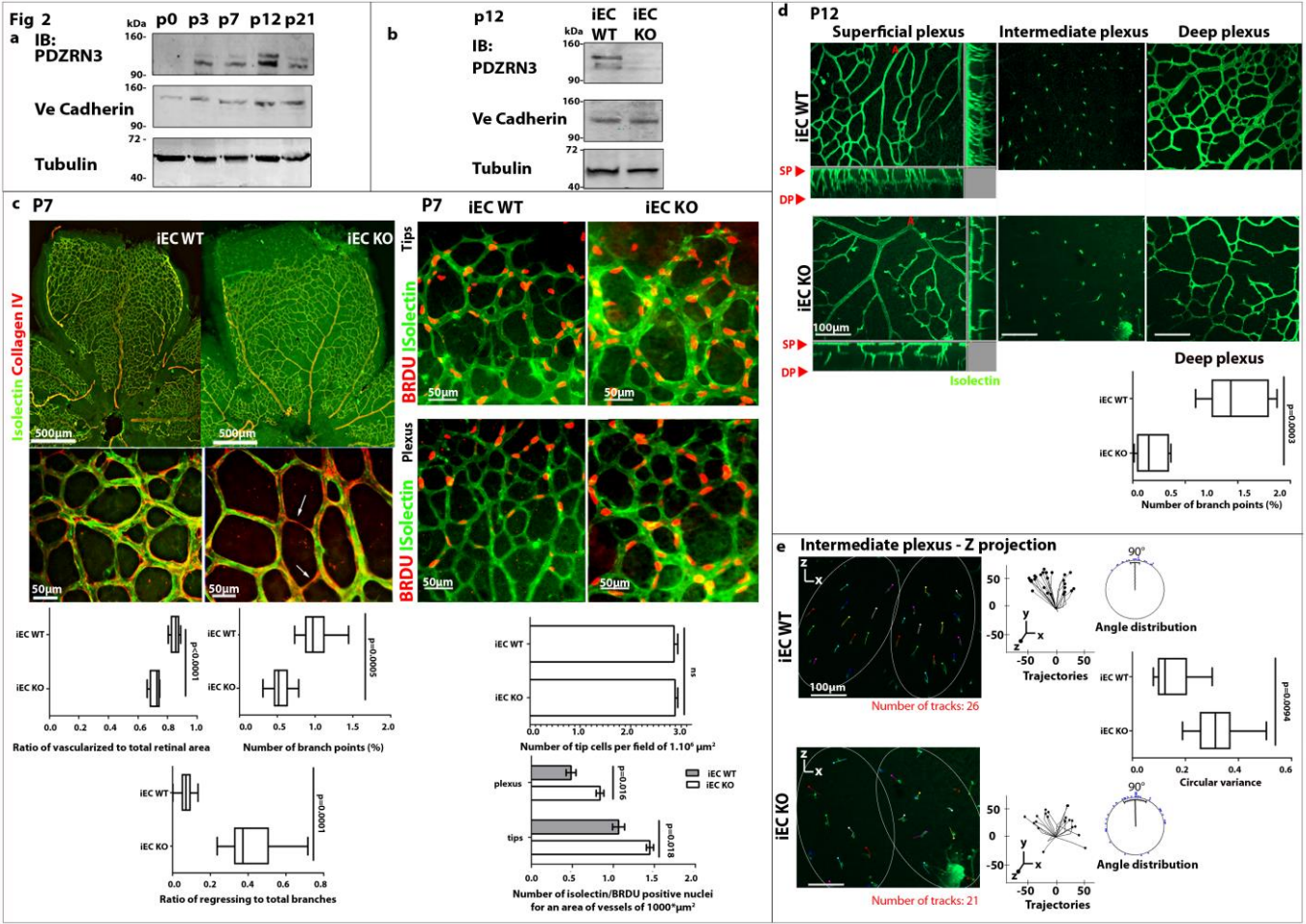
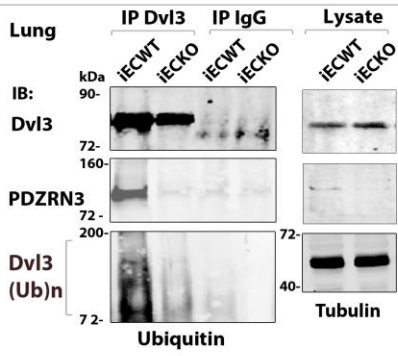
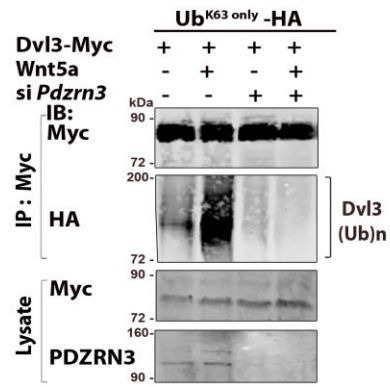


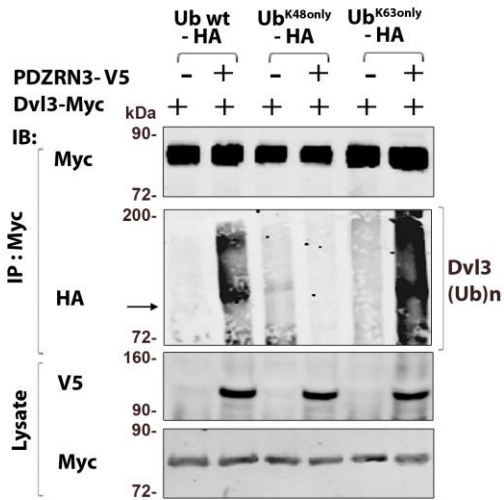
Fig 4
a



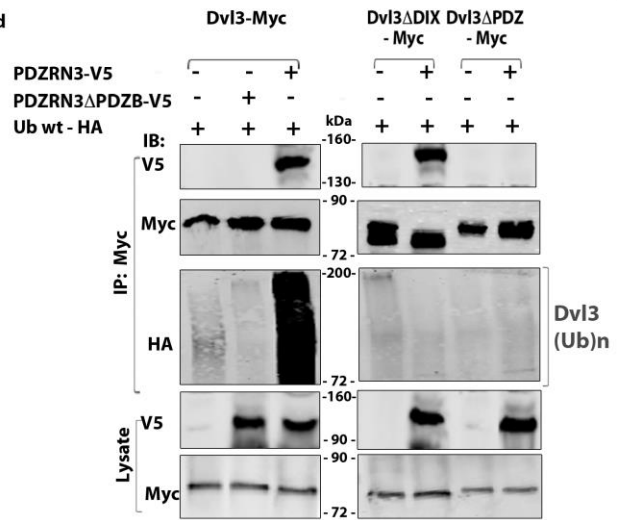
c



b



d



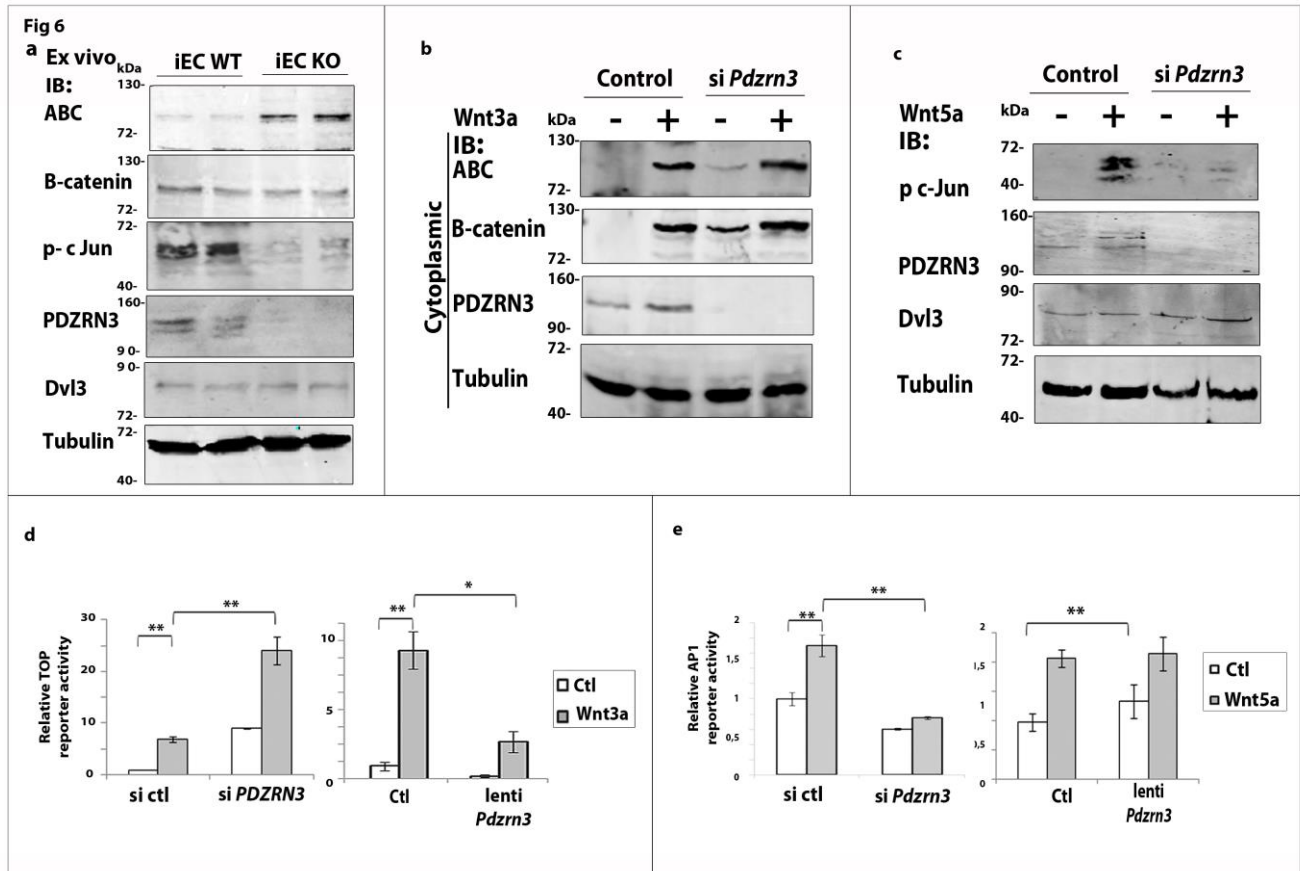
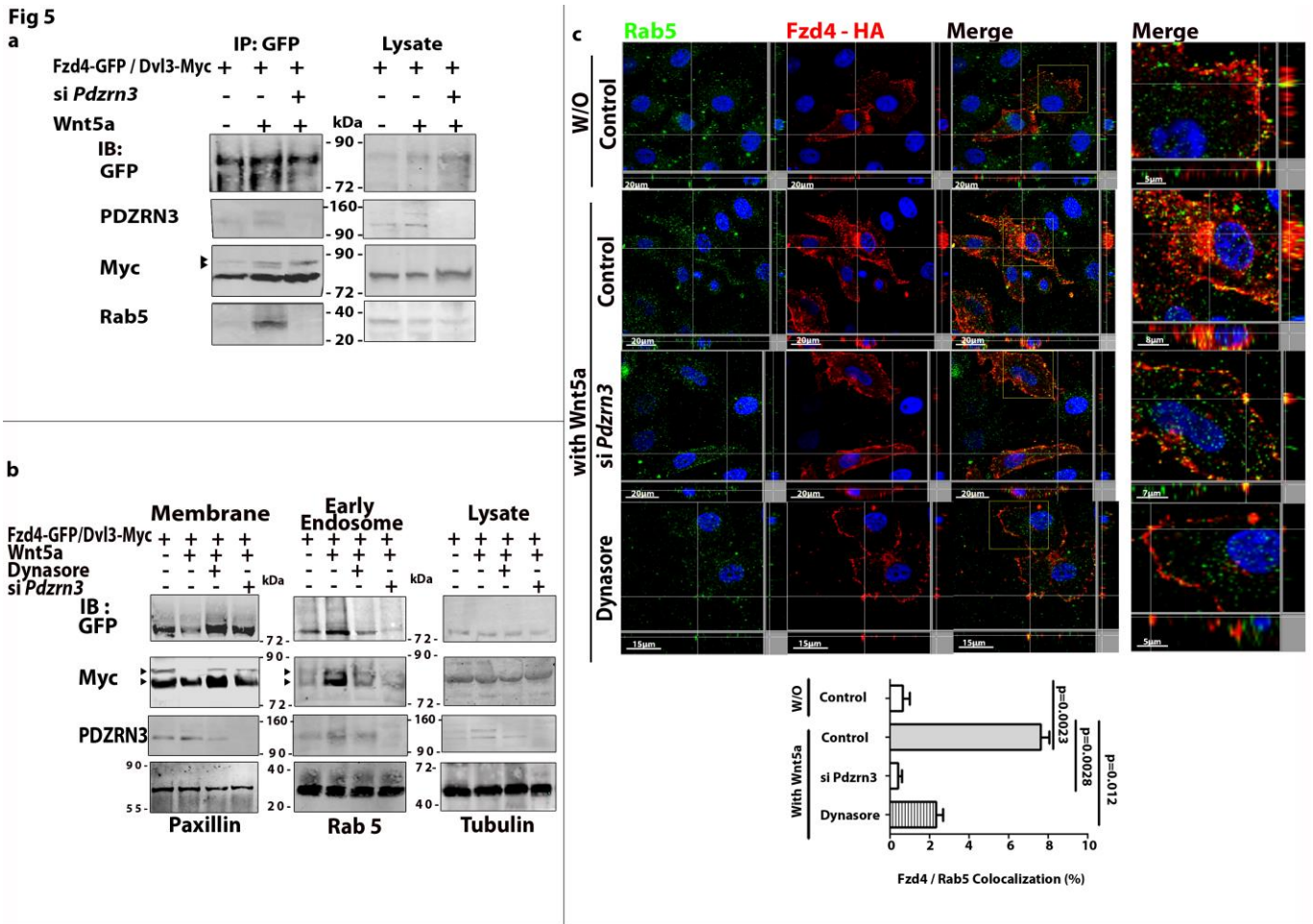
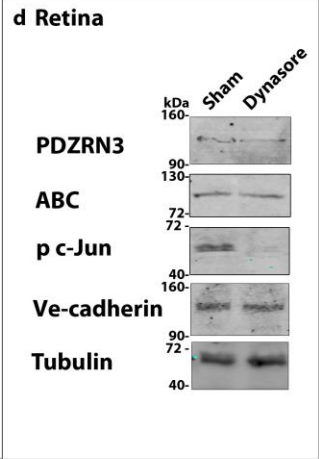
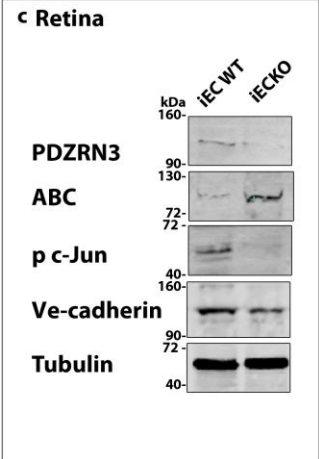
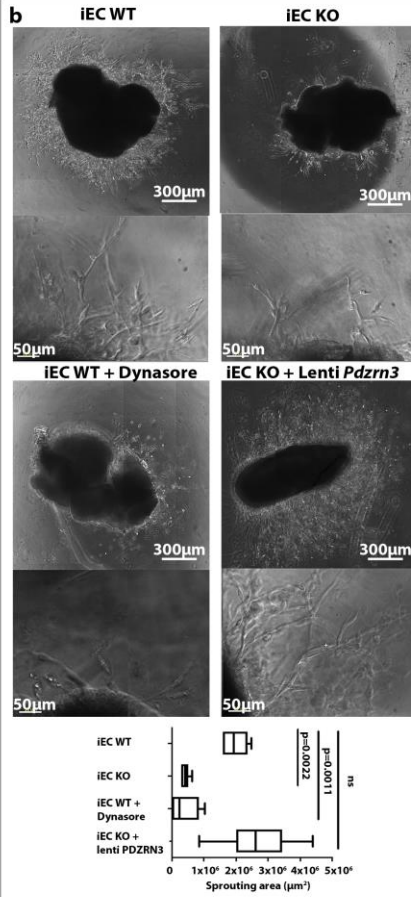
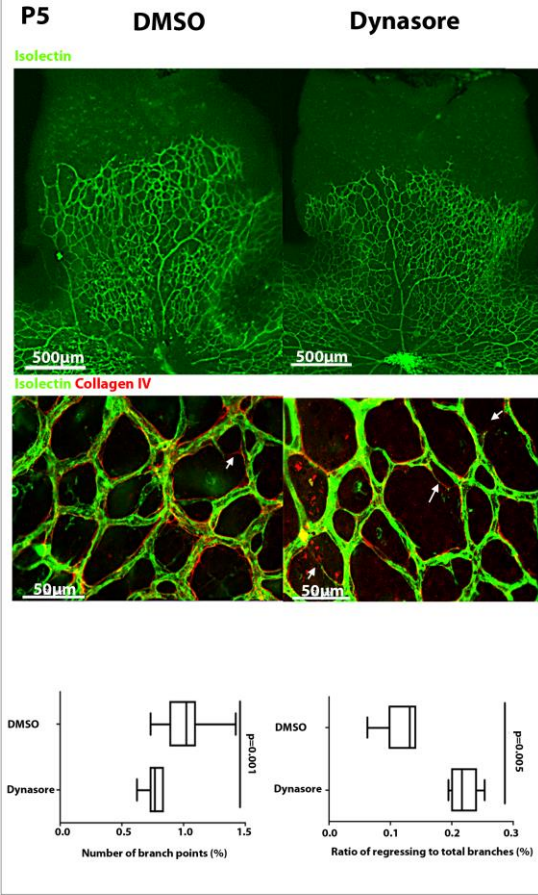
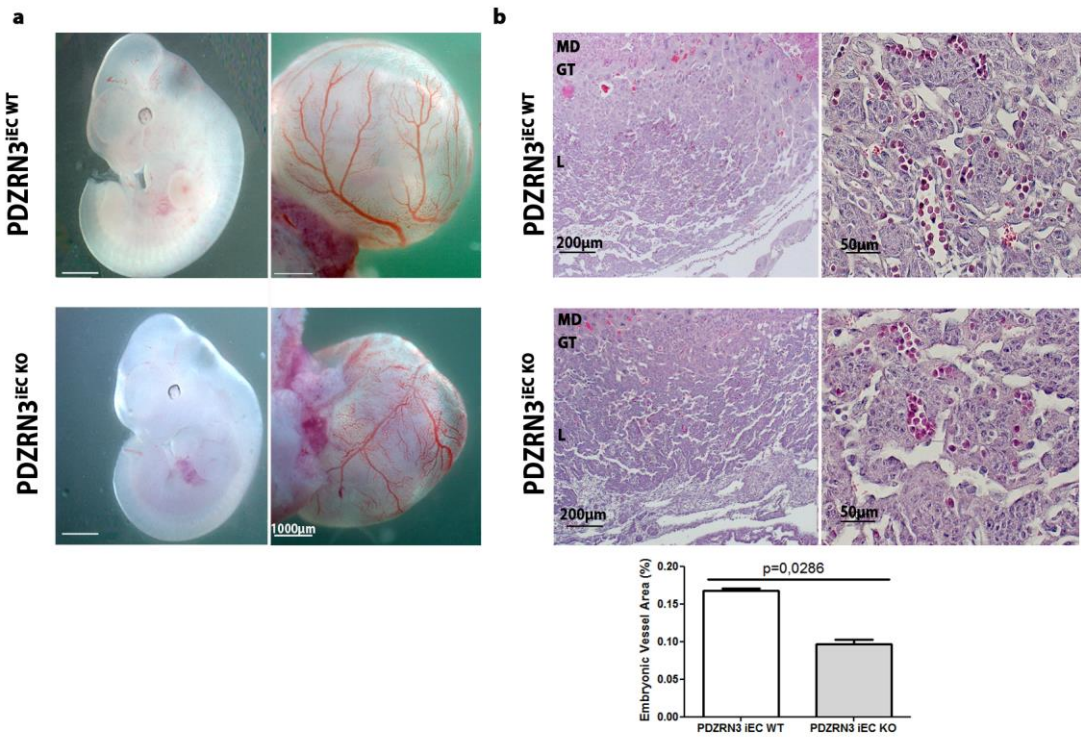
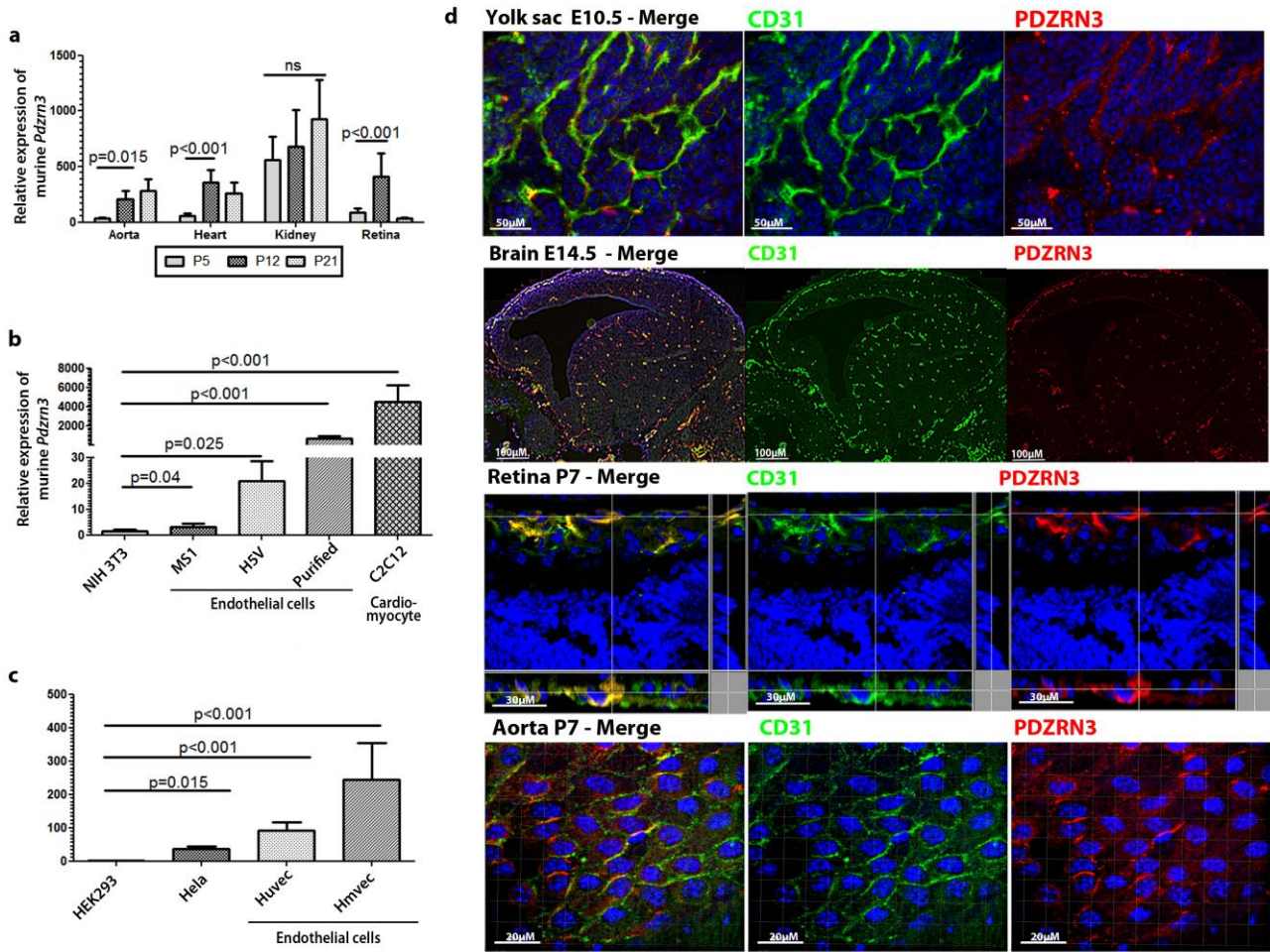


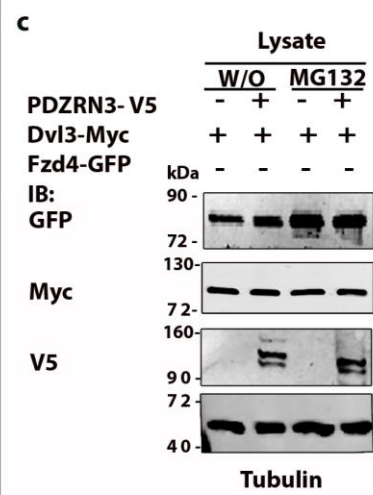
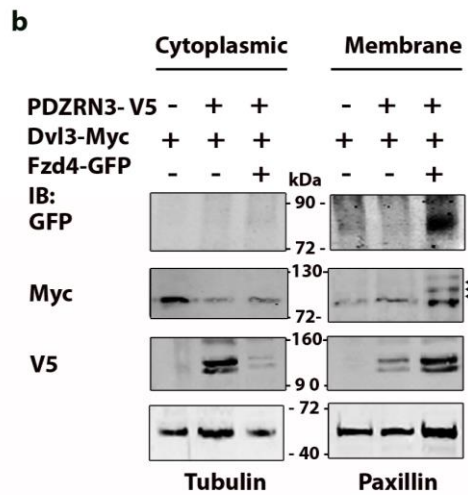
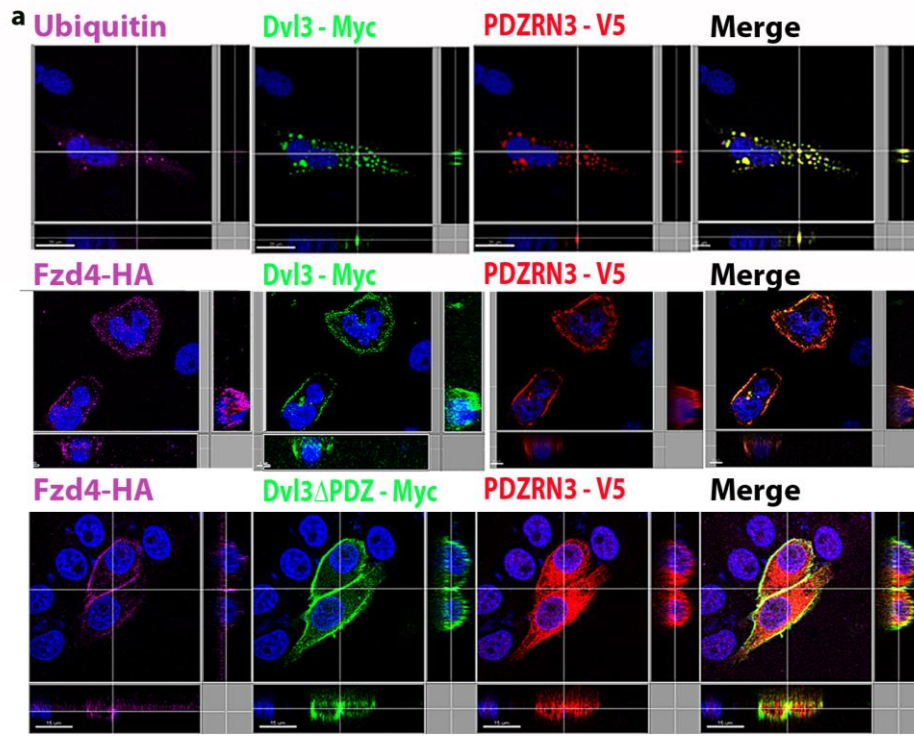
Fig 7 a



Supplementary1



Supplementary2



Supplementary3

Article 3

The ubiquitin ligase PDZRN3 regulates blood brain barrier integrity by controlling tight junctions stability via a Wnt dependant mechanism

Rationnel	Les voies de signalisation Wnt/Fzd sont impliquées dans l'angiogenèse cérébrale au cours de l'embryogenèse et jouent par la suite un rôle dans le maintien des jonctions serrées des cellules endothéliales cérébrales et le contrôle de la barrière hémato-encéphalique (BHE). Le mécanisme d'action des voies Wnt dans ce contexte reste méconnu.
Résultats	Nous avons développé un modèle murin d'œdème cérébral par occlusion transitoire de l'artère cérébrale moyenne (ACM), modèle d'ischémie focale. Nous montrons que la délétion de <i>Pdzrn3</i> dans ce modèle rend la BHE plus résistante et réduit la taille de la zone lésée après ischémie. PDZRN3 régule la perméabilité endothéliale en induisant la relocalisation au noyau de protéines clés des jonctions serrées (ZO-1) par l'ubiquitination de la protéine d'échaffaudage MUPP1. ZO1 est une protéine qui est associée aux jonctions serrées en condition basale et qui induit la dissociation des jonctions serrées lorsqu'elle se détache. Les voies Wnt sont activées dans le modèle d'ischémie cérébrale avec une induction de l'expression de cibles des voies Wnt telles que c-Jun. La délétion endothéliale de PDZRN3 ne bloque pas la synthèse des ligands Wnt après ischémie, mais réprime l'expression de c-Jun. Nous montrons que PDZRN3 est phosphorylé lorsqu'il est actif et que cette phosphorylation dépend du corecepteur de Fzd4, Ror2. L'activation de Ror2 dépend de PKC- ζ , l'injection d'un inhibiteur de PKC- ζ après occlusion de l'ACM réduit fortement l'œdème cérébral.
Conclusion	Nous proposons un mécanisme par lequel PDZRN3 lorsqu'il est activé par la signalisation Ror2 / PKC- ζ dépendante ubiquitinerait MUPP1, ce qui provoquerait le décrochage de ZO1 et favoriserait la dissociation des jonctions serrées et la perméabilité de la BHE.

a) State of art

PDZRN3 is remarkable as it possesses PDZ domains/ PDZ binding domains and a RING domain. The RING domain is functional and identifies PDZRN3 as an ubiquitin ligase, a protein that gives the specificity to the reaction of ubiquitinylation. The PDZ binding domain of PDZRN3 indicates that it potentially interacts with proteins containing PDZ domains such as components of Tight Junctions.

b) Hypothesis

Our hypothesis is that PDZRN3 could interact with junctions via PDZ interactions and regulate TJ function.

c) Preliminary Results

Preliminary results indicated a role of *Pdzrn3* signaling in endothelial junction maintenance. Transwell assay indicated that depletion of *Pdzrn3* reduced permeability of the endothelial layer. We also observed a delay to EDTA treatment (Calcium chelation) of *Pdzrn3* depleted endothelial cells. The endothelial cells would detach more slowly than their control after EDTA treatment (Fig 94).

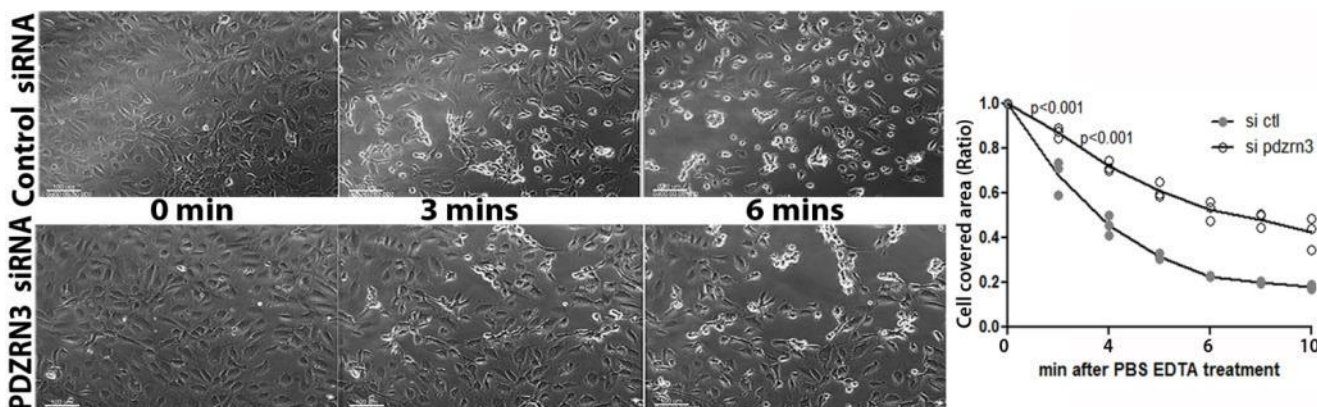


Figure 94: EDTA treatment induces disruption of cell to cell junctions in control HUVECs; a delay is observed in *Pdzrn3* depleted cells

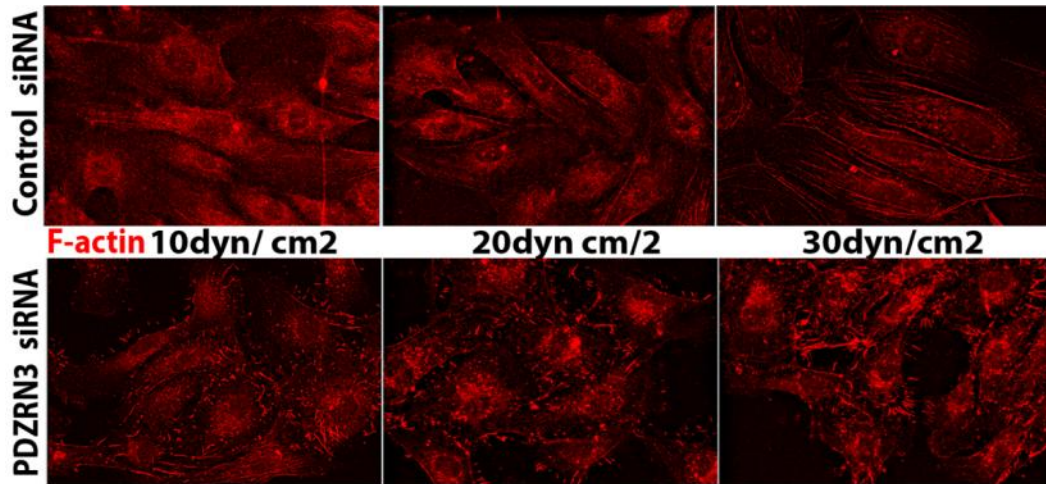


Figure 95: HUVEC cells are orientated in a flow of 10, 20 or 30dyn/cm²; Pdzn3 depleted cells are unable to align to the flow and reorganize their junctions accordingly

Interestingly, we found that control HUVECs were able to reorganize their actin skeleton and elongate/ align according to the flow (10 to 30 dyn/cm²). *Pdzn3* depleted cells were unable to reorganize in a flow of 10 to 20 dyn/cm² (Fig 95). The cells would detach progressively in a flow of 30dyn/cm² suggesting defects of the reorganization of the actin cytoskeleton and/ or cell / cell junctions.

d)Methods

To test our hypothesis, we developed transgenic models to delete PDZRN3 in EC and analyze its impacts on EC TJ functions. Experiments in this article were carried out on *PDGF icre; pdzn3^{ff}* mice. Vessels preparation was realized from non infarcted and infarcted hemispheres from iEC WT and iEC KO mice after cerebral artery occlusion, and subjected to quantitative RT PCR. Enrichment of the preparations was assessed by measuring expression of *Ve-cadherin* and *Tie2*. Vessel fractions strongly expressed both genes when compared to the wash fraction (Fig 97). Validation of the specificity of the *PDGF icre* mice was done by crossing *PDGF icre* mice with *mT/mG* mice that expresses membrane-targeted tandem dimer Tomato (mT) prior to Cre-mediated excision and membrane-targeted green fluorescent protein (mG) after excision. Vessels express GFP in *PDGF icre* mice but not in control mice, where they express Tomato only as shown on vibratome slices of the cortex and on purified

vessels extract (Fig 96). Confocal imaging shows that the endothelial cells express the GFP and the mural cells only express tomato in vessel purification from *PDGF icre* mice.

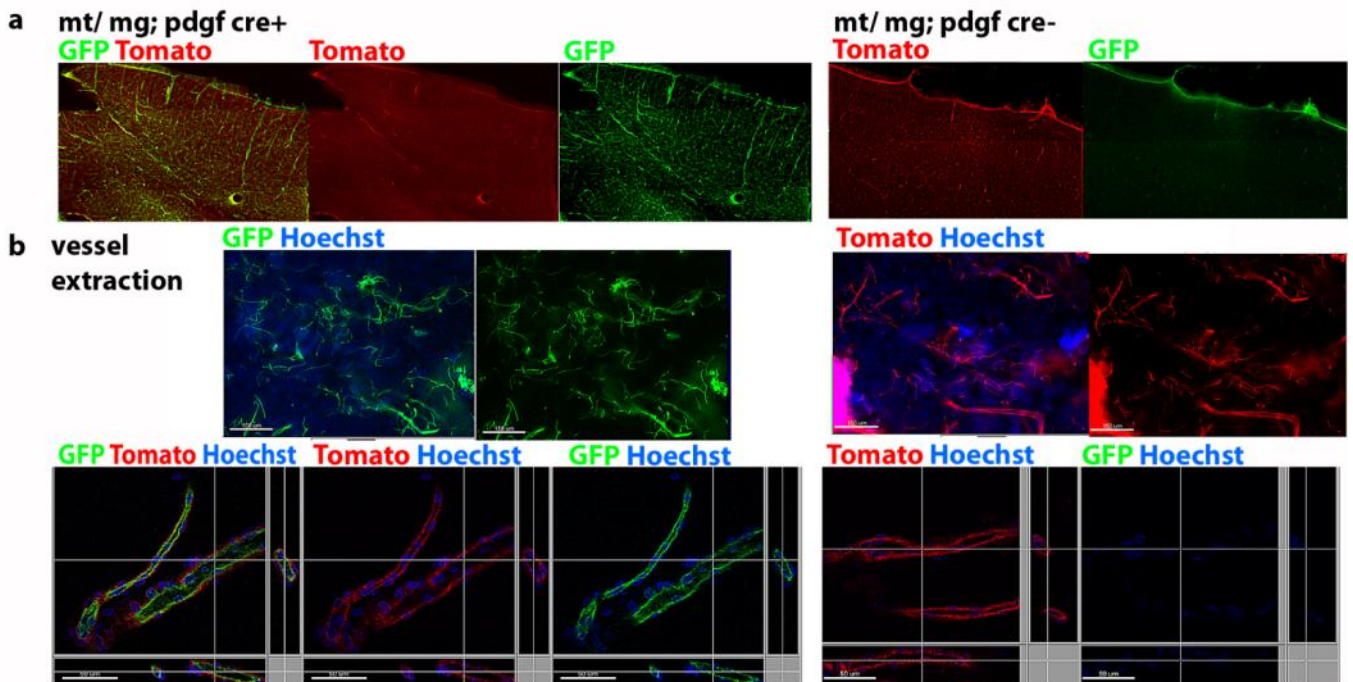


Figure 96: a - validation of the *PDGF iCre* activation using a *mT/mG* reporter; b- vessel extracts were purified from *PDGF icre*; *mT/mG* mice and subjected to confocal microscopy

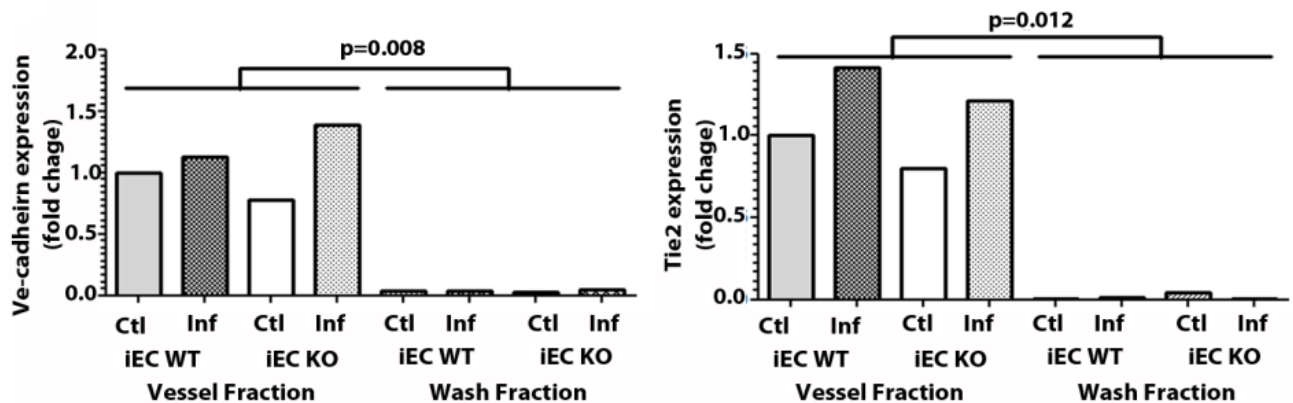


Figure 97: Validation of the enrichment of the brain vessel fraction by q RT PCR

Interestingly, the level of expression of *Pdzrn3* was not modified after cerebral ischemia in the vessel fraction. *Pdzrn3* was found essentially in the vessel fraction when compared to the wash fraction indicating that the protein is essentially expressed in the vessels in the brain (Fig 98).

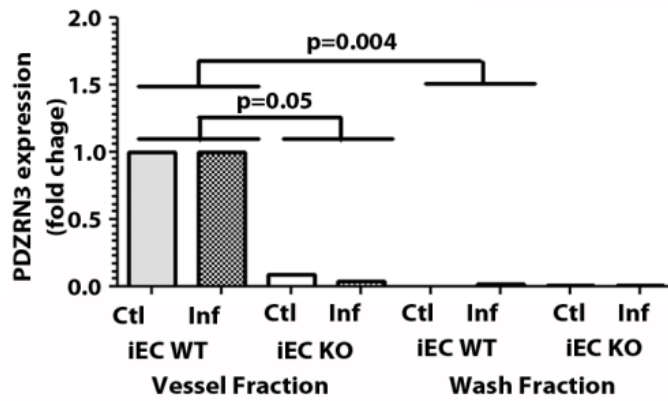


Figure 98: Expression of PDZRN3 in vessel / wash fraction

We also developed transgenic models to over-express PDZRN3 in endothelial cells by taking advantage of the tetracyclin activated system. Mice having integrated the gene coding for PDZRN3-V5 were crossed with mice expressing the transactivator (tta) under the control of the Tie2 promoter. The gene over-expression was conditional as in the presence of doxycycline, the transactivator could not interact with its target (tet off system). A β -Gal reporter cassette was also under the control of the Tie2-tta promoter, making it possible to reveal cell specific expression of the transactivator.

e) Summary

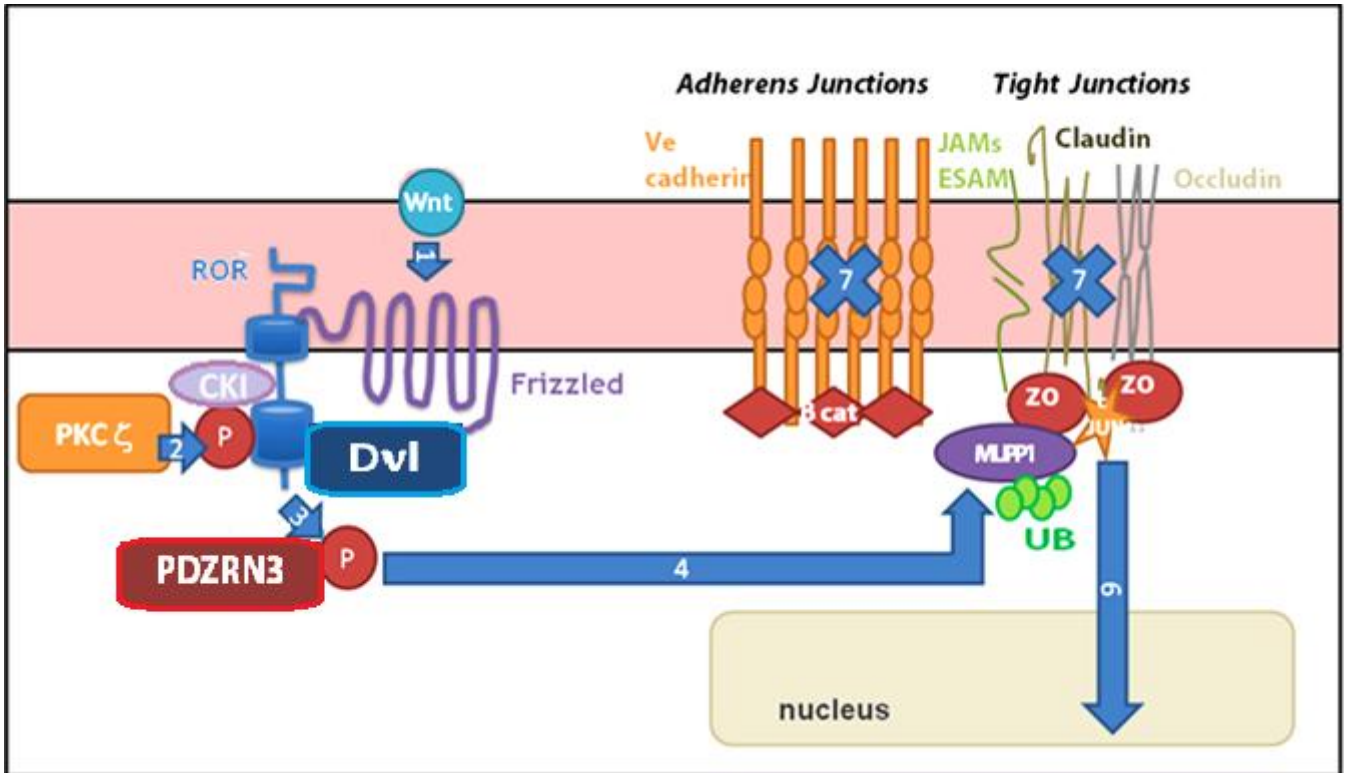


Figure 99: Proposed Model

This work identifies PDZRN3 as a link between Wnt signaling and Tight junction stability. After Wnt activation (Fig 96- 1), PKC Zeta would be activated leading to phosphorylation Ror2 via Casein Kinase 1(2). Ror2 is then active and would phosphorylate PDZRN3 (3) on a tyrosine residue. PDZRN3 would then ubiquitinylate MUPP1 leading to its degradation (4, 5). This would lead to detachment of ZO1; ZO2 and c-Jun from the tight junctions and their relocation to the nucleus (6) where they act as transcription factors. Tight junctions are disrupted leading to endothelial permeability (7). PDZRN3 would be found under an inactive form in normal conditions (where Wnt ligands are expressed in a small quantity); and activated by tyrosine phosphorylation after cerebral occlusion (where Wnt ligands are expressed strongly) – leading to disruption of the blood brain barrier.

The ubiquitin ligase PDZRN3 regulates blood brain barrier integrity by controlling tight junctions stability via a Wnt dependant mechanism

Raj N. Sewduth¹, Vincent Jecko³, Béatrice Jaspard-Vinassa^{1, 2}, Nicolas Fritsch, Mathieu Pernot^{1, 3}, Pascale Dufourcq^{1,2}, Thierry Couffinhal^{1,2,3}, Cécile Dupl  a^{1,2}.

1 INSERM, Adaptation cardiovasculaire   l'isch mie, U1034, F-33600 Pessac, France

2 Univ. Bordeaux, Adaptation cardiovasculaire   l'isch mie, U1034, F-33600 Pessac, France

3 CHU de Bordeaux, Service des Maladies Cardiaques et Vasculaires, F-33000 Bordeaux, France

Summary

Development of the Central Nervous System vasculature requires the coordination of multiple signaling processes. Wnt signaling is critical during vascular invasion of the brain and regulates acquisition of the 'barrier' properties of the newly formed brain vessels. Here, we demonstrate that the permeability of the blood brain barrier and stability of endothelial tight junctions are regulated by Wnt signaling via the ubiquitin ligase PDZRN3. Overexpression of PDZRN3 in endothelium leads to severe growth retardation in embryos as from 8.5 dpc. Specific *Pdzrn3* endothelial cell deletion in mouse mutants altered stability of endothelial junctions, as loss of PDZRN3 protects from blood brain barrier disruption in a cerebral artery occlusion model (MCAO), associated to a blockade of c-jun activation. MCAO induced secretion of several Wnt factors such as Wnt5a or Wnt7a/b. PDZRN3 regulates the response of endothelial cells to these stimuli as it promotes disruption of the tight junction associated complex composed of ZO1 / MUPP1 and c-Jun by ubiquitinylation of MUPP1, leading to its degradation & translocation of ZO1 and c-Jun from tight junctions to the nucleus, promoting permeability. Interestingly, we were able to show that PDZRN3 is tyrosine-phosphorylated in a Ror2 dependent manner after Wnt activation; and that this activation is required for the interaction of the protein with MUPP1. These results highlight the role of PDZRN3 in Wnt signaling and broadly implicate this pathway in regulation of vascular permeability.

Introduction

The planar cell polarity regulates properties of endothelial cells such as proliferation¹ or angiogenesis. Many recent studies have implicated the role of Wnt/PCP pathway in the regulation of blood brain barrier (BBB) development and permeability. The Wnt ligands, Wnt7a and Wnt7b were shown to be expressed by the neuroepithelium of the developing central nervous system (CNS) during vascular invasion. These ligands would induce activation of the Wnt pathway in the vascular endothelium, leading to formation and differentiation of the vasculature². Notably, the Wnt canonical pathway would be required for acquisition of the blood brain barrier characteristics of the CNS vasculature. In a similar manner, activation of the canonical Wnt signaling would induce β -catenin stabilization in glioblastoma endothelium, making the tumor vessels quiescent and less permeable by acquisition of the BBB characteristics. Expression of β -catenin would lead to secretion of platelet-derived growth factor B (PDGF-B), leading to mural cell recruitment^{3,4}. β -catenin would also interfere with the action of the transcription factor Foxo1 that can be relocated to the nucleus to regulate expression of TJ components such as Claudin 5. Interestingly, loss of the Fzd4 receptor leads to massive leakage in the cerebellum and cortex⁵ as *fzd4* deficient endothelial cells are unable to form correct tight junctions, as shown by their inability to express claudin5, indicating a requirement of the Wnt/ Fzd signaling for the maintenance of the barrier characteristic of the CNS vessels. Recent evidences have shown that expression B catenin would be able to rescue the defects observed in the *Fzd4* *-/-* mice⁶, confirming the interplay between Fzd4 and B catenin signaling for the acquisition of BBB characteristics and maintenance of endothelial integrity.

We previously showed that the ubiquitin ligase PDZRN3 was a novel regulator of Wnt/PCP signaling, as it promoted endocytosis of the Frizzled/Dvl complex enabling activation of the downstream effectors of the pathway. PDZRN3 was also found to be essential for angiogenesis during development and retinal vascular patterning. Here we show that overexpression of PDZRN3 in endothelial cells leads to severe growth retardation due to vascular defects, correlating with accumulation of c-Jun. We demonstrate that mice deleted for *Pdzrn3* in endothelial cells (iEC KO) present less vascular leakage in a model of middle cerebral artery occlusion (MCAO). Loss of *Pdzrn3* also stabilizes junctions and reduces

permeability of the endothelial cell layer in vitro. Finally, PDZRN3 was found to attach the tight junctions by interacting with MUPP1 that in turns binds the tight junction protein ZO1. PDZRN3 would ubiquitinylate MUPP1 leading to its degradation and subsequently, to disruption of the tight junctions. We also provide evidence of the role of Ror2 on the activation of PDZRN3. After Wnt activation, Ror2 is threonin- phosphorylated by Casein Kinase 1 in a PKC ζ dependant process; Ror2 would then be able to phosphorylate PDZRN3 on tyrosine 972. Interestingly, deleting this tyrosine impairs interaction of PDZRN3 with MUPP1; suggesting that phosphorylation of PDZRN3 is required for its interaction with MUPP1 and the subsequent signal transduction.

Results

PDZRN3 stabilizes endothelial cells in vitro

Incubation with Wnt ligands such as Wnt3a impacts on tight junction stability³, leading to a state of enhanced permeability/ migration of endothelial cells. As PDZRN3 is a regulator of the Wnt pathway, we wanted to assess the effect of PDZRN3 on the permeability of the endothelial cell layer. We used a strategy of silencing using siRNA targeted against *Pdzrn3* and over expression using a lentiviral construct to evaluate junctional integrity. In control condition, confluent endothelial cells form linear junctions as shown by ZO1 and Ve-cadherin staining; while incubation with Wnt CM leads to disruption of the junctions between EC that appeared irregular and discontinuous (Fig 1a). Interestingly, cells depleted for *Pdzrn3* were not affected by Wnt treatment while junctions of cell transduced with PDZRN3-V5 appeared disjointed in both control and Wnt conditions (Fig 1b, c). In a similar manner, incubation with Wnt Conditioned Medium (Wnt CM) strongly increased permeability of the endothelial cell monolayer in a model of transwell. Depletion of *Pdzrn3* reduces Wnt induced permeability by 50% (Fig 1d). Overexpression of PDZRN3 by lentiviral transduction enhances endothelial permeability in a Wnt independent manner (Fig 1e). Depletion and overexpression of *Pdzrn3* in the Huvecs cells were validated by Western Blot. Deletion of *Pdzrn3* favors accumulation of active B catenin accorded to our previous results. Overexpression of *Pdzrn3* (*Pdzrn3*-V5) strongly increases activation of c-jun indicating this pathway is impacted. Level of activation of Foxo-1 that was also described as a regulator of endothelial permeability

was not impacted by *Pdzn3*. Level of the components of tight and adherent junctions, ZO1 and Ve-cadherin respectively were not modified in both conditions (Fig 1f).

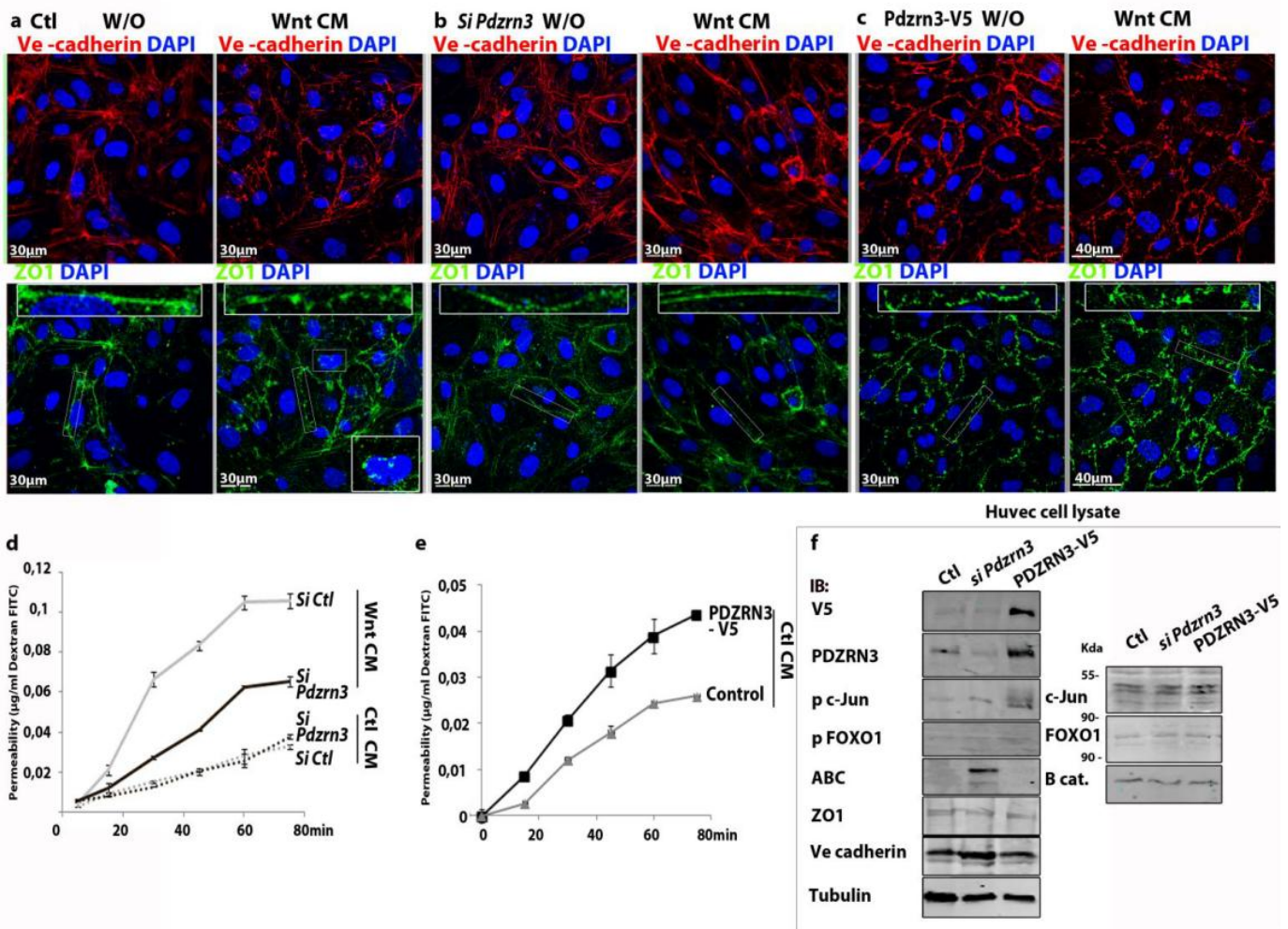


Fig 1. Loss of PDZRN3 stabilizes endothelial cells *in vitro*

a. Evaluation of junctional integrity of confluent endothelial cells was assessed by immunostaining with Ve-cadherin (red) and ZO1 (green) antibodies. Confluent endothelial cells form linear junctions while incubation with Wnt CM disrupts junctions between endothelial cells that appear punctiform. Interestingly, membrane staining of ZO1 appears discontinuous and ZO1 staining was detected at nuclear membrane in Wnt treated cells (see inset).

b, c. Cells depleted for *Pdzn3* did not lose their junctional integrity after incubation with Wnt CM. Junctions of cell transduced with PDZRN3-V5 were altered independently of Wnt activation. Images taken with an Olympus FSV 100 Confocal microscope; scale bar= 30µm.

d, e. PDZRN3 regulates permeability *in vitro*. Knock-down of *Pdzn3* by siRNA reduces permeability of the endothelial cell layer when incubated with Wnt conditioned medium (CM) as quantified by the concentration of FITC Dextran that diffuses in the lower chamber of the transwell. No differences are noted between control or PDZRN3 siRNA treated cells, when incubated with Control (Ctl) CM. Overexpression of PDZRN3 using a lentiviral construct increases the permeability of the endothelial layer independently of Wnt activation. Whiskers denote standard deviation between replicated experiments. Experiments repeated three times.

f. Endothelial cell lysates depleted for *Pdzn3* or overexpressing PDZRN3-V5 were subjected to Western Blot. Depletion of *Pdzn3* induces activation of B-catenin as revealed by the active B catenin staining (ABC). Overexpression of PDZRN3-V5 induces phosphorylation of c-Jun that is the active form of the protein accumulated upon Wnt signaling activation. The level of activity of the Foxo-1 protein is not modulated as indicated by p- Foxo1 blotting, indicating that the Foxo-1 pathway is not impacted by PDZRN3. Lysates are normalized with Ve-cadherin and Tubulin.

Overexpression of PDZRN3 leads to growth arrest during embryonic development

We created a mouse with conditional endothelial specific overexpression of PDZRN3, via crosses of a TetO-flanked *PDZRN3-V5* gene with tetracycline transactivator (*tta*) expression driven by *tie2* tetracyclin-off promoter. Expression of the transgene was validated by immunostaining and B galactosidase revelation on 10.5dpc brain vibratome slices (Fig 2a; Supplementary 2c). The *tie2 tta; PDZRN3- V5* embryos appeared growth retarded at E10.5. The vascularization of *tie2 tta; PDZRN3- V5* embryos appeared abnormal at E10.5, as the vessels appeared dilated. Presence of blood clots in the head was also detected in some of the mutant (Fig 2a). Approximately 50% of the *tie2 tta; pdzrn3 fl/fl* embryos were already regressed at E10.5. The rest of the embryos were smaller when compared to their wild-type littermates and hemorrhages were detected in most of the surviving embryos. Yolk Sac vascular defects and pericardial edema were detected in some of the embryos. No *tie2 tta; V5* embryos were detected at birth indicating that the phenotype observed in the mutants was lethal (Fig 2b). Taken together, our results suggest that overexpression of PDZRN3 in EC leads to severe growth retardation and embryonic death, at mid gestation.

Expression of PDZRN3-V5 was validated by Western Blot on E10.5 brain lysates. Overexpression of the protein correlated with an increase of phosphorylation of the Wnt target c-Jun, suggesting that the Wnt/ PCP signaling is activated by PDZRN3 overexpression. Phosphorylation of Foxo1 is not modified under expression of *Pdzrn3* indicating that the claudin5/ Foxo1 pathway is not modulated by *Pdzrn3* (Fig 2c). Subcellular localization of ZO1 and c-Jun was assessed by cell fractionation on embryo lysates. ZO1 is present at the nucleus or at the adhesion complex (NACos) depending on context, being located at the membrane in confluent endothelial cell layer and detected at the nucleus when permeability is enhanced⁷. C-Jun is also segregated at the TJ by interacting with ZO1 & 2 when the Wnt pathway is off; activation of the Wnt pathway leads to the relocalization of c-Jun from the TJ to the nucleus^{8,9}. Interestingly, over-expression of PDZRN3-V5 leads to relocalization of ZO1 and c-Jun from the membrane to the nucleus, suggesting that PDZRN3 alters stability of the tight junction complex (Fig 2d).

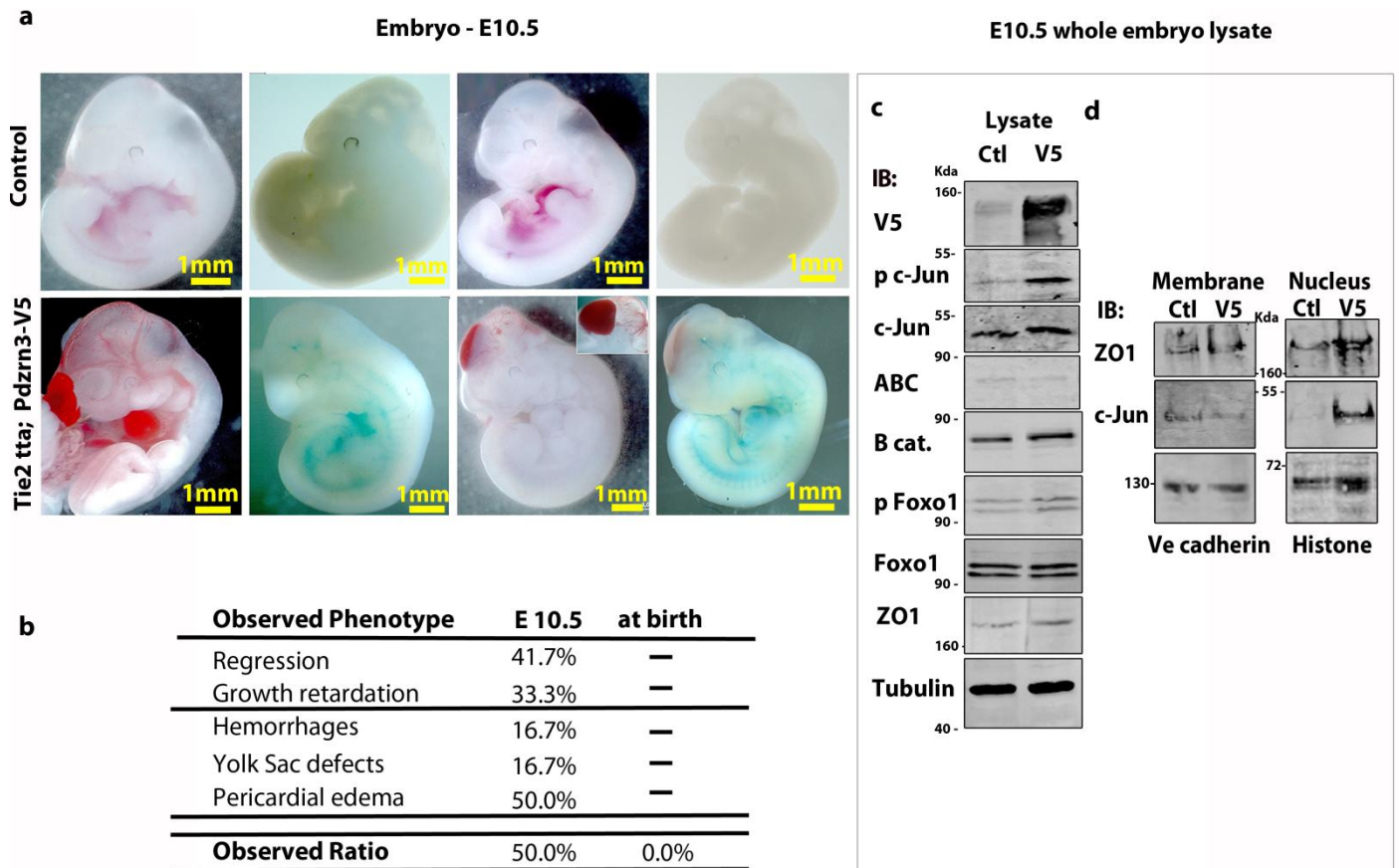


Fig2. Overexpression of PDZRN3 in EC induces hemorrhages during embryogenesis

a. Overexpression of PDZRN3 in endothelial cells leads to hemorrhages as observed at E10.5. *Tie2-tta; pdzrn3-v5* embryos were smaller and exhibited abnormal vascularization as vessels appeared dilated in the mutant. Presence of blood clots in the head was detected in the mutant. Imaged using a ZEISS Axiozoom, scale bar= 1000 μ m

b. Morphological phenotypes *Tie2-tta; pdzrn3-v5* embryo was observed at E10.5 (total number of mutant embryos=12). Survival rate of *Tie2-tta; pdzrn3-v5* embryo was measured between E10.5 and birth. Overexpression of PDZRN3 leads to early embryonic lethality as no mutants is detected at birth.

c. Lysates of brain of embryo at 10.5dpc were subjected to Western Blot. Overexpression of PDZRN3-V5 induces activation of c-Jun. The level of and the phosphorylation of Foxo-1/ B catenin proteins is not modulated, suggesting that the B-catenin / Foxo-1 pathway is not impacted by overexpression of PDZRN3. Lysates are normalized with Tubulin.

d. Lysates of brain of embryo at 10.5dpc were subjected to cell fractionation and Western Blot. ZO1 is relocated to the nucleus when junctions are disrupted²⁵, c-Jun is also relocated to the nucleus when Wnt signaling is activated and in sparse cells²⁶. Interestingly, Overexpression of PDZRN3-V5 induces relocalisation of c-Jun and ZO1 to the nucleus. The membrane fraction was normalized with Ve-cadherin and nuclear fraction with Histone.

Loss of PDZRN3 protects from stroke

These evidences lead us to propose that loss of PDZRN3 could reduce permeability of endothelial cells. In order to confirm this hypothesis, we used a strategy of middle cerebral artery occlusion (MCAO)¹⁰. The reperfusion after occlusion of the middle central artery induces cytotoxic and vascular

edemas in one of hemisphere of the brain (Infarcted- Inf). The other hemisphere is not altered (Contralateral - Ctl). For this purpose, we created a mice with targeted deletions of *Pdzrn3*, via crosses of a LoxP-flanked *Pdzrn3* gene with a Cre expression driven by *Pdgf* tamoxifen-inducible promoter which targets ECs ¹¹. The mice expressing (*Pdgf- iCre+*; *pdzrn3*^{f/f} noted as PDZRN3^{iECKO}) and littermates; (*pdzrn3*^{f/f} noted as PDZRN3^{iECWT}) were treated by 4 consecutive injections of Tamoxifen (1mg). We waited 1 month prior realize to the MCAO as tamoxifen is known to induce vascular inflammation/leakage ¹². No lethality was observed and the vessel network of the brain was not affected after these injections as indicated my 3D brain vasculature analysis (Supplementary 1d).

Damage of the BBB was assessed by injection of FITC Dextran (70 kDa). Leakage was observed in the infarcted hemisphere of both groups of mice at 24hours after surgery; it was significantly reduced in the PDZRN3^{iECKO} group (Fig 3a). Confocal analysis of the vessels of non infarcted areas of the cortex revealed that the endothelial cells can be delineated clearly and form a circular lumen (ZO1 in red), while Dextran (in green) was contained in the vessels. In infarcted areas of the cortex of PDZRN3 iEC WT mice, vessels appeared irregular-shaped and the lumen was collapsed, associated with a massive leakage of Dextran. Leakage was reduced 2h after surgery and vessels structure less altered in the infarcted hemisphere of the PDZRN3 iEC KO mice (Fig 3b). Damage of the BBB was also visualized and quantified by measuring diffusion of Evans Blue. Extravagated Evans Blue was extracted and dosed by spectrometry 24 hours after MCAO. Interestingly, the quantity of extravagated Evans Blue in the infarcted hemisphere was significantly reduced in the PDZRN3^{iECKO} mice compared to control mice (Fig 3c). To confirm this observation, we realized paraffin sections and mouse igG staining of the brain subjected to MCAO, 24 hours after reperfusion. Mouse igG extravagation indicates disruption of the BBB. The area of extravagation was measured showing that it was much more important in the infarcted hemisphere of PDZRN3^{iECWT} mice when compared to the PDZRN3 deleted group (Fig 3d).

2 hours after MCAO

24 hours after MCAO

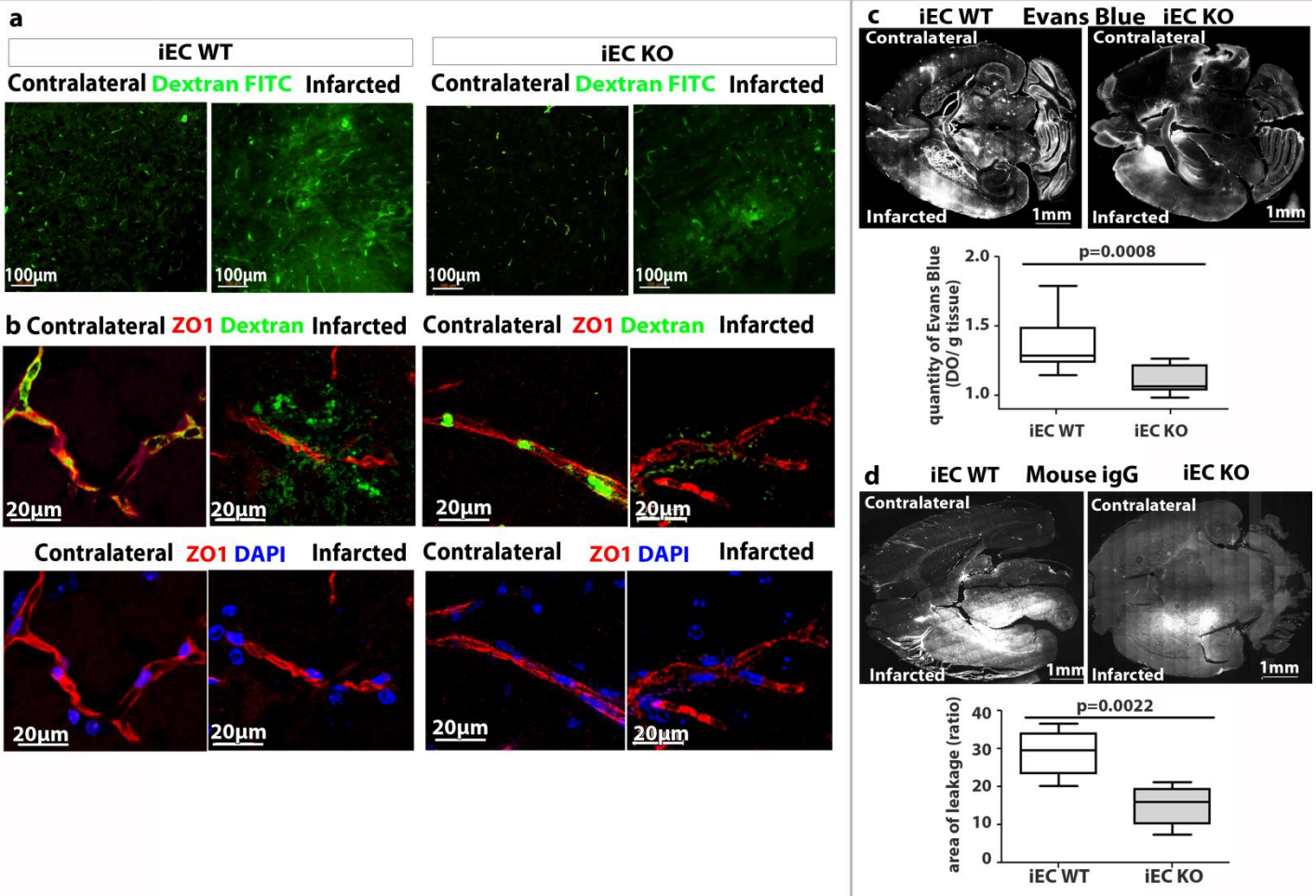


Fig3. Loss of PDZRN3 reduces Blood brain barrier disruption after middle cerebral artery artery

a. Large regions of Dextran leakage were detected in the infarcted cortex of PDZRN3 iEC WT mice as observed on 10µm sagittal slices of brain as observed 2 hours after MCAO. The regions of leakage were less present and much smaller in the infarcted regions in PDZRN3 iEC KO mice. Cryosection. Imaged using a ZEISS Axiobserver, scale bar=100µm.

b. ZO1 immunostaining was realized on Dextran-injected brains. In the controlateral hemisphere, Dextran was found to be localized in the vessels; ZO1 staining was linear and vessel formed lumen. In the infarcted area of iEC WT mice, the lumen of vessels appeared collapsed and dextran was detected outside of the vessels. In the infarcted area of iEC KO mice, dextran was detected outside of vessels but ZO1 staining was not altered. Cryosection. Imaged using a ZEISS Axiobserver, scale bar=20µm.

c. Occlusion / Reperfusion is realized on the cerebral artery of the right side of the animal leading to infarct in the corresponding hemisphere (Inf); the other hemisphere is noted as controlateral (Ctl). Evans Blue diffuses only on area where the vessels are altered and fluoresces at 565nm. 24 hours after MCAO, a large of leakage was detected in the PDZRN3 iEC WT mice; the area of leakage was reduced in PDZRN3 iEC KO mice as observed on 100µm sagittal slices of brain (vibratome, observed on Axiobserver (Zeiss) using the mosaic function). Imaged using a ZEISS Axiobserver, scale bar=1mm. Quantity of Evans Blue having diffused (µg per g of tissue) was measured by spectrophotometry after extraction from brain lysates. Diffusion of Evans Blue increased strongly in the infarcted hemisphere in PDZRN3 iEC WT mice, but increased only moderately in PDZRN3 iEC KO mice. Imaged using a ZEISS Axiobserver, scale bar=1mm. N=10 iEC WT mice; N=9 iEC KO mice. Unpaired t test.

d. Mouse IgG diffuses out of the vessels only in area where the vessels are altered. Mouse IgG staining reveals a large region of leakage in PDZRN3 iEC WT mice was observed on 7µm sagittal slices of brain (paraffin, observed on Axiobserver (Zeiss) using the mosaic function). The area of leakage was smaller in iEC KO mice. Imaged using a ZEISS Axiobserver, scale bar=1mm. N=6 iEC WT mice; N=6 iEC KO mice. Unpaired t test.

PDZRN3 is required for transduction of Wnt signaling after MCAO

We then realized vessel extracts from infarcted (Inf) and Contralateral (Ctl) hemisphere of brains of mice subjected to MCAO. Confocal analysis of the vessels of non infarcted areas of the cortex revealed that the endothelial cells can be delineated clearly and form a circular lumen as indicated by ZO1 and CD31 staining, while aquaporin that stains the astrocyte end-feet was present around the vessels (Fig 4a, b). In infarcted areas of the cortex of PDZRN3 iEC WT mice, vessels appeared irregular shaped and in some regions, loss of ZO1 and Aquaporin 4 staining were even observed. The structure of cortical vessels was less affected in infarcted areas in PDZRN3 iEC KO mice as expression of ZO1 and aquaporin were maintained (Fig 4a, b). This reduction of expression of ZO1 and Aquaporin was also detected by Western Blot (Fig 4c). To assess if Wnt pathways were activated in our model, level of various Wnt ligands and targets was assessed by qRT-PCR on vessel extracts of the non infarcted and infarcted hemisphere from PDZRN3^{iECWT} and PDZRN3^{iECKO} mice brains. Level of Wnt3a, Wnt5a, Wnt7a & b was significantly increased in infarcted when compared to non infarcted hemisphere similarly between PDZRN3 iEC WT and KO mice, indicating that in both cases, MCAO induces Wnts secretion (Supplementary 2a, b, c). Depletion of Pdzrn3 in the PDZRN3^{iECKO} mice was validated by Western Blot realized on the vessel extracts. Interestingly, cerebral ischemia correlated with an increase of phosphorylation of the Wnt targets c-Jun in PDZRN3^{iECWT} but not in PDZRN3^{iECKO} mice, confirming that the Wnt/ PCP is indeed activated by PDZRN3. Phosphorylation of Foxo1 is activated by cerebral ischemia in both groups indicating that the Foxo1 pathway is modulated by cerebral ischemia but not by Pdzrn3 signaling. Accumulation of active B catenin was stronger in iEC KO mice independently of the MCAO (Fig 4c). Subcellular localization of ZO1 and c-Jun was assessed by cell fractionation on the vessel extracts. Cerebral ischemia leads to relocalization of ZO1 and c-Jun from the membrane to the nucleus in PDZRN3^{iECWT} but not in PDZRN3^{iECKO} mice, confirming that PDZRN3 signaling is required for destabilization of the tight junction complex (Fig 4d).

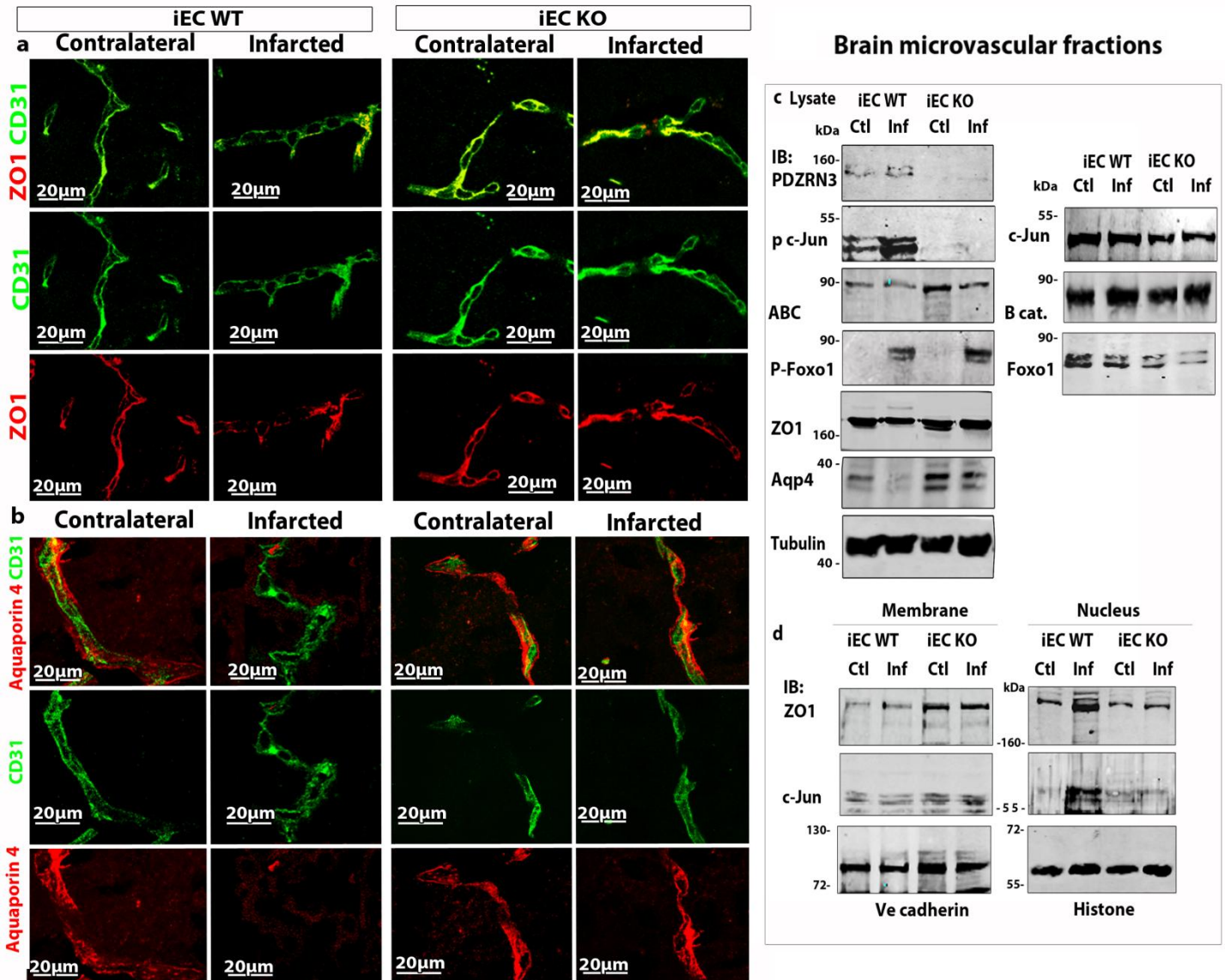


Fig 4. MCAO leads to activation & loosening of TJ in a PDZRN3 dependant manner

a. Confocal analysis of the cortical vessels of contralateral areas of the cortex revealed that the endothelial cells can form a delineated lumen as indicated by ZO1 (red) and CD31 (green) staining. In infarcted areas of the cortex of PDZRN3 iEC WT mice, vessels were collapsed and in some regions, partial loss of ZO1 staining observed. The structure of cortical vessels was less affected in infarcted areas in the PDZRN3 iEC KO mice and expression of ZO1 was not lost.

b. Aquaporin that stains the astrocyte end-feet was present around the CD31 stained endothelial cells in the contralateral area. In infarcted areas of the cortex of PDZRN3 iEC WT mice, vessels were irregular shaped and in some regions, loss of aquaporin staining observed. The structure of the cortical vessels was mildly affected in infarcted areas in PDZRN3 iEC KO mice and expression of aquaporin was maintained.

c. Brain Microvessel fractions were purified from the infarcted and contralateral hemisphere and subjected to Western Blot. An increase of the level of activation of c-Jun was detected in infarcted conditions in iEC WT mice but not in iEC KO mice, indicating that Wnt signaling is activated after MCAO and that this activation requires PDZRN3. Level of active B catenin is sensibly higher in the PDZRN3 iEC KO mice, independently of the MCAO. The activity of the Foxo-1 protein is modulated by the Infarct but not by PDZRN3 deletion as indicated by p-Foxo1 blotting, indicating that the Foxo-1 pathway is not impacted by PDZRN3. A small reduction of expression of ZO1 and a massive reduction of expression of aquaporin was detected in iEC WT mice but not in iEC KO mice. Lysates are normalized with Tubulin.

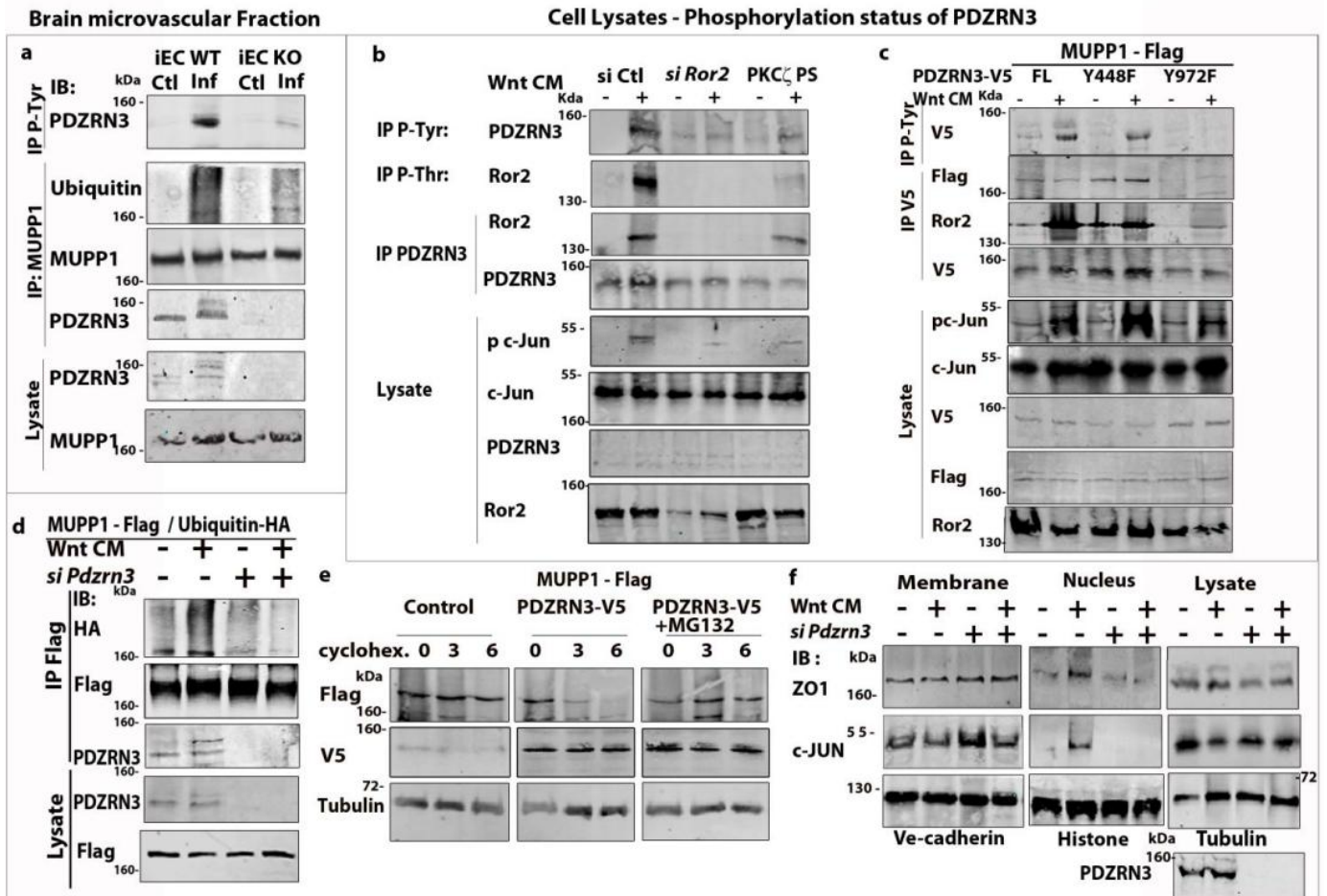
d. Subcellular fractionation was realized on vessel preparations from infarcted and non infarcted brain. ZO1 and c-Jun are accumulated in the nucleus of the infarcted area of the iEC WT but not iEC KO mice, indicating that PDZRN3 is required for translocation of ZO1 and c-Jun from the membrane to the nucleus. Shift of phosphorylation indicates that ZO1 is more mobile and was observed strongly in iECWT and to a lesser extent in iEC KO nuclear lysates. Membrane fraction normalized with Ve-cadherin and nuclear fraction with Histone.

PDZRN3 is activated by tyrosine phosphorylation and interacts with MUPP1 upon Wnt activation

We then wanted to assess whether PDZRN3 was phosphorylated when activated. To test this hypothesis, brain microvascular fractions and HUVEC cells were subjected to immunoprecipitation using a P-threonine & P-Tyrosine antibody. Cerebral Ischemia and Wnt CM treatment induced coprecipitation of PDZRN3 with the P-Tyrosine antibody, indicating that PDZRN3 was phosphorylated on tyrosine residue when cells are activated. Level of phosphorylation of PDZRN3 correlated with induction of c-Jun phosphorylation, suggesting that PDZRN3 was activated when phosphorylated (Fig 5a, b). We then assessed which tyrosine kinase could phosphorylate PDZRN3. One of the candidates was Ror2. Ror2 is a co-receptor of Fzd but also possesses a tyrosine-kinase activity; Ror2 is activated by phosphorylation of serine and threonine residues, in a process that requires the serine/ threonine kinases PKC ζ and CKI¹³. Ror2 was threonine-phosphorylated in endothelial cells activated with WntCM. Depletion of Ror2 using siRNA blocked Wnt-induced phosphorylation of PDZRN3; while blockade of the activity of PKC ζ using a pseudosubstrate blocked Wnt-induced phosphorylation of Ror2 & PDZRN3 (Fig 5b). As the PDZRN3 protein was shown to be tyrosine –phosphorylated previously and contains only two tyrosine residues (Supplementary 3d), we generated two constructions of PDZRN3 deleted for each tyrosine (Y448F and Y972F) and expressed the proteins in HeLa cells. Interestingly, PDZRN3 Y448F was tyrosine phosphorylated after Wnt treatment but not PDZRN3 Y972F (Fig 5c). To assess if the kinase activity of Ror2 and CKI were required for the activation of Pdzn3, HeLa cells were transfected with kinase dead or full length forms of Ror2 and CKI. Expression of full length CKI but not kinase dead (KD) CKI induced phosphorylation of PDZRN3 and Ror2 at a similar level as activation with Wnt CM; while expression of full but not KD Ror2 induced phosphorylation of PDZRN3 (Supplementary 3e). In a similar manner, PDZRN3-Y972F is not tyrosin- phosphorylated in any of the conditions (Supplementary 3e).

To identify how PDZRN3 interacts with TJ, we used a strategy of immunoprecipitation. PDZRN3 did not interact with ZO1 or c-Jun directly. One of the potential partners of PDZRN3 at the TJ is MUPP1. MUPP1 was characterized as a member of the Crumbs complex¹⁴, is expressed in EC from the brain¹⁵ and interacts directly with ZO1 via its PDZ binding domain¹⁶. Endogenous MUPP1 coprecipitated PDZRN3

in brain lysates, and MUPP1 also coprecipitated PDZRN3 in transfected HeLa cells (Fig 5 a, d). We then analyzed if MUPP1 was a substrate of PDZRN3. We were able to detect an increase of ubiquitinylation of MUPP1 in the hemisphere subjected to MCAO of PDZRN3 iEC WT but not of iEC KO mice (Fig 5a); suggesting that MUPP1 is a specific substrate of PDZRN3-mediated ubiquitinylation. In a similar manner, Wnt treatment of HeLa cells induced coprecipitation of MUPP1 – Flag with Ubiquitin –HA in control cells but not in cells depleted for *Pdzn3* (Fig 5d); confirming that *Pdzn3* is required for Wnt-induced ubiquitinylation of MUPP1. Ubiquitinylation can elicit different processes. We questioned whether ubiquitinylation of MUPP1 by PDZRN3 would regulate its level of expression. To this intent, we treated MUPP1-Flag transfected HeLa cells with cycloheximide that blocks *de novo* traduction. The level of MUPP1-Flag was stable in control cells but rapidly decreased in cells transfected with PDZRN3-V5. Treatment of PDZRN3-V5 transfected cells with MG132 (that blocks the activity of the proteasome) stabilized the level of expression of MUPP1-Flag (Fig 5e), suggesting that PDZRN3 mediated ubiquitinylation of MUPP1 induces degradation of the protein. Activation of Huvec cells with Wnt CM induced relocalization of ZO1 and c-Jun to the nucleus in a *Pdzn3* dependant manner (Fig 5f) (Fig 1a) echoing the findings on brain vessel fractions after MCAO (Fig 4d). These evidence suggest that PDZRN3 by ubiquitinyllating MUPP1, induces its degradation that would trigger dissociation of the TJ associated proteins ZO1 and c-Jun. As phosphorylation of PDZRN3 would be a major regulator of its activity and MUPP1 is an important substrate of PDZRN3, we wanted to assess if the phosphorylation of PDZRN3 could modulate its interaction with MUPP1. While PDZRN3 Y972F was able to interact with Ror2; PDZRN3 FL and Y448F- V5 but not PDZRN3 Y972-V5 were able to coprecipitate MUPP1-Flag, suggesting that the Tyrosine 972 residue of PDZRN3 is phosphorylated after Wnt treatment and required for its interaction with MUPP1 (Fig 5c). These results collectively indicate that the kinase activity and activation by phosphorylation of Ror2 were required for phosphorylation of *Pdzn3* on the tyrosine 972 and that this phosphorylation is required for its interaction with MUPP1, and dissociation of the TJ complex.



Cell Lysates - Ubiquitinylation activity of PDZRN3

Fig5. PDZRN3 is tyrosine phosphorylated and interacts with the tight junction complex via MUPP1

a. Brain vessel fractions were subjected to additional protein analysis. PDZRN3 was shown to be tyrosine phosphorylated after cerebral infarct as indicated by coprecipitation of the protein with anti-phospho tyrosine antibody. Western blot analysis also showed that PDZRN3 ubiquitinylates the TJ associated protein MUPP1 in infarcted brain after Middle cerebral artery occlusion. MUPP1 immunoprecipitation was realized on vessel preparations from the infarcted and control hemisphere of brains subjected to MCAO. MUPP1 coprecipitates with PDZRN3 and ubiquitin chains in infarcted conditions in iEC WT but not in the iEC KO mice, when compared to non infarcted conditions, indicating that an endogenous interaction between PDZRN3 & MUPP1 exists.

b. Wnt mediated phosphorylation of PDZRN3 and Ror2 was assessed in HUVEC cells treated with Ctl or Wnt CM and subjected to immunoprecipitation with a P-tyrosine and P-Threonine antibody. The tyrosine kinase Ror2 is required for the phosphorylation of PDZRN3, as depletion of *Ror2* blocks Wnt-induced phosphorylation of PDZRN3. The serine/ threonine kinase PKC- ζ is required for the phosphorylation of Ror2, as depletion of PKC- ζ (using the pseudosubstrate) blocks Wnt-induced phosphorylation of Ror2. Interestingly, blockade of PKC- ζ also blocks Wnt-induced phosphorylation of PDZRN3.

c. HeLa cells were transfected with the three forms of PDZRN3, treated with or without Wnt CM and subjected to immunoprecipitation with Phospho-tyrosine antibody. Interestingly, PDZRN3 Y448F was tyrosine phosphorylated after Wnt treatment but not PDZRN3 Y972F, indicating that Tyrosine 972 is the site of Wnt mediated phosphorylation of PDZRN3. Interestingly, PDZRN3 FL and Y448F- V5 but not PDZRN3 Y972-V5 were able to coprecipitate MUPP1-Flag, indicating that the Tyrosine 972 residue of PDZRN3 is required for its interaction with MUPP1. Lysates normalized with tubulin.

d. To assess if the ubiquitinylation of MUPP1 is modulated by Wnt signaling, HeLa cells were transfected with MUPP1-Flag, Ubiquitin-HA plasmids and/or *Pdzrn3* siRNA, treated with Ctl or Wnt CM, before being subjected to Flag immunoprecipitation. MUPP1 coprecipitates strongly with Ubiquitin -HA after activation of cells with Wnt CM. Interestingly, depletion of *Pdzrn3* blocks coprecipitation of Ubiquitin chains by MUPP1 even in Wnt treated cells, indicating that PDZRN3 is required for Wnt mediated ubiquitinylation of MUPP1.

e. To assess if the ubiquitinylation of MUPP1 induces degradation of the protein, we treated MUPP1-Flag transfected Hela cells with cycloheximide that blocks *de novo* traduction. The level of MUPP1-Flag was stable in control cells but decreased after cycloheximide treatment in cells co-transfected with PDZRN3-V5. Interestingly, treatment of PDZRN3-V5 transfected cells with MG132 that blocks the activity of the proteasome, stabilized the level of expression of MUPP1-Flag, suggesting that PDZRN3 mediated ubiquitinylation of MUPP1 induces degradation of the protein.

f. Localization of ZO1 was also evaluated by cell fractionation on Huvec cells depleted for *Pdzrn3*. ZO1 is detected in the nuclear and membrane fraction after Wnt treatment but essentially in the membrane fraction in untreated endothelial cells. Depletion of *Pdzrn3* blocked Wnt induced relocalization of ZO1 and c-Jun to the nucleus. Extinction of the expression of PDZRN3 was also validated on cell lysates. Normalization of membrane fraction with Ve-cadherin, of nuclear fraction with Histone and lysate with Tubulin.

Tyrosine phosphorylation of PDZRN3 972 is required for its activity

We then assessed if the phosphorylation of PDZRN3 has relevance *in vivo* and *in vitro*, using the PKC- ζ pseudosubstrate and transfection of the tyrosine –mutated forms of PDZRN3 respectively. Evans Blue diffusion was used to measure the leakage in the brain of mice subjected to MCAO and injected with the PKC- ζ pseudosubstrate or with the carrier only at the reperfusion. Diffusion of Evans Blue increased strongly in the infarcted hemisphere in control mice, but increased only moderately in the infarcted hemisphere of PKC- ζ pseudosubstrate injected mice as indicated by the quantity of extravagated Evans Blue 24h after MCAO (Fig 6a). In order to assess if the phosphorylation of PDZRN3 & *ror2* were modulated by ischemia in the model of MCAO, P-Threonine and P-tyrosine immunoprecipitation were realized on vessel preparations from infarcted and control brain from control and PKC- ζ pseudosubstrate injected mice. PDZRN3 and Ror2 were found to be phosphorylated in the infarcted hemisphere of control mice 6h after MCAO. Depletion of PKC- ζ blocked infarct-induced phosphorylation of PDZRN3 and Ror2 (Fig 6b). These results indicate that phosphorylation of PDZRN3 is a process that participates to the establishment of vascular edema after MCAO. To assess if the two constructs were functional *in vitro*, we transfected Huvec cells with siRNA targetting *Pdzrn3* and transduced them with PDZRN3-FL or PDZRN3-Y972 and incubated the cellswith Ctl or Wnt CM. Expression of PDZRN3-FL in *Pdzrn3* depleted cells restored the ability of EC to disjoint their junction after Wnt activation, while expression of PDZRN3-972 did not restore their ability to disrupt their junctions (Fig 6c). Depletion of *Pdzrn3* by siRNA and expression of the PDZRN3-FL-V5 and PDZRN3-972-V5 in Huvecs cell was controlled by Western Blotting (Fig 6d). In a similar manner, we expressed both constructs in *Pdzrn3* depleted Huvecs, that reduces permeability of the endothelial cell layer. Expression of PDZRN3-FL restored Wnt induced

permeability of the EC monolayer, while expression of PDZRN3-972 did not (Fig 6e), clearly indicating that the phosphorylation of PDZRN3 on Tyrosine 972 is essential for its function.

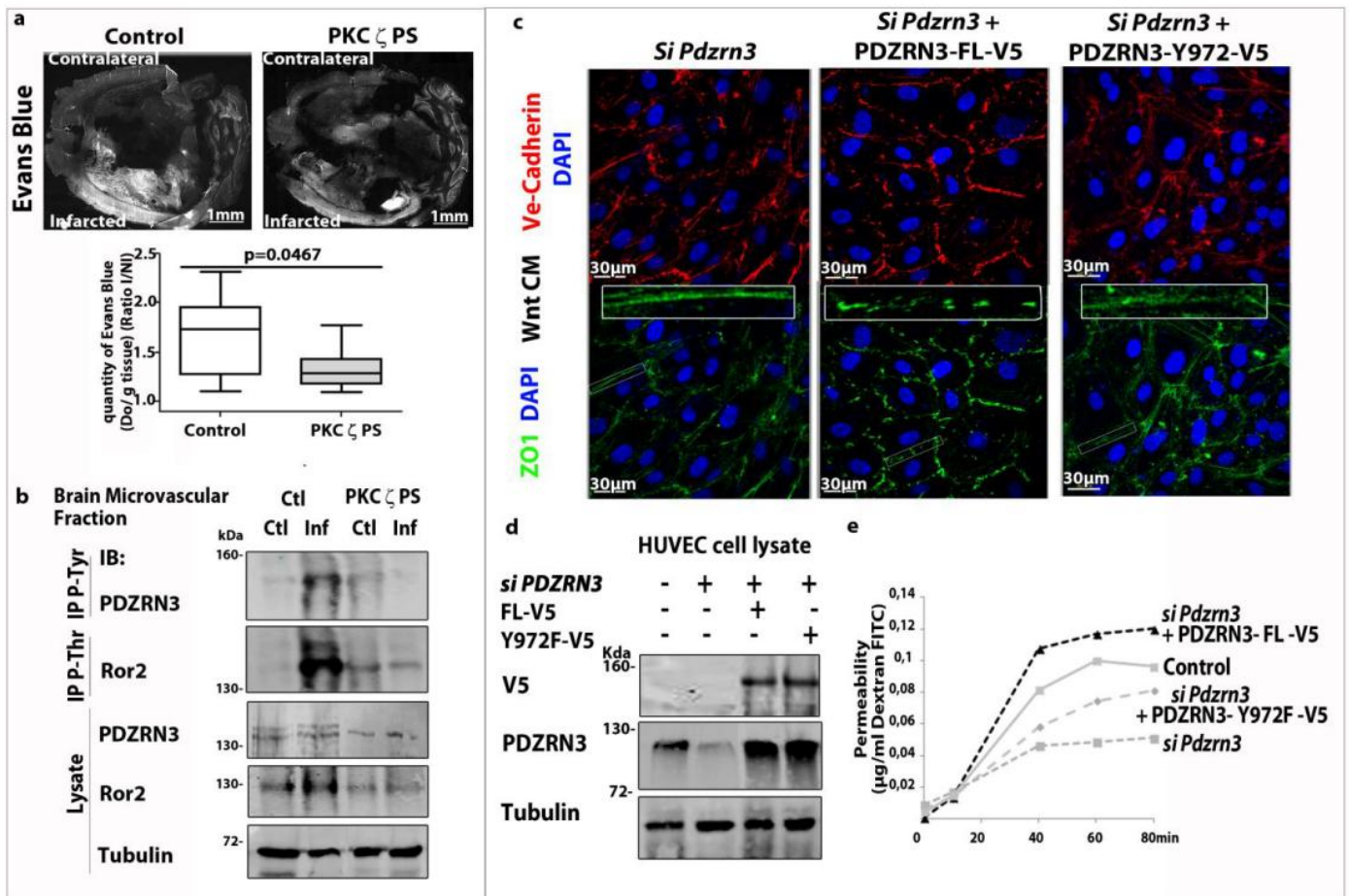


Fig7. Tyrosine phosphorylation of PDZRN3 on tyrosine 972 is required for its functions

- a. Evans Blue diffusion was used to measure the leakage in the brain of mice subjected to MCAO and injected with the PKC- ζ pseudosubstrate or with the carrier only at the reperfusion. Diffusion of Evans Blue increased strongly in the infarcted hemisphere in control mice, but increased only moderately in the infarcted hemisphere of PKC- ζ pseudosubstrate injected mice as indicated by the quantity of extravasated Evans Blue 24h after MCAO. Imaged using a ZEISS Axiobserver, scale bar=1mm. N=6 in each group. Unpaired t test
- b. P-Threonine and P-tyrosine immunoprecipitation were realized on vessel preparations from infarcted and non infarcted brain from control and PKC- ζ pseudosubstrate injected mice to assess the level of phosphorylation of PDZRN3 and Ror2. Interestingly, PDZRN3 and Ror2 were highly phosphorylated in the infarcted hemisphere of control mice 6h after ischemia, while depletion of PKC- ζ also blocks ischemia-induced phosphorylation of PDZRN3 and Ror2. The total level of PDZRN3 and Ror2 were not affected by the injection of PKC- ζ pseudosubstrate. Lysates normalized with Ve-cadherin.
- c. As depletion of *Pdzrn3* stabilizes junctions in HUVECs cells activated with Wnt CM, *Pdzrn3* depleted HUVECs were transduced with PDZRN3-FL or PDZRN3-Y972 and incubated with Ctl or Wnt CM. Expression of PDZRN3-FL in *Pdzrn3* depleted cells restored the ability of EC to disjoint their junction after Wnt activation. Expression of PDZRN3-972 in *Pdzrn3* depleted cells did not restore their ability to disrupt their junctions.
- d. Depletion of *Pdzrn3* by siRNA and expression of the PDZRN3-FL-V5 and PDZRN3-972-V5 in HUVECs cell was controlled by Western Blot using the PDZRN3 and V5 antibodies. Lysates normalized with tubulin.
- e. Knock-down of PDZRN3 by siRNA reduces permeability of the endothelial cell layer when incubated with Wnt conditioned medium (CM) as quantified by diffusion of FITC Dextran. Interestingly, expression of PDZRN3-FL in *Pdzrn3* depleted cells restored Wnt induced permeability of the EC monolayer. Expression of PDZRN3-972 in *Pdzrn3* depleted cells did not restore permeability of the EC monolayer. Experiments repeated three times.

Discussion

We show that depletion of PDZRN3 protects from TJ disruption, and reduces the impact of ischemia on the BBB. We propose a model where upon Wnt binding to its ligands, PDZRN3 is activated by tyrosine phosphorylation by Ror2 and binds MUPP1 at the TJs. PDZRN3 ubiquitinylates MUPP1, promoting dissociation of the claudin/ ZO1/ c-Jun complex. The TJs are then loosened and ZO1 / c-Jun translocate to the nucleus. Loss of PDZRN3 would make TJ less flexible and more static, while overexpression of PDZRN3 would make the junctions unstable, leading to vessel leakage. Similar phenotypes have been observed in the KO mice for Fzd4, that shows massive leakage in the cerebellum⁵ or the KO mice for the effector of Wnt signaling Rho Kinase II, where embryos are hemorrhagic¹⁷. The effector of Wnt signaling, c-Jun is one of the first proteins to be activated after MCAO¹⁰, while inhibition of c-Jun leads to reduction of vascular permeability¹⁸. Recent evidence have also shown that expression of B catenin would favor acquisition of BBB characteristics; as loss of PDZRN3 favors activation of B catenin – this could also explain why deletion of Pdzrn3 would make junctions less permeable. This body of work indicates a key role of Wnt signaling via c-Jun in the regulation of vascular permeability and notably blood brain barrier integrity. The fact that PDZRN3 is strongly expressed in CNS during its vascular invasion and that its expression is reduced progressively afterwards suggests that it is a key protein for the balance between angiogenesis and acquisition of the barrier characteristics of the CNS vasculature.

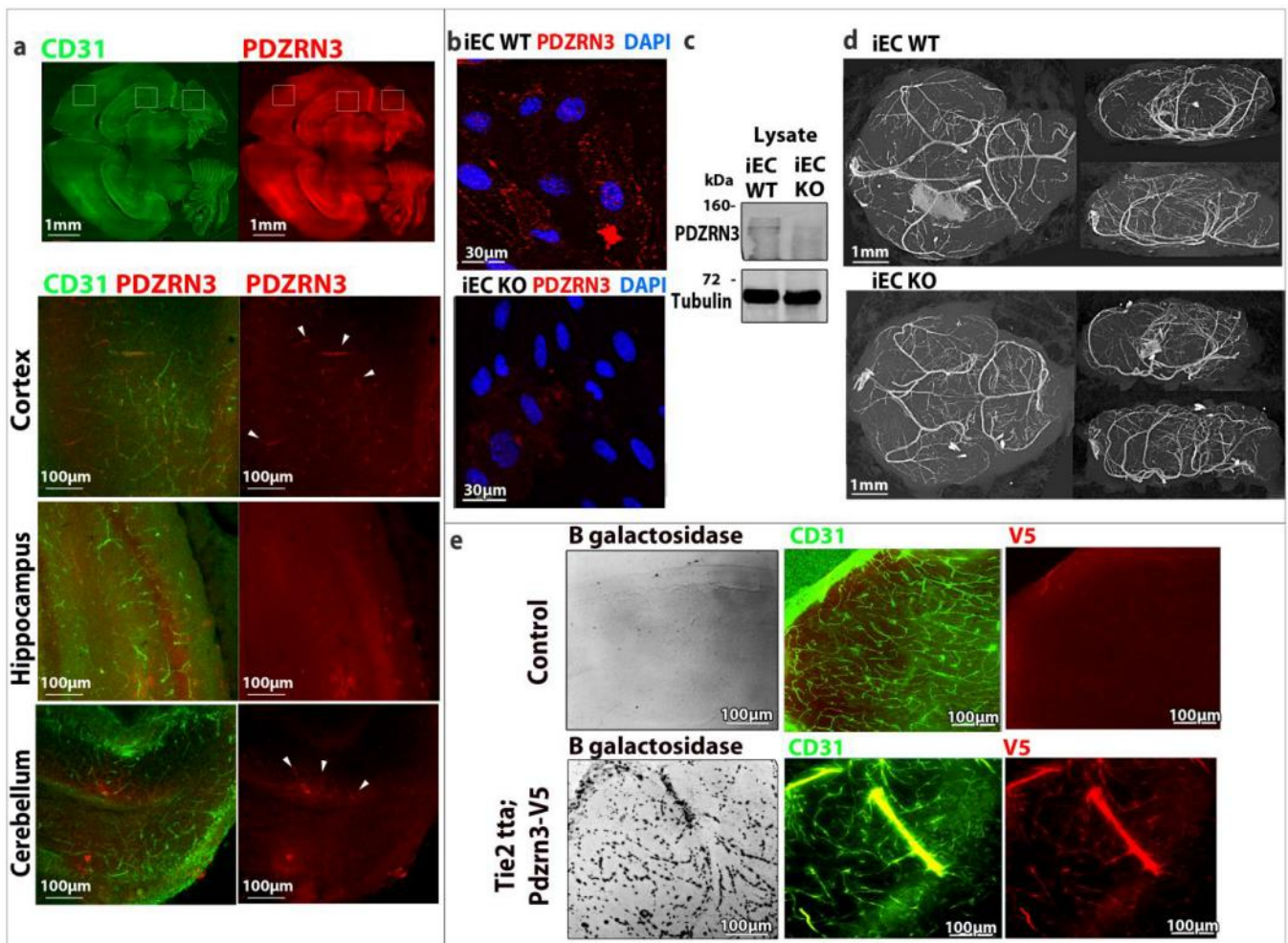
Acknowledgements

This work was supported by grants from the Agence Nationale de la Recherche (ANR-2010-Blanc-1135-01), from Region Aquitaine (20101301039MP), from Fondation de la Recherche Médicale (FDT20130928208) and from Communauté de Travail Pyrénéenne.

References

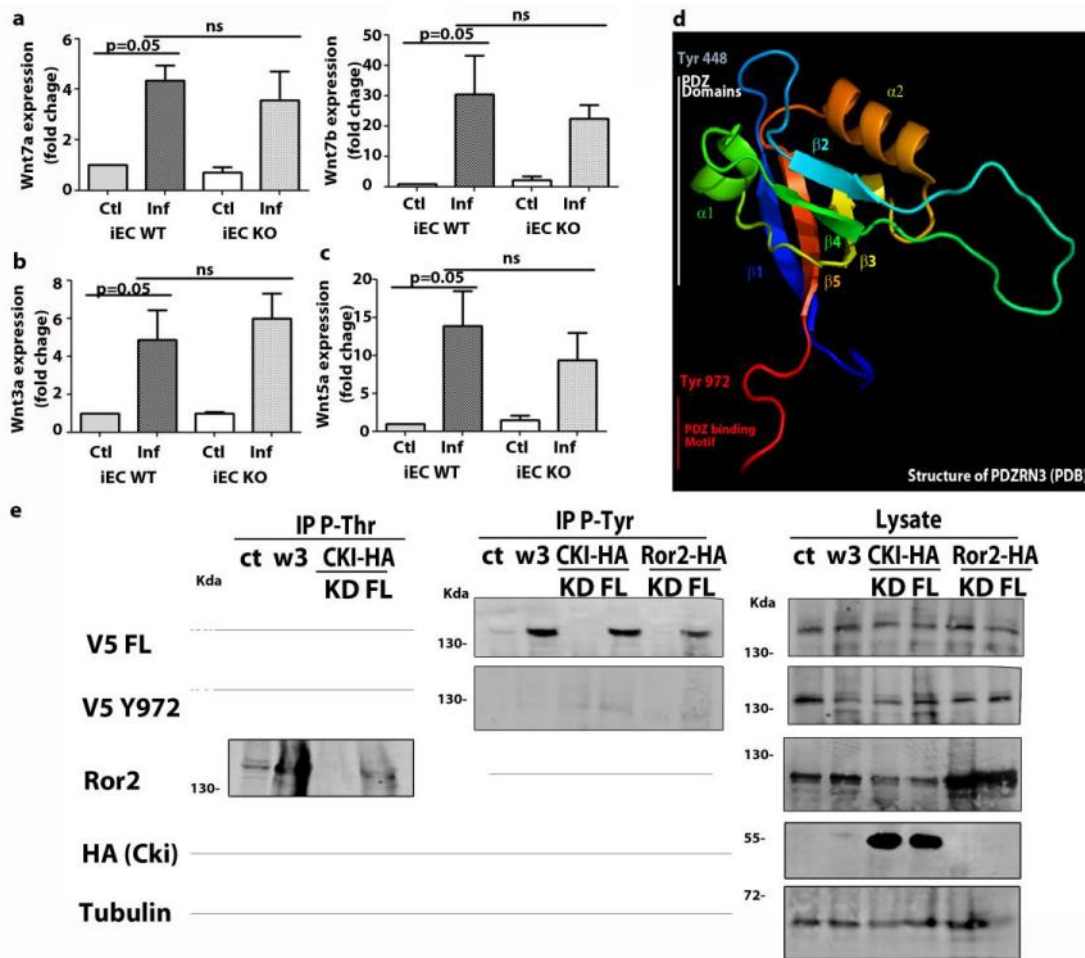
- 1 Masckauchan, T. N. *et al.* Wnt5a signaling induces proliferation and survival of endothelial cells in vitro and expression of MMP-1 and Tie-2. *Molecular biology of the cell* 17, 5163-5172, doi:10.1091/mbc.E06-04-0320 (2006).
- 2 Jan M. Stenman, J. R., 1,2 Thomas J. Carroll,1† Makoto Ishibashi,1‡ & Jill McMahon, A. P. M., 3§. Canonical Wnt Signaling Regulates Organ-Specific Assembly and Differentiation of CNS Vasculature. *Science* (2008).
- 3 Cattelino, A. *et al.* The conditional inactivation of the beta-catenin gene in endothelial cells causes a defective vascular pattern and increased vascular fragility. *The Journal of cell biology* 162, 1111-1122, doi:10.1083/jcb.200212157 (2003).
- 4 Reis, M. *et al.* Endothelial Wnt/beta-catenin signaling inhibits glioma angiogenesis and normalizes tumor blood vessels by inducing PDGF-B expression. *The Journal of experimental medicine* 209, 1611-1627, doi:10.1084/jem.20111580 (2012).
- 5 Wang, Y. *et al.* Norrin/Frizzled4 signaling in retinal vascular development and blood brain barrier plasticity. *Cell* 151, 1332-1344, doi:10.1016/j.cell.2012.10.042 (2012).
- 6 Zhou, Y. *et al.* Canonical WNT signaling components in vascular development and barrier formation. *The Journal of clinical investigation*, doi:10.1172/JCI76431 (2014).
- 7 Kausalya, P. J., Phua, D. C. & Hunziker, W. Association of ARVCF with zonula occludens (ZO)-1 and ZO-2: binding to PDZ-domain proteins and cell-cell adhesion regulate plasma membrane and nuclear localization of ARVCF. *Molecular biology of the cell* 15, 5503-5515, doi:10.1091/mbc.E04-04-0350 (2004).
- 8 Betanzos, A. *et al.* The tight junction protein ZO-2 associates with Jun, Fos and C/EBP transcription factors in epithelial cells. *Experimental cell research* 292, 51-66, doi:10.1016/j.yexcr.2003.08.007 (2004).
- 9 Jaramillo, B. E. *et al.* Characterization of the tight junction protein ZO-2 localized at the nucleus of epithelial cells. *Experimental cell research* 297, 247-258, doi:10.1016/j.yexcr.2004.03.021 (2004).
- 10 McColl, B. W., Rothwell, N. J. & Allan, S. M. Systemic inflammation alters the kinetics of cerebrovascular tight junction disruption after experimental stroke in mice. *The Journal of neuroscience : the official journal of the Society for Neuroscience* 28, 9451-9462, doi:10.1523/JNEUROSCI.2674-08.2008 (2008).
- 11 Claxton, S. *et al.* Efficient, inducible Cre-recombinase activation in vascular endothelium. *Genesis* 46, 74-80, doi:10.1002/dvg.20367 (2008).
- 12 Jones, M. E., Kondo, M. & Zhuang, Y. A tamoxifen inducible knock-in allele for investigation of E2A function. *BMC developmental biology* 9, 51, doi:10.1186/1471-213X-9-51 (2009).
- 13 Grumolato, L. *et al.* Canonical and noncanonical Wnts use a common mechanism to activate completely unrelated coreceptors. *Genes & development* 24, 2517-2530, doi:10.1101/gad.1957710 (2010).
- 14 Knust, N. A. B. a. E. The Crumbs complex: from epithelial-cell polarity to retinal degeneration. *Journal of cell science*, doi:10.1242/jcs (2009).
- 15 Sitek, B. *et al.* Expression of MUPP1 protein in mouse brain. *Brain research* 970, 178-187, doi:10.1016/s0006-8993(03)02338-2 (2003).
- 16 Lanaspa, M. A. *et al.* The tight junction protein, MUPP1, is up-regulated by hypertonicity and is important in the osmotic stress response in kidney cells. *Proceedings of the National Academy of Sciences of the United States of America* 104, 13672-13677, doi:10.1073/pnas.0702752104 (2007).
- 17 Thumkeo, D. *et al.* Targeted Disruption of the Mouse Rho-Associated Kinase 2 Gene Results in Intrauterine Growth Retardation and Fetal Death. *Molecular and cellular biology* 23, 5043-5055, doi:10.1128/mcb.23.14.5043-5055.2003 (2003).
- 18 Fahmy, R. G. *et al.* Suppression of vascular permeability and inflammation by targeting of the transcription factor c-Jun. *Nature biotechnology* 24, 856-863, doi:10.1038/nbt1225 (2006).
- 19 Honda, T., Yamamoto, H., Ishii, A. & Inui, M. PDZRN3 negatively regulates BMP-2-induced osteoblast

- differentiation through inhibition of Wnt signaling. *Molecular biology of the cell* 21, 3269-3277, doi:10.1091/mbc.E10-02-0117 (2010).
- 20 Wu, C. *et al.* Rab13-dependent trafficking of RhoA is required for directional migration and angiogenesis. *The Journal of biological chemistry* 286, 23511-23520, doi:10.1074/jbc.M111.245209 (2011).
- 21 Descamps, B. *et al.* Frizzled 4 regulates arterial network organization through noncanonical wnt/planar cell polarity signaling. *Circulation research* 110, 47-58, doi:10.1161/CIRCRESAHA.111.250936 (2012).
- 22 Dufourcq, P. *et al.* Secreted frizzled-related protein-1 enhances mesenchymal stem cell function in angiogenesis and contributes to neovessel maturation. *Stem Cells* 26, 2991-3001, doi:10.1634/stemcells.2008-0372 (2008).
- 23 Tirziu, D. & Simons, M. Angiogenesis in the human heart: gene and cell therapy. *Angiogenesis* 8, 241-251, doi:10.1007/s10456-005-9011-z (2005).
- 24 Oses, P. *et al.* Mapping 3-dimensional neovessel organization steps using micro-computed tomography in a murine model of hindlimb ischemia-brief report. *Arteriosclerosis, thrombosis, and vascular biology* 29, 2090-2092, doi:10.1161/ATVBAHA.109.192732 (2009).
- 25 Balda, M. Epithelial cell adhesion and the regulation of gene expression. *Trends in Cell Biology* 13, 310-318, doi:10.1016/s0962-8924(03)00105-3 (2003).
- 26 Gan, X. Q. *et al.* Nuclear Dvl, c-Jun, beta-catenin, and TCF form a complex leading to stabilization of beta-catenin-TCF interaction. *The Journal of cell biology* 180, 1087-1100, doi:10.1083/jcb.200710050 (2008).
- 27 Hudak, A. M. *et al.* Cytotoxic and vasogenic cerebral oedema in traumatic brain injury: Assessment with FLAIR and DWI imaging. *Brain injury : [BI]*, 1-8, doi:10.3109/02699052.2014.936039 (2014).
- 28 Huisman, T. A. State of the art in diffusion tensor imaging. *Pediatric radiology* 43, 14, doi:10.1007/s00247-012-2518-8 (2013).



Supplementary 1. Evaluation of *Pdzrn3* expression & impact of its deletion on physiological angiogenesis

- Expression of PDZRN3 was assessed by immunostaining on vibratome slices of mice adult brain. Expression of the protein was found to be localized to the vessels of the cortex and to a lesser extent to vessels of the cerebellum, as assessed by co-immunostaining with CD31. The fact that PDZRN3 expression is found essentially in brain vessels correlates with our protein analysis of vessel extracts. Imaged using an Olympus FSV100 confocal microscope. Scale bar=1mm and 100 μ M respectively.
- Endothelial cells were purified from kidney of iEC WT and iEC KO mice. Extinction of the expression of PDZRN3 was also validated by immunostaining imaged using an Olympus FSV100 confocal microscope. Scale bar=30 μ M.
- Level of expression of PDZRN3 was assessed on the purified EC by Western Blot. Extinction of the expression of the protein was verified. Normalization with tubulin.
- To analyze if deletion of *Pdzrn3* at the age of 3weeks by tamoxifen injection affected the brain vasculature, we injected mice with a contrast agent. The brain vasculature was found to be similar in both group of mice as analyzed using a Bruker Micro Computer Tomography Imager.
- Overexpressing of PDZRN3-V5 in the transgenic mice was validated on brain slices of embryos at 12.5 dpc. V5 staining was used to control expression of the integrated protein. LacZ expression can also be used to measure the expression of the PDZRN3-V5 transgene promoter. Vibratome slices of cortex were incubated with B galactosidase for 30min. Imaged using an Olympus FSV 100 microscope, scale bar= 100 μ m



Supplementary 2. Additional information

a, b, c. The level of expression of several Wnt ligands was measured by quantitative RT-PCR. Level of Wnt3a, Wnt5a, Wnt7a and b was increased in hemispheres subjected to MCAO of iEC WT and iEC KO mice. . N=3 iEC WT mice; N=3 iEC KO mice. Unpaired t test.

d. In silico predictions (3D structure of the protein from the PDB database) indicate that the the first tyrosine is placed between two PDZ domains; while the second tyrosine is placed just before the C-terminal PDZ binding (Threonin; Threonin; Valine motif). As the PDZRN3 protein contains only two tyrosine residues, we generated two constructions of PDZRN3 deleted for each tyrosine (Y448F and Y972F).

e. To assess if the kinase activity of the tyrosine kinase Ror2 and the serine/ threonin kinase CKI would impact phosphorylation of PDZRN3 and Ror2, Hela cells were transfected with full-length and kinase dead forms of both enzymes and subjected to immunoprecipitation. Interestingly, expression of Ror2 Full Length (FL) but not Kinase dead (KD) induces phosphorylation of PDZRN3. Expression of CKI FL but not KD induces phosphorylation of Ror2 and PDZRN3 respectively, indicating that kinase activity of CKI is essential for the phosphorylation of Ror2 and its activity, while activation and kinase activity of Ror2 are both required for the phosphorylation of PDZRN3. PDZRN3 Y972F is not phosphorylated in any of the conditions.

CONCLUSION and PROSPECTS

Conclusion et Perspectives

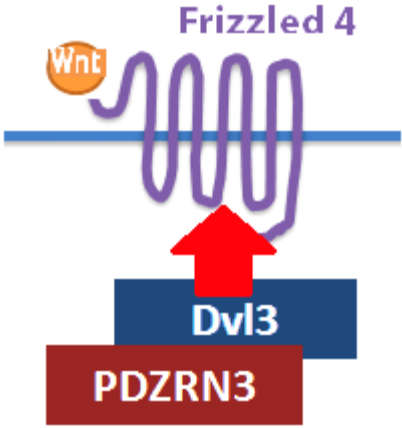
Pendant ce travail de thèse, nous avons pu étendre nos connaissances sur le rôle des voies Wnt/ Frizzled dans les processus d'angiogenèse au cours du développement et dans le maintien de l'intégrité de la barrière hémato-encéphalique. Ce travail s'est notamment axé sur un nouvel acteur des voies Wnt, l'ubiquitine ligase PDZRN3.

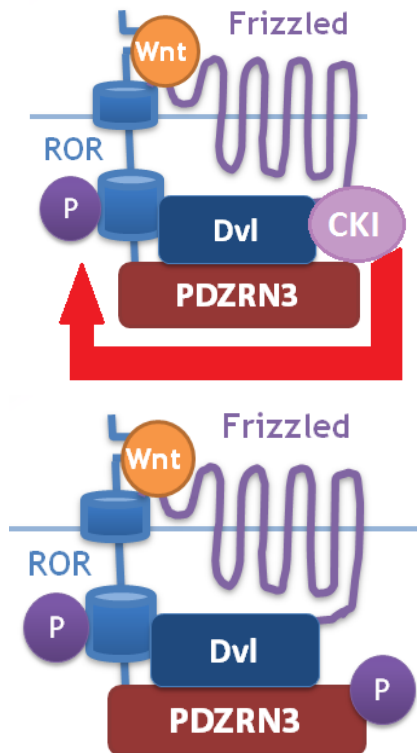
Nous proposons un modèle par lequel PDZRN3 ubiquitine la protéine adaptatrice Dvl3 pour induire l'endocytose du complexe Fzd4/ Dvl3 et favoriser la transduction du signal en aval de la fixation du ligand Wnt sur le récepteur Fzd4. Ce mécanisme novateur serait essentiel pour le développement vasculaire régulé par les voies Wnt : notamment la vascularisation du sac amniotique et de la rétine. Ce rôle clé de la protéine ouvre des perspectives intéressantes pour le traitement de pathologie ischémique. Activer la voie Wnt via PDZRN3 pourrait permettre de récupérer un réseau vasculaire fonctionnel plus rapidement. Cette protéine pourrait également être ciblée dans des pathologies tumorales où l'angiogenèse est suractivée. En effet, PDZRN3 est surexprimé dans certains cancers tels que le cancer du sein (Oncomine™).

Dans un second temps, nous proposons un modèle par lequel PDZRN3 régulerait la stabilité des jonctions serrées en induisant le décrochage de la protéine associée aux jonctions ZO1 par ubiquitination de la protéine d'échaffaudage MUPP1. Ce processus serait essentiel pour le maintien de l'intégrité de la barrière hématoencéphalique au cours du développement et dans un contexte ischémique. En effet, la surexpression de PDZRN3 induit une létalité embryonnaire et la délétion de PDZRN3 stabilise les jonctions des cellules endothéliales dans un modèle d'ischémie cérébrale. Ce rôle clé de la protéine ouvre des perspectives intéressantes pour le traitement des accidents vasculaires cérébraux (AVC). Ainsi, bloquer la voie Wnt via PDZRN3 pourrait réduire l'impact délétère de l'AVC sur les vaisseaux cérébraux en permettant une meilleure résistance à la montée de pression de la BHE.

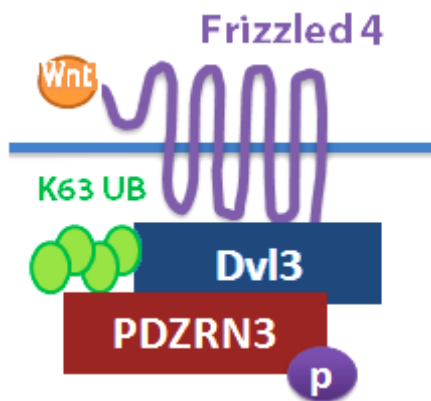
1) Proposed Model

This work identifies PDZRN3 as a novel regulator of Wnt signalling and tight junctions regulation. The protein was identified using a Yeast Two Hybrid screening using the adaptor protein Dvl3 as bait. We were able to confirm that Dvl3 was a substrate of PDZRN3 *in vitro* and *in vivo*, and that this interaction triggers induction of the c-Jun dependant Wnt pathway.

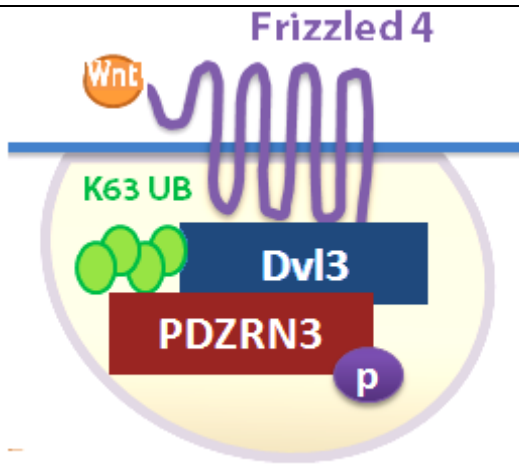
	<p>Our proposed model is that endogenously PDZRN3 is located in many subcellular compartments. It can interact with membrane proteins or vesicular proteins via its PDZ binding domain. When realizing immunostaining on cells culture, PDZRN3 was found in cytoplasmic puncta that were identified as Rab positive vesicles but also at the cytoplasmic membrane or the nucleus. This indicates that many pools of the protein exist, which might have different functions. Endogenous Dvl3 also form cytoplasmic puncta.</p>
	<p>When Fzd4 is tranfected, we were able to detect a massive relocation of Dvl3 and PDZRN3 to the cytoplasmic membrane. This suggests that Fzd4 is able to trigger cell signalling cues leading to the recruitment of both proteins to the membrane. Interestingly, a form of PDZRN3 deleted from its interaction domain with Dvl3 was not recruited to the membrane, indicating that the interaction between PDZRN3 and Dvl3 is a prerequisite for the relocation of PDZRN3.</p>



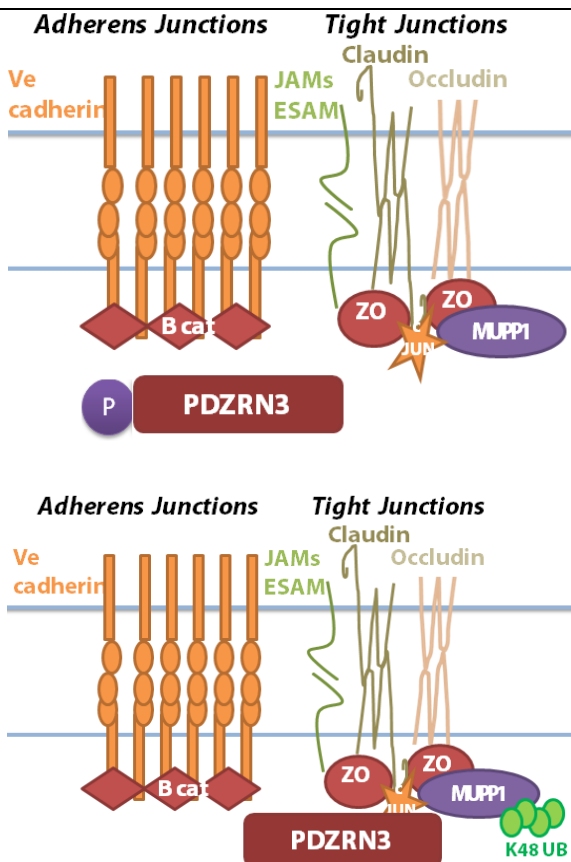
We were able to show that PDZRN3 was phosphorylated on a tyrosine residue close to its PDZ binding domain after Wnt activation. This process required the Tyrosine Kinase Ror2 as depletion of the protein blocked the phosphorylation. Ror2 is a correceptor of Fzd4 and was shown to be phosphorylated by CKI in a process depending on PKC- ζ when specific Wnt ligands bind the Fzd receptor. We were able to confirm this *in vitro* and *in vivo*. Our work identifies a cascade of phosphorylation induced by binding of Wnt to Frizzled: Ror2 is phosphorylated and would then phosphorylate PDZRN3.



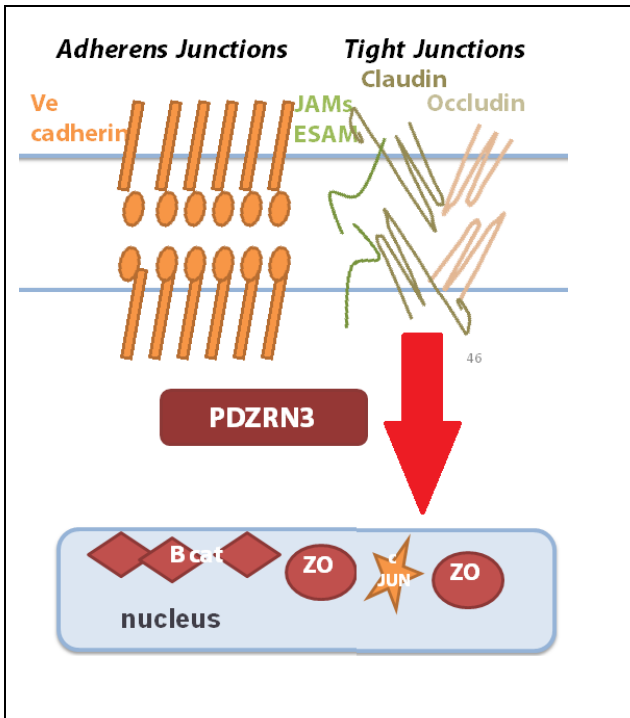
When cells are activated with Wnt ligands, we were also able to detect ubiquitinylation of the Dvl protein. The process required PDZRN3 as depletion of the protein blocked the ubiquitinylation. Ubiquitinylation can activate various intra-cellular mechanisms. We were able to identify that Dvl3 was ubiquitinated using Ubiquitin chains linked by lysine 63. This type of ubiquitinylation triggers recruitment of the cargo to endocytic vesicles.



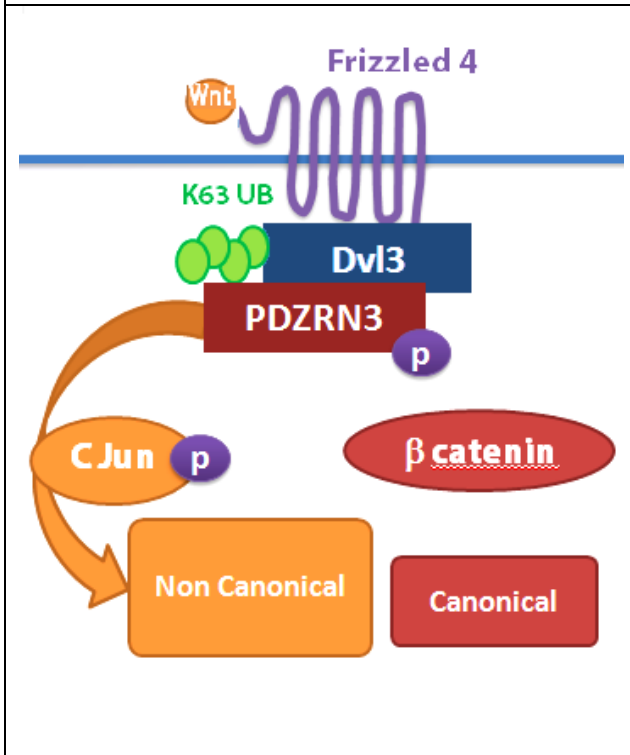
To confirm that the Fzd4/ Dvl complex was recruited to endocytic vesicles after Wnt activation, we used a strategy of immunostaining on Fzd4-transfected cells. Fzd4 was found at the membrane in control cells but was found in Rab- positive structures in Wnt activated cells. This indicates that Fzd4 is endocytosed via a clathrin/ rab dependant pathway after Wnt activation. Interestingly, depletion of Pdzn3 blocked the process of internalization of the receptor, suggesting that Pdzn3 is required for signal transduction after binding of Wnt ligands to Fzd receptors.



Interestingly, PDZRN3 was also found to interact with a protein associated to tight junctions MUPP1 when tyrosine - phosphorylated. MUPP1 was ubiquitinated after activation of cells with Wnt in a process that required PDZRN3. More specifically, PDZRN3 ubiquitinated MUPP1 with ubiquitin chains linked by Lysine 48, inducing the degradation of MUPP1 as demonstrated *in vitro*. This degradation induced dissociation of proteins segregated to the transmembrane components of the TJ such as ZO1 or c-Jun.



These proteins were then relocated to the nucleus where they would act as transcription factors to activate their respective target genes. We were able to demonstrate this relocation by cell fractionation. C Jun is activated in the nucleus and triggers target of Wnt non canonical pathway.



To confirm this hypothesis, we assessed if Wnt targets were modulated by depletion / overexpression of PDZRN3. PDZRN3 was shown to favour the non canonical – c Jun dependant pathway over the canonical – β-catenin pathway; as depletion of the protein blocked activation of c Jun and induced activation of β-catenin.

2) Prospects

a) Expression of PDZRN3 in pathologies

This work identifies PDZRN3 as a regulator of vital vessel functions. However, many points have to be resolved. Expression of PDZRN3 was found to be up-regulated in many cancers such as Carcinoma or Melanoma in a micro-array database, Oncomine (Fig 100). This is interesting as Wnt signalling has been shown to be upregulated in cancers. The link between PDZRN3 and transformation of normal cells into tumor cells would be an interesting topic, as this process also implicates translocation of ZO1 and c-JUN to the nucleus (Polette et al. 2007).

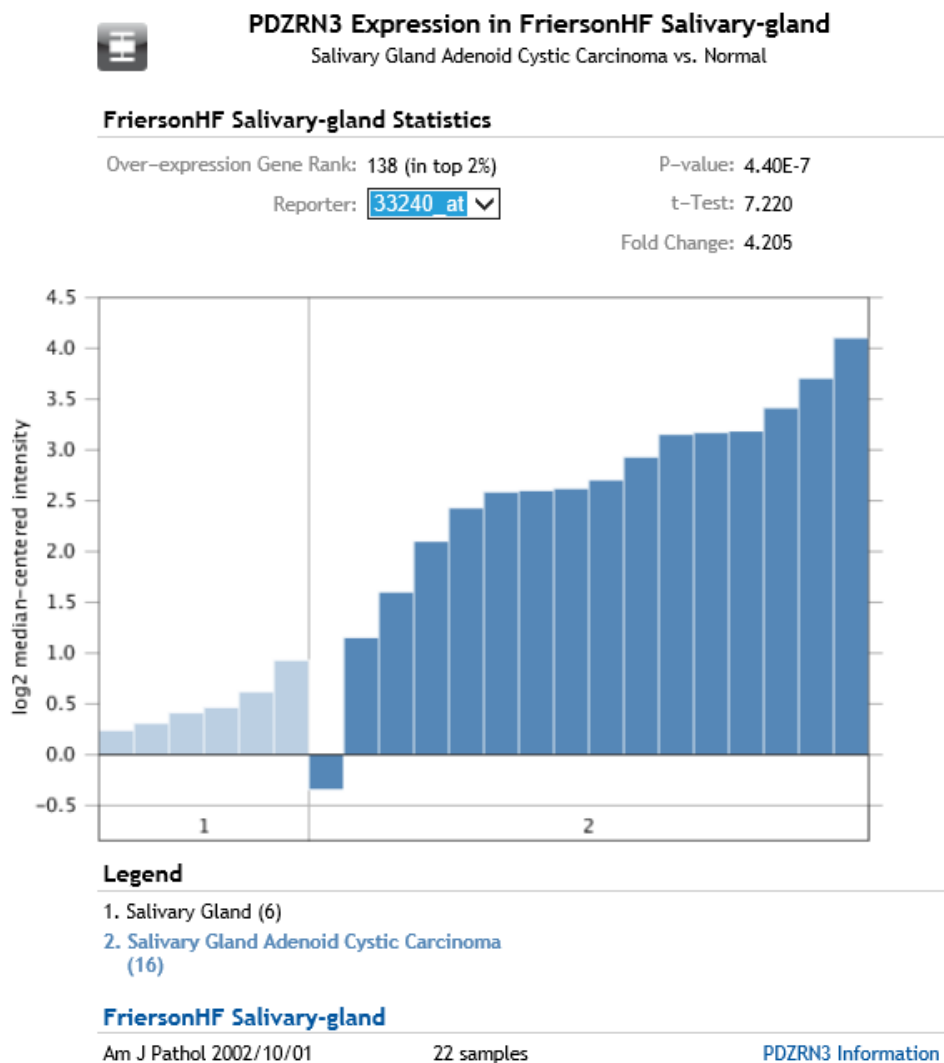


Figure 100: Expression of the Pdzn3 in Carcinoma (Oncomine)

Correlation of expression of PDZRN3 with other genes can be also be found in the database. Level of expression of PDZRN3 was found to correlate with levels of such as PDGFRA, ICAM, PECAM, VWF (Van Willebrand Factor) (Fig 101). These factors are linked to neo-angiogenesis, suggesting that upregulation of PDZRN3 in cancer cells could be linked to tumor angiogenesis.

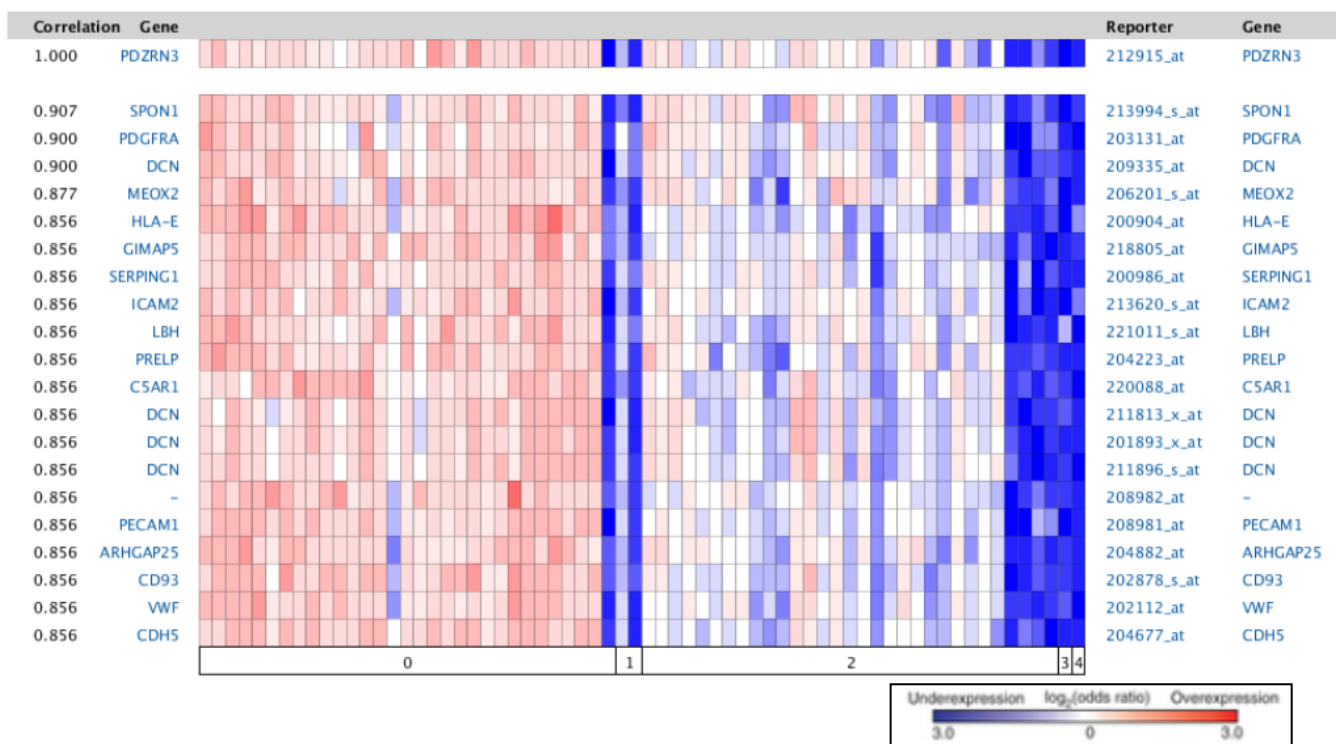


Figure 101: Correlation of expression of PDZRN3 with other genes in Carcinoma – inset represent the scaling colour (Oncomine)

It would also be interesting to look at the expression of PDZRN3 in other pathologies where vessel dysfunction can be observed such as Alzheimer/ Stroke or Parkinson.

b) Interaction of PDZRN3 with MUPP1

This work identifies PDZRN3 as a partner of the TJ associated protein MUPP1. MUPP1 has a dual function as it participates in the Crumbs complex. This complex regulates targeting of RhoA to the leading edge of migrating cells. It would be interesting to assess whether loss of PDZRN3 affects the activity of the Crumbs complex positively or negatively. It would also important to confirm the direct interaction between MUPP1 and PDZRN3 using another method such as precipitation of a HIS-tag protein using a Cobalt agarose resin column.

c) Phosphorylation status of PDZRN3

We were able to identify a phosphorylation site of PDZRN3. It would be interesting to see whether this phosphorylation modifies the 3D structure of the protein and accessibility of the PDZ binding domain, using crystallography. This would confirm that this phosphorylation is vital for activity of the protein. Similar approaches have been realized on PSD-95 and were highly successful (Fig 95) (Zhang et al. 2011). . It would also important to confirm the existence of the Tyrosine 972 - phosphorylation site of PDZRN3 using another method such as Mass Spectrometry.

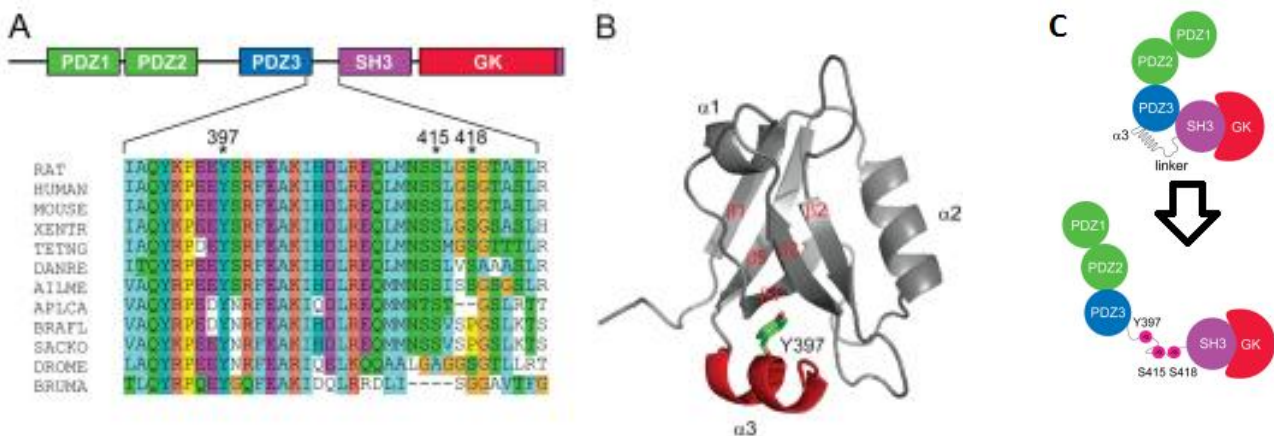


Figure 102: Phosphorylation of PSD-95 on Y397 makes access to the 3rd PDZ domain of PSD 95 possible (Zhang et al. 2011)

d) Chemical inhibition of PDZRN3

No chemical inhibitors of PDZRN3 (or other members of the family) were identified for the moment. A molecule that binds the PDZ domain of Dvl was identified (Grandy et al. 2009). It would be interesting to test this molecule in angiogenic assays to test whether it is able to modulate the properties of EC to understand whether PDZ scaffolding is important in Wnt signalling.

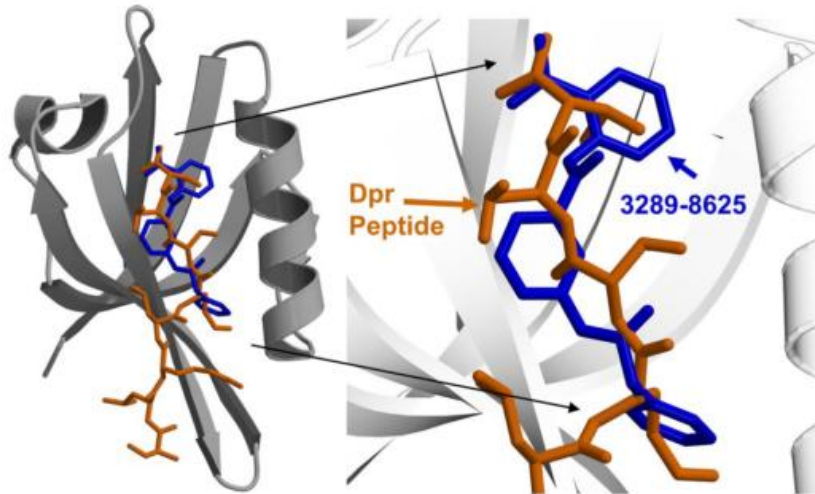


Figure 103: Interaction of compound 3289-8625 (blue) and Dpr peptide(brown) with the PDZ domain of Dvl (Grandy et al. 2009)

e) PDZRN3 in other tissues

PDZRN3 was first identified at the neuromuscular junction where it regulates integrity of the junction by ubiquitinating MUSK1. We were able to show that PDZRN3 was expressed in the endothelium in the brain/ retina/ yolk sac and placenta. Interestingly, PDZRN3 was also found to be expressed in the cardiomyocytes in the heart. As overexpression of Dvl1 induces a cardiac hypertrophy and dysfunction and ubiquitin signalling have been linked to similar pathologies, it would be interesting to test whether loss or over-expression of PDZRN3 would affect similar functions (Malekar et al. 2010, Powell et al. 2012).

BIBLIOGRAPHY

Avila-Flores, A., E. Rendon-Huerta, J. Moreno, S. Islas, A. Betanzos, M. Robles-Flores and L. Gonzalez-Mariscal (2001). "Tight-junction protein zonula occludens 2 is a target of phosphorylation by protein kinase C." *Biochem J* **360**(Pt 2): 295-304.

Badaut, J., S. Ashwal, A. Adami, B. Tone, R. Recker, D. Spagnoli, B. TERNON and A. Obenaus (2011). "Brain water mobility decreases after astrocytic aquaporin-4 inhibition using RNA interference." *J Cereb Blood Flow Metab* **31**(3): 819-831.

Balda, M. (2003). "Epithelial cell adhesion and the regulation of gene expression." *Trends in Cell Biology* **13**(6): 310-318.

Barandon, L., F. Casassus, L. Leroux, C. Moreau, C. Allieres, J. M. Lamaziere, P. Dufourcq, T. Couffignal and C. Duplaa (2011). "Secreted frizzled-related protein-1 improves postinfarction scar formation through a modulation of inflammatory response." *Arterioscler Thromb Vasc Biol* **31**(11): e80-87.

Barolo, S. (2006). "Transgenic Wnt/TCF pathway reporters: all you need is Lef?" *Oncogene* **25**(57): 7505-7511.

Bei Li., L. Z., Xiangling Yang, Tommy Andersson, Min Huang, Shao-Jun Tang (2011). "WNT5A Signaling Contributes to Ab-Induced Neuroinflammation and Neurotoxicity." *PLOS ONE*.

Berndt, J. D., A. Aoyagi, P. Yang, J. N. Anastas, L. Tang and R. T. Moon (2011). "Mindbomb 1, an E3 ubiquitin ligase, forms a complex with RYK to activate Wnt/beta-catenin signaling." *J Cell Biol* **194**(5): 737-750.

Betanzos, A., M. Huerta, E. Lopez-Bayghen, E. Azuara, J. Amerena and L. González-Mariscal (2004). "The tight junction protein ZO-2 associates with Jun, Fos and C/EBP transcription factors in epithelial cells." *Exp Cell Res* **292**(1): 51-66.

Bignon, M., C. Pichol-Thievend, J. Hardouin, M. Malbouyres, N. Brechot, L. Nasciutti, A. Barret, J. Teillon, E. Guillon, E. Etienne, M. Caron, R. Joubert-Caron, C. Monnot, F. Ruggiero, L. Muller and S. Germain (2011). "Lysyl oxidase-like protein-2 regulates sprouting angiogenesis and type IV collagen assembly in the endothelial basement membrane." *Blood* **118**(14): 3979-3989.

Bijur, G. N. and R. S. Jope (2001). "Proapoptotic stimuli induce nuclear accumulation of glycogen synthase kinase-3 beta." *J Biol Chem* **276**(40): 37436-37442.

Bilic, J., Y. L. Huang, G. Davidson, T. Zimmermann, C. M. Cruciat, M. Bienz and C. Niehrs (2007). "Wnt induces LRP6 signalosomes and promotes dishevelled-dependent LRP6 phosphorylation." *Science* **316**(5831): 1619-1622.

Biron, K. E., D. L. Dickstein, R. Gopaul and W. A. Jefferies (2011). "Amyloid triggers extensive cerebral angiogenesis causing blood brain barrier permeability and hypervascularity in Alzheimer's disease." *PLoS One* **6**(8): e23789.

Boulday, G., N. Rudini, L. Maddaluno, A. Blecon, M. Arnould, A. Gaudric, F. Chapon, R. H. Adams, E. Dejana and E. Tournier-Lasserre (2011). "Developmental timing of CCM2 loss influences cerebral cavernous malformations in mice." *J Exp Med* **208**(9): 1835-1847.

Bouleti, C., T. Mathivet, B. Coqueran, J. M. Serfaty, M. Lesage, E. Berland, C. Ardidie-Robouant, G. Kauffenstein, D. Henrion, B. Lapergue, M. Mazighi, C. Duyckaerts, G. Thurston, D. M. Valenzuela, A. J. Murphy, G. D. Yancopoulos, C. Monnot, I. Margail and S. Germain (2013). "Protective effects of angiopoietin-like 4 on cerebrovascular and functional damages in ischaemic stroke." *Eur Heart J* **34**(47): 3657-3668.

Bryja, V., G. Schulte, N. Rawal, A. Grahn and E. Arenas (2007). "Wnt-5a induces Dishevelled phosphorylation and dopaminergic differentiation via a CK1-dependent mechanism." *J Cell Sci* **120**(Pt 4): 586-595.

Cattelino, A., S. Liebner, R. Gallini, A. Zanetti, G. Balconi, A. Corsi, P. Bianco, H. Wolburg, R. Moore, B. Oreda, R. Kemler and E. Dejana (2003). "The conditional inactivation of the beta-catenin gene in endothelial cells causes a defective vascular pattern and increased vascular fragility." *J Cell Biol* **162**(6): 1111-1122.

Chan, D. W., C. Y. Chan, J. W. Yam, Y. P. Ching and I. O. Ng (2006). "Prickle-1 negatively regulates Wnt/beta-catenin pathway by promoting Dishevelled ubiquitination/degradation in liver cancer." *Gastroenterology* **131**(4): 1218-1227.

Chen, W., D. ten Berge, J. Brown, S. Ahn, L. A. Hu, W. E. Miller, M. G. Caron, L. S. Barak, R. Nusse and R. J. Lefkowitz (2003). "Dishevelled 2 recruits beta-arrestin 2 to mediate Wnt5A-stimulated endocytosis of Frizzled 4." *Science* **301**(5638): 1391-1394.

Cheng, X., T. L. Huber, V. C. Chen, P. Gadue and G. M. Keller (2008). "Numb mediates the interaction between Wnt and Notch to modulate primitive erythropoietic specification from the hemangioblast." *Development* **135**(20): 3447-3458.

Choi, H. (2011). "Minimally invasive molecular delivery into the brain using optical modulation of vascular permeability." *PNAS*.

Claxton, S., V. Kostourou, S. Jadeja, P. Chambon, K. Hodivala-Dilke and M. Fruttiger (2008). "Efficient, inducible Cre-recombinase activation in vascular endothelium." *Genesis* **46**(2): 74-80.

Descamps, B., R. Sewduth, N. Ferreira Tojais, B. Jaspard, A. Reynaud, F. Sohet, P. Lacolley, C. Allieres, J. M. Lamaziere, C. Moreau, P. Dufourcq, T. Couffinhal and C. Duplaa (2012). "Frizzled 4 regulates arterial network organization through noncanonical wnt/planar cell polarity signaling." *Circ Res* **110**(1): 47-58.

Djiane, A. and M. Mlodzik (2010). "The Drosophila GIPC homologue can modulate myosin based processes and planar cell polarity but is not essential for development." *PLoS One* **5**(6): e11228.

Dobrowolski, R. and E. M. De Robertis (2011). "Endocytic control of growth factor signalling: multivesicular bodies as signalling organelles." *Nat Rev Mol Cell Biol* **13**(1): 53-60.

Dufourcq, P., B. Descamps, N. F. Tojais, L. Leroux, P. Oses, D. Daret, C. Moreau, J. M. Lamaziere, T. Couffinhal and C. Duplaa (2008). "Secreted frizzled-related protein-1 enhances mesenchymal stem cell function in angiogenesis and contributes to neovessel maturation." *Stem Cells* **26**(11): 2991-3001.

Ernkvist, M., N. Luna Persson, S. Audebert, P. Lecine, I. Sinha, M. Liu, M. Schlueter, A. Horowitz, K. Aase, T. Weide, J. P. Borg, A. Majumdar and L. Holmgren (2009). "The Amot/Patj/Syx signaling complex spatially controls RhoA GTPase activity in migrating endothelial cells." *Blood* **113**(1): 244-253.

Ezan, J., L. Lasvaux, A. Gezer, A. Novakovic, H. May-Simera, E. Belotti, A. C. Lhoumeau, L. Birnbaumer, S. Beer-Hammer, J. P. Borg, A. Le Bivic, B. Nurnberg, N. Sans and M. Montcouquiol (2013). "Primary cilium migration depends on G-protein signalling control of subapical cytoskeleton." *Nat Cell Biol* **15**(9): 1107-1115.

Ezan, J., L. Leroux, L. Barandon, P. Dufourcq, B. Jaspard, C. Moreau, C. Allieres, D. Daret, T. Couffinhal and C. Duplaa (2004). "FrzA/sFRP-1, a secreted antagonist of the Wnt-Frizzled pathway, controls vascular cell proliferation in vitro and in vivo." *Cardiovasc Res* **63**(4): 731-738.

Fiedler, M., C. Mendoza-Topaz, T. J. Rutherford, J. Mieszczanek and M. Bienz (2011). "Dishevelled interacts with the DIX domain polymerization interface of Axin to interfere with its function in down-regulating beta-catenin." *Proc Natl Acad Sci U S A* **108**(5): 1937-1942.

Fishman-Jacob, T., L. Reznichenko, M. B. Youdim and S. A. Mandel (2009). "A sporadic Parkinson disease model via silencing of the ubiquitin-proteasome/E3 ligase component SKP1A." *J Biol Chem* **284**(47): 32835-32845.

Flynn, M., O. Saha and P. Young (2011). "Molecular evolution of the LNX gene family." *BMC Evol Biol* **11**: 235.

Ford, C. E., S. S. Qian Ma, A. Quadir and R. L. Ward (2013). "The dual role of the novel Wnt receptor tyrosine kinase, ROR2, in human carcinogenesis." *Int J Cancer* **133**(4): 779-787.

Fornai, F., O. M. Schluter, P. Lenzi, M. Gesi, R. Ruffoli, M. Ferrucci, G. Lazzeri, C. L. Busceti, F. Pontarelli, G. Battaglia, A. Pellegrini, F. Nicoletti, S. Ruggieri, A. Paparelli and T. C. Sudhof (2005). "Parkinson-like syndrome induced by continuous MPTP infusion: convergent roles of the ubiquitin-proteasome system and alpha-synuclein." *Proc Natl Acad Sci U S A* **102**(9): 3413-3418.

Franco, C. A., S. Liebner and H. Gerhardt (2009). "Vascular morphogenesis: a Wnt for every vessel?" *Curr Opin Genet Dev* **19**(5): 476-483.

Fruttiger, M. (2007). "Development of the retinal vasculature." *Angiogenesis* **10**(2): 77-88.

Funato, Y., T. Terabayashi, R. Sakamoto, D. Okuzaki, H. Ichise, H. Nojima, N. Yoshida and H. Miki (2010). "Nucleoredoxin sustains Wnt/beta-catenin signaling by retaining a pool of inactive dishevelled protein." *Curr Biol* **20**(21): 1945-1952.

Gagliardi, M., E. Piddini and J. P. Vincent (2008). "Endocytosis: a positive or a negative influence on Wnt signalling?" *Traffic* **9**(1): 1-9.

Gan, X. Q., J. Y. Wang, Y. Xi, Z. L. Wu, Y. P. Li and L. Li (2008). "Nuclear Dvl, c-Jun, beta-catenin, and TCF form a complex leading to stabilization of beta-catenin-TCF interaction." *J Cell Biol* **180**(6): 1087-1100.

Gao, C. and Y. G. Chen (2010). "Dishevelled: The hub of Wnt signaling." *Cell Signal* **22**(5): 717-727.

Gavard, J. and J. S. Gutkind (2008). "VE-cadherin and claudin-5: it takes two to tango." *Nat Cell Biol* **10**(8): 883-885.

Giese, A. P., J. Ezan, L. Wang, L. Lasvaux, F. Lembo, C. Mazzocco, E. Richard, J. Reboul, J. P. Borg, M. W. Kelley, N. Sans, J. Brigande and M. Montcouquiol (2012). "Gipc1 has a dual role in Vangl2 trafficking and hair bundle integrity in the inner ear." *Development* **139**(20): 3775-3785.

Gonzalez-Mariscal, L., A. Betanzos and A. Avila-Flores (2000). "MAGUK proteins: structure and role in the tight junction." *Semin Cell Dev Biol* **11**(4): 315-324.

Grandy, D., J. Shan, X. Zhang, S. Rao, S. Akunuru, H. Li, Y. Zhang, I. Alpatov, X. A. Zhang, R. A. Lang, D. L. Shi and J. J. Zheng (2009). "Discovery and characterization of a small molecule inhibitor of the PDZ domain of dishevelled." *J Biol Chem* **284**(24): 16256-16263.

Grant, B. D. and J. G. Donaldson (2009). "Pathways and mechanisms of endocytic recycling." *Nat Rev Mol Cell Biol* **10**(9): 597-608.

Grumolato, L., G. Liu, P. Mong, R. Mudbhary, R. Biswas, R. Arroyave, S. Vijayakumar, A. N. Economides and S. A. Aaronson (2010). "Canonical and noncanonical Wnts use a common mechanism to activate completely unrelated coreceptors." *Genes Dev* **24**(22): 2517-2530.

Hellstrom, M., L. K. Phng, J. J. Hofmann, E. Wallgard, L. Coultas, P. Lindblom, J. Alva, A. K. Nilsson, L. Karlsson, N. Gaiano, K. Yoon, J. Rossant, M. L. Iruela-Arispe, M. Kalen, H. Gerhardt and C. Betsholtz (2007). "Dll4 signalling through Notch1 regulates formation of tip cells during angiogenesis." *Nature* **445**(7129): 776-780.

Herbert, S. P. and D. Y. Stainier (2011). "Molecular control of endothelial cell behaviour during blood vessel morphogenesis." *Nat Rev Mol Cell Biol* **12**(9): 551-564.

Hoffmann, A., J. Bredno, M. Wendland, N. Derugin, P. Ohara and M. Wintermark (2011). "High and Low Molecular Weight Fluorescein Isothiocyanate (FITC)-Dextrans to Assess Blood-Brain Barrier Disruption: Technical Considerations." *Transl Stroke Res* **2**(1): 106-111.

Honda, T., H. Yamamoto, A. Ishii and M. Inui (2010). "PDZRN3 negatively regulates BMP-2-induced osteoblast differentiation through inhibition of Wnt signaling." *Mol Biol Cell* **21**(18): 3269-3277.

Jaramillo, B. E., A. Ponce, J. Moreno, A. Betanzos, M. Huerta, E. Lopez-Bayghen and L. Gonzalez-Mariscal (2004). "Characterization of the tight junction protein ZO-2 localized at the nucleus of epithelial cells." *Exp Cell Res* **297**(1): 247-258.

Ji-Ae Ko, Y. K., Kenji Matsuura, Hisato Yamamoto, Toshikazu Gondo and Makoto Inui, (2006). "PDZRN3 (LNX3, SEMCAP3) is required for the differentiation of C2C12 myoblasts into myotube." *Journal of Cell Science*.

Jibin Zhou, T. A. F., 2 Firdos Ahmad,1 Xiyang Shang,1 Emily Mangano,3 Erhe Gao,1 John Farber,4 Yajing Wang,5 Xin-Liang Ma,5 James Woodgett,6 Ronald J. Vagnozzi,1,4 Hind Lal,1 and Thomas Force1 (2005). "GSK-3 α is a central regulator of age-related pathologies in mice." *The Journal of Clinical Investigation*.

Ju, R., P. Cirone, S. Lin, H. Griesbach, D. C. Slusarski and C. M. Crews (2010). "Activation of the planar cell polarity formin DAAM1 leads to inhibition of endothelial cell proliferation, migration, and angiogenesis." *Proc Natl Acad Sci U S A* **107**(15): 6906-6911.

Kani, S., I. Oishi, H. Yamamoto, A. Yoda, H. Suzuki, A. Nomachi, K. Iozumi, M. Nishita, A. Kikuchi, T. Takumi and Y. Minami (2004). "The receptor tyrosine kinase Ror2 associates with and is activated by casein kinase Iepsilon." *J Biol Chem* **279**(48): 50102-50109.

Kansaku, A., S. Hirabayashi, H. Mori, N. Fujiwara, A. Kawata, M. Ikeda, C. Rokukawa, H. Kurihara and Y. Hata (2006). "Ligand-of-Numb protein X is an endocytic scaffold for junctional adhesion molecule 4." *Oncogene* **25**(37): 5071-5084.

Kelly, J. C., P. Lungchukiet and R. J. Macleod (2011). "Extracellular Calcium-Sensing Receptor Inhibition of Intestinal Epithelial TNF Signaling Requires CaSR-Mediated Wnt5a/Ror2 Interaction." *Front Physiol* **2**: 17.

Kemp, C. R., E. Willems, D. Wawrzak, M. Hendrickx, T. Agbor Agbor and L. Leyns (2007). "Expression of Frizzled5, Frizzled7, and Frizzled10 during early mouse development and interactions with canonical Wnt signaling." *Dev Dyn* **236**(7): 2011-2019.

Kim, K. I., H. J. Cho, J. Y. Hahn, T. Y. Kim, K. W. Park, B. K. Koo, C. S. Shin, C. H. Kim, B. H. Oh, M. M. Lee, Y. B. Park and H. S. Kim (2006). "Beta-catenin overexpression augments angiogenesis and skeletal muscle regeneration through dual mechanism of vascular endothelial growth factor-mediated endothelial cell proliferation and progenitor cell mobilization." *Arterioscler Thromb Vasc Biol* **26**(1): 91-98.

Kimelman, D. and W. Xu (2006). "beta-catenin destruction complex: insights and questions from a structural perspective." *Oncogene* **25**(57): 7482-7491.

Kitazawa, M., D. Cheng, M. R. Tsukamoto, M. A. Koike, P. D. Wes, V. Vasilevko, D. H. Cribbs and F. M. LaFerla (2011). "Blocking IL-1 signaling rescues cognition, attenuates tau pathology, and restores neuronal beta-catenin pathway function in an Alzheimer's disease model." *J Immunol* **187**(12): 6539-6549.

Kortekaas, R., K. L. Leenders, J. C. van Oostrom, W. Vaalburg, J. Bart, A. T. Willemsen and N. H. Hendrikse (2005). "Blood-brain barrier dysfunction in parkinsonian midbrain in vivo." *Ann Neurol* **57**(2): 176-179.

Lanaspa, M. A., N. E. Almeida, A. Andres-Hernando, C. J. Rivard, J. M. Capasso and T. Berl (2007). "The tight junction protein, MUPP1, is up-regulated by hypertonicity and is important in the osmotic stress response in kidney cells." *Proc Natl Acad Sci U S A* **104**(34): 13672-13677.

Larrivee, B., C. Freitas, M. Trombe, X. Lv, B. Delafarge, L. Yuan, K. Bouvree, C. Breant, R. Del Toro, N. Brechet, S. Germain, F. Bono, F. Dol, F. Claes, C. Fischer, M. Autiero, J. L. Thomas, P. Carmeliet, M. Tessier-Lavigne and A. Eichmann (2007). "Activation of the UNC5B receptor by Netrin-1 inhibits sprouting angiogenesis." *Genes Dev* **21**(19): 2433-2447.

Leroux, L., B. Descamps, N. F. Tojais, B. Seguy, P. Oses, C. Moreau, D. Daret, Z. Ivanovic, J. M. Boiron, J. M. Lamaziere, P. Dufourcq, T. Couffinhal and C. Duplaa (2010). "Hypoxia preconditioned mesenchymal stem cells

improve vascular and skeletal muscle fiber regeneration after ischemia through a Wnt4-dependent pathway." *Mol Ther* **18**(8): 1545-1552.

Leyns, L., T. Bouwmeester, S. H. Kim, S. Piccolo and E. M. De Robertis (1997). "Frzb-1 is a secreted antagonist of Wnt signaling expressed in the Spemann organizer." *Cell* **88**(6): 747-756.

Li, Y., S. Schrodi, C. Rowland, K. Tacey, J. Catanese and A. Grupe (2006). "Genetic evidence for ubiquitin-specific proteases USP24 and USP40 as candidate genes for late-onset Parkinson disease." *Hum Mutat* **27**(10): 1017-1023.

Liebner, S., M. Corada, T. Bangsow, J. Babbage, A. Taddei, C. J. Czapalla, M. Reis, A. Felici, H. Wolburg, M. Fruttiger, M. M. Taketo, H. von Melchner, K. H. Plate, H. Gerhardt and E. Dejana (2008). "Wnt/beta-catenin signaling controls development of the blood-brain barrier." *J Cell Biol* **183**(3): 409-417.

Liu, Y., B. Rubin, P. V. Bodine and J. Billiard (2008). "Wnt5a induces homodimerization and activation of Ror2 receptor tyrosine kinase." *J Cell Biochem* **105**(2): 497-502.

Liu, Z. J., T. Shirakawa, Y. Li, A. Soma, M. Oka, G. P. Dotto, R. M. Fairman, O. C. Velazquez and M. Herlyn (2003). "Regulation of Notch1 and Dll4 by Vascular Endothelial Growth Factor in Arterial Endothelial Cells: Implications for Modulating Arteriogenesis and Angiogenesis." *Mol Cell Biol* **23**(1): 14-25.

Lu, W., V. Yamamoto, B. Ortega and D. Baltimore (2004). "Mammalian Ryk is a Wnt coreceptor required for stimulation of neurite outgrowth." *Cell* **119**(1): 97-108.

Lu, Z., H. S. Je, P. Young, J. Gross, B. Lu and G. Feng (2007). "Regulation of synaptic growth and maturation by a synapse-associated E3 ubiquitin ligase at the neuromuscular junction." *J Cell Biol* **177**(6): 1077-1089.

Malekar, P., M. Hagenmueller, A. Anyanwu, S. Buss, M. R. Streit, C. S. Weiss, D. Wolf, J. Riffel, A. Bauer, H. A. Katus and S. E. Hardt (2010). "Wnt signaling is critical for maladaptive cardiac hypertrophy and accelerates myocardial remodeling." *Hypertension* **55**(4): 939-945.

Marchesi, V. T. (2011). "Alzheimer's dementia begins as a disease of small blood vessels, damaged by oxidative-induced inflammation and dysregulated amyloid metabolism: implications for early detection and therapy." *FASEB J* **25**(1): 5-13.

McColl, B. W., N. J. Rothwell and S. M. Allan (2008). "Systemic inflammation alters the kinetics of cerebrovascular tight junction disruption after experimental stroke in mice." *J Neurosci* **28**(38): 9451-9462.

Meray, R. K. and P. T. Lansbury, Jr. (2007). "Reversible monoubiquitination regulates the Parkinson disease-associated ubiquitin hydrolase UCH-L1." *J Biol Chem* **282**(14): 10567-10575.

Mikels, A., Y. Minami and R. Nusse (2009). "Ror2 receptor requires tyrosine kinase activity to mediate Wnt5A signaling." *J Biol Chem* **284**(44): 30167-30176.

Mikels, A. J. and R. Nusse (2006). "Purified Wnt5a protein activates or inhibits beta-catenin-TCF signaling depending on receptor context." *PLoS Biol* **4**(4): e115.

Montcouquiol, M., N. Sans, D. Huss, J. Kach, J. D. Dickman, A. Forge, R. A. Rachel, N. G. Copeland, N. A. Jenkins, D. Bogani, J. Murdoch, M. E. Warchol, R. J. Wenthold and M. W. Kelley (2006). "Asymmetric localization of Vangl2 and Fz3 indicate novel mechanisms for planar cell polarity in mammals." *J Neurosci* **26**(19): 5265-5275.

Mukai, A., M. Yamamoto-Hino, W. Awano, W. Watanabe, M. Komada and S. Goto (2010). "Balanced ubiquitylation and deubiquitylation of Frizzled regulate cellular responsiveness to Wg/Wnt." *EMBO J* **29**(13): 2114-2125.

Nassia Methia, P. A., Ali Hafezi-Moghadam, Maria Economopoulos, Kennard L. Thomas, and Denisa D. Wagner (2001). "ApoE Deficiency Compromises the Blood Brain Barrier Especially After Injury." *Molecular Medicine* **7**(12): 810-815.

Ngok, S. P., R. Geyer, M. Liu, A. Kourtidis, S. Agrawal, C. Wu, H. R. Seerapu, L. J. Lewis-Tuffin, K. L. Moodie, D. Huvelde, R. Marx, J. M. Baraban, P. Storz, A. Horowitz and P. Z. Anastasiadis (2012). "VEGF and Angiopoietin-1 exert opposing effects on cell junctions by regulating the Rho GEF Syx." *J Cell Biol* **199**(7): 1103-1115.

Nie, J., S. S. Li and C. J. McGlade (2004). "A novel PTB-PDZ domain interaction mediates isoform-specific ubiquitylation of mammalian Numb." *J Biol Chem* **279**(20): 20807-20815.

Nie, M., S. Aijaz, I. V. Leefa Chong San, M. S. Balda and K. Matter (2009). "The Y-box factor ZONAB/DbpA associates with GEF-H1/Lfc and mediates Rho-stimulated transcription." *EMBO Rep* **10**(10): 1125-1131.

Nikopoulos, K., H. Venselaar, R. W. Collin, R. Riveiro-Alvarez, F. N. Boonstra, J. M. Hoymans, A. Mukhopadhyay, D. Shears, M. van Bers, I. J. de Wijs, A. J. van Essen, R. H. Sijmons, M. A. Tilanus, C. E. van Nouhuys, C. Ayuso, L. H. Hoefsloot and F. P. Cremers (2010). "Overview of the mutation spectrum in familial exudative vitreoretinopathy and Norrie disease with identification of 21 novel variants in FZD4, LRP5, and NDP." *Hum Mutat* **31**(6): 656-666.

Nomachi, A., M. Nishita, D. Inaba, M. Enomoto, M. Hamasaki and Y. Minami (2008). "Receptor tyrosine kinase Ror2 mediates Wnt5a-induced polarized cell migration by activating c-Jun N-terminal kinase via actin-binding protein filamin A." *J Biol Chem* **283**(41): 27973-27981.

Ohkawara, B., A. Glinka and C. Niehrs (2011). "Rspo3 binds syndecan 4 and induces Wnt/PCP signaling via clathrin-mediated endocytosis to promote morphogenesis." *Dev Cell* **20**(3): 303-314.

Oses, P., M. A. Renault, R. Chauvel, L. Leroux, C. Allieres, B. Seguy, J. M. Lamaziere, P. Dufourcq, T. Couffignal and C. Duplaa (2009). "Mapping 3-dimensional neovessel organization steps using micro-computed tomography in a murine model of hindlimb ischemia-brief report." *Arterioscler Thromb Vasc Biol* **29**(12): 2090-2092.

Paes, K. T., E. Wang, K. Henze, P. Vogel, R. Read, A. Suwanichkul, L. L. Kirkpatrick, D. Potter, M. M. Newhouse and D. S. Rice (2011). "Frizzled 4 is required for retinal angiogenesis and maintenance of the blood-retina barrier." *Invest Ophthalmol Vis Sci* **52**(9): 6452-6461.

Paolinelli, R., M. Corada, F. Orsenigo and E. Dejana (2011). "The molecular basis of the blood brain barrier differentiation and maintenance. Is it still a mystery?" *Pharmacol Res* **63**(3): 165-171.

Polakis, P. (2008). "Formation of the blood-brain barrier: Wnt signaling seals the deal." *J Cell Biol* **183**(3): 371-373.

Polette, M., C. Gilles, B. Nawrocki-Raby, J. Lohi, W. Hunziker, J. M. Foidart and P. Birembaut (2005). "Membrane-type 1 matrix metalloproteinase expression is regulated by zonula occludens-1 in human breast cancer cells." *Cancer Res* **65**(17): 7691-7698.

Polette, M., M. Mestdagt, S. Bindels, B. Nawrocki-Raby, W. Hunziker, J. M. Foidart, P. Birembaut and C. Gilles (2007). "Beta-catenin and ZO-1: shuttle molecules involved in tumor invasion-associated epithelial-mesenchymal transition processes." *Cells Tissues Organs* **185**(1-3): 61-65.

Powell, S. R., J. Herrmann, A. Lerman, C. Patterson and X. Wang (2012). "The ubiquitin-proteasome system and cardiovascular disease." *Prog Mol Biol Transl Sci* **109**: 295-346.

Pozzi, A. and R. Zent (2010). "ZO-1 and ZONAB interact to regulate proximal tubular cell differentiation." *J Am Soc Nephrol* **21**(3): 388-390.

R.Hutton. (2010). "Role of blood brain barrier in parkinson's disease."

Rajasekaran, A. K., M. Hojo, T. Huima and E. Rodriguez-Boulan (1996). "Catenins and zonula occludens-1 form a complex during early stages in the assembly of tight junctions." *J Cell Biol* **132**(3): 451-463.

Rebagay, G., S. Yan, C. Liu and N. K. Cheung (2012). "ROR1 and ROR2 in Human Malignancies: Potentials for Targeted Therapy." *Front Oncol* **2**: 34.

Reis, M., C. J. Czupalla, N. Ziegler, K. Devraj, J. Zinke, S. Seidel, R. Heck, S. Thom, J. Macas, E. Bockamp, M. Fruttiger, M. M. Taketo, S. Dimmeler, K. H. Plate and S. Liebner (2012). "Endothelial Wnt/beta-catenin signaling inhibits glioma angiogenesis and normalizes tumor blood vessels by inducing PDGF-B expression." *J Exp Med* **209**(9): 1611-1627.

Reis, M. and S. Liebner (2013). "Wnt signaling in the vasculature." *Exp Cell Res* **319**(9): 1317-1323.

Rite, I., A. Machado, J. Cano and J. L. Venero (2007). "Blood-brain barrier disruption induces in vivo degeneration of nigral dopaminergic neurons." *J Neurochem* **101**(6): 1567-1582.

RN, Kalaria. (2002). "Small vessel disease and alzheimer's dementia: Pathological consideration." *Cerebrovascular disease* **13**: 48-52.

Robitaille, J., M. L. MacDonald, A. Kaykas, L. C. Sheldahl, J. Zeisler, M. P. Dube, L. H. Zhang, R. R. Singaraja, D. L. Guernsey, B. Zheng, L. F. Siebert, A. Hoskin-Mott, M. T. Trese, S. N. Pimstone, B. S. Shastry, R. T. Moon, M. R. Hayden, Y. P. Goldberg and M. E. Samuels (2002). "Mutant frizzled-4 disrupts retinal angiogenesis in familial exudative vitreoretinopathy." *Nat Genet* **32**(2): 326-330.

Robitaille, J. M., B. Zheng, K. Wallace, M. J. Beis, C. Tatlidil, J. Yang, T. G. Sheidow, L. Siebert, A. V. Levin, W. C. Lam, B. W. Arthur, C. J. Lyons, E. Jaakkola, E. Tsilou, C. A. Williams, R. G. Weaver, Jr., C. L. Shields and D. L. Guernsey (2011). "The role of Frizzled-4 mutations in familial exudative vitreoretinopathy and Coats disease." *Br J Ophthalmol* **95**(4): 574-579.

Saadeddin, A., R. Babaei-Jadidi, B. Spencer-Dene and A. S. Nateri (2009). "The links between transcription, beta-catenin/JNK signaling, and carcinogenesis." *Mol Cancer Res* **7**(8): 1189-1196.

Saadi-Kheddouci, S., D. Berrebi, B. Romagnolo, F. Cluzeaud, M. Peuchmaur, A. Kahn, A. Vandewalle and C. Perret (2001). "Early development of polycystic kidney disease in transgenic mice expressing an activated mutant of the beta-catenin gene." *Oncogene* **20**(42): 5972-5981.

Sadowski, L., I. Pilecka and M. Miaczynska (2009). "Signaling from endosomes: location makes a difference." *Exp Cell Res* **315**(9): 1601-1609.

Sandoval, K. E. and K. A. Witt (2008). "Blood-brain barrier tight junction permeability and ischemic stroke." *Neurobiol Dis* **32**(2): 200-219.

Schorpp-Kistner, W., Angel, Wagner (1999). "JunB is essential for mammalian placentation." *EMBO J* **18**(4): 934-948.

Schreiber, W., Jochum, Fetka, Elliott, Wagner (2000). "Placental vascularisation requires the AP-1 component Fra1." *Development* **127**: 4937-4948.

Schulte, G., A. S. , a. Vite and Zslav Bryja3 (2010). "b-arrestins – scaffolds and signalling elements essential for WNT/Frizzled signalling pathways?" *British Journal of Pharmacology* (159): 1051–1058.

Schulte, G. (2010). "International Union of Basic and Clinical Pharmacology. LXXX. The class Frizzled receptors." *Pharmacol Rev* **62**(4): 632-667.

Schulte, G., A. Schambony and V. Bryja (2010). "beta-Arrestins - scaffolds and signalling elements essential for WNT/Frizzled signalling pathways?" *Br J Pharmacol* **159**(5): 1051-1058.

Schulte, G. and S. K. Shenoy (2011). "beta-Arrestin and dishevelled coordinate biased signaling." *Proc Natl Acad Sci U S A* **108**(50): 19839-19840.

Shimura, H., N. Hattori, S. Kubo, Y. Mizuno, S. Asakawa, S. Minoshima, N. Shimizu, K. Iwai, T. Chiba, K. Tanaka and T. Suzuki (2000). "Familial Parkinson disease gene product, parkin, is a ubiquitin-protein ligase." *Nat Genet* **25**(3): 302-305.

Simons, M. and G. Walz (2006). "Polycystic kidney disease: cell division without a clue?" *Kidney Int* **70**(5): 854-864.

Smadja, D. M., C. d'Audigier, L. B. Weiswald, C. Badoual, V. Dangles-Marie, L. Mauge, S. Evrard, I. Laurendeau, F. Lallemand, S. Germain, F. Grelac, B. Dizier, M. Vidaud, I. Bieche and P. Gaussem (2010). "The Wnt antagonist Dickkopf-1 increases endothelial progenitor cell angiogenic potential." *Arterioscler Thromb Vasc Biol* **30**(12): 2544-2552.

Stefater, J. A., 3rd, I. Lewkowich, S. Rao, G. Mariggi, A. C. Carpenter, A. R. Burr, J. Fan, R. Ajima, J. D. Molkentin, B. O. Williams, M. Wills-Karp, J. W. Pollard, T. Yamaguchi, N. Ferrara, H. Gerhardt and R. A. Lang (2011). "Regulation of angiogenesis by a non-canonical Wnt-Flt1 pathway in myeloid cells." *Nature* **474**(7352): 511-515.

Tauriello, D. V., A. Haegebarth, I. Kuper, M. J. Edelmann, M. Henraat, M. R. Canninga-van Dijk, B. M. Kessler, H. Clevers and M. M. Maurice (2010). "Loss of the tumor suppressor CYLD enhances Wnt/beta-catenin signaling through K63-linked ubiquitination of Dvl." *Mol Cell* **37**(5): 607-619.

Then, C., T. Bergler, R. Jeblick, B. Jung, B. Banas and B. K. Kramer (2011). "Hypertonic stress promotes the upregulation and phosphorylation of zonula occludens 1." *Nephron Physiol* **119**(2): p11-21.

Tian-Qiang Sun, B. L., Jia-Jia Feng, Christoph Reinhard, Yuh Nung Jan, Wendy J. Fantl and L. T. Williams (2001). "PAR-1 is a Dishevelled-associated kinase and a positive regulator of Wnt signalling." *Nature cell biology*.

Tirziu, D. and M. Simons (2005). "Angiogenesis in the human heart: gene and cell therapy." *Angiogenesis* **8**(3): 241-251.

Tomo-o Ishikawa, Y. T., Aaron M. Zorn, Hisahiro Yoshida, Michael F. Seldin, and M. M. T. Shin-ichi Nishikawa (2001). "Mouse Wnt receptor gene Fzd4 is required for yolk sac angiogenesis." *Development* **128**(5).

Toomes, C., H. M. Bottomley, R. M. Jackson, K. V. Towns, S. Scott, D. A. Mackey, J. E. Craig, L. Jiang, Z. Yang, R. Trembath, G. Woodruff, C. Y. Gregory-Evans, K. Gregory-Evans, M. J. Parker, G. C. Black, L. M. Downey, K. Zhang and C. F. Inglehearn (2004). "Mutations in LRP5 or FZD4 underlie the common familial exudative vitreoretinopathy locus on chromosome 11q." *Am J Hum Genet* **74**(4): 721-730.

Topol, L., X. Jiang, H. Choi, L. Garrett-Beal, P. J. Carolan and Y. Yang (2003). "Wnt-5a inhibits the canonical Wnt pathway by promoting GSK-3-independent beta-catenin degradation." *J Cell Biol* **162**(5): 899-908.

Tsuji, T., Y. Ohta, Y. Kanno, K. Hirose, K. Ohashi and K. Mizuno (2010). "Involvement of p114-RhoGEF and Lfc in Wnt-3a- and dishevelled-induced RhoA activation and neurite retraction in N1E-115 mouse neuroblastoma cells." *Mol Biol Cell* **21**(20): 3590-3600.

Tung, J. J., I. W. Tattersall and J. Kitajewski (2012). "Tips, stalks, tubes: notch-mediated cell fate determination and mechanisms of tubulogenesis during angiogenesis." *Cold Spring Harb Perspect Med* **2**(2): a006601.

Ullrich, C., R. Mlekusch, A. Kuschig, J. Marksteiner and C. Humpel (2010). "Ubiquitin enzymes, ubiquitin and proteasome activity in blood mononuclear cells of MCI, Alzheimer and Parkinson patients." *Curr Alzheimer Res* **7**(6): 549-555.

Valiente, M., A. Andres-Pons, B. Gomar, J. Torres, A. Gil, C. Tapparel, S. E. Antonarakis and R. Pulido (2005). "Binding of PTEN to specific PDZ domains contributes to PTEN protein stability and phosphorylation by microtubule-associated serine/threonine kinases." *J Biol Chem* **280**(32): 28936-28943.

van Amerongen, R. and R. Nusse (2009). "Towards an integrated view of Wnt signaling in development." *Development* **136**(19): 3205-3214.

Verkaar, F., A. A. van der Doelen, J. F. Smits, W. M. Blankesteyn and G. J. Zaman (2011). "Inhibition of Wnt/beta-catenin signaling by p38 MAP kinase inhibitors is explained by cross-reactivity with casein kinase Idelta/varepsilon." *Chem Biol* **18**(4): 485-494.

Wang, C. Y., W. Zheng, T. Wang, J. W. Xie, S. L. Wang, B. L. Zhao, W. P. Teng and Z. Y. Wang (2011). "Huperzine A activates Wnt/beta-catenin signaling and enhances the nonamyloidogenic pathway in an Alzheimer transgenic mouse model." *Neuropsychopharmacology* **36**(5): 1073-1089.

Wang, L. H., R. G. Kalb and S. M. Strittmatter (1999). "A PDZ protein regulates the distribution of the transmembrane semaphorin, M-SemF." *J Biol Chem* **274**(20): 14137-14146.

Wang, Y., N. Guo and J. Nathans (2006). "The role of Frizzled3 and Frizzled6 in neural tube closure and in the planar polarity of inner-ear sensory hair cells." *J Neurosci* **26**(8): 2147-2156.

Wang, Y., D. Huso, H. Cahill, D. Ryugo and J. Nathans (2001). "Progressive cerebellar, auditory, and esophageal dysfunction caused by targeted disruption of the frizzled-4 gene." *J Neurosci* **21**(13): 4761-4771.

Wang, Y., A. Rattner, Y. Zhou, J. Williams, P. M. Smallwood and J. Nathans (2012). "Norrin/Frizzled4 signaling in retinal vascular development and blood brain barrier plasticity." *Cell* **151**(6): 1332-1344.

Wang, Y., J. Tong, D. Zou, B. Chang, B. Wang and B. Wang (2013). "Elevated expression of forkhead box protein O1 (FoxO1) in alcohol-induced intestinal barrier dysfunction." *Acta Histochem*.

Wong, C. K., W. Luo, Y. Deng, H. Zou, Z. Ye and S. C. Lin (2004). "The DIX domain protein coiled-coil-DIX1 inhibits c-Jun N-terminal kinase activation by Axin and dishevelled through distinct mechanisms." *J Biol Chem* **279**(38): 39366-39373.

Wong, T., K. K. Matthay, W. J. Boscardin, R. A. Hawkins, P. R. Brakeman and S. G. DuBois (2013). "Acute changes in blood pressure in patients with neuroblastoma treated with (1)(3)(1)I-metaiodobenzylguanidine (MIBG)." *Pediatr Blood Cancer* **60**(9): 1424-1430.

Wu, C., S. Agrawal, A. Vasanji, J. Drazba, S. Sarkaria, J. Xie, C. M. Welch, M. Liu, B. Anand-Apte and A. Horowitz (2011). "Rab13-dependent trafficking of RhoA is required for directional migration and angiogenesis." *J Biol Chem* **286**(26): 23511-23520.

Xia, Y.-R., Gong (2010). "LRP5 Is Required for Vascular Development in Deeper Layers of the Retina." *PLoS One* **5**(7).

Xu, Q., Y. Wang, A. Dabdoub, P. M. Smallwood, J. Williams, C. Woods, M. W. Kelley, L. Jiang, W. Tasman, K. Zhang and J. Nathans (2004). "Vascular development in the retina and inner ear: control by Norrin and Frizzled-4, a high-affinity ligand-receptor pair." *Cell* **116**(6): 883-895.

Yamamoto, H., H. Sakane, T. Michiue and A. Kikuchi (2008). "Wnt3a and Dkk1 regulate distinct internalization pathways of LRP6 to tune the activation of beta-catenin signaling." *Dev Cell* **15**(1): 37-48.

Yamamoto, H., S. K. Yoo, M. Nishita, A. Kikuchi and Y. Minami (2007). "Wnt5a modulates glycogen synthase kinase 3 to induce phosphorylation of receptor tyrosine kinase Ror2." *Genes Cells* **12**(11): 1215-1223.

Ye, X., Y. Wang and J. Nathans (2010). "The Norrin/Frizzled4 signaling pathway in retinal vascular development and disease." *Trends Mol Med* **16**(9): 417-425.

Youdim, M. B., T. Amit, M. Falach-Yogev, O. Bar Am, W. Maruyama and M. Naoi (2003). "The essentiality of Bcl-2, PKC and proteasome-ubiquitin complex activations in the neuroprotective-antiapoptotic action of the anti-Parkinson drug, rasagiline." *Biochem Pharmacol* **66**(8): 1635-1641.

Yu, A., J. F. Rual, K. Tamai, Y. Harada, M. Vidal, X. He and T. Kirchhausen (2007). "Association of Dishevelled with the clathrin AP-2 adaptor is required for Frizzled endocytosis and planar cell polarity signaling." *Dev Cell* **12**(1): 129-141.

Zeng, X., H. Huang, K. Tamai, X. Zhang, Y. Harada, C. Yokota, K. Almeida, J. Wang, B. Doble, J. Woodgett, A. Wynshaw-Boris, J. C. Hsieh and X. He (2008). "Initiation of Wnt signaling: control of Wnt coreceptor Lrp6 phosphorylation/activation via frizzled, dishevelled and axin functions." *Development* **135**(2): 367-375.

Zhang, J., C. M. Petit, D. S. King and A. L. Lee (2011). "Phosphorylation of a PDZ domain extension modulates binding affinity and interdomain interactions in postsynaptic density-95 (PSD-95) protein, a membrane-associated guanylate kinase (MAGUK)." *J Biol Chem* **286**(48): 41776-41785.

Zhou, Y., Y. Wang, M. Tischfield, J. Williams, P. M. Smallwood, A. Rattner, M. M. Taketo and J. Nathans (2014). "Canonical WNT signaling components in vascular development and barrier formation." *J Clin Invest*.